AD

EARTHQUAKE ENGINEERING SUPPORT
PHASE 5

Final Technical Report

by

R S Steedman

August 2002

United States Army

EUROPEAN OFFICE OF THE U.S. ARMY

London England

CONTRACT NUMBER: N68171-01-M-5037

PRINCIPAL INVESTIGATOR: DR R S STEEDMAN

SUMMARY

This report summarizes the findings of an experimental study supported by the U.S. Army Centrifuge Research Center and Engineer Earthquake Engineering Research Program (EQEN) into the behavior of saturated sands under high initial effective confining stresses subjected to strong ground shaking. The research was conducted using the Army Centrifuge at the U.S. Army Engineering Research and Development Center (ERDC), located in Vicksburg, MS. A large dataset of the response of saturated sand to dynamic shaking under 'level ground' conditions has been compiled and a series of verification models have been conducted. Several techniques were used to investigate the response of deep soil sites (in excess of 70m) including surcharges, lowered water table and higher acceleration (gravities). The most effective approach was to test specimens at higher gravity, as the interpretation of data from specimens tested using a heavy surcharge on the ground surface, or a deep water table has proved difficult. Many deep samples showed a limit to the excess pore pressure generated during shaking at a level much less than 100% of the initial vertical effective stress. A range of explanations has been proposed, including container effects, saturation, compression of the soil, redistribution of pore pressure and dynamic response of the surcharge. The verification tests eliminated container effects, and parallel research by others has shown that there are several reasons for pore pressure generation at depth to be limited. However, as postulated in earlier stages of this research, there is no absolute limit: in a fully saturated specimen of broadly uniform permeability, liquefaction was observed within a few cycles of strong shaking throughout (to an equivalent field depth of around 65m). A second key finding indicates that dense layers overlying loose layers may still be readily liquefied as a consequence of the high excess pore pressures generated below. These findings are highly significant for designers.

LIST OF KEYWORDS

liquefaction
centrifuge
earthquake
model
experiment
sand
dam safety

TABLE OF CONTENTS

1.0 BACKGROUND

This research contract addressed a further phase in the completion of an experimental and analytical research programme in support of the Earthquake Engineering Research Program under the direction of the USAE ERDC (formerly the Waterways Experiment Station), Vicksburg, Mississippi. The phase was entitled Earthquake Induced Liquefaction in Deep Sand Deposits. This study was a continuation of earlier research under Contract Nos. N68171-98-C-9014, N68171-97-M-5710, N68171-97-C-9012, N68171-99-C-9021 and N68171-00-M-5505. The research involved further interpretation of the early experimental data, design of verification experiments, interpretation and analysis of new experimental data and preparation of technical papers for publication. The work was completed in September 2001.

2.0 INTRODUCTION

The current state-of-practice for the evaluation of liquefaction potential and for remediation design and analysis depends on empirical correlations of in-situ measurements of strength versus field experience of liquefaction at shallow depth and laboratory data of the behavior of confined elements under cyclic loading. (Liquefaction is defined here to mean the development of pore pressure equal to 100% of the initial vertical effective stress.) This approach is known as the "simplified procedure". Opinions vary as to the maximum depth in the field at which liquefaction has been observed, but there is no established field evidence from historic earthquakes of liquefaction at depths greater than a few tens of meters. The NCEER Workshop in 1996 on the Evaluation of Liquefaction Resistance of Soils noted that the simplified procedure was developed from evaluations of field observations and field and laboratory test data, Youd and Idriss (1997). The report notes, "These data were collected mostly from sites ... at shallow depths (less than 15m). The original procedure was verified for and is applicable only to these site conditions".

Hence, in design practice the assessment of liquefaction under high initial effective confining stress, such as might relate to the foundations of large earth dams, is based on the extrapolation of observed behavior and correlations at shallow depths. In practice, the behavior of saturated soil under these conditions is not well understood. Based on the results of laboratory tests, researchers have postulated that there is a reduction in the liquefaction resistance of such soil compared to shallow depths. This reduction is accounted for in standard approaches by a ratio known as K_σ, a "correction factor" developed by Seed (1983) in the simplified procedure. This strength ratio is postulated to reduce with increasing initial effective confining stress, which has a large impact potentially on the extent and method (hence cost) of remedial construction required to assure adequate seismic performance of large dams. For example, it may reduce the cyclic shear stress ratio predicted to cause liquefaction in a soil layer under a typical large dam (of the order of 30m high) to about 50% of its value in the absence of the dam. The predicted deformations and resistance and the remedial strength required are a direct function of the reduced shear strength. The K_σ strength reduction therefore

has a strong influence on the decision to remediate a large dam and on the costs of that remediation.

The factor K_σ quantifies the curvature in the cyclic shear strength envelope (cyclic shear stress required to cause liquefaction versus confining stress) for a soil as observed in laboratory tests on discrete specimens. Although some curvature may be expected, such large reductions in cyclic shear strength ratios are counter-intuitive. It is generally accepted that increased confining stress should broadly improve the capacity of a soil to resist applied loads, not reduce it. Clearly the volume of soil that requires to be treated and the difficulty and expense of that treatment are highly dependent on an accurate assessment of the potential for and consequences of liquefaction.

There is therefore strong motivation for owners of large dams to investigate the behavior of saturated sands subject to strong ground shaking under high initial effective confining stresses. In the absence of field data, the use of a centrifuge was considered to be the only practical option to realistically represent a deep soil deposit subjected to earthquake shaking. The experiments reported herein relate exclusively to level ground initial stress conditions in a single layer (loose) or two-layer (dense over loose) deposit of clean, fine sand.

Liquefaction of a level sand bed has previously been the subject of research by many others. Experiments using Nevada sand were conducted at many centrifuge centers under the VELACS project, Arulanandan and Scott (1994). The objective of the ERDC study is to investigate the onset of liquefaction under much higher initial effective overburden stresses than used in the VELACS experiments. Nevada sand, which was used in the VELACS research and has been extensively studied in the laboratory, was adopted for the series of experiments under the ERDC centrifuge test program.

3.0 THE ERDC CENTRIFUGE FACILITY

The design specification for the ERDC centrifuge followed a review of the Army's research needs and a study of the available academic facilities, Ledbetter (1991). Many of the field problems with which the U.S. Army Corps of Engineers is concerned are physically large, such as earth dams, locks and river control structures, environmental problems and military research. It was determined that a new facility with a high payload capacity and high g capability was required to meet future Army needs. A large beam centrifuge was commissioned, Figure 1, termed the Acutronic 684, based on the French designed Acutronic 661, 665 and 680 series of geotechnical centrifuges, Ledbetter et al. (1994a). The capacity of the ERDC centrifuge is a payload of 8 tonnes at up to 143 g, reducing to 2 tonnes at 350 g, with a platform area of 1.3m square. This high capacity enables field problems of the order of up to 300m in breadth, 300m in depth, and 1000m in length to be simulated under a wide variety of loading conditions. The facility is equipped with a large range of equipment and appurtenances.

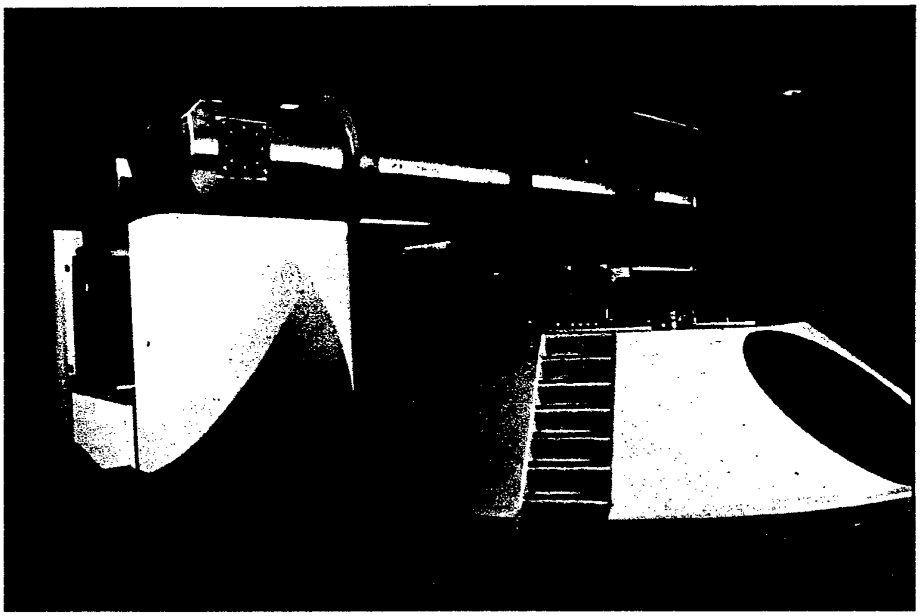

Figure 1. The WES centrifuge

The research approach for this high confining stress liquefaction study uses the large capacity of the WES centrifuge to investigate the generation of excess pore pressure and liquefaction under conditions that much more closely resemble those at depth in the field, Ledbetter et al. (1999). To do this required the design and construction of a large dynamic actuator. The history, design and characteristics of the actuator and specimen container have been discussed in a previous Technical Report, Steedman (2000) and are not repeated here.

4.0 RESEARCH PROGRAM

Table 1 summarises the experiments conducted during 1998 and 2001. The models are grouped in series, where each series corresponds to a different target range of vertical effective overburden stress in the loose layer.

Model series	Models in series	Effective overburden stress near bottom	Equivalent field depth (approx)	Depth of specimen	Notes (all specimens constructed from Nevada Sand, tested at 50g unless specified)
2	a, b, c, d, e, f	110 KPa (1 tsf)	15 m	300 mm	Fully submerged
3	a, b, c, d, e, f	210 KPa (2 tsf)	26 m	525 mm	Fully submerged (3f at 100g)
4	a, b, c, d	320 – 540 KPa (3 – 5 tsf)	26 – 40 m	525 mm	Lowered phreatic surface or surcharge (weights)
	e, f, g, h, i, j	420 – 1040 KPa (3.9 – 9.7 tsf)	30 – 60 m	525 mm	Surcharge (weights) and fully submerged, tested up to 125g
	k	200 – 510 KPa (1.9 – 4.8 tsf)	25 – 39 m	525 mm	No surcharge, fully submerged, tested up to 125g
5	a, b, c, d, e	750 – 1070 Kpa (7 – 10 tsf)	54 – 63 m	525 mm	Surcharge (weights), fully submerged
	f, g	740 KPa (6.9 tsf)	41 m	525 mm	Surcharge (weights), fully submerged (5g reused Model 3e)
	h	610 KPa (5.7 tsf)	41 m	525 mm	No surcharge, fully submerged, tested up to 125g
	i	730 KPa (6.8 tsf)	41 m	460 mm	No surcharge, lowered phreatic surface, tested at 125g

Table 1. Outline summary of centrifuge model test program

Model Code	Overall depth (mm)	Relative Density (D_r)*	σ_v' near base of specimen (tsf)	OCR	Number of earthquakes	Comments (all models constructed from Nevada Sand and tested at 50g unless specified)
2a	300	44% loose, 83% dense	1	1	3	Fully submerged
2b	300	50% loose, 75% dense	1	1	2	Fully submerged
2c	300	49% loose, 74% dense	1	1	5	Fully submerged
2d	300	50% loose, 75% dense	1	1	4	Fully submerged
2e	300	49% loose, 73% dense	1	2.5	4	Fully submerged
2f	300	50% loose, 75% dense	1	2.5	4	Fully submerged
3a	525	34% loose, 73% dense	2	1	2	Fully submerged
3b	525	49% loose, 77% dense	2	1	3	Fully submerged
3c	525	49% loose, 79% dense	2	1	3	Fully submerged
3d	525	54% loose, 80% dense	2	2.5	4	Fully submerged
3e	525	50% loose, 75% dense	2	1	1	Fully submerged
3f	262	50% loose, 75% dense	2	1	1	182 mm dense layer overlying 80 mm loose layer, fully submerged, no surcharge, 100g
4a	525	49% loose, 80% dense	3	1	4	Saturated to top of loose layer only.
4b	525	56% loose, 74% dense	3	2.5	4	Saturated to top of loose layer only.
4c	525	50% loose, 75% dense	4.7	1	4	Fully submerged, surcharge (weights)
4d	525	50% loose, 68% dense	4.7	2.5	4	Fully submerged, surcharge (weights)
4e	525	47% uniform	3.9 – 7.8	1	2,1,1	Fully submerged, surcharge (weights), Shaking at 50, 80, 100g
4f	525	55% uniform	3.9 – 9.7	1	1,1,2,1	Fully submerged, surcharge (weights), Shaking at 50, 80, 100, 125g
4g	525	50% uniform	3.9 – 9.7	1	1,1, 1,2	Fully submerged, surcharge (weights), Shaking at 50, 80, 100, 125g
4h	525	50% uniform	3.9 – 9.7	1	1,1, 1,1	Fully submerged, surcharge (weights), Shaking at 50, 80, 100, 125g
4i	525	50% uniform	3.9 – 9.7	1	1,1, 1,1	Fully submerged, surcharge (weights), Shaking at 50, 80, 100, 125g
4j	525	50% uniform	3.9 – 9.7	1	1,1, 1,2	Fully submerged, surcharge (weights), Shaking at 50, 80, 100, 125g.
4k	525	50% uniform	1.9 – 4.8	1	1,1, 1,2	Fully submerged, no surcharge, Shaking at 50, 80, 100, 125g.
4l	525	Densities uncertain	4.8	1	1	Fully submerged, surcharge (weights)
5a	525	51% loose, 72% dense	7.4	1	4	Fully submerged, surcharge (weights)
5b	525	49% loose, 76% dense	7.4	2.5	4	Fully submerged, surcharge (weights)
5c	525	52% loose, 75% dense	9.2	1	3	Fully submerged, surcharge (weights)
5d	525	57% loose, 80% dense	9.2	1	1	Fully submerged, surcharge (weights)
5e	525	50% uniform	8.4	1	7	Fully submerged, surcharge (weights)
5f	525	50% loose, 75% dense	6.9	1	1	Fully submerged, surcharge (weights)
5g	525	50% loose, 75% dense	6.9	1	1	Fully submerged, surcharge (same model as 3e with surcharge added)
5h	525	49% loose, 74% dense	5.7	1	1	Fully submerged, no surcharge, 125g
5i	460	50% loose, 75% dense	6.8	1	1	396 mm dense layer, saturated to depth of 250mm only, overlying 64 mm loose layer, no surcharge, 125g

*Relative density of the portion of the model termed 'loose', generally refers to a 160 mm thick layer placed at the bottom of the model. For the 'model of the model' experiments, this loose layer was reduced in depth. Relative density of the portion of the model termed 'dense', refers to that portion of the model above the 'loose' layer (ranged in thickness from 140 to 365 mm). Model 4l was understood to have been built to the standard specification, i.e. 75% dense over 50% loose.

Table 2. Summary description of centrifuge model test program

Generally, specimens were up to 525mm deep with the bottom 160mm placed at around 50% Relative Density (RD) and the upper portion at around 75% RD. The 'early' models were shaken at 50g; later models were shaken at up to 125g. During the verification phase modelling of models was carried out at 100g and 125g. Some models were overconsolidated by a factor of 2.5 prior to shaking (achieved by running the centrifuge up to 125g and then dropping back to 50g). The size of the dataset and number of repetitions provided the opportunity to characterise the data on the basis of the quality of the output. This is seen in Appendix A, where the summary data for each transducer and each earthquake analysed is presented. A quality rating of low/medium/high and * was assigned to each time history based on the consistency and reliability of the data and the quality of the experiment itself. For example, higher 'quality ratings' would be assigned to transducers which showed internal consistency in terms of static pore pressures, physical location in the model, response during shaking etc.

The Nevada sand used in the models was characterized by standard laboratory tests to determine parameters such as dry density and gradation. Table 3 presents key material parameters for this sand.

Specific gravity	2.64
Maximum void ratio	0.757 (density 93.8 pcf)
Minimum void ratio	0.516 (density 108.7 pcf)
D_{50}	0.18 mm (approx)
D_{10}	0.11 mm (approx)

Table 3. Nevada Sand (parameters as measured)

The pore fluid comprised a mixture of glycerine and water, 80% by weight for experiments conducted at 50g. Measurements of the viscosity of glycerine-water mixes at a range of temperatures and proportions show that the viscosity is sensitive to both parameters.

The density of a glycerine-water mix was calculated from:

$$\rho_m = \rho_g(m_g + m_w)/(m_g + \rho_g m_w)$$

where ρ_m is the density of the mix, ρ_g is the density of glycerine, m_g is the mass of glycerine, and m_w is the mass of water. Table 4. summarizes the properties of the glycerine-water solution used as the pore fluid.

Density	1200 kg/m^3
Viscosity	50 cs
Specific Gravity	1.26
Composition	80% glycerine-water mix (by weight)

Table 4. Parameters for pore fluid (as measured)

The models were poured dry from a hopper and saturated under vacuum, or slowly under gravity. Instrumentation was placed in the model as it was being constructed.

The typical arrangement of the model specimens for the different test series is shown in Figure 2. Instrumentation was positioned through the depth of the models, and comprised pore pressure transducers and accelerometers. The location of the instrumentation for Model 5b is shown in Figure 3.

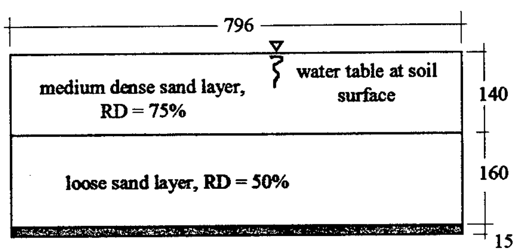

Typical cross section through Model series 1 and 2

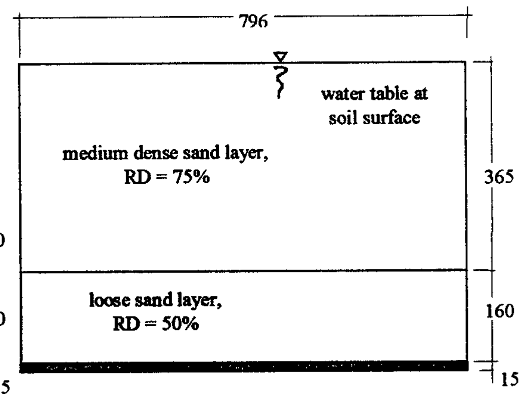

Typical cross section through Model series 3

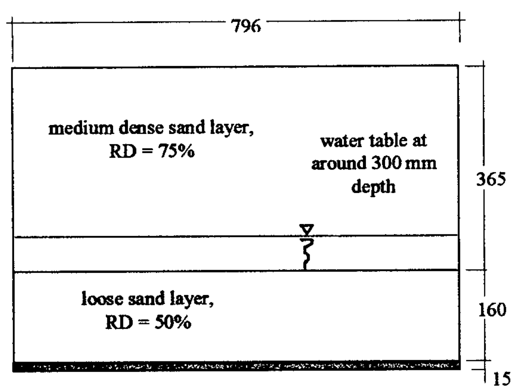

Typical cross section through Models 4a, 4b

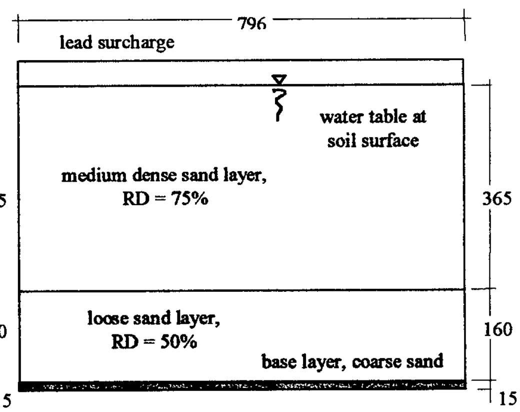

Typical cross section through Models 4c, 4d and 5

Figure 2. Cross sections through the different model configurations

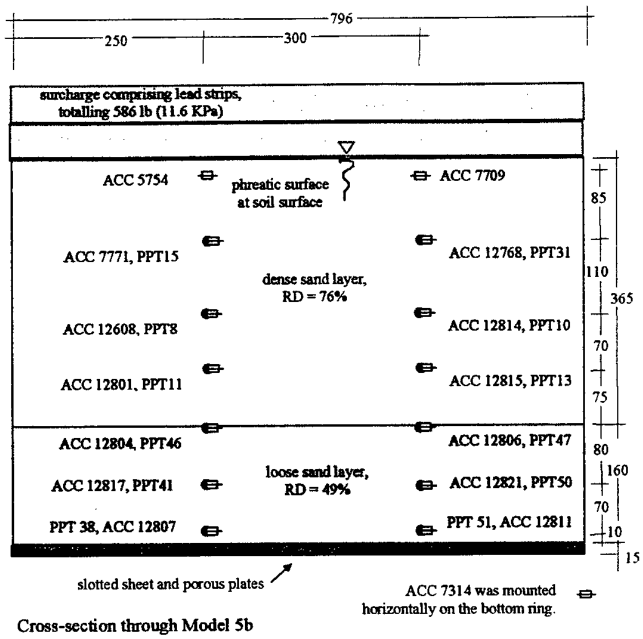

Figure 3. Instrumentation for Model 5b

5.0 RESULTS

Earlier reports, Steedman (1999), (2000) have presented analysis of the data using a range of approaches. In this report, the data from the verification models is summarized alongside the earlier experimental results, and in the same format.

Appendix A presents the dataset of limiting excess pore pressures, by model and by transducer. Comments are added concerning the quality of each record, and the experiment in general.

From this set a number of time histories were selected as of particularly high quality for possible future interpretation. This selection was made in part based on the internal consistency of the experimental results, and in part using subjective judgment based on past experience. These data are presented in Figures 4a and 4b, and 5a and 5b, below. In each case, the model reference number and earthquake is given, which can be checked against the commentary in Appendix A. Figures 4a and 5a present the pore pressure records; Figures 4b and 5b present the (matching) base input acceleration time history from the same model test.

A summary of selected data and recommendations for future centrifuge testing of level ground conditions under high effective confining stress has been prepared, Sharp and Steedman (2002).

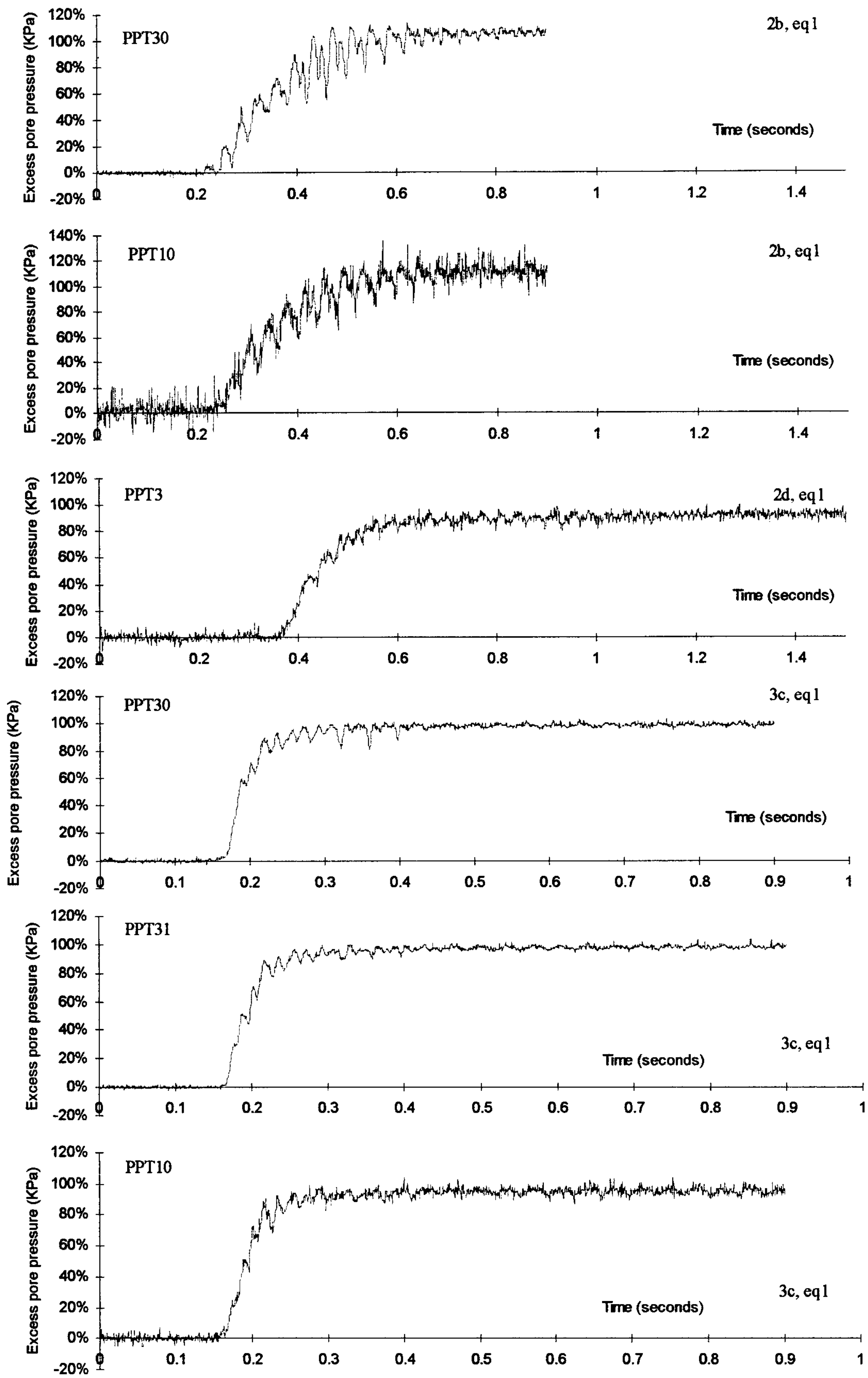

Figure 4a. Selected pore pressure time histories (I)

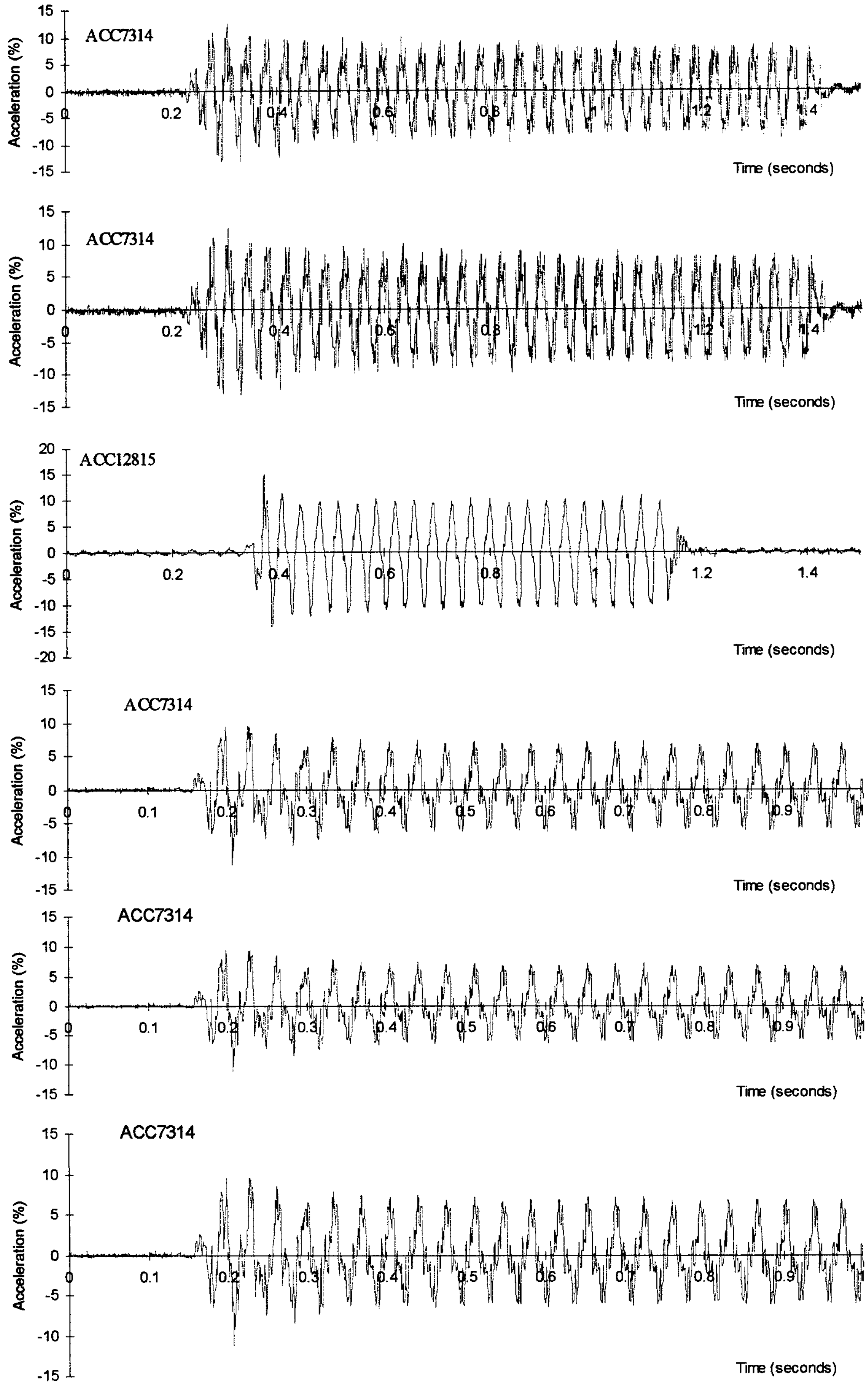

Figure 4b. Matching acceleration (base input) time histories (I)

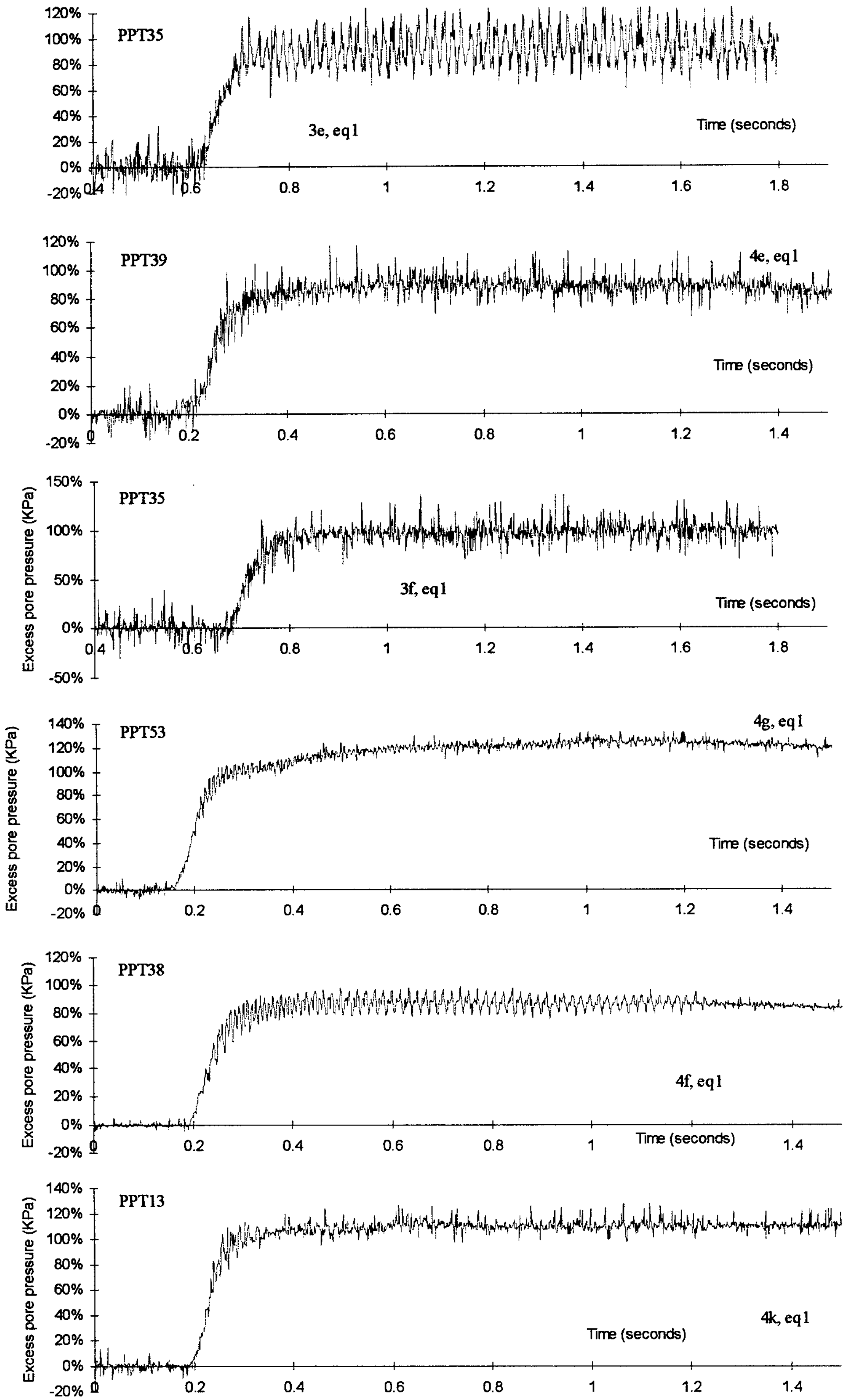

Figure 5a. Selected pore pressure time histories (II)

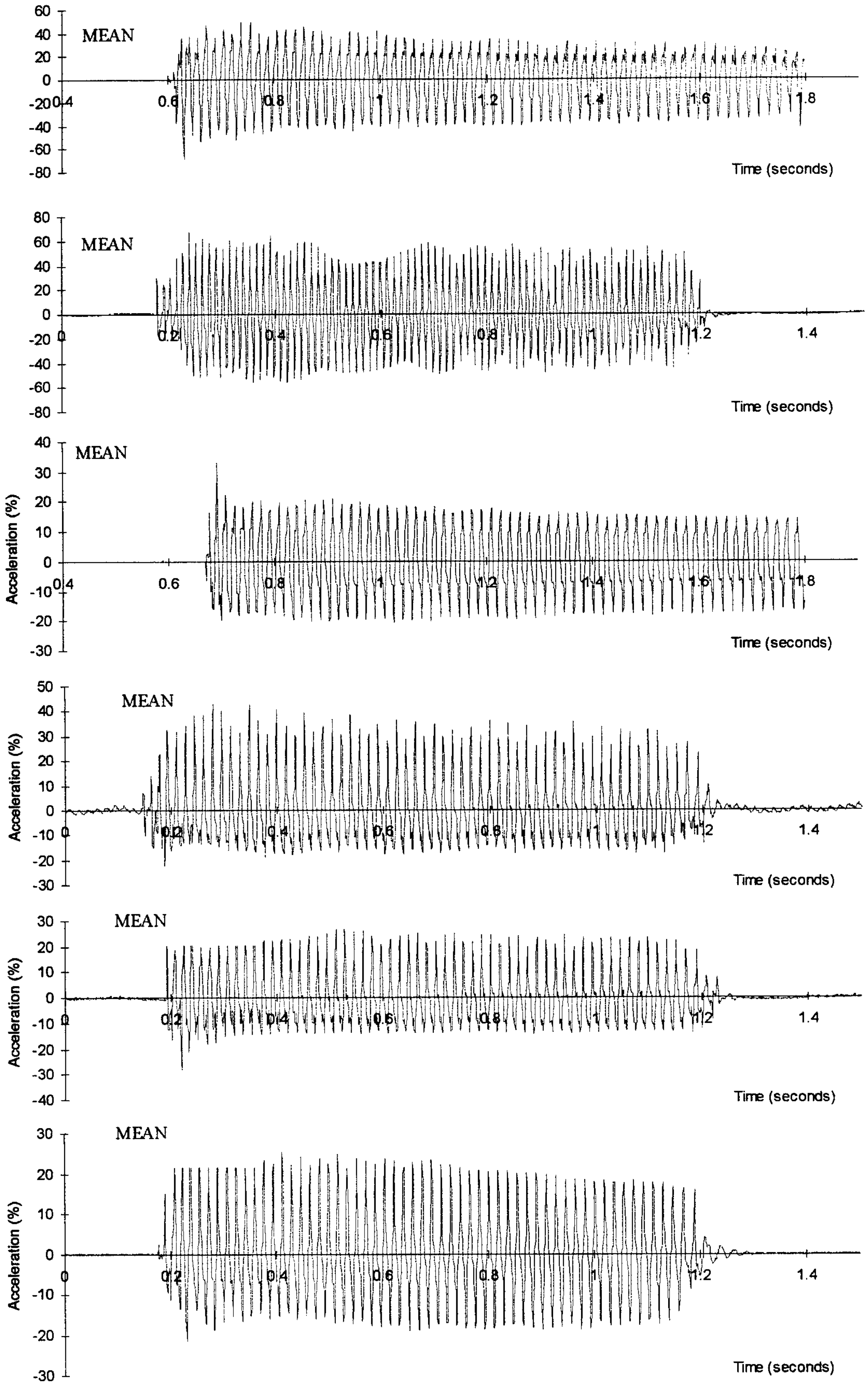

Figure 5b. Matching acceleration (base input) time histories (II)

6.0 DETERMINATION OF SHEAR STRESS-STRAIN HISTORIES

All of the experiments undertaken in this study addressed level ground conditions, with no initial static shear stress. The only shear stress and subsequent shear strain was that imposed by the loading. Level ground liquefaction is therefore a special case of the cyclic mobility phenomenon that occurs when the static shear stress is less than the shear strength of the liquefied soil. Level ground liquefaction failures are caused by the upward flow of water that occurs when seismically induced excess pore pressures dissipate. Depending on the length of time required to reach hydraulic equilibrium, level ground liquefaction failure may occur well after ground shaking has ceased and this was seen in a number of the experiments. References in Appendix A to transducers 'still climbing at the end of shaking' are evidence of pore pressure redistribution affecting the pore pressure generation caused by shaking.

A critical aspect in the assessment of these model experiments was to compute the stress strain time histories for comparison with laboratory element and field experience. This was done in collaboration with researchers at WES and RPI.

The method adopted to compute the stress and strain time histories was known as System Identification or SI. The method is described in a paper by Zeghal et. al. (1995), where the authors proposed that accelerometer and pore pressure time histories could offer a direct and effective means of evaluating seismic soil properties, in particular, a second order accurate estimation of shear stress and shear strain. This SI technique was utilized for analysis of the earthquake data.

Stress strain figures are shown here for Models 4k (Figure 6) and 5b (Figure 7), windowed during similar stages of shaking, Steedman and Sharp (2001).

The left column of plots are the traditional stress-strain loops computed for the early time data, as the excess pore pressures are developing strongly. This may be seen by comparison with the time history of vertical effective stress below the stress strain figures. For Model 4k this shows the largest amount of straining near the surface at nearly 1%, decreasing to a strain of 0.6% at a depth of 24 m. The remaining columns of figures show how the stress strain loops are altered by the development of excess pore pressure. In the case of Model 4k, the specimen reaches close to 100% excess pore pressure, and the upper layers become isolated from the straining at the base. In the case of Model 5b, the excess pore pressure is limited and the response of the soil column becomes nearly linear. The marked contrast in response between the two specimens confirm the observation that the stabilization of the excess pore pressure development in the deeper specimens is a genuine phenomenon associated with a stable cycling of applied load at a level significantly below 100% excess pore pressure, and with the soil retaining considerable reserves of strength and stiffness.

One explanation for the limiting level of excess pore pressure may be associated with upward drainage of the excess pore pressures.
Appendix B presents isochrones of stress and strain levels from each experiment, based on this method.

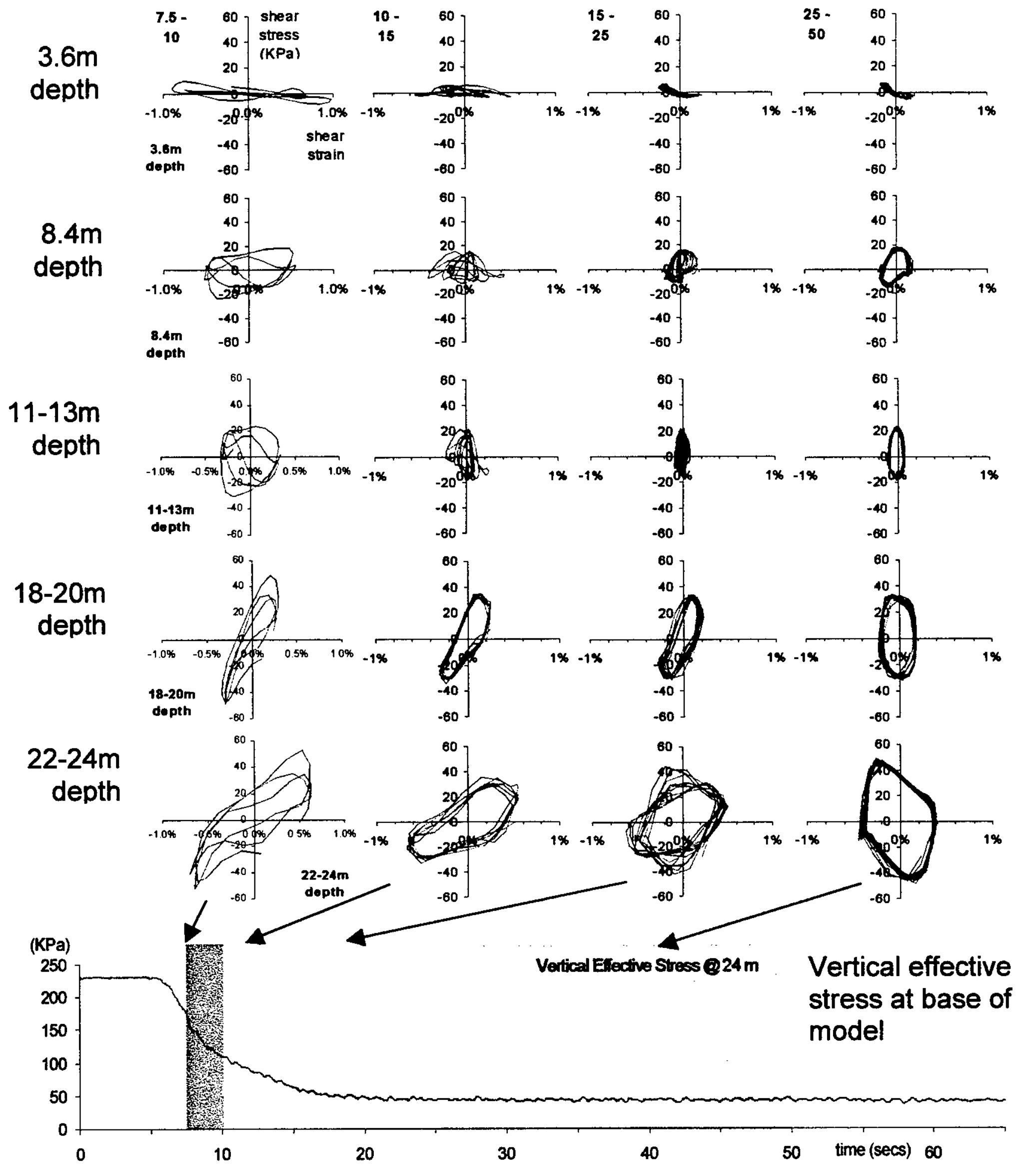

Figure 6. Stress strain time histories, Model 4k

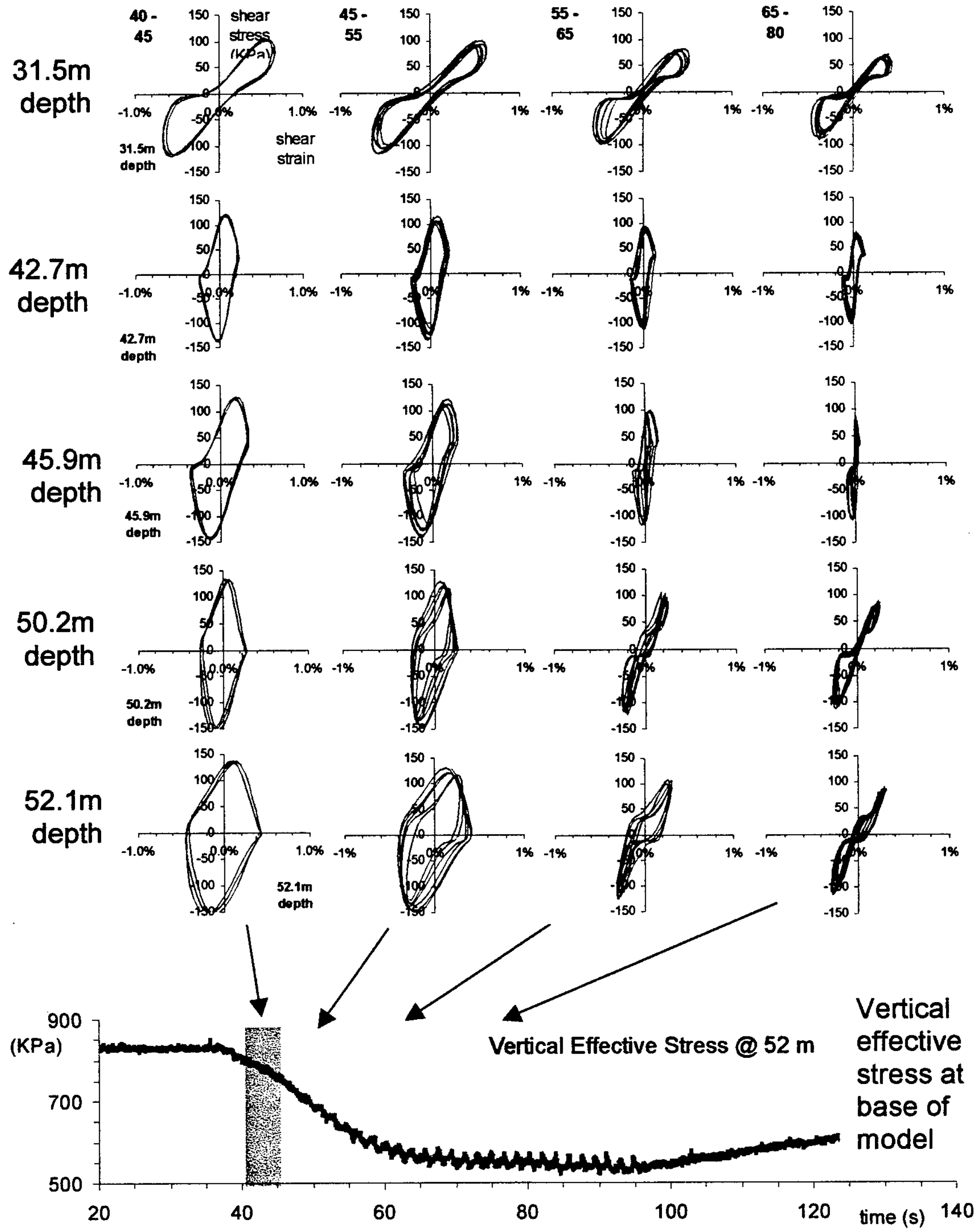

Figure 7. Stress strain time histories, Model 5b

A very large dataset of the behavior of Nevada sand subject to shaking under level ground conditions has been accumulated as a result of this work. Review of the stress-strain data alongside the time histories of excess pore pressure provided considerable additional insight into the explanation of the pore pressure response in many cases. The verification models that were tested during 2000-2001 were successful in validating the performance of the specimen chamber and shaker in many respects. The verification models showed that the use of surcharges may indeed be having an effect on the response of the soil column, although exactly how the surcharge affects the soil column has not yet been conclusively

determined; many other factors, including soil density, compression and saturation may also be influencing the 'true' response under cyclic loading at high effective confining stress. It is clear that the most effective method of investigating the influence of very high effective confining stress is to use the centrifuge at high g, with or without dry sand surcharging, as for example was achieved with the final experiments in the series, Models 5h and 5i.

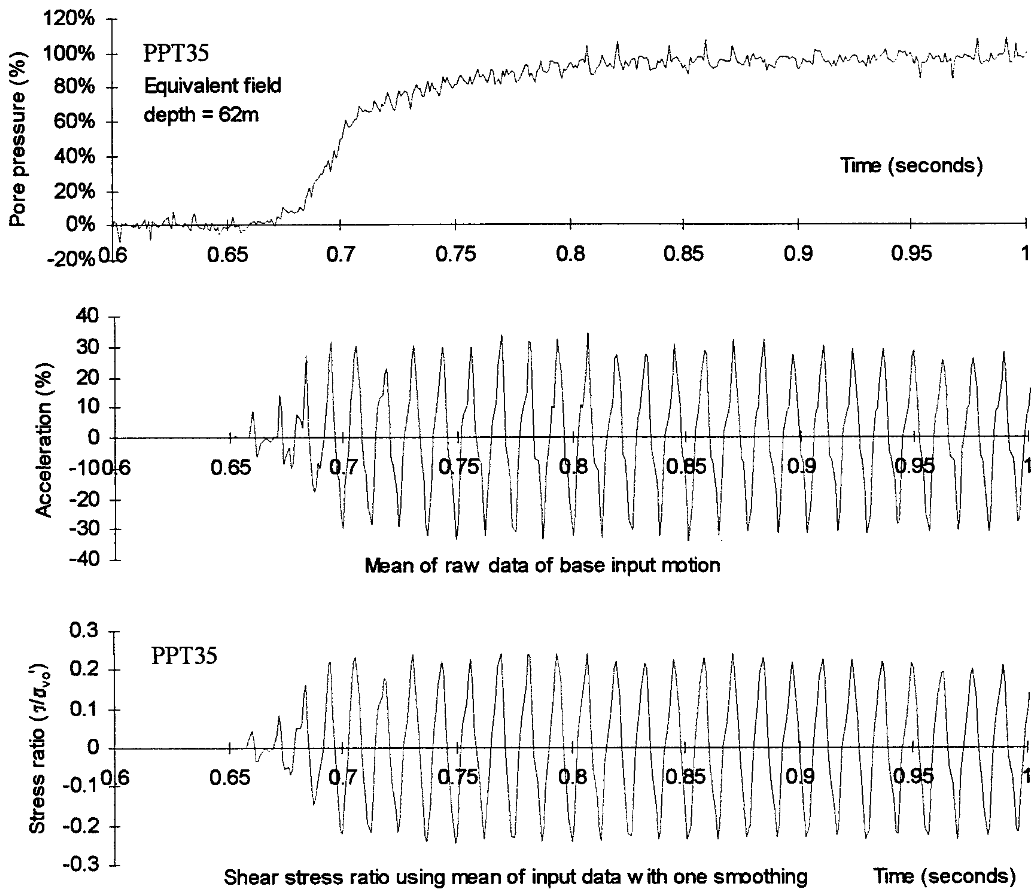

Figure 8. Liquefaction at 62m equivalent depth, Model 5h

Figure 8 presents data from PPT35, Model 5h, which shows 100% excess pore pressure reached after a few cycles of strong shaking in a fully saturated deep specimen without surcharge, at 125g. The shear stress ratio time history shown here was calculated using the simplified method, Steedman (2000) and may be compared to the isochrones of stress ratio calculated using the SI method, Appendix B. Appendix B also shows the long term response after the end of shaking, where consolidation effects and pore pressure redistribution last for a very long period after the end of the earthquake.

7.0 CONCLUSIONS

1. A large data-set of the behavior of loose saturated sands under high initial effective confining stresses and subject to earthquake-like shaking has been collected during an extensive experimental program on the ERDC Centrifuge, Vicksburg MS.

2. Early findings from the centrifuge experiments showed that under high effective confining stress, the potential to generate excess pore pressures was limited, and this may be of considerable importance if verified.

3. Detailed investigation into the early findings has provided a range of explanations for the limiting values, including experimental problems such as specimen saturation, chamber effects or the distorting effects of large surcharges on the soil surface. Of these possible effects, detailed investigation of the response of the chamber effectively eliminated movement, or distortion of the ESB container as an explanation.

4. The effect of surcharging was investigated by comparison with changing g level and using different methods of surcharging, or no surcharges at all. The use of dry sand appeared preferable to lead or steel weights; this method was used in early experiments as well as in later models.

5. In the final experiments, which were carried out at high g without the use of surcharges, liquefaction occurred throughout the entire depth within a few cycles. This experiment confirmed that with sufficient input shaking, large excess pore pressures are generated in a saturated soil column of broadly uniform permeability.

6. A key finding of the study has been to recognise the importance of pore pressure redistribution in deep soil columns, which can cause an 'up-welling' of excess pore pressure from lower layers leading to liquefaction of upper layers some time after shaking has ceased. This is an effect not widely considered in standard design methods.

7.0 REFERENCES AND BIBLIOGRAPHY

This research work has made use of a wide range of references; these are presented below for completeness:

Arulanandan, A. and Scott, R.F. (1994) editors, Proc. Int. Conf. on Verification of Numerical Procedures for the Analysis of Soil Liquefaction Problems, at U.C. Davis; Volumes 1 & 2; Balkema.

Arulmoli, K., Muraleetharan, K.K., Hossain, M.M., and Fruth, L.S., (1992). "VELACS Verification of Liquefaction Analyses by Centrifuge Studies Laboratory Testing Program Soil Data Report." National Science Foundation Report.

Butler, G.D. (2000). A dynamic analysis of the stored energy angular momentum actuator used with the equivalent shear beam container, PhD thesis, Engineering Department, Cambridge University.

Elgamal, A-W, Zeghal, M., Tang, H.T., and Stepp, J.C., (1995). "Lotung Downhole Array. I: Evaluation of Site Dynamic Properties", Journal of Geotechnical Engineering, Vol, 121, No. 4, pp. 350-362.

Finn, W.D.L. and Yogendrakumar, M., Yoshida, N. and Yoshida, H., (1986), "TARA-3: A Program to Compute the Response of 2-D Embankments and Soil-Structure Interaction Systems to Seismic Loadings", Department of Civil Engineering University of British Columbia, Canada.

Finn, W.D.L., Ledbetter, R.H., and Marcuson, W.F. III (1995). "Seismic Deformations in Embankments and Slopes", Symposium on Developments in Geotechnical Engineering - From Harvard to New Delhi, 1936-1994, Bangkok, Thailand, A.A. Balkema, Rotterdam.

Finn, W.D.L. and Yogendrakumar, M., (1989) "TARA-3FL; Program for Analysis of Liquefaction Induced Flow Deformations", Department of Civil Engineering, University of British Columbia, Vancouver, Canada.

Gonzals, L., Abdoun, T., and Sharp, M.K., (2002). "Modeling of Seismically Induced Liquefaction Under High Confining Stress", submitted International Journal of Physical Modeling and Geotechnics.

Harder, L.F., (1988). "Use of Penetration Tests to determine the Cyclic loading Resistance of Gravelly Soils during Earthquake Shaking", PhD Dissertation, University of California at Berkeley.

Hynes, M.E. and Olsen, R., (1998). "Influence of Confining Stress on Liquefaction Resistance." Proceedings of the International Symposium on the Physics and Mechanics of Liquefaction, John Hopkins University, Baltimore, MD, 10-11 September 1998.

Hynes, M.E., (1988). A Pore pressure characterization of gravels under undrained cyclic loading, PhD Dissertation, University of California at Berkeley.

Ledbetter, R.H. (ed) (1991) Large centrifuge: a critical Army capability for the future, Misc. Paper GL-91-12, Dept. of the Army, Waterways Experiment Station, Vicksburg, MS, May.

Ledbetter, R.H., and Finn, W.D.L. (1993). "Development and Evaluation of Remediation Strategies by Deformation Analysis", ASCE Specialty Conference on Geotechnical Practice In Dam Rehabilitation, Raleigh, North Carolina, April, pp 386 - 401.

Steedman, R.S. and Habibian A. (1987) Modelling the failure of coastal dykes during earthquakes. 9th European Conf. Soil Mech. Found. Eng. Vol 2, pp 633-636, Dublin, 31 Aug - 3 Sept.

Steedman, R.S. (1998) Initial earthquake centrifuge model experiments for the study of liquefaction, Final Technical Report, Contract No. N68171-97-M-5710, European Office of the U.S. Army, London, March.

Steedman, R.S. (1999) Earthquake engineering support, Phase 2, Final Technical Report, Contract No. N68171-98-C-9014, European Office of the U.S. Army, London, January.

Steedman, R.S. (1999) Earthquake engineering support, Phase 3, Final Technical Report, Contract No. N68171-99-C-9021, European Office of the U.S. Army, London, November.

Steedman, R.S. (2000) Earthquake Engineering Support Phase 4, Final Technical Report, USAE WES, Contract No. N68171-00-M-5505, European Office of the US Army, London, September.

Steedman, R.S., Ledbetter, R.H., and Hynes, M.E. (2000). "The influence of high confining stress on the cyclic behavior of saturated sand", ASCE Geotechnical Special Publication No. 107, Soil Dynamics and Liquefaction 2000, Eds. Ronald Y.S. Pak and Jerry Yamamura,pp. 35-57.

Steedman, R.S. and Sharp, M. (2001) Liquefaction of deep saturated sands under high effective confining stress, Proc 4th Int Conf Recent Advances in Geotech Earthquake Engineering and Soil Dynamics, San Diego, California, March 26-31, Univ Missouri-Rolla.

Taboada, V. and Dobry, R. (1998), "Centrifuge Modeling of Earthquake-Induced Lateral Spreading in Sand", *Jour. of Geotech. and Geoenv. Eng.*, ASCE, Vol. 120, No. 12, pp. 1195-1206.

Vaid, Y. P. and Thomas, J., (1995). "Liquefaction and post liquefaction behavior of sand." Journal of Geotechnical Engineering, ASCE, Vol. 121, No. 2, February, pg 163-173.

Vaid, Y.P., Chern, J.C. and Tumi, H., (1985). "Confining pressure, grain angularity, and liquefaction." Journal of Geotechnical Engineering, ASCE, October, Vol. 111, No. 10, pg 1229-1235.

Youd, L. and Idriss, I., Eds (1997) Workshop on Evaluation of Liquefaction Resistance of Soils, Proceedings, Salt Lake City, Technical Report NCEER-97-0022, sponsored by FHWA, NSF and WES, published by NCEER.

Youd, T.L., Idriss, I.M., Andrus, R.D., Arango, I., Castro, G., Christian, J.T., Dobry, R., Finn, W.D.L., Harder, L.F., Hynes, M.E., Ishihara, K., Koester, J.P., Liao, S.C., Marcuson, W.F., Martin, G.R., Mitchell, J.K., Moriwaki, Y., Power,

M.S., Robertson, P.K., Seed, R.B., Stokoe, K.H. (2001), "Liquefaction Resistance of Soils: Summary Report from the 1996 NCEER and 1998 NCEER/NSF Workshops on Evaluation of Liquefaction Resistance of Soils, *Jour. Of Geotech. And Geoenv. Eng.*, ASCE, Vol. 127, No. 10, pp. 817-833.

Zeghal, M., Elgamal, A.-W., Tang, H.T., and Steep, J.C., (1995). Lotung downhole array. II: Evaluation of Soil Nonlinear Properties, J. Geotech. Engrg., ASCE, 121(4), 363-378.

APPENDIX A

EARTHQUAKE DATASET

Data of limiting pore pressures, Models and cycles (1998-2001)

EARTHQUAKE DATASET

Data of limiting pore pressures, Models and cycles

Model, Earthquake	Eq	Centrif'g acc'n	Total vertical stress (KPa)	Effective Overburden Pressure (KPa)	Cycles to upper limit	Cycles to 50% excess	Pore pressure Upper limit (%)	Upper value (KPa)	Peak Cyclic stress ratio	0.65 Stress ratio 0.65xPeak	Relative Density (%)	Quality low/med/high/*	PPT	Comments	Summary details and WES Model Ref
Model 1a, 1	1	50	67.6	34	10.8		59	20.06	0.105	0.068	70	low	31	Uncertain measured depth of transducers, showed double frequency	
Model 1a, 1	1												10	Still climbing at end of datacapture	
Model 1a, 1	1												9	Still climbing at end of datacapture	
Model 1a, 2	2	50	67.6	35	12.4		100	35		0.0511	70	low	31	Ottawa sand. Second eq showed slow rise to final limit	
Model 1a, 2	2												10	Still climbing at end of datacapture	
Model 1a, 2	2												9	Still climbing at end of datacapture	
Model 2a, 1	1	50	70.3	30	2.51		100	30	0.318	0.207	83	low		Near surface acceleration clearly shows liquefaction	20/2/1998, Ref 2
Model 2a, 2	2	50	70.3	30	2.48		100	30	0.25	0.162	83	low	na	Estimated as no ppts functioning	300mm depth
Model 2a, 3	3												na	Probably did not liquefy	44% loose, 83% dense
Model 2b, 1	1	50	221	106	10.719	2.187	110	116.6	0.18	0.117	50	*	10	Clearly over 100%, large cycles affect 50% point	30/4/1998, Ref 5
Model 2b, 1	1	50	223	106	11.529	2.349	105	111.3	0.181	0.118	50	*	30	Double frequency just over 100%, large cycles affect 50% point	300mm depth
Model 2b, 1	1	50	68.9	27	10.611	2.16	110	29.7	0.292	0.19	75	*	31	Clearly over 100%, large cycles affect 50% point	50% loose, 75% dense
Model 2b, 2	2	50	230	111	5.4		104	115.44	0.221	0.143	50	*	10	Very clearly 100%	
Model 2b, 2	2	50	236	115	4.59		98	112.7	0.216	0.141	50	*	30	Rapid rise to 100%	
Model 2b, 2	2	50	76.4	32	5.4		100	32	0.33	0.214	75	*	31	Clear 100%, rapid rise	
Model 2c, 1	1	50	240	98	27.5	13.095	100	98	0.092	0.059	49	high	46	Possibly just reached limit before being cut off	6/6/98, Ref 8
Model 2c, 1	1	50	256	98	27.5	8.343	103	100.94	0.097	0.063	49	high	41	Seems to be very close to limit at the end of the eq	300mm depth
Model 2c, 1	1	50		99		21.978			0.0899	0.0585	49	high	49	Still climbing when data cut off	49% loose, 74% dense
Model 2c, 1	1	50	69.2	30	8.59	5.238	70	21	0.114	0.074	74	high	37	Reached upper limit early, unlike other depths, high freq rapid rise affects 50% point	
Model 2c, 1	1												42	Erratic response, still climbing at end	
Model 2c, 1	1												39	Erratic response, still climbing at end	
Model 2c, 2	2	50	240	98	46		96	94.08	0.094	0.061	49	high	46	Very close to limit at end	
Model 2c, 2	2	50	256	98	46		100	98	0.1	0.065	49	high	41	Very close to limit at end	
Model 2c, 2	2												49	Still climbing at end of shaking	
Model 2c, 2	2	50	70.8	27.6	6.6		75	20.7	0.132	0.085	74	med	37	Reached upper limit early, unlike other depths	
Model 2c, 2	2												42	Erratic response, still climbing at end	
Model 2c, 2	2	50	74.1	30.3	12.8		90	27.27	0.123	0.08	74	med	39	Reached upper limit early, like ppt37	
Model 2c, 3	3												46	Still climbing at end of shaking	
Model 2c, 3	3												41	Still climbing at end of shaking	
Model 2c, 3	3												49	Still climbing at end of shaking	
Model 2c, 3	3	50	70.8	27.6	7.7		70	19.32	0.127	0.083	74	med	37	Reached upper limit early, very noisy response	
Model 2c, 3	3												42	Erratic response, still climbing at end	
Model 2c, 3	3	50	74.1	30.3	15.4		80	24.24	0.069	0.045	74	med	39	Reached upper limit later than ppt37, very noisy	
Model 2c, 4	4												46	Still climbing at end of shaking	
Model 2c, 4	4												41	Still climbing at end of shaking	
Model 2c, 4	4												49	Still climbing at end of shaking	
Model 2c, 4	4	50	70.8	27.6	5.4		70	19.32	0.107	0.07	74	med	37	Reached upper limit early, very noisy response	
Model 2c, 4	4												42	Erratic response, still climbing at end	
Model 2c, 4	4	50	74.1	30.3	36.5		75	22.725	0.1	0.065	74	med	39	Possibly reached limit, very noisy	
Model 2c, 5	5												46	No excess pore pressure	
Model 2c, 5	5												41	No excess pore pressure	

Model 2c, 5	5												49	No excess pore pressure	
Model 2c, 5	5												37	No excess pore pressure	
Model 2c, 5	5												42	No excess pore pressure	
Model 2c, 5	5												39	No excess pore pressure	
Model 2d, 1	1	50	188	76	9.45	2.0	106	80.56	0.26	0.169	74	*	3	Good record, dense/loose boundary	12/8/98, Ref 9
Model 2d, 1	1	50	203	88	5	1.5	83	73.04	0.174	0.113	49	*	31	Double frequency at upper limit suggests 100% excess pwp	300mm depth
Model 2d, 1	1	50	317	133	13	2.6	76	101.08	0.187	0.121	49	high	46	Difficult to identify upper limit, which rises slowly, large cycles affect 50% point	50% loose, 75% dense
Model 2d, 1	1	50	124	50	10	2.3	92	46	0.25	0.162	74	high	7	Sank during earthquake, clearly reached limit	
Model 2d, 1	1	50	150	59.4	8.4	1.8	93	55.242	0.242	0.158	74	*	41	Clearly reached limit, dense/loose boundary, large cycles affect 50% point	
Model 2d, 1	1	50	264	112	12.2	2.3	92	103.04	0.193	0.126	49	high	51	Reached limit, cyclic response, large cycles affect 50% point	
Model 2d, 1	1	50		135		3.3			0.186	0.121	49	high	8	Still climbing slowly at end of shaking, large cycles affect 50% point	
Model 2d, 2	2	50	195	76	9.2		88	66.88	0.338	0.22	74	*	3	Good record, dense/loose boundary	
Model 2d, 2	2	50	204	86.6	4		80	69.28	0.299	0.194	49	*	31	Double frequency at upper limit suggests 100% excess pwp	
Model 2d, 2	2												46	Still climbing at end of earthquake	
Model 2d, 2	2	50	132	49.7	4.3		82	40.754	0.388	0.252	74	med	7	Sank during earthquake, clearly reached limit	
Model 2d, 2	2	50	154	59.4	5.1		90	53.46	0.364	0.236	74	*	41	Clearly reached limit, dense/loose boundary	
Model 2d, 2	2	50	267	112	9.7		90	100.8	0.286	0.186	49	high	51	Reached limit, cyclic response	
Model 2d, 2	2												8	Still climbing slowly at end of shaking	
Model 2d, 3	3	50	196	76	7.7		88	66.88	0.309	0.201	74	*	3	Good record, dense/loose boundary	
Model 2d, 3	3	50	203	87.8	3.6		78	68.484	0.266	0.173	49	*	31	Double frequency at upper limit suggests 100% excess pwp	
Model 2d, 3	3												46	Still climbing at end of earthquake	
Model 2d, 3	3	50	133	50	5		83	41.5	0.353	0.23	74	med	7	Sank during earthquake, clearly reached limit	
Model 2d, 3	3	50	153	59.4	5.9		90	53.46	0.327	0.213	74	*	41	Clearly reached limit, dense/loose boundary	
Model 2d, 3	3												51	Still climbing slowly at end of shaking	
Model 2d, 3	3												8	Still climbing slowly at end of shaking	
Model 2d, 4	4	50	196	76	7.7		84	63.84	0.281	0.183	74	*	3	Good record, dense/loose boundary	
Model 2d, 4	4	50	203	87.8	4.4		78	68.484	0.242	0.157	49	*	31	Double frequency at upper limit suggests 100% excess pwp	
Model 2d, 4	4												46	Still climbing at end of earthquake	
Model 2d, 4	4	50	133	49.7	5		83	41.251	0.321	0.208	74	med	7	Sank during earthquake, clearly reached limit	
Model 2d, 4	4	50	154	59.6	5		88	52.448	0.297	0.193	74	*	41	Clearly reached limit, dense/loose boundary	
Model 2d, 4	4												51	Close, but still climbing slowly at end of shaking	
Model 2d, 4	4												8	Still climbing slowly at end of shaking	
Model 2e, 1	1	125	162	60	13.4	4.2	100	60	0.225	0.147	73	med	52	Kink in pore pressure time history, static readings at 50g unreliable	26/8/98, Ref 10
Model 2e, 1	1	125	270	129	13.2	8.9	72	92.88	0.153	0.1	49	high	47	Static readings at 50g not totally reliable	300mm depth
Model 2e, 1	1	125	373	175	22.4	7.6	76	133	0.144	0.093	49	high	49	Static readings at 50g not totally reliable	49% loose, 73% dense
Model 2e, 1	1	125		38		2.0			0.163	0.106	73	med	43	Dense layer, rose rapidly at first, but then started to drop after 0.2 seconds, large cycle affects 50%	
Model 2e, 2	2	125	169	66.8	8		90	60.12	0.211	0.137	73	high	52	Good record	
Model 2e, 2	2	125	269	129	11.2		71	91.59	0.158	0.103	49	high	47	Clear limit, but static readings at 50g not totally reliable	
Model 2e, 2	2	125	381	184	5.3		69	126.96	0.142	0.092	49	high	49	Very rapid rise to limit, but static readings at 50g not totally reliable	
Model 2e, 2	2	125	68.9	42.4	6.9		70	29.68	0.158	0.103	73	med	43	Dense layer, reached some sort of limit but noisy signal	
Model 2e, 3	3	125	169	66.8	9.3		85	56.78	0.218	0.142	73	high	52	Limit, but with cyclic behaviour	
Model 2e, 3	3	125	269	129	14.7		70	90.3	0.163	0.106	49	high	47	Clear limit, but static readings at 50g not totally reliable	
Model 2e, 3	3	125	381	184	3.9		70	128.8	0.146	0.095	49	high	49	Very rapid rise to limit, but static readings at 50g not totally reliable	
Model 2e, 3	3	125	68.9	42.4	3.9		63	26.712	0.163	0.106	73	med	43	Dense layer, reached some sort of limit but noisy signal	
Model 2e, 4	4	125	169	66.8	20.6		83	55.444	0.222	0.144	73	high	52	Limit, but with strong cyclic behaviour	
Model 2e, 4	4	125	269	129	17.9		70	90.3	0.166	0.108	49	high	47	Good record, but static readings at 50g not totally reliable	
Model 2e, 4	4	125	381	184	11.1		68	125.12	0.149	0.097	49	high	49	Very rapid immediate response, then slow rise to limit, as above	
Model 2e, 4	4	125	68.9	42.4	7.1		67	28.408	0.166	0.108	73	med	43	Dense layer, reached some sort of limit but noisy signal	
Model 2f, 1	1	125	172	63	15.4	6.6	99	62.37	0.288	0.187	50	*	31	Excellent, loose/dense interface	22/9/98, Ref 14
Model 2f, 1	1	125	251	101	13.5	7.2	88	88.88	0.237	0.154	50	*	47	Excellent, up to 7.911 for 50%	300mm depth

Model 2f, 1	1	125	320	136	7.34	3.1	85	115.6	0.207	0.134	50	*	46	Excellent	50% loose, 75% dense
Model 2f, 1	1	125	104	32.2	5.21	1.7	115	37.03	0.395	0.257	75	*	38	Excellent	
Model 2f, 1	1	125	102	31.7	5.4	2.4	115	36.455	0.397	0.258	75	*	51	Clear limit, very rapid rise with one or two big cycles, affecting 50%	
Model 2f, 1	1	125	172	62.6	13.5	7.5	93	58.218	0.293	0.191	50	*	15	Good record, loose/dense interface	
Model 2f, 1	1	125	337	138	10.8	3.9	90	124.2	0.213	0.138	50	*	41	Bottom of loose layer, rapid rise to limit, with cycles which may affect 50%	
Model 2f, 2	2	125	177	69	8.6		88	60.72	0.287	0.187	50	*	31	Excellent	
Model 2f, 2	2	125	254	103.5	14		79	81.765	0.248	0.161	50	*	47	Good record	
Model 2f, 2	2	125	320	136	2.2		85	115.6	0.222	0.144	50	*	46	Very rapid rise to limit	
Model 2f, 2	2	125	113	41.4	3.2		80	33.12	0.341	0.222	75	*	38	Clear limit, slightly noisy	
Model 2f, 2	2	125	112	41.9	4.1		82	34.358	0.336	0.218	75	*	51	Clear limit, again noisy	
Model 2f, 2	2	125	177	67.6	20.3		85	57.46	0.294	0.191	50	*	15	Two stage rise to final limit	
Model 2f, 2	2	125	339	140.3	6.8		86	120.658	0.225	0.146	50	*	41	Bottom of model, rapid rise to limit	
Model 2f, 3	3	125	177	69	19.7		92	63.48	0.38	0.247	50	high	31	Reached limit near end of shaking, loose/dense interface	
Model 2f, 3	3	125	254	103.5	34.8		92	95.22	0.328	0.213	50	high	47	Just reached limit near end	
Model 2f, 3	3	125	320	136	4.3		92	125.12	0.293	0.191	50	*	46	Bottom of model, very rapid rise to limit	
Model 2f, 3	3	125	113	41.4	6.2		100	41.4	0.452	0.293	75	*	38	Clear limit, slightly noisy	
Model 2f, 3	3	125	112	41.9	4.9		93	38.967	0.444	0.288	75	*	51	Clear limit, again noisy	
Model 2f, 3	3												15	Still rising at end of shaking	
Model 2f, 3	3	125	339	140	10.3		93	130.2	0.298	0.193	50	*	41	Bottom of model, rapid rise to limit	
Model 2f, 4	4	125	177	69	26.2		83	57.27	0.39	0.254	50	high	31	Reached limit near end of shaking, cyclic response	
Model 2f, 4	4	125	254	103.5	23.5		84	86.94	0.337	0.219	50	high	47	Reached limit near end	
Model 2f, 4	4	125	320	135.7	4.6		86	116.702	0.301	0.196	50	*	46	Bottom of model, very rapid rise to limit	
Model 2f, 4	4	125	113	41.4	7.3		78	32.292	0.463	0.301	75	*	38	Clear limit, slightly noisy	
Model 2f, 4	4	125	112	41.9	4.6		77	32.263	0.455	0.296	75	*	51	Clear limit, again noisy	
Model 2f, 4	4												15	Still rising at end of shaking	
Model 2f, 4	4	125	339	140.3	15.4		82	115.046	0.305	0.199	50	*	41	Bottom of model, slower rise to limit	
Model 3a, 1	1	50	474	181	4.2	1.9	102	184.62	0.314	0.204	34	high	9	Spikey acceleration record, but excellent pore pressure data, rapid rise affects 50%	30/3/98, Ref 3
Model 3a, 1	1	50	429	182	3.8	1.8	110	200.2	0.281	0.183	34	high	10	Low static pore pressure value, good dynamic response, rapid rise affects 50%	525mm depth
Model 3a, 2	2	50	477	186	7.9		98	182.28	0.288	0.187	34	high	9	Slow rise contrasts with ppt10	34% loose, 73% dense
Model 3a, 2	2	50	432	184	3.6		102	187.68	0.258	0.168	34	high	10	Good limit, spikey acceleration on eqs 1 and 2	
Model 3b, 2	2	50	466	198	5.4		90	178.2	0.124	0.081	49	med	16	Calibration adjusted to bring into line with ppt2	1/5/98, Ref 6
Model 3b, 2	2	50	469	200	5.7		90	180	0.124	0.081	49	high	2	Good record	525mm depth
Model 3b, 2	2	50	528	228	4.5		82	186.96	0.117	0.076	49	high	11	Clearly reached limit	49% loose, 77% dense
Model 3b, 2	2	50	385	164	25.1		90	147.6	0.132	0.086	49	high	1	Just reached limit	
Model 3b, 3	3	50	466	190	5.2		85	161.5	0.135	0.088	50	med	16	Calibration adjusted to bring into line with ppt2	
Model 3b, 3	3	50	469	197	4.9		90	177.3	0.135	0.088	50	high	2	Good record	
Model 3b, 3	3	50	528	220	6.5		66	145.2	0.127	0.083	50	high	11	Clearly reached limit	
Model 3b, 3	3	50	385	164	19.7		90	147.6	0.144	0.093	50	high	1	Just reached limit	
Model 3c, 1	1	50	457	194	4.3	1.0	100	194	0.225	0.146	50	*	30	Excellent, exactly 100%, less than 1 cycle to 50% query amplitude	5/5/98, Ref 7
Model 3c, 1	1	50	468	196	4.1	1.2	100	196	0.228	0.148	50	*	31	Excellent, again exactly 100%	525mm depth
Model 3c, 1	1	50	524	222	4.2	1.2	95	210.9	0.216	0.141	50	*	10	Excellent	49% loose, 79% dense
Model 3c, 1	1	50	296	130	17.6	2.2	87	113.1	0.247	0.161	75	high	11	Limit rises slowly	
Model 3c, 1	1	50	320	129	14.9	1.9	90	116.1	0.268	0.174	75	high	16	Limit rises slowly	
Model 3c, 1	1	50	382	160	7.5	1.2	100	160	0.243	0.158	75	high	15	Rapid rise time, liquefaction could be affected by loose layer below	
Model 3c, 1	1	50	115	53.5	5.4	2.1	84	44.94	0.3	0.195	75	high	5	Clear limit, noisy record affects 50%	
Model 3c, 1	1	50	123	54	6.8	1.9	96	51.84	0.315	0.205	75	high	2	Clear limit, noisy record affects 50%	
Model 3c, 1	1	50	252	100	9.5	1.7	96	96	0.296	0.192	75	high	1	Limit rises slowly affects 50%	
Model 3c, 2	2	50	457	194	6.5		98	190.12	0.218	0.142	50	high	30	Rapid rise to 90% +	
Model 3c, 2	2	50	468	196	5.7		96	188.16	0.221	0.143	50	high	31	Very rapid rise to 90% +	
Model 3c, 2	2	50	524	222	12.0		92	204.24	0.209	0.136	50	med	10	First limit reached at 82%, then rose to 92%	

Model 3c, 2	2	50	296	130	37.8		90	117	0.239	0.156	76	low	11	Still climbing slowly at end of shaking	
Model 3c, 2	2	50	320	129	36.8		92	118.68	0.26	0.169	75	low	16	Still climbing slowly at end of shaking	
Model 3c, 2	2	50	382	160	21.6		100	160	0.235	0.153	75	high	15	Reached limit, probably influenced by loose layer below	
Model 3c, 2	2	50	115	53.5	24.3		77	41.195	0.29	0.189	75	high	5	Clear limit, noisy record	
Model 3c, 2	2	50	123	54	32.4		83	44.82	0.305	0.198	75	high	2	Clear limit, noisy record	
Model 3c, 2	2	50	252	100	31.1		95	95	0.286	0.186	75	high	1	Close to 100% at end of shaking	
Model 3c, 3	3	50	457	194	8.1		97	188.18	0.207	0.134	50	high	30	Rapid rise to 90% +	
Model 3c, 3	3	50	468	196	7.6		98	192.08	0.209	0.136	50	high	31	Very rapid rise to 90% +	
Model 3c, 3	3	50	524	222	15.3		95	210.9	0.199	0.129	50	med	10	Again, double stage rise, as eq2	
Model 3c, 3	3	50	296	130	44.3		92	119.6	0.227	0.148	75	low	11	Still climbing slowly at end of shaking	
Model 3c, 3	3	50	320	129	45.9		93	119.97	0.246	0.16	75	low	16	Still climbing slowly at end of shaking	
Model 3c, 3	3	50	382	160	22.7		100	160	0.223	0.145	75	high	15	Probably influenced by loose layer below	
Model 3c, 3	3	50	115	53.5	24.3		76	40.66	0.275	0.179	75	high	5	Clear limit, noisy record	
Model 3c, 3	3	50	123	54	23.0		82	44.28	0.29	0.188	75	high	2	Clear limit, noisy record	
Model 3c, 3	3												1	Still rising at end of shaking	
Model 3d, 1	1	125	434	226	8.6	4.9	63	142.38	0.147	0.09	54	*	48	Excellent	3/9/98, Ref 11
Model 3d, 1	1	125	515	245	17.6	4.9	78	191.1	0.147	0.095	54	med	37	Slow buildup makes definition of limit difficult	525mm depth
Model 3d, 1	1	125	522	243	12.4	3.4	75	182.25	0.149	0.097	54	high	35	Slow buildup makes definition of limit difficult	54% loose, 80% dense
Model 3d, 1	1	125	434	223	7.9	4.2	65	144.95	0.141	0.092	54	*	40	Excellent, cycles affect 50%	
Model 3d, 1	1												38	Still climbing at end of shaking	
Model 3d, 1	1												44	Still climbing at end of shaking	
Model 3d, 2	2	125	523	283	14.8		70	198.1	0.163	0.106	54	high	37	Rapid rise to 60%, then slow climb	
Model 3d, 2	2	125	522	273	11.8		73	199.29	0.169	0.11	54	high	35	Rapid rise to 60%, then slow climb	
Model 3d, 2	2												48	Still climbing slowly at end of shaking	
Model 3d, 2	2												40	Still climbing at end of shaking	
Model 3d, 2	2												38	Still climbing at end of shaking	
Model 3d, 2	2												44	Still climbing at end of shaking	
Model 3d, 3	3	125	523	283	8.0		70	198.1	0.168	0.109	54	high	37	Good record	
Model 3d, 3	3	125	522	273	8.5		75	204.75	0.174	0.113	54	high	35	Good record	
Model 3d, 3	3												48	Still climbing slowly at end of shaking	
Model 3d, 3	3												40	Still climbing at end of shaking	
Model 3d, 3	3												38	Still climbing at end of shaking	
Model 3d, 3	3												44	Still climbing at end of shaking	
Model 3d, 4	4	125	508	268	28.6		72	192.96	0.182	0.118	54	high	37	Two stage rise	
Model 3d, 4	4	125	522	273	27.2		70	191.1	0.184	0.12	54	high	35	Two stage rise	
Model 3d, 4	4	125	435	257	28.1		62	159.34	0.171	0.111	54	high	48	Clear limit	
Model 3d, 4	4	125	438	257	25.9		61	156.77	0.172	0.112	54	high	40	Clear limit	
Model 3d, 4	4												38	Still climbing at end of shaking	
Model 3d, 4	4												44	Still climbing at end of shaking	
Model 3e, 1	1	50	521	235	10.9		100	235	0.652	0.424	50	*	35	Classic rise to 100%, some cycling at limit	3/10/01, Ref 35
Model 3e, 1	1	50	369	170							75		39	Noisy, no clear limit, steady rise	525mm depth
Model 3e, 1	1	50	239	239							75		43	u/s	50% loose, 75% dense
Model 3e, 1	1	50	359	359							50		48	u/s	No surcharge on flight 1
Model 3e, 1	1	50	231	105	21.2		88	92	0.828	0.538	75	*	56	Classic response to near 100%	50g
Model 3e, 1	1	50	108	67	18.8		85	57	0.716	0.465	75	high	57	Good rsponse, slightly noisy	See also Model 5g
Model 3f, 1	1	100	471	191	9.4		93	178	0.341	0.222	50	*	35	Classis rise to limit near 100%, noisy	16/10/01, Ref 37
Model 3f, 1	1	100	394	426							50		39	Static pore pressure u/s	262mm depth
Model 3f, 1	1	100	316	131							75		56	Steady climb	50% loose, 75% dense
Model 3f, 1	1	100	375	169	4.1		54	91	0.327	0.213	75	high	57	Quick rise to early limit, flat then slow climb	No surcharge
															100g
Model 4a, 1	1	50	477	347	24.8	14.0	80	278	0.078	0.051	49	high	45	Clearly reached upper limit	14/9/98, Ref 12

Model 4a, 1	1	50	483	348	26.7	22.1	75	261	0.078	0.051	49	high	35	Clearly reached upper limit	525mm depth
Model 4a, 1	1												52	Still climbing at end of shaking	49% loose, 80% dense
Model 4a, 1	1												43	Still climbing at end of shaking	
Model 4a, 2	2	50	469	339	40		27	91.53	0.098	0.064	49	med	45	Reached some sort of limit, much less than eq1	
Model 4a, 2	2	50	474	340	40		16	54.4	0.098	0.064	49	med	35	Reached some sort of limit, much less than eq1	
Model 4a, 2	2												52	Still climbing at end of shaking	
Model 4a, 2	2												43	Still climbing at end of shaking	
Model 4a, 3	3												45	Very little excess pore pressure generated	
Model 4a, 3	3												35	Very little excess pore pressure generated	
Model 4a, 3	3												52	Very little excess pore pressure generated	
Model 4a, 3	3												43	Very little excess pore pressure generated	
Model 4a, 4	4												45	No excess pore pressure at all	
Model 4a, 4	4												35	No excess pore pressure at all	
Model 4a, 4	4												52	No excess pore pressure at all	
Model 4a, 4	4												43	No excess pore pressure at all	
Model 4b, 1	1												39	Very noisy signal, minimal excess pore pressure	15/9/98, Ref 13
Model 4b, 1	1												40	Very noisy signal, minimal excess pore pressure	525mm depth
Model 4b, 1	1												44	Very noisy signal, minimal excess pore pressure	56% loose, 74% dense
Model 4b, 2	2	125	465	369	24.4		85	313.65	0.165	0.107	56	low	39	Clear limit, surprising after eq1	
Model 4b, 2	2												40	Climbing at end of earthquake	
Model 4b, 2	2												44	Climbing at end of earthquake	
Model 4b, 3	3												39	No excess pore pressure at all	
Model 4b, 3	3												40	Almost no excess pore pressure	
Model 4b, 3	3												44	Climbing at end of earthquake	
Model 4b, 4	4												39	No excess pore pressure at all	
Model 4b, 4	4												40	Almost no excess pore pressure	
Model 4b, 4	4												44	Almost no excess pore pressure	
Model 4c, 1	1	50	808	533	19.5	13.338	60	319.8	0.073	0.048	50	high	51	Good record : (6 other ppts in upper layer showed	22/10/98, Ref 17
Model 4c, 1	1	50	806	534	20.6	15.903	59	315.06	0.073	0.048	50	high	38	Good record : no response in any Model 4c eq)	525mm depth
Model 4c, 1	1												47	Still climbing at end of shaking	50% loose, 75% dense
Model 4c, 1	1												46	Still climbing at end of shaking	292 lb surcharge
Model 4c, 1	1												50	Still climbing at end of shaking	
Model 4c, 1	1												41	Still climbing at end of shaking	
Model 4c, 2	2												51	Still climbing at end of shaking	
Model 4c, 2	2												38	Still climbing at end of shaking	
Model 4c, 2	2												47	Still climbing at end of shaking	
Model 4c, 2	2												46	Still climbing at end of shaking	
Model 4c, 2	2												50	Still climbing at end of shaking	
Model 4c, 2	2												41	Still climbing at end of shaking	
Model 4c, 3	3												51	Still climbing at end of shaking	
Model 4c, 3	3												38	Still climbing at end of shaking	
Model 4c, 3	3												47	Still climbing at end of shaking	
Model 4c, 3	3												46	Still climbing at end of shaking	
Model 4c, 3	3												50	Still climbing at end of shaking	
Model 4c, 3	3												41	Still climbing at end of shaking	
Model 4c, 4	4												51	Almost no excess pore pressure	
Model 4c, 4	4												38	Almost no excess pore pressure	
Model 4c, 4	4												47	Almost no excess pore pressure	
Model 4c, 4	4												46	Almost no excess pore pressure	
Model 4c, 4	4												50	Almost no excess pore pressure	
Model 4c, 4	4												41	Almost no excess pore pressure	

Model 4d, 1	1	125	813	543	11.9	47	255.21	0.079	0.051	50	high	38	Excellent : (6 ppts in upper layer showed	4/11/98, Ref 18
Model 4d, 1	1	125	813	543	12.42	48	260.64	0.079	0.051	50	high	51	Excellent : almost no response in any 4d eq)	525mm depth
Model 4d, 1	1											47	Climbing at end of earthquake	50% loose, 68% dense
Model 4d, 1	1											46	Climbing at end of earthquake	292 lb surcharge
Model 4d, 1	1											50	Still climbing at end of shaking	
Model 4d, 1	1											41	Still climbing at end of shaking	
Model 4d, 2	2	125	813	543	12.4	44	238.92	0.085	0.055	50	high	38	Good record	
Model 4d, 2	2	125	813	543	11.8	45	244.35	0.085	0.055	50	high	51	Good record	
Model 4d, 2	2											47	Climbing at end of earthquake	
Model 4d, 2	2											46	Climbing at end of earthquake	
Model 4d, 2	2											50	Still climbing slowly at end of shaking	
Model 4d, 2	2											41	Still climbing slowly at end of shaking	
Model 4d, 3	3	125	813	543	47	37	200.91	0.083	0.054	50	med	38	Possible limit at end of shaking	
Model 4d, 3	3	125	813	543	47	38	206.34	0.083	0.054	50	med	51	Possible limit at end of shaking	
Model 4d, 3	3											47	Climbing at end of earthquake	
Model 4d, 3	3											46	Climbing at end of earthquake	
Model 4d, 3	3	125	739	515	37.9	41	211.15	0.083	0.054	50	high	50	Appears to reach limit near end of shaking	
Model 4d, 3	3	125	741	512	36	41	209.92	0.083	0.054	50	high	41	Appears to reach limit near end of shaking	
Model 4d, 4	4											38	Still climbing at end of shaking	
Model 4d, 4	4											51	Still climbing at end of shaking	
Model 4d, 4	4											47	Climbing at end of earthquake	
Model 4d, 4	4											46	Climbing at end of earthquake	
Model 4d, 4	4											50	Still climbing at end of shaking	
Model 4d, 4	4											41	Still climbing at end of shaking	
Model 4e, 1	1	50	738	430	20.2	87	374	0.439	0.285	50	*	39	Excellent early response	14/7/00, Ref 24
Model 4e, 1	1	50	648	415	30.6	77	320	0.416	0.270	50	high	38	Classic rise to near 100%	525mm depth
Model 4e, 1	1	50	505	337								50	Steady climb throughout duration	50% uniform density
Model 4e, 1	1	50	586	353	13.1	74	261	0.464	0.302	50	high	46	Rapid rise to early limit, slight increase later	211 lb surcharge
Model 4e, 1	1	50	439	310								6	Steady climb throughout duration	50, 80,100, 125g
Model 4e, 1	1	50	500	346								54	Steady climb throughout duration	
Model 4f, 1	1	50	313	267							low	1	No significant excess pore pressure	2/8/00, Ref 25
Model 4f, 1	1	50	220	220								8	u/s	525 mm depth
Model 4f, 1	1	50	573	371	8.9	21	78	0.178	0.116	55	high	10	Quick rise to early limt, then flat	Densities uncertain
Model 4f, 1	1	50	555	555								16	u/s	211 lb surcharge
Model 4f, 1	1	50	728	445	12.4	89	396	0.173	0.112	55	*	38	Excellent response, absolutely flat limit	50, 80, 100, 125g
Model 4f, 1	1	50	472	379	9.5	24	91	0.15	0.098	55	med	39	Quick rise to limit, very noisy	Average RD = 54.7%
Model 4f, 1	1	50	431	431								14	u/s	
Model 4f, 1	1	50	424	314	13.6	17	53	0.171	0.111	55	high	41	Quick rise to limit, then flat	
Model 4f, 1	1	50	335	237							low	48	Very noisy	
Model 4f, 1	1	50	647	407	8.3	17	69	0.176	0.114	55	high	54	Quick rise to limit, then steady climb	
Model 4g, 1	1	50	698	342	8.1	101	345	0.273	0.177	50	*	53	Excellent early response, slight rise later	5,7/8/00, Ref 26
Model 4g, 1	1	50	562	383	4	19	73	0.206	0.134	50	high	43	Clear early limit, flat then long rise	525mm depth
Model 4g, 1	1	50	670	385	6.9	78	300	0.233	0.151	50	high	37	Good early rise to limit, then slow rise later	50% uniform density
Model 4g, 1	1	50	508	336	6.9	15	50	0.221	0.144	50	high	6	Good early rise to limit, then steady rise later	50, 80, 100, 125g
Model 4g, 1	1	50	751	403	10.4	81	326	0.24	0.156	50	high	35	Good early rise to limit, then slow climb, noisy	
Model 4g, 1	1	50	248	220							low	13	Rise, drop and rise	
Model 4g, 1	1	50	505	338	7.5	14	47	0.219	0.142	50	high	42	Good early rise, flat then steady climb	
Model 4g, 1	1	50	450	291	6.4	12	35	0.237	0.154	50	high	50	Good early rise, flat then steady climb	
Model 4g, 1	1	50	330	247								46	No significant excess pore pressure	
Model 4h, 1	1	50	631	446	31.5	81	361	0.183	0.119	48	high	43	Steady convex rise to limit	23/8/00, Ref 27
Model 4h, 1	1	50	511	335	6.7	20.6	69	0.216	0.140	51	high	53	Quick rise to early limit, drop and then steady rise to end	525mm depth

Model 4h, 1	1	50	571	381	7.3		36	137	0.203	0.132	48 high	13	Quick rise to early limit, flat and then steady rise to end	211 lb surcharge
Model 4h, 1	1	50	432	317	10.1		20	63	0.202	0.131	51 high	50	Quick rise to limit	50% uniform density
Model 4h, 1	1	50	607	625								8	u/s	50, 80, 100, 125g
Model 4h, 1	1	50	219	229	14		34	78	0.172	0.112	51 med	10	Quick rise to limit, then steady fall	
Model 4h, 1	1	50	711	457	31.5		86	393	0.194	0.126	48 high	35	Rapid initial rise, then steady climb	
Model 4h, 1	1	50	624	452	29.8		88	398	0.179	0.116	48 med	48	Good but slow rise to high limit	
Model 4h, 1	1	50	322	263	11.2		10.6	28	0.199	0.129	51 med	41	Noisy, but clear limit, then slow rise	
Model 4h, 1	1	50	497	354	11.2		15	53	0.199	0.129	51 med	42	Clear limit, then flat and long steady rise	
Model 4i, 1	1	50	242	237							50 med	6	No excess pore pressure	25/8/00, Ref 28
Model 4i, 1	1	50	659	402	13.1		59	237	0.21	0.137	50 high	46	Good limit, held for about 0.2 sec before rising again	525mm depth
Model 4i, 1	1	50	431	452								38	u/s	211 lb surcharge
Model 4i, 1	1	50	656	407	13.7		68	277	0.206	0.134	50 high	39	Clear limit	50% uniform density
Model 4i, 1	1	50	574	370	8.7		39	144	0.208	0.135	50 high	54	Clear limit	50, 80, 100, 125g
Model 4i, 1	1	50	502	343	10.9		21	72	0.205	0.133	50 high	8	Clear limit	
Model 4i, 1	1	50	320	264	8.4		8	21	0.195	0.127	50 med	1	Very noisy, but clear limit	
Model 4i, 1	1	50	720	437								37	No limit, steady rise to 300kpa plus	
Model 4i, 1	1	50	376	401								14	u/s	
Model 4j, 1	1	50	593	342	8.6		76	260	0.251	0.163	50 high	48	Limit held for 0.2 secs before rising again	8/9/00, Ref 29
Model 4j, 1	1	50	445	296	4.5		35	104	0.238	0.155	50 high	54	Limit held for about 0.1 secs before rising	525mm depth
Model 4j, 1	1	50	518	323	11.2		40.6	131	0.242	0.157	50 high	43	Limit held for about 0.1 secs before rising	211 lb surcharge
Model 4j, 1	1	50	330	244								6	No clear early limit, but steady rise	50% uniform density
Model 4j, 1	1	50	333	240								46	No clear early limit, but steady rise	50, 80, 100, 125g
Model 4j, 1	1	50	670	390	15.9		87	339	0.237	0.154	50 high	37	Note 70% at 4.1 cycles, rising to 97% at 42.6 cycles	
Model 4j, 1	1	50	736	412	36		83	342	0.238	0.155	50 high	35	Sharp early rise, then slow rise to final limit	
Model 4j, 1	1	50	238	211	15.6		8.2	17	0.214	0.139	50 high	42	Pretty much constant over the duration	
Model 4j, 1	1	50	669	387	83		27.1	105	0.239	0.155	50 high	39	Sharp early rise to 50% plus, then slow rise to limit	
Model 4j, 1	1	50	519	317	29		4.4	14	0.248	0.161	50 high	50	Limit at 29%, but then rose steadily later	
Model 4k, 1	1	50	232	91	21		108	98	0.401	0.261	48 high	41	Very rapid rise to c. 60% then slower rise to 100%	14/9/00, Ref 30
Model 4k, 1	1	50	447	193	14		90	174	0.299	0.194	50 high	10	Rise to 80% in 5.1 cycles, then slower rise to 90/100%	525 mm depth
Model 4k, 1	1	50										16	u/s	No surcharge
Model 4k, 1	1	50	521	226	16.4		88	199	0.284	0.185	50 high	1	Steady rise to 88/100%	50% uniform density
Model 4k, 1	1	50	455	179	4.9		100	179	0.328	0.213	50 *	13	Straight to 100% exactly	50, 80, 100, 125g
Model 4k, 1	1	50	313	109	7		82	89	0.42	0.273	48 high	53	Straight to 82%, then later to 130%	
Model 4k, 1	1	50	298	131	26.3		87	114	0.332	0.216	48 high	8	Rise to 60% in 5 cycles, then slower rise to 90/100%	
Model 4k, 1	1	50	38	15	13		106	16	0.581	0.378	48 high	46	Very noisy, but straight to 100%	
Model 4k, 1	1	50	113	50	20		80	40	0.423	0.275	48 high	42	Good steady rise to high limit	
Model 4l, 1	1	50	510	388	32		21	81	0.62	0.403	54 med	53	Initial limit, but noisy and slowly continued to climb	15/2/01, Ref 33
Model 4l, 1	1	50	394	339								46	Steady climb	525 mm depth
Model 4l, 1	1	50	813	515								37	Steady climb	295 lb surcharge
Model 4l, 1	1	50	648	446	52		18	80	0.631	0.410	54 med	43	Initial good rise, then upper limit reached very slowly	Densities uncertain
Model 4l, 1	1	50	732	481								48	Steady climb	Average used here
Model 4l, 1	1	50	582	418	25		16	67	0.628	0.408	54 med	41	Good upper limit	
Model 4l, 1	1	50	732	481								39	Noisy, steady climb	
Model 4l, 1	1	50	813	515								35	Noisy, steady climb	
Model 5a, 1	1	50	1101	823	13.9	14.067	50	411.5	0.055	0.036	51 high	51	Shows double frequencies : (note upper 4 ppts showed minimal	7/10/98, Ref 15
Model 5a, 1	1	50	1105	825	15	13.419	50	412.5	0.055	0.036	51 high	38	Shows double frequencies : dynamic response) only just reached 50%	525mm depth
Model 5a, 1	1	50	1040	797	34		30	239.1	0.055	0.036	51 low	41	Still climbing slowly at end of shaking	586 lb surcharge
Model 5a,1	1	50	1038	797	34		31	247.07	0.055	0.036	51 low	50	Still climbing slowly at end of shaking	51% loose, 72% dense
Model 5a, 1	1											13	Still climbing at end of shaking	
Model 5a, 1	1											11	Still climbing at end of shaking	
Model 5a, 1	1											47	Still climbing at end of shaking	

Model 5a, 1	1										46	Still climbing at end of shaking	
Model 5a, 2	2	50	1113	824	30.9	41	337.84	0.056	0.036	51 high	51	Reaches limit showing double frequency behaviour	
Model 5a, 2	2	50	1113	825	30.9	39	321.75	0.056	0.036	51 high	38	Note strong double frequency behaviour	
Model 5a, 2	2	50	1044	799	35	24	191.76	0.056	0.036	51 med	41	Just reached limit	
Model 5a, 2	2	50	1047	805	35	26	209.3	0.055	0.036	51 med	50	Just reached limit	
Model 5a, 2	2										13	Still climbing at end of shaking	
Model 5a, 2	2										11	Still climbing at end of shaking	
Model 5a, 2	2										47	Still climbing at end of shaking	
Model 5a, 2	2										46	Still climbing at end of shaking	
Model 5a, 3	3										51	Still climbing slowly at end of shaking	
Model 5a, 3	3										38	Still climbing slowly at end of shaking	
Model 5a, 3	3										41	Still climbing at end of shaking	
Model 5a, 3	3										50	Still climbing at end of shaking	
Model 5a, 3	3										13	Still climbing at end of shaking	
Model 5a, 3	3										11	Still climbing at end of shaking	
Model 5a, 3	3										47	Still climbing at end of shaking	
Model 5a, 3	3										46	Still climbing at end of shaking	
Model 5a, 4	4										51	Very small excess pore pressure, still climbing at end	
Model 5a, 4	4										38	Very small excess pore pressure, still climbing at end	
Model 5a, 4	4										41	Still climbing at end of shaking	
Model 5a, 4	4										50	Still climbing at end of shaking	
Model 5a, 4	4										13	Almost no excess pore pressure	
Model 5a, 4	4										11	Almost no excess pore pressure	
Model 5a, 4	4										47	Still climbing at end of shaking	
Model 5a, 4	4										46	Still climbing at end of shaking	
Model 5b, 1	1	50	1118	830	20	33	273.9	0.068	0.044	49 high	51	Reaches limit which rises slowly : (note 6 ppts in upper layer showed	14/9/98, Ref 16
Model 5b, 1	1	50	1119	830	18.25	34	282.2	0.068	0.044	49 high	38	Reaches limit which rises slowly : no dynamic excess pore pressure)	525mm depth
Model 5b, 1	1										47	Very little excess pore pressure	586 lb surcharge
Model 5b, 1	1										46	Very little excess pore pressure	49% loose, 76% dense
Model 5b, 1	1	50	1043	801							50	Rising steadily at end of shaking	125, then 50g
Model 5b, 1	1	50	1042	799							41	Rising steadily at end of shaking	
Model 5b, 2	2										51	Rising steadily at end of shaking	
Model 5b, 2	2										38	Rising steadily at end of shaking	
Model 5b, 2	2										47	Rising steadily at end of shaking	
Model 5b, 2	2										46	Rising steadily at end of shaking	
Model 5b, 2	2										50	Rising steadily at end of shaking	
Model 5b, 2	2										41	Rising steadily at end of shaking	
Model 5b, 3	3										51	Small excess pore pressure, rising steadily at end of shaking	
Model 5b, 3	3										38	Small excess pore pressure, rising steadily at end of shaking	
Model 5b, 3	3										47	Small excess pore pressure, rising steadily at end of shaking	
Model 5b, 3	3										46	Small excess pore pressure, rising steadily at end of shaking	
Model 5b, 3	3										50	Almost no excess pore pressure, slight rise at end of shaking	
Model 5b, 3	3										41	Almost no excess pore pressure, slight rise at end of shaking	
Model 5b, 4	4										51	Very little excess pore pressure	
Model 5b, 4	4										38	Very little excess pore pressure	
Model 5b, 4	4										47	Almost no excess pore pressure	
Model 5b, 4	4										46	Almost no excess pore pressure	
Model 5b, 4	4										50	Very little excess pore pressure	
Model 5b, 4	4										41	Very little excess pore pressure	
Model 5c, 1	1										46	Almost no excess pore pressure, noisy signal	11/12/98, Ref 19
Model 5c, 1	1										47	Almost no excess pore pressure, noisy signal	525mm depth

Model 5c, 1	1											41	Still climbing at end of shaking	775 lb surcharge
Model 5c, 1	1											50	Still climbing at end of shaking	52% loose, 75% dense
Model 5c, 1	1											38	Starting to climb steeply at end of shaking	50g
Model 5c, 1	1											51	Starting to climb steeply at end of shaking	
Model 5c, 2	2											46	Climbing at end of earthquake	
Model 5c, 2	2											47	Climbing at end of earthquake	
Model 5c, 2	2											41	Climbing at end of earthquake	
Model 5c, 2	2											50	Climbing at end of earthquake	
Model 5c, 2	2											38	Climbing steeply at end of shaking	
Model 5c, 2	2											51	Climbing steeply at end of shaking	
Model 5c, 3	3											46	Climbing at end of earthquake	
Model 5c, 3	3											47	Climbing at end of earthquake	
Model 5c, 3	3	50	1222	974								41	Climbing at end of shaking, but possible flat top just at end	
Model 5c, 3	3	50	1221	975								50	Climbing at end of earthquake	
Model 5c, 3	3	50	1291	1009								38	Climbing steadily at end of shaking	
Model 5c, 3	3	50	1291	1009	28		17	171.53	0.042	0.028	52 low	51	Climbing at end of shaking, but possible flat top just at end	
Model 5d,1	1	50	1223	978	47.3	34.4	33	322.74	0.092	0.06	39 high	31	Filtered acceleration record : (note 6 ppts in upper layer showed	17/12/99, Ref 20
Model 5d,1	1	50	1217	985	37	26.918	35	344.75	0.091	0.059	39 high	43	Filtered acceleration record : no significant response during shaking)	525mm depth
Model 5d,1	1	50	1280	1037	34.4	22.79	52	539.24	0.088	0.047	39 high	39	Filtered acceleration record	775 lb surcharge
Model 5d,1	1											13	Climbing at end of shaking	57% loose, 80% dense
Model 5e, 1	1	50	1125	925								37	Initial limit around 27%, then drift upwards	10/7/00, Ref 23
Model 5e, 1	1	50	1140	900								43	Initial limit around 25%, then drift upwards	525mm depth
Model 5e, 1	1	50	1224	911	31.3		50	456	0.203	0.132	50 high	35	Good response, clear flat top	708 lb surcharge
Model 5e, 1	1	50	1070	851								10	Less than 5%, then steady drift upwards	50% density, assumed
Model 5f, 1	1	50	1012	722	17.6		61	440	0.569	0.370	50 high	35	Good response, with cycles at upper limit	31/8/01, Ref 34
Model 5f, 1	1	50	724									48	u/s	525mm depth
Model 5f, 1	1	50	784									43	u/s	495 lb surcharge
Model 5f, 1	1	50	661									37	u/s	50% loose, 74% dense
Model5f, 1	1	50	865									39	u/s	50g
Model 5g, 1	1	50	1021	712	16.4		74	527	0.247	0.161	48 high	35	Shows strong cyclic behaviour	4/10/01, Ref 35
Model 5g, 1	1	50	870	645	14.5		46.5	300	0.249	0.162	48 med	39	Quite noisy, but clearly limited response	525mm depth
Model 5g, 1	1	50	730									43	u/s	495 lb surcharge on
Model 5g, 1	1	50	850									48	u/s	2nd flight only (eq2)
Model 5g, 1	1	50	733	579	7.9		11.5	67	0.251	0.163	74 med	56	Very low response, with drop after peak	48% loose, 74% dense
Model 5g, 1	1	50	610	540	12.7		8	43	0.239	0.155	74 med	57	Very low response, but clear flat upper limit	50g, 2 flights
Model 5h, 1	1	125	1285	607	14.4		97	589	0.243	0.158	49 high	35	Sharp rise to liquefaction	11/10/01, Ref 36
Model 5h, 1	1	125	733	384								57	Rapid initial rise, then steady climb	525mm depth
Model 5h, 1	1	125	954	374								48	u/s	No surcharge
Model 5h, 1	1	125	554	317								56	Very noisy signal, appears to be climbing	49% loose, 74% dense
Model 5h, 1	1	125	1119	546	13.6		97	530	0.251	0.163	49 high	39	Only marred by uncertain static pore pressure	125g
Model 5i, 1	1	125	597	581								10374	Characterised by falling acceleration input. Depth of phreatic	14/11/01, Ref 39
Model 5i, 1	1	125	737	740								10375	surface probably closer to 390mm deep, rather than the intended	460mm total depth
Model 5i, 1	1	125	473	437								10376	250mm, hence 10374-10378 probably unsaturated.	No surcharge, 64mm
Model 5i, 1	1	125	695	645								10378		50% loose, 75% dense
Model 5i, 1	1	125	803	800	38		32	256	0.115	0.075	50 med	10379	Delayed peak due to redistribution	phreatic surface at
Model 5i, 1	1	125	881	839	16		50	420	0.116	0.075	50 high	56	Good rise to peak	250mm depth, 125g
Model 5i, 1	1	125	934	835	11		64	534	0.122	0.079	50 high	57	Strong rise to peak	

APPENDIX B

SUMMARY OF DATA

Time histories of acceleration, excess pore pressure and model configurations
Stress and strain histories

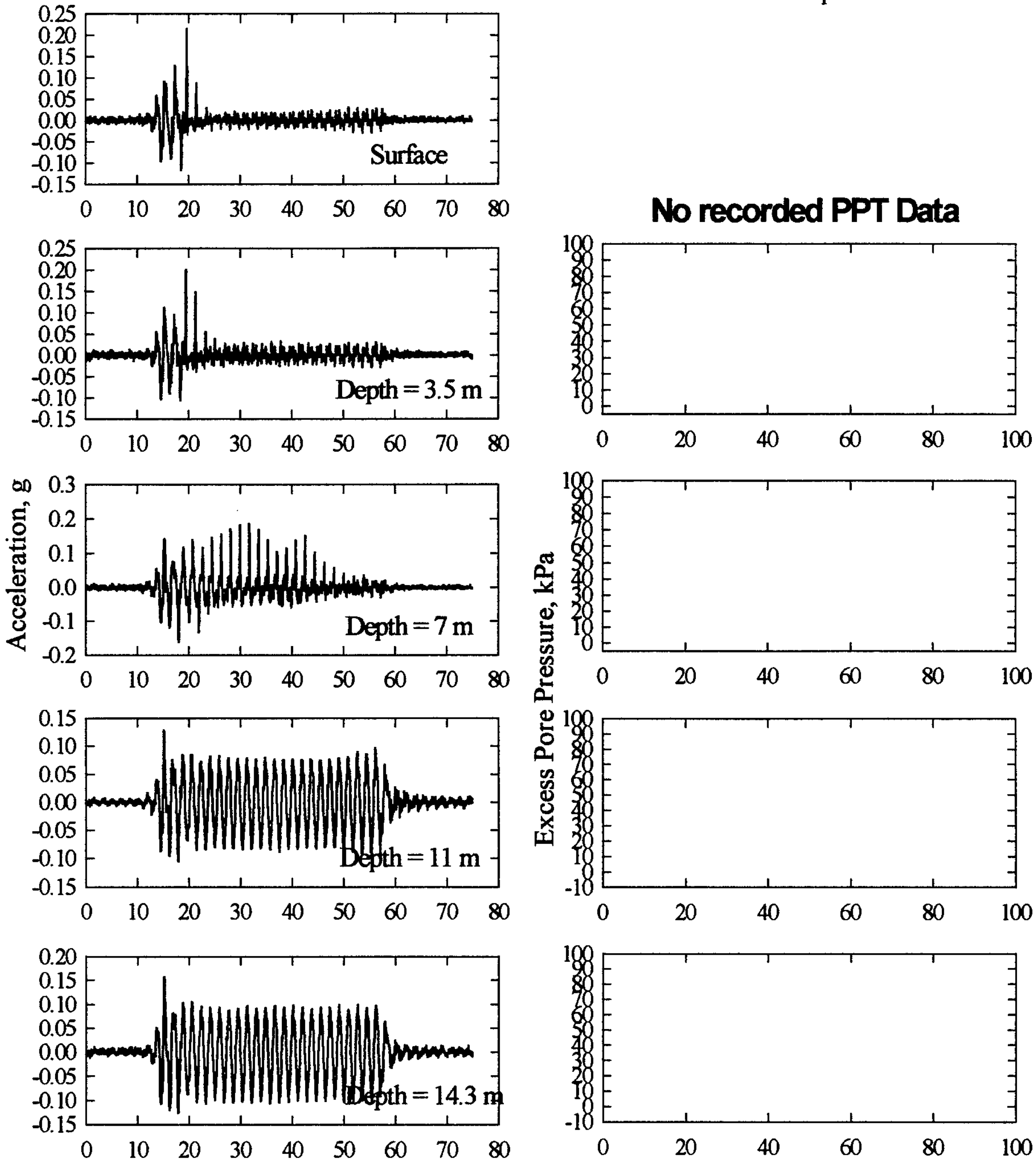
Acceleration, g
Surface
Depth = 3.5 m
Depth = 7 m
Depth = 11 m
Depth = 14.3 m
No recorded PPT Data
Excess Pore Pressure, kPa

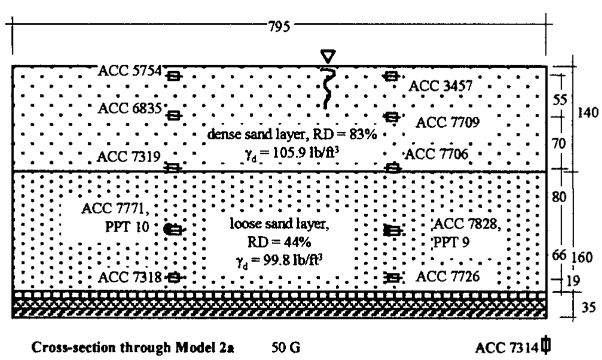
795
ACC 5754
ACC 6835
ACC 7319
ACC 3457
ACC 7709
ACC 7706
dense sand layer, RD = 83%
γ_d = 105.9 lb/ft³
ACC 7771,
PPT 10
ACC 7318
loose sand layer,
RD = 44%
γ_d = 99.8 lb/ft³
ACC 7828,
PPT 9
ACC 7726
55
70
140
80
66
160
19
35
Cross-section through Model 2a
50 G
ACC 7314

Model 2a

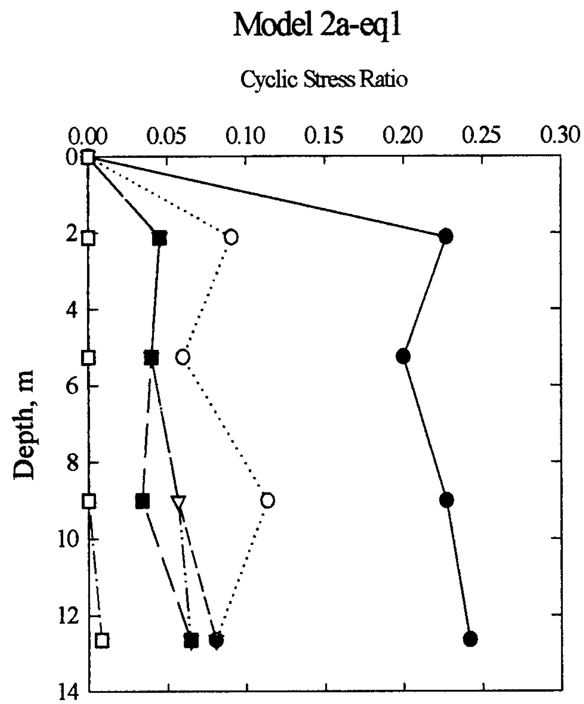

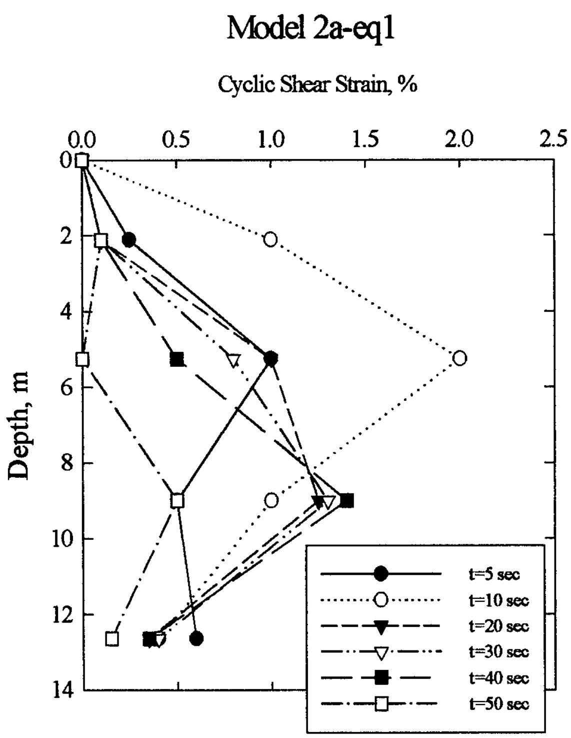

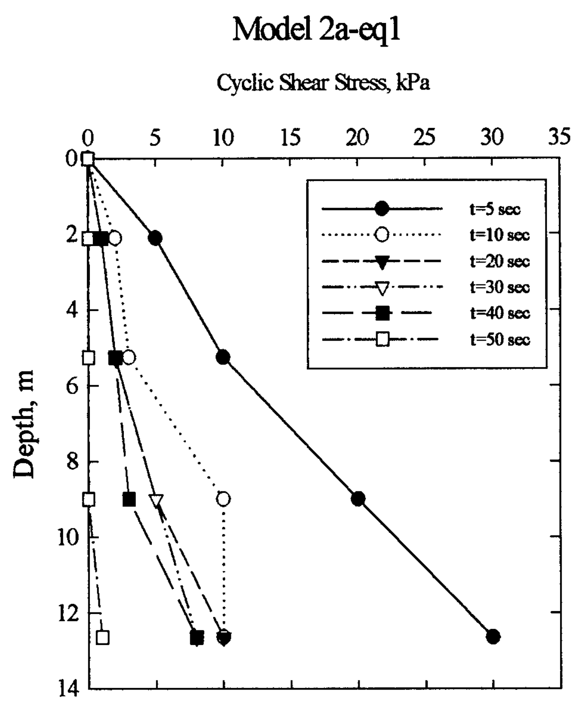

Model 2a Stress and strain isochrones

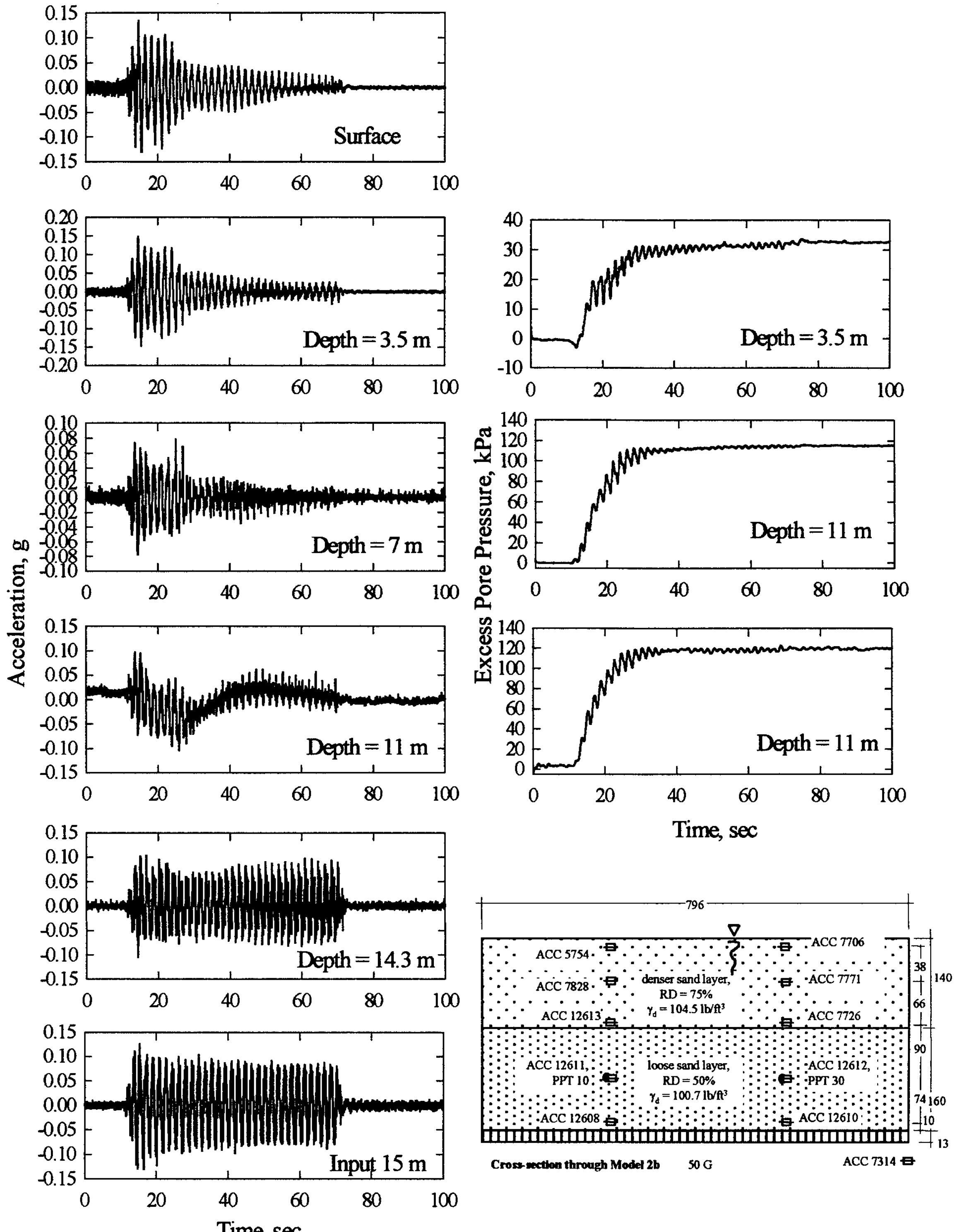
Surface
Depth = 3.5 m
Depth = 7 m
Depth = 11 m
Depth = 14.3 m
Input 15 m
Acceleration, g
Time, sec
Depth = 3.5 m
Depth = 11 m
Depth = 11 m
Excess Pore Pressure, kPa
Time, sec
796
ACC 5754
ACC 7706
ACC 7828
denser sand layer,
RD = 75%
γ_d = 104.5 lb/ft^3
ACC 7771
ACC 12613
ACC 7726
ACC 12611,
PPT 10
loose sand layer,
RD = 50%
γ_d = 100.7 lb/ft^3
ACC 12612,
PPT 30
ACC 12608
ACC 12610
38
66
140
90
74
160
10
13
Cross-section through Model 2b
50 G
ACC 7314

Model 2b

Model 2b-eq1

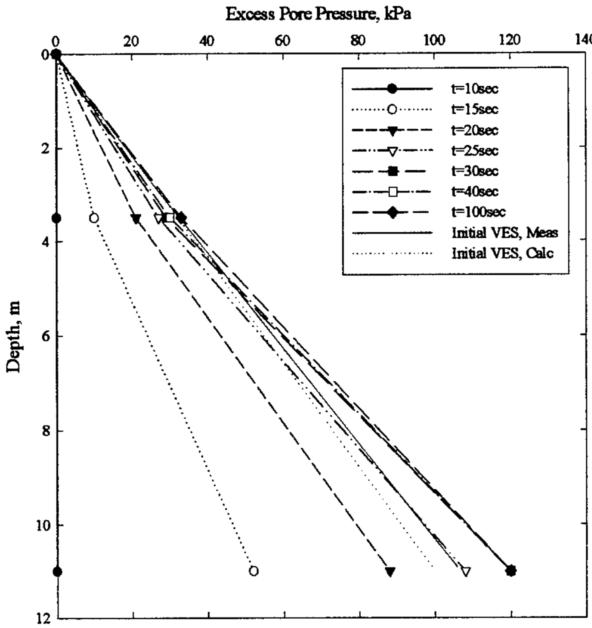

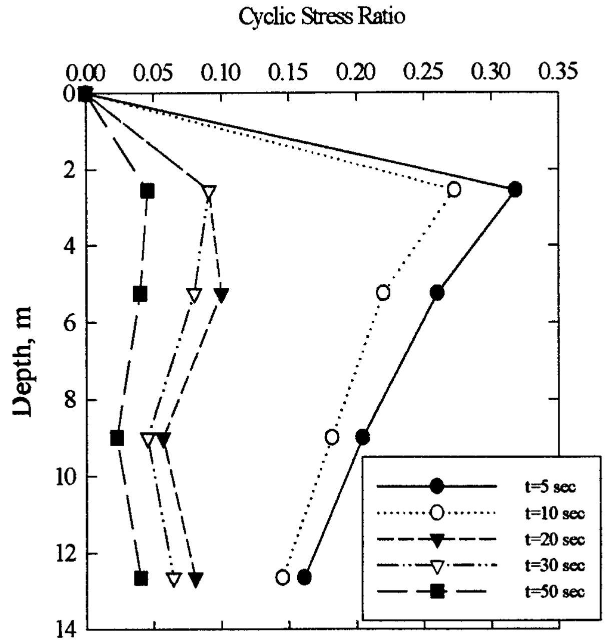

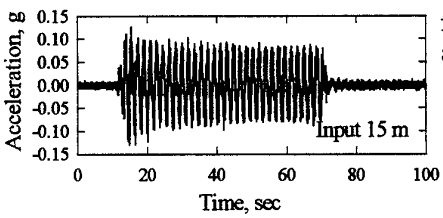

f = 0.6 Hz
a_{max} = 0.08 g

Model 2b-eq1

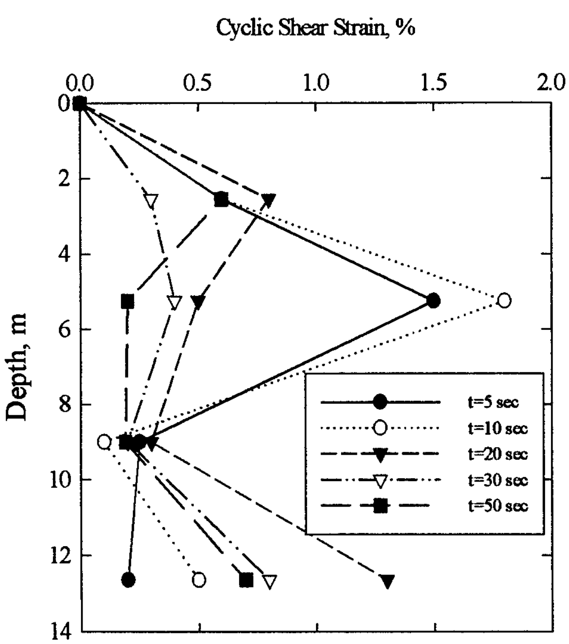

Model 2b-eq1

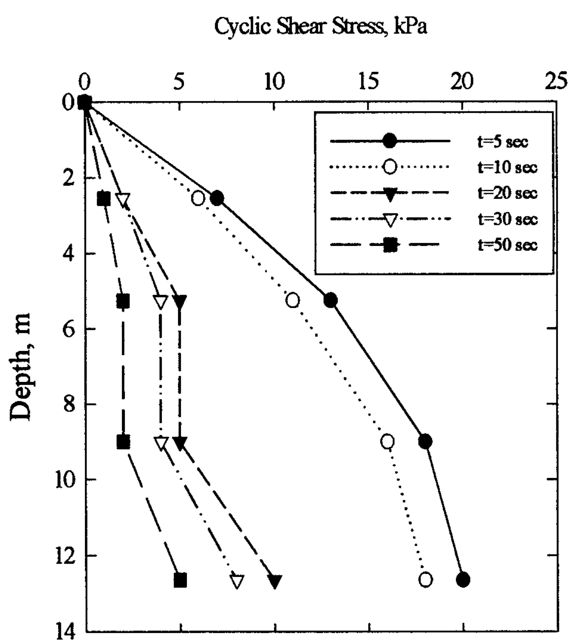

Model 2b Stress and strain isochrones

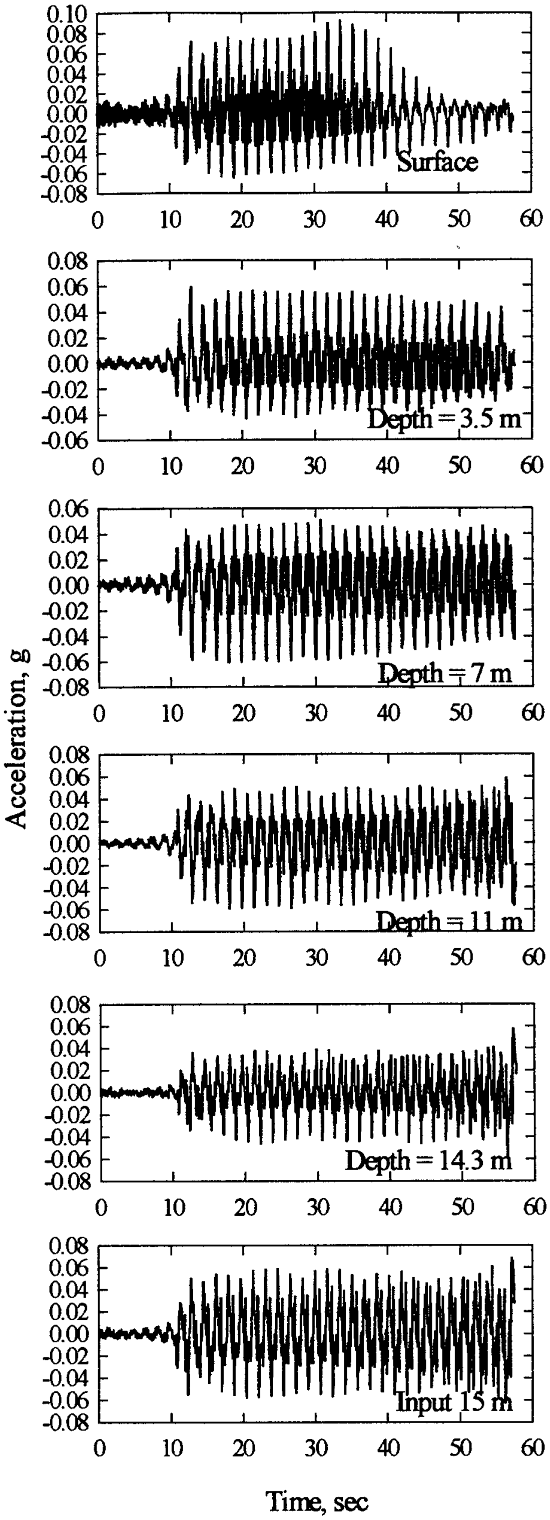

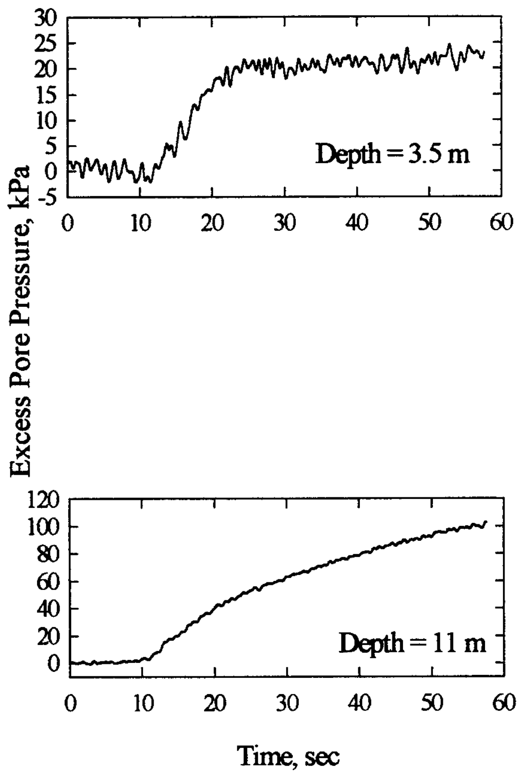

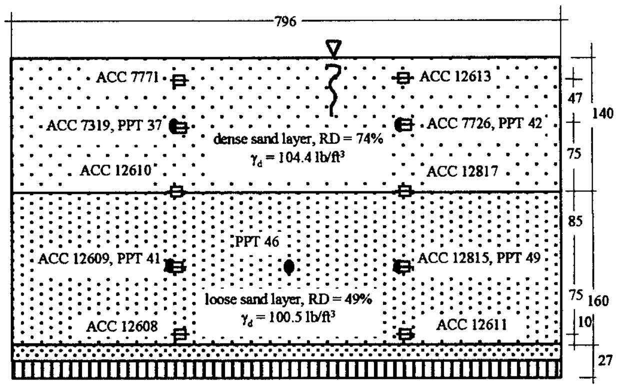

Cross-section through Model 2c 50 G

Model 2c

Model 2c-eq1

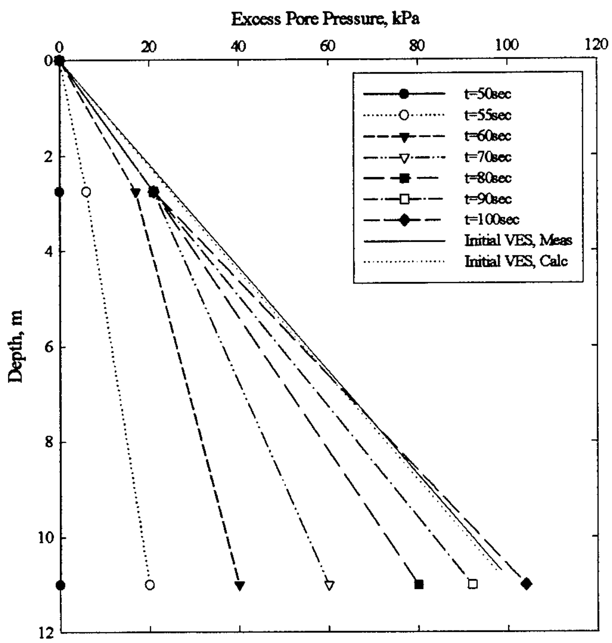

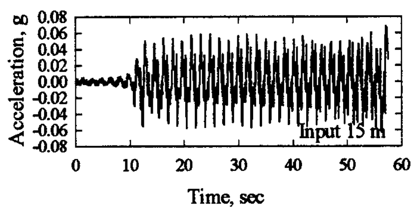

f = 0.6 Hz
a_{max} = 0.06 g

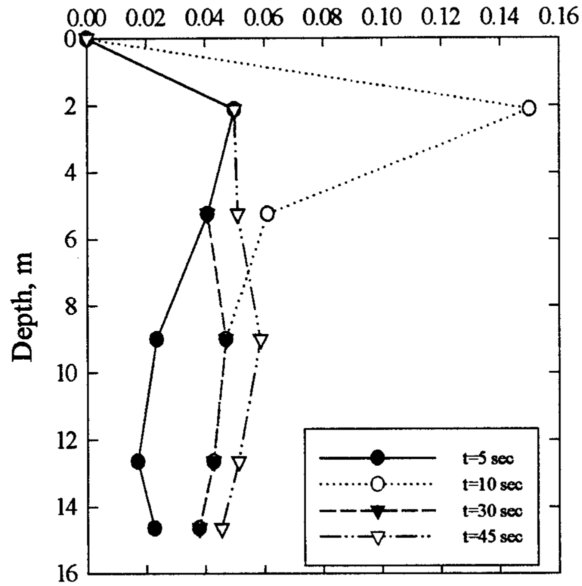

Model 2c-eq1

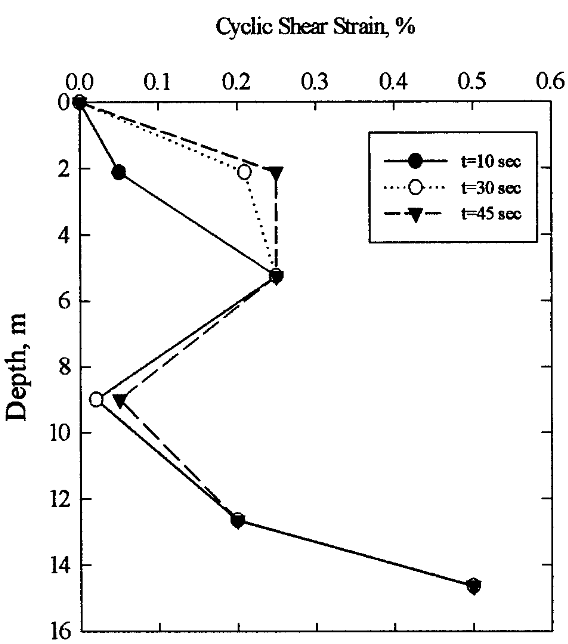

Model 2c-eq1

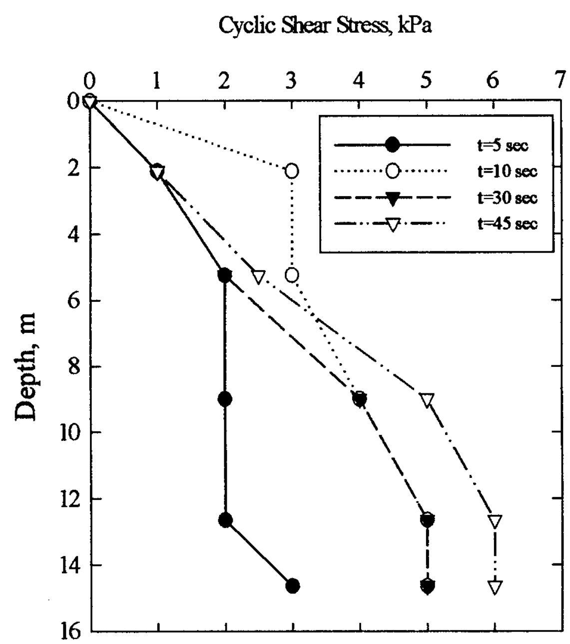

Model 2c Stress and strain isochrones

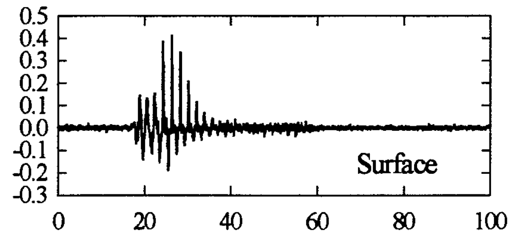
Surface

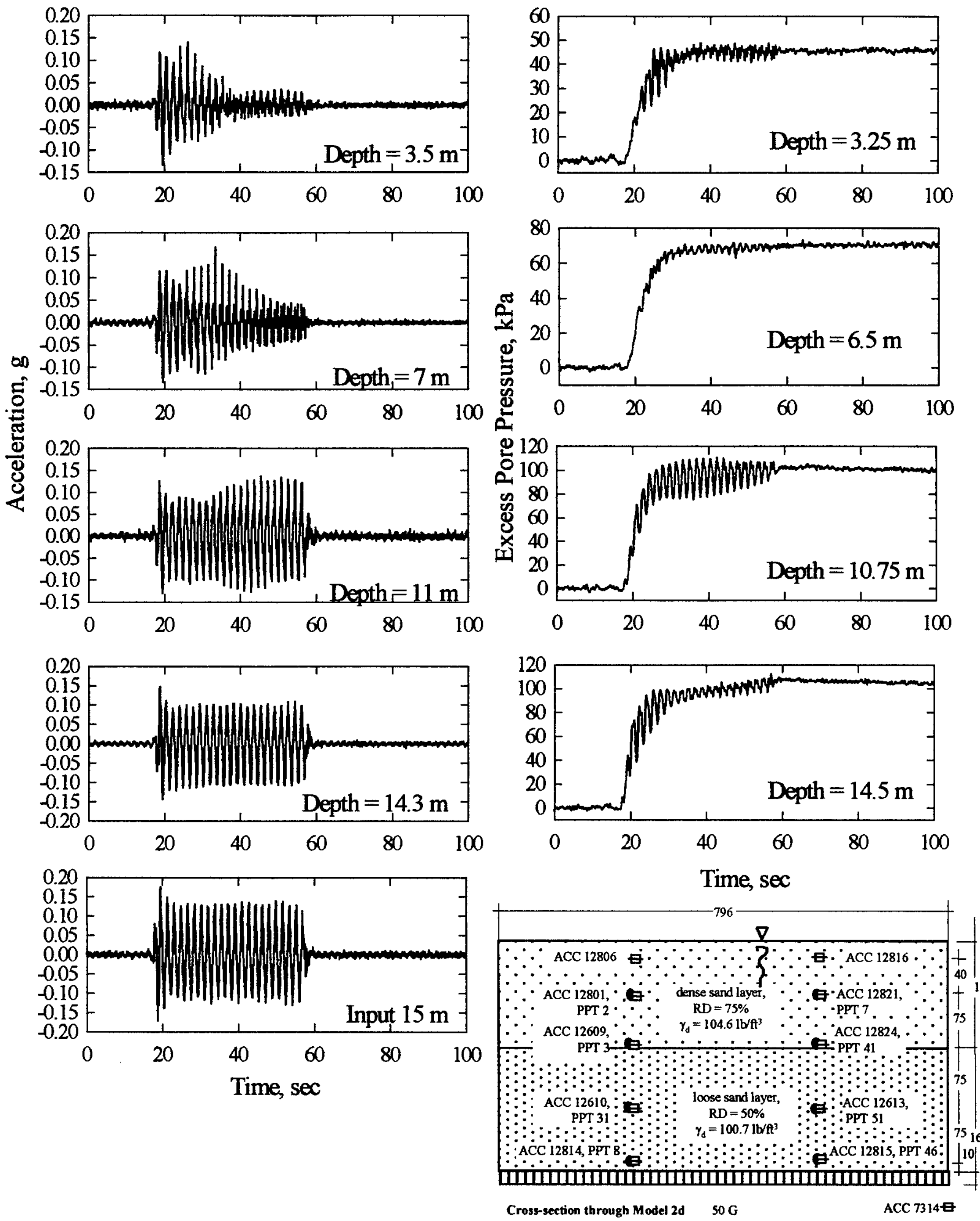
Acceleration, g
Excess Pore Pressure, kPa
Depth = 3.5 m
Depth = 3.25 m
Depth = 7 m
Depth = 6.5 m
Depth = 11 m
Depth = 10.75 m
Depth = 14.3 m
Depth = 14.5 m
Input 15 m
Time, sec
Time, sec
796
ACC 12806
ACC 12816
ACC 12801, PPT 2
dense sand layer, RD = 75%
γd = 104.6 lb/ft³
ACC 12821, PPT 7
ACC 12609, PPT 3
ACC 12824, PPT 41
ACC 12610, PPT 31
loose sand layer, RD = 50%
γd = 100.7 lb/ft³
ACC 12613, PPT 51
ACC 12814, PPT 8
ACC 12815, PPT 46
40
75
140
75
75
160
10
13
Cross-section through Model 2d
50 G
ACC 7314

Model 2d

Model 2d-eq1

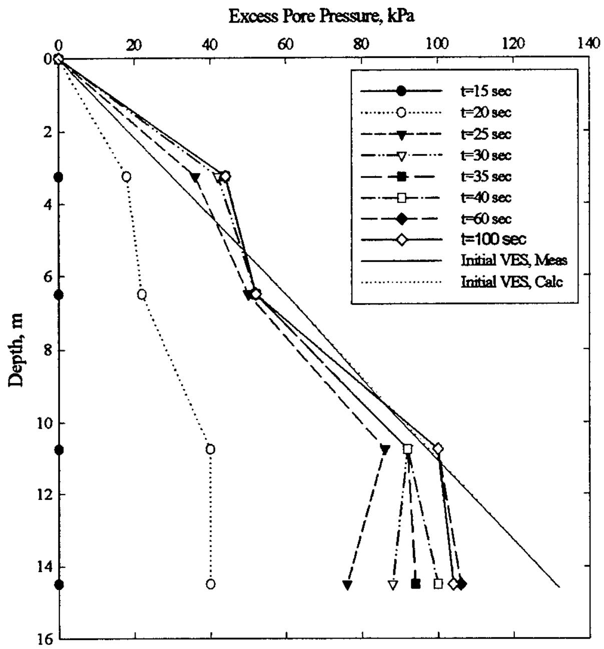

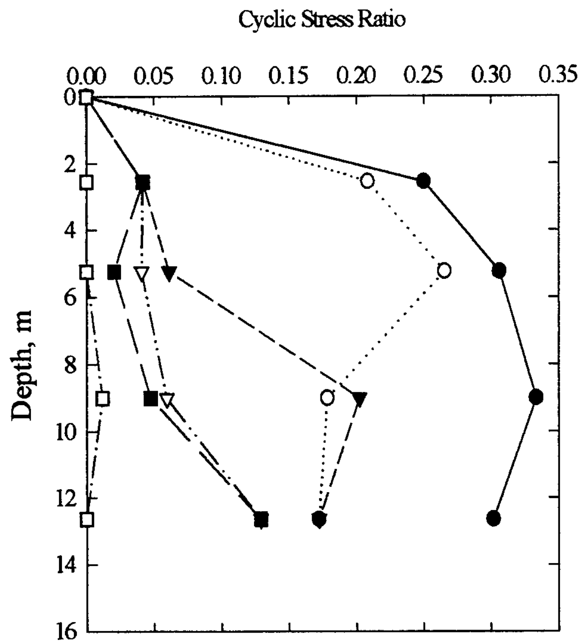

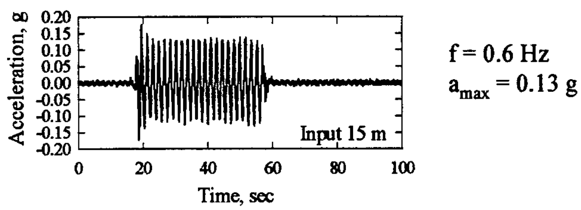

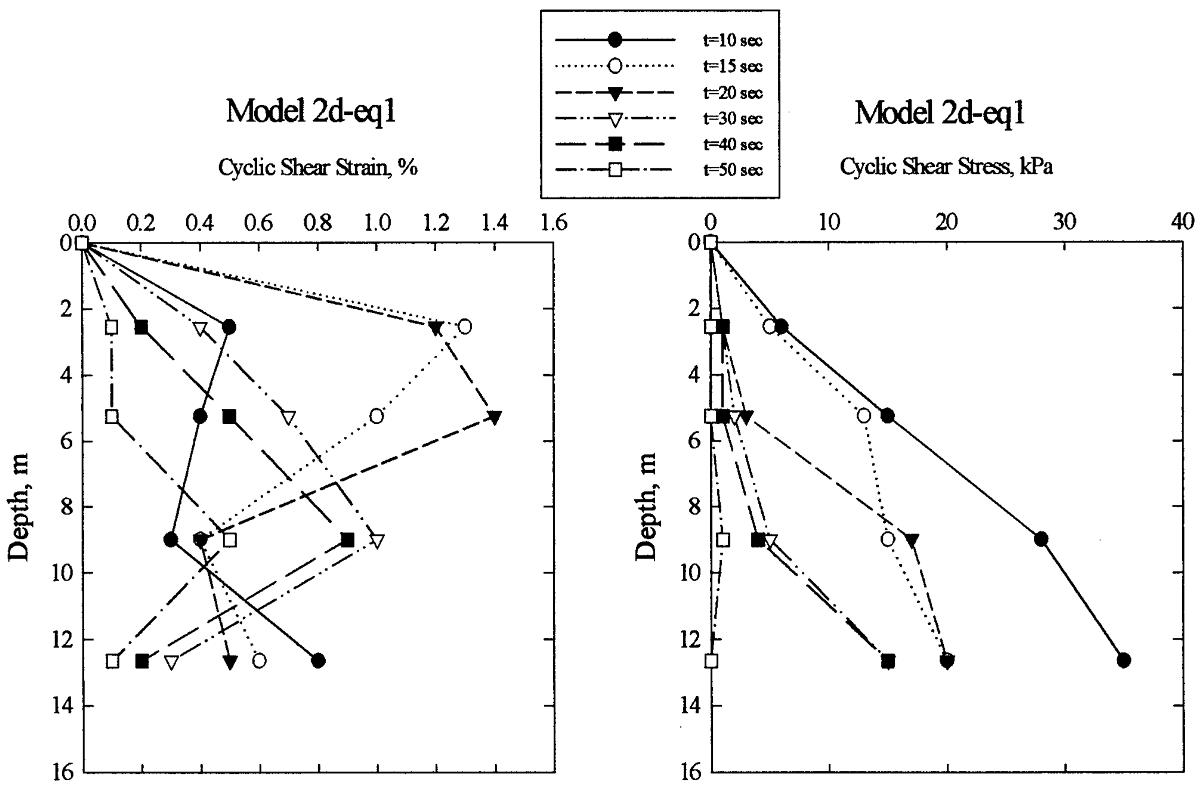

Model 2d Stress and strain isochrones

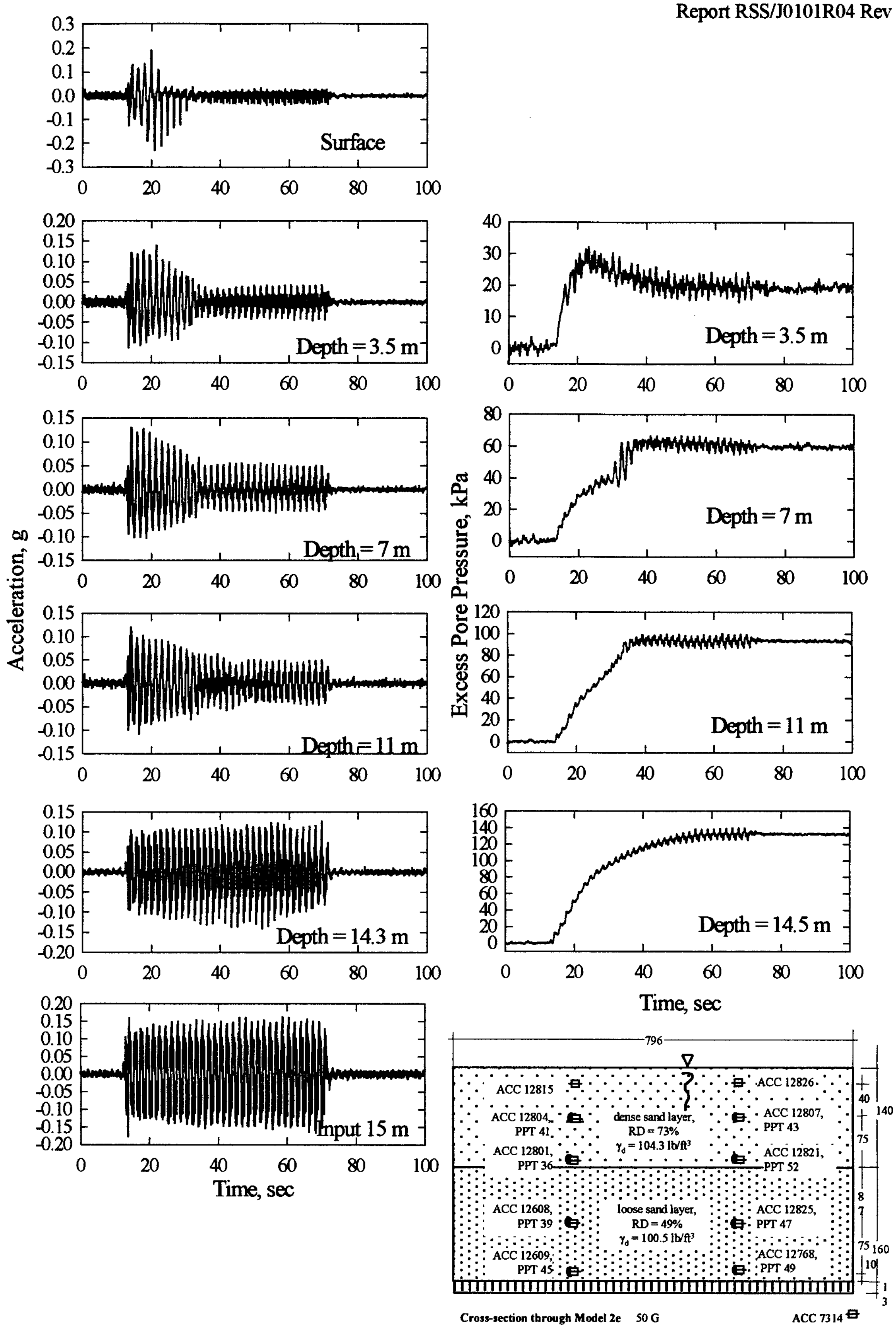
Acceleration, g
Surface
Depth = 3.5 m
Depth = 7 m
Depth = 11 m
Depth = 14.3 m
Input 15 m
Time, sec
Excess Pore Pressure, kPa
Depth = 3.5 m
Depth = 7 m
Depth = 11 m
Depth = 14.5 m
Time, sec
796
ACC 12815
ACC 12826
ACC 12804, PPT 41
dense sand layer, RD = 73%
γ_d = 104.3 lb/ft^3
ACC 12807, PPT 43
ACC 12801, PPT 36
ACC 12821, PPT 52
ACC 12608, PPT 39
loose sand layer, RD = 49%
γ_d = 100.5 lb/ft^3
ACC 12825, PPT 47
ACC 12609, PPT 45
ACC 12768, PPT 49
40
75
140
8
75
160
10
1
3
Cross-section through Model 2e 50 G
ACC 7314

Model 2e

Model 2e-eq1

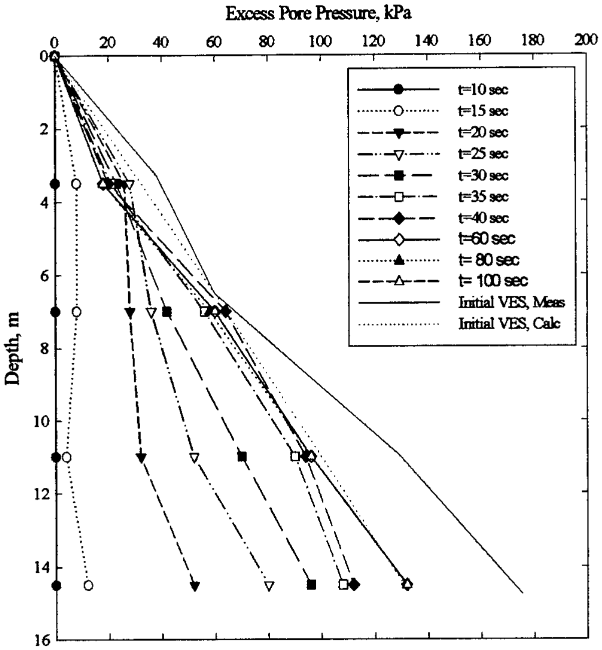

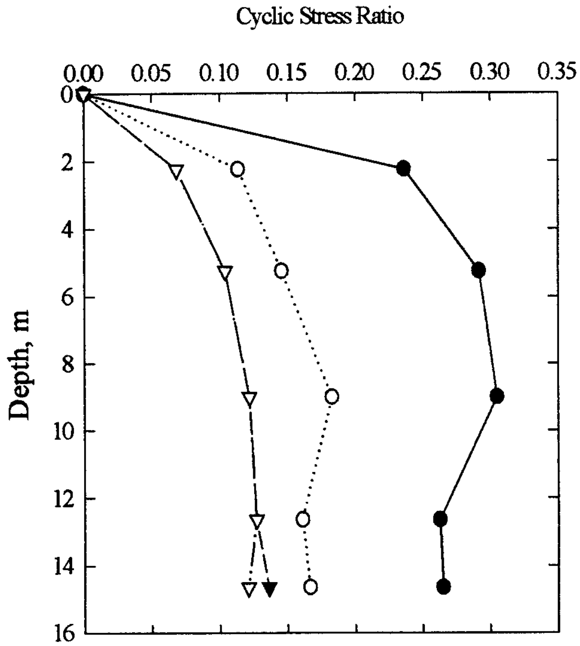

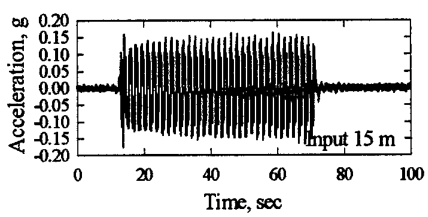

f = 0.6 Hz
a_{max} = 0.15 g

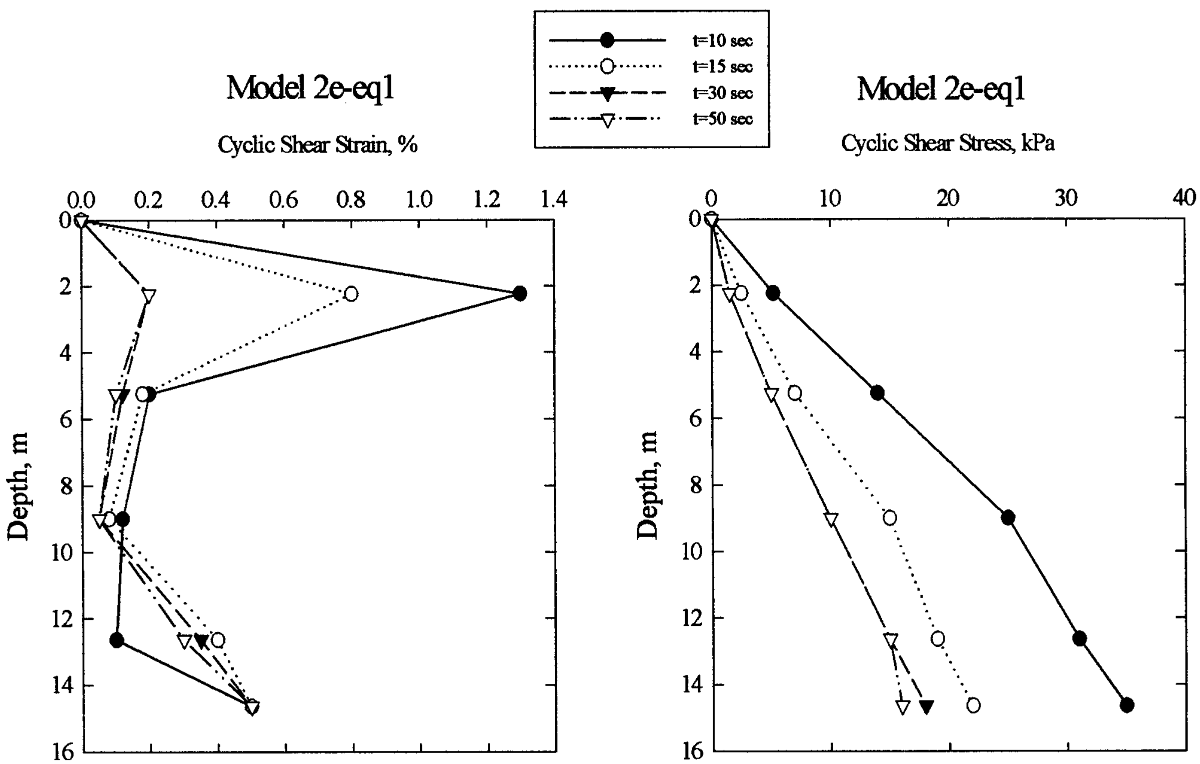

Model 2e Stress and strain isochrones

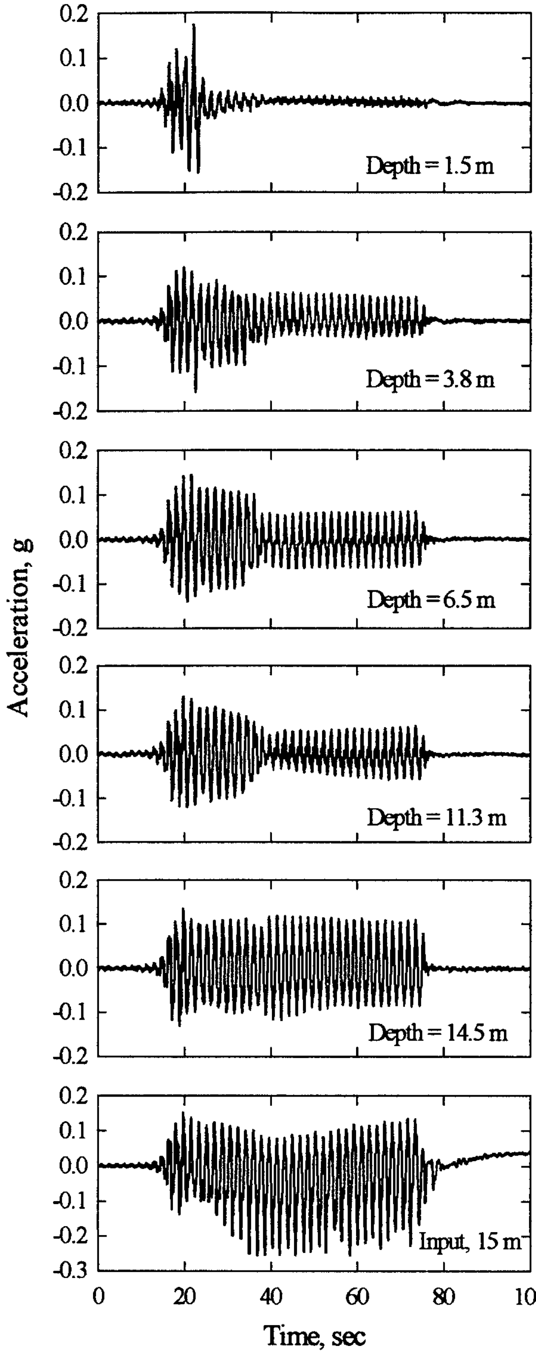
Acceleration, g
Depth = 1.5 m
Depth = 3.8 m
Depth = 6.5 m
Depth = 11.3 m
Depth = 14.5 m
Input, 15 m
Time, sec

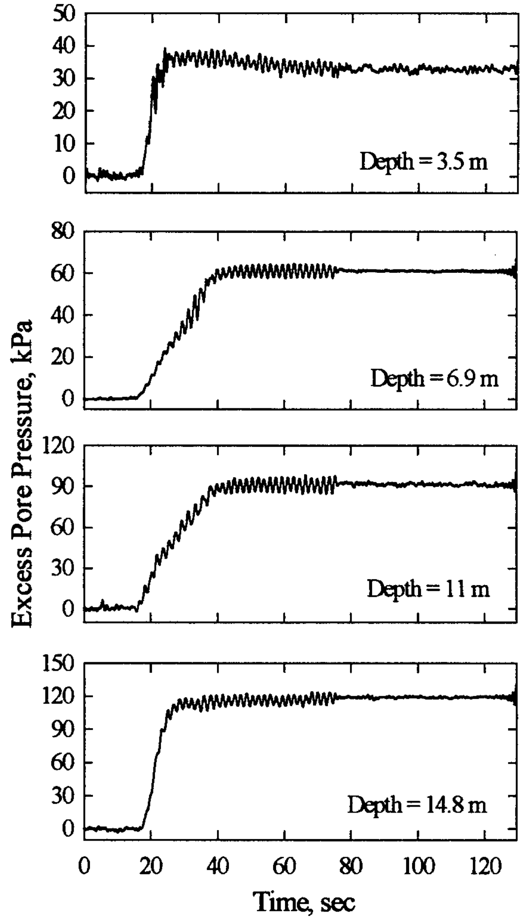
Excess Pore Pressure, kPa
Depth = 3.5 m
Depth = 6.9 m
Depth = 11 m
Depth = 14.8 m
Time, sec

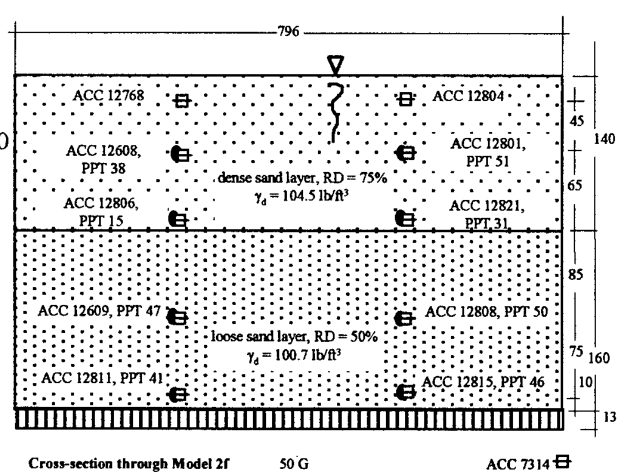
796
ACC 12768
ACC 12804
ACC 12608,
PPT 38
ACC 12801,
PPT 51
dense sand layer, RD = 75%
γ_d = 104.5 lb/ft³
ACC 12806,
PPT 15
ACC 12821,
PPT 31
ACC 12609, PPT 47
ACC 12808, PPT 50
loose sand layer, RD = 50%
γ_d = 100.7 lb/ft³
ACC 12811, PPT 41
ACC 12815, PPT 46
45
140
65
85
75
160
10
13
Cross-section through Model 2f
50 G
ACC 7314

Model 2f

Model 2f-eq1

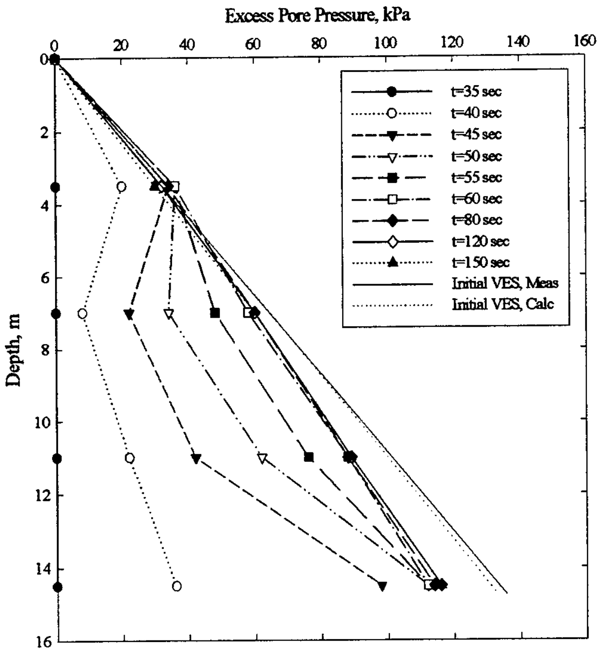

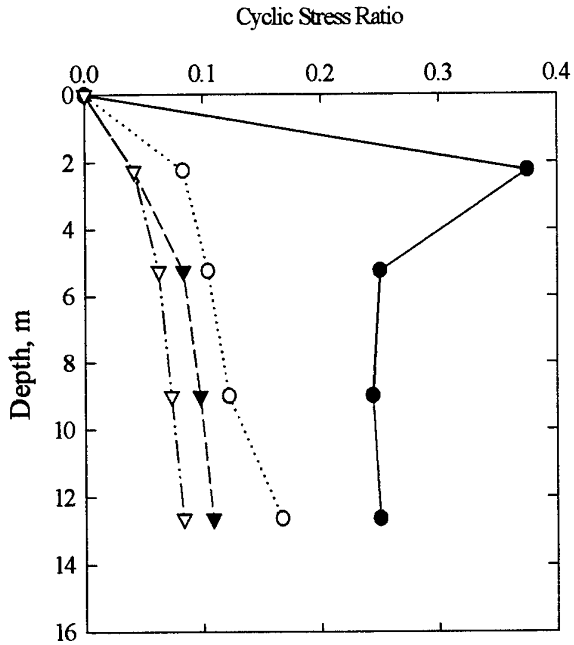

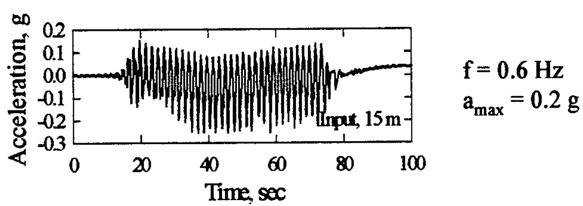

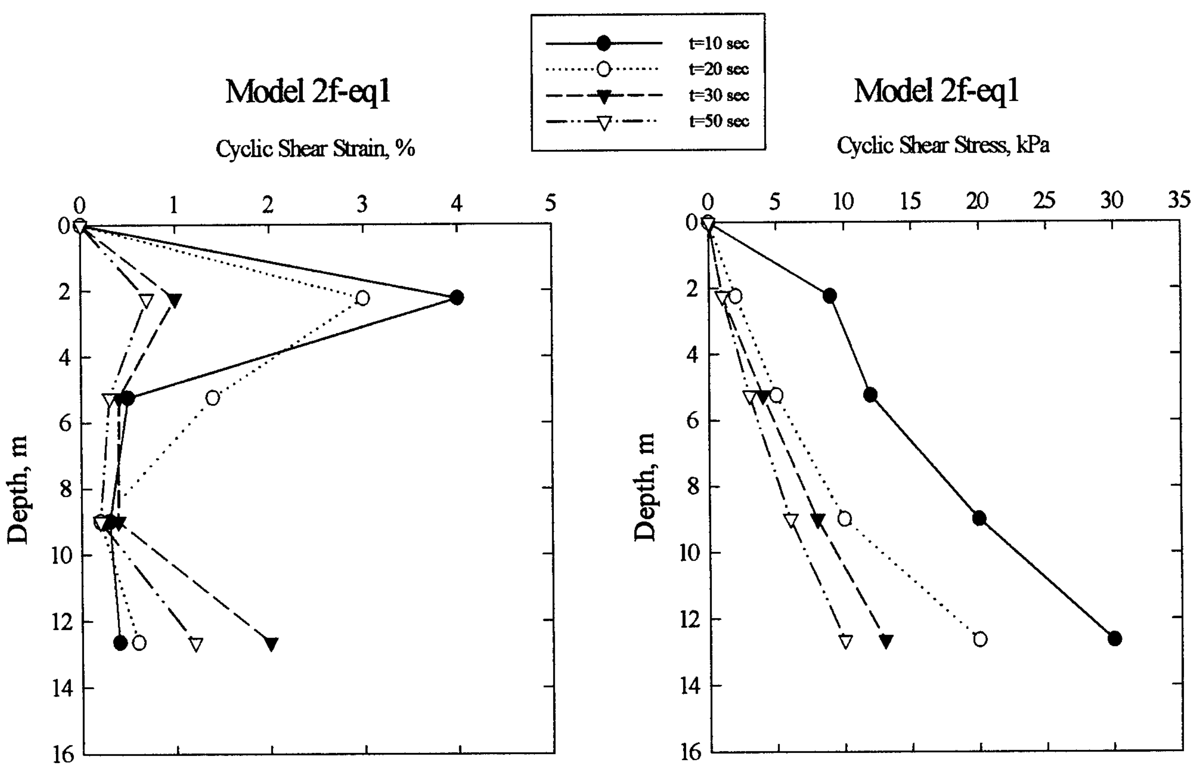

Model 2f Stress and strain isochrones

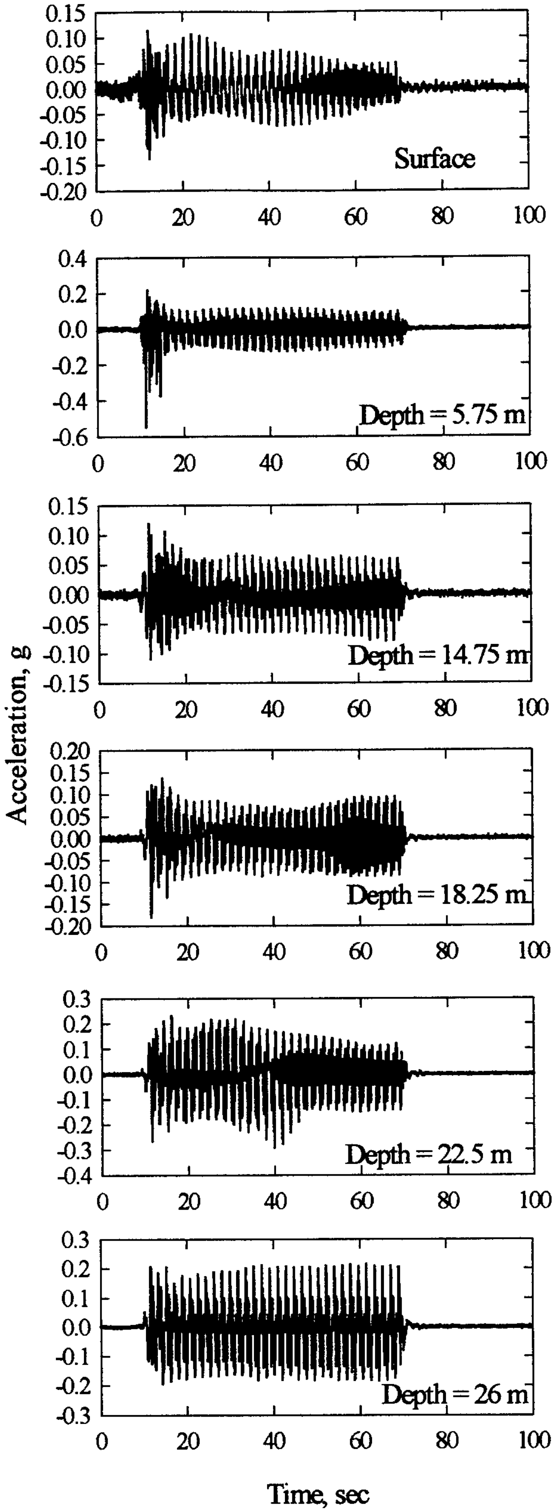
Surface
Depth = 5.75 m
Depth = 14.75 m
Depth = 18.25 m
Depth = 22.5 m
Depth = 26 m
Acceleration, g
Time, sec

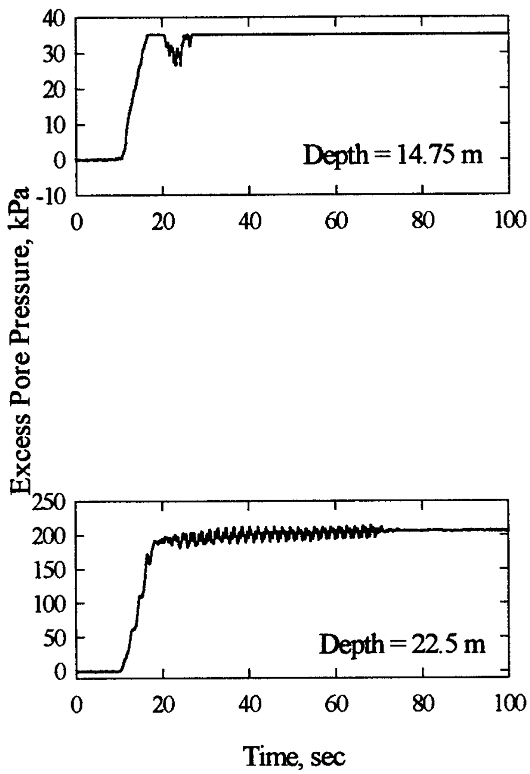
Depth = 14.75 m
Depth = 22.5 m
Excess Pore Pressure, kPa
Time, sec

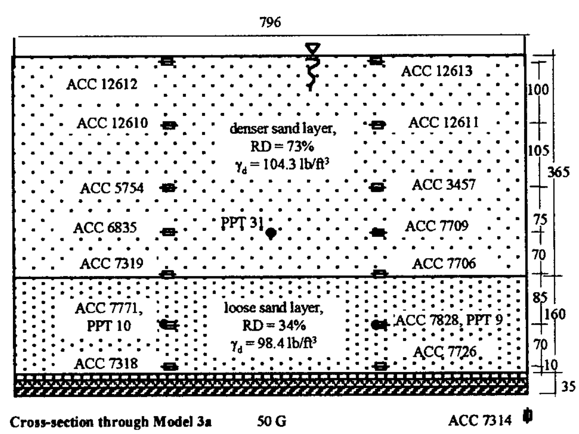
796
ACC 12612
ACC 12613
ACC 12610
ACC 12611
denser sand layer,
RD = 73%
γ_d = 104.3 lb/ft^3
ACC 5754
ACC 3457
ACC 6835
PPT 31
ACC 7709
ACC 7319
ACC 7706
ACC 7771,
PPT 10
loose sand layer,
RD = 34%
γ_d = 98.4 lb/ft^3
ACC 7828, PPT 9
ACC 7726
ACC 7318
100
105
365
75
70
85
160
70
10
35
Cross-section through Model 3a
50 G
ACC 7314

Model 3a

Model 3a-eq1

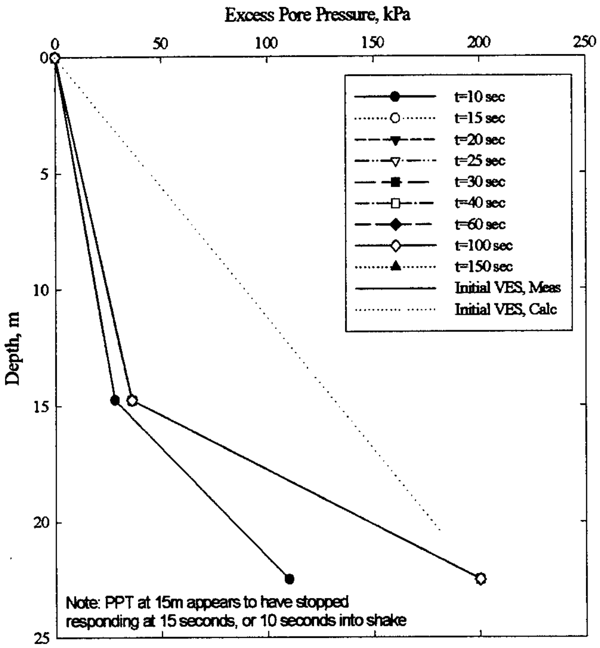

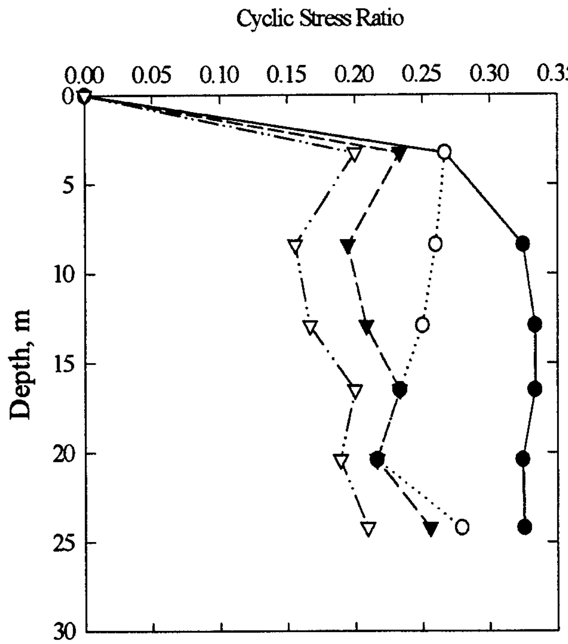

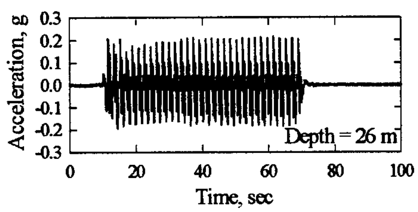

f = 0.6 Hz
a_{max} = 0.2 g

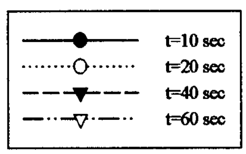

Model 3a-eq1

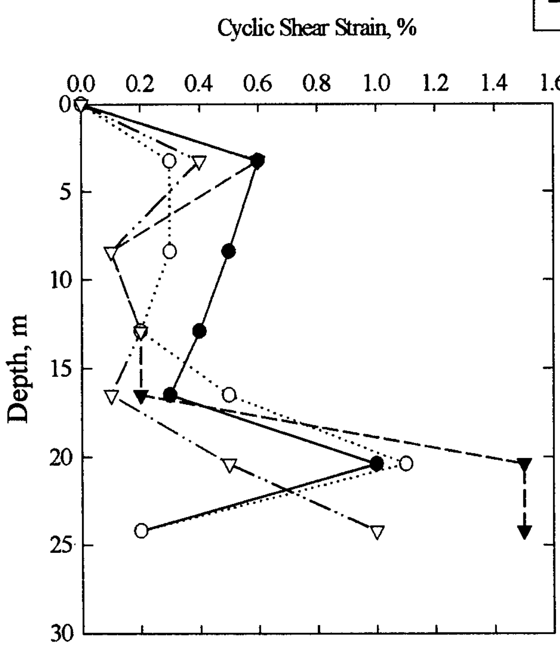

Model 3a-eq1

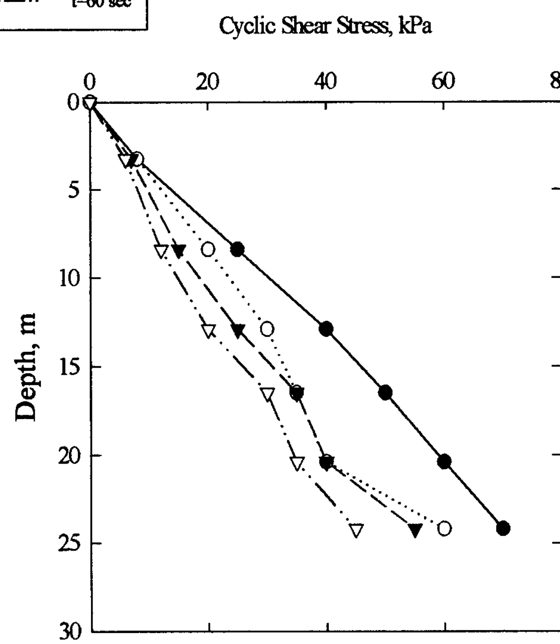

Model 3a Stress and strain isochrones

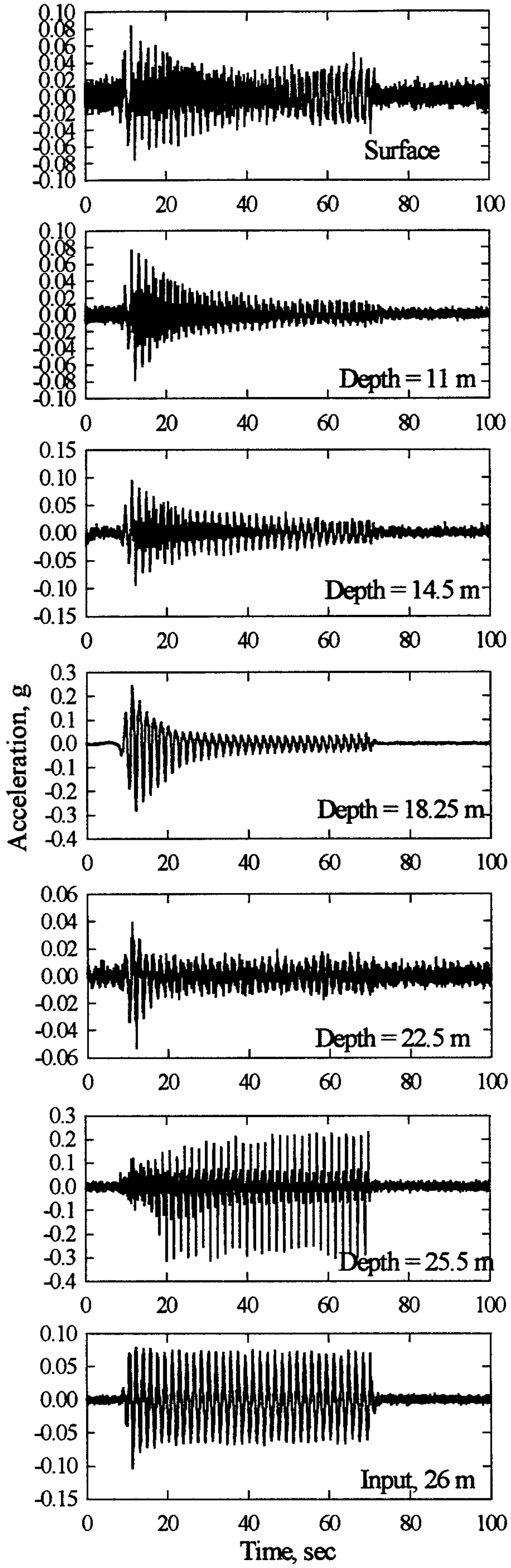

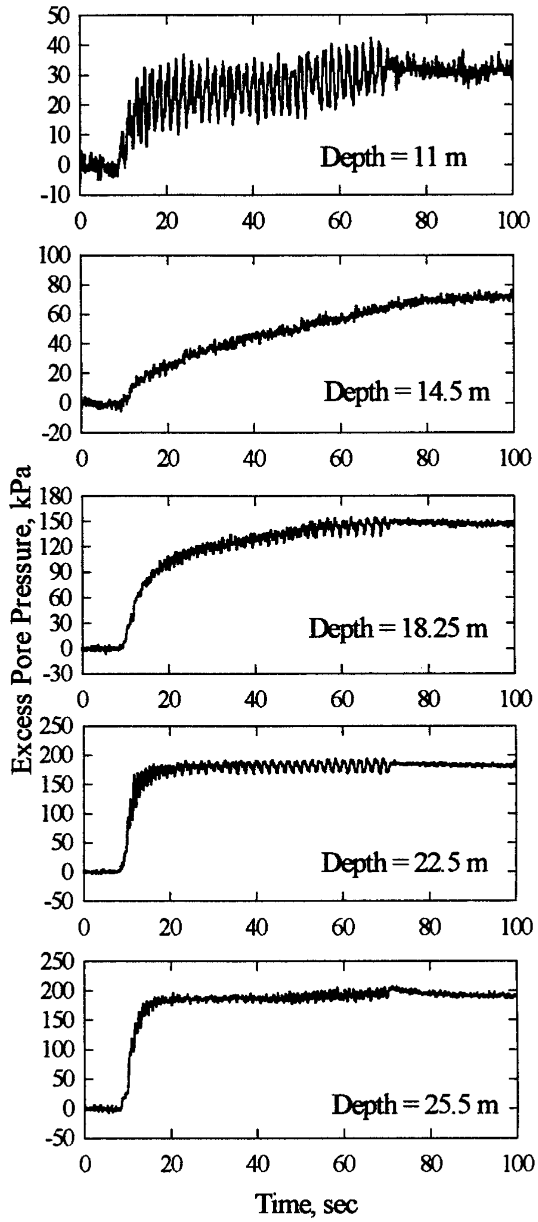

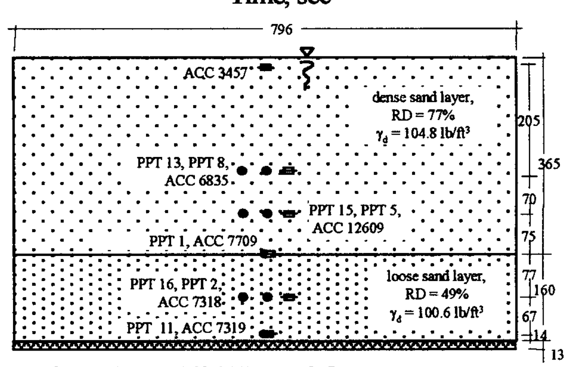

Cross-section through Model 3b 50 G ACC 7314

Model 3b

Model 3b-eq2

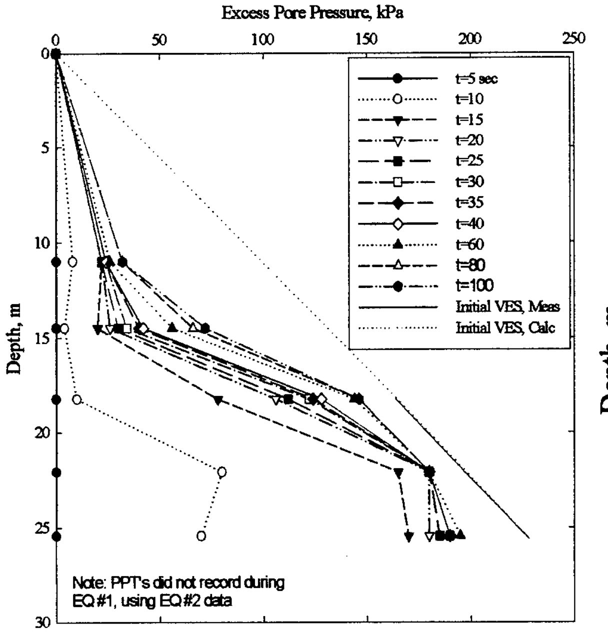

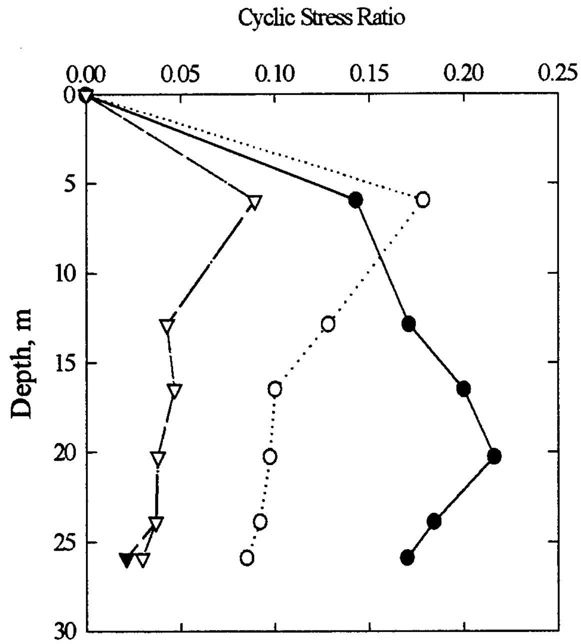

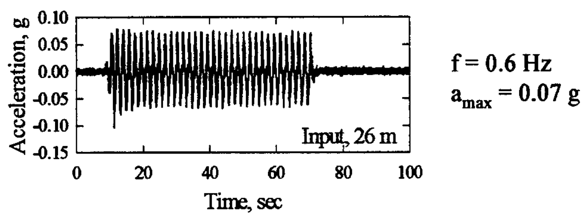

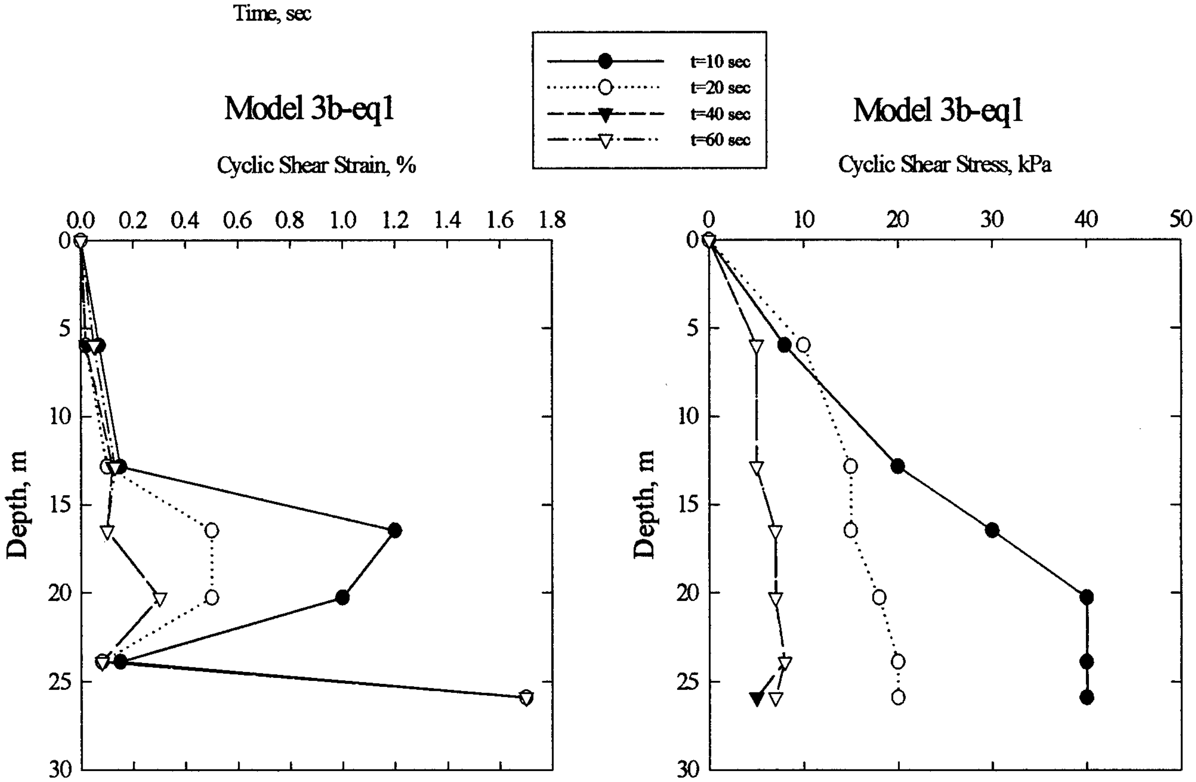

Model 3b Stress and strain isochrones

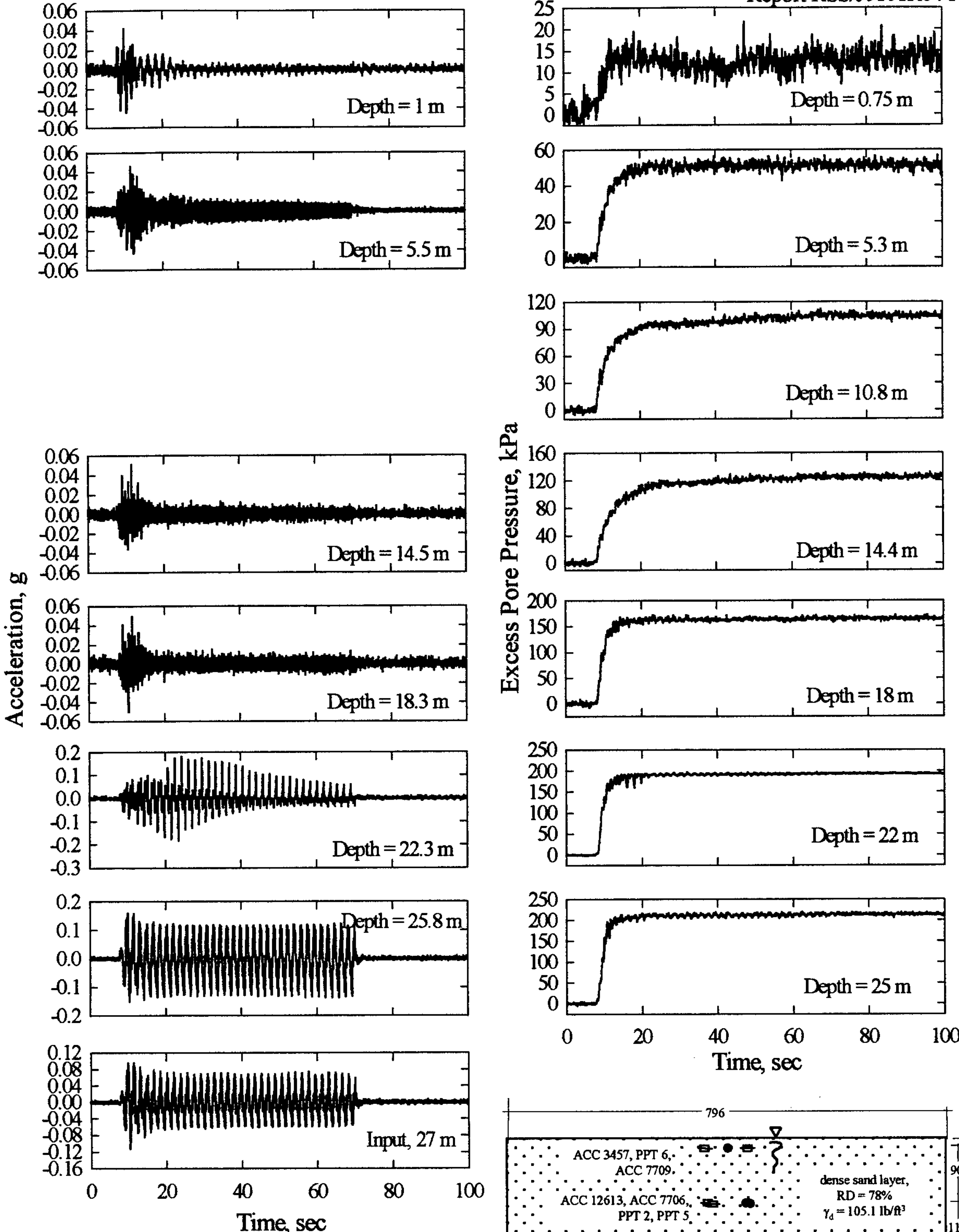
Depth = 1 m
Depth = 5.5 m
Depth = 14.5 m
Depth = 18.3 m
Depth = 22.3 m
Depth = 25.8 m
Input, 27 m
Acceleration, g
Time, sec
Depth = 0.75 m
Depth = 5.3 m
Depth = 10.8 m
Depth = 14.4 m
Depth = 18 m
Depth = 22 m
Depth = 25 m
Excess Pore Pressure, kPa
Time, sec

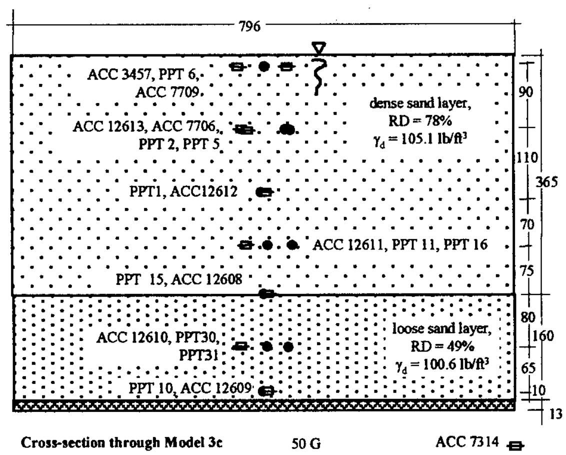
796
ACC 3457, PPT 6, ACC 7709
ACC 12613, ACC 7706, PPT 2, PPT 5
dense sand layer, RD = 78% γ_d = 105.1 lb/ft³
PPT1, ACC12612
ACC 12611, PPT 11, PPT 16
PPT 15, ACC 12608
ACC 12610, PPT30, PPT31
loose sand layer, RD = 49% γ_d = 100.6 lb/ft³
PPT 10, ACC 12609
90
110
365
70
75
80
160
65
10
13
Cross-section through Model 3c
50 G
ACC 7314

Model 3c

Model 3c-eq1

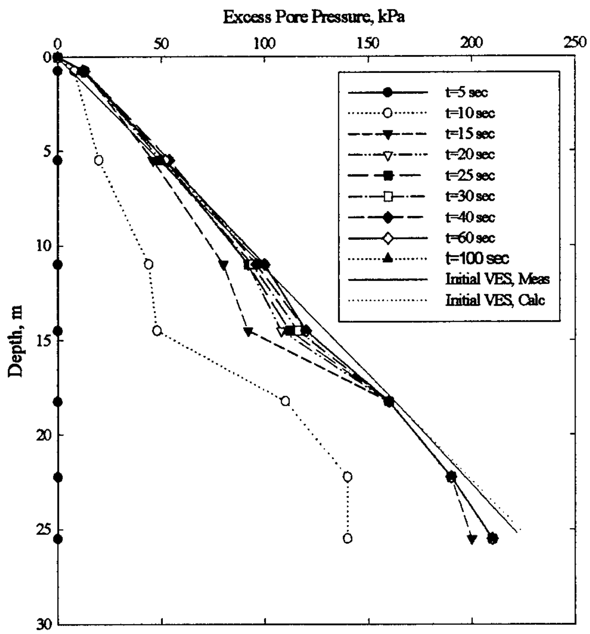

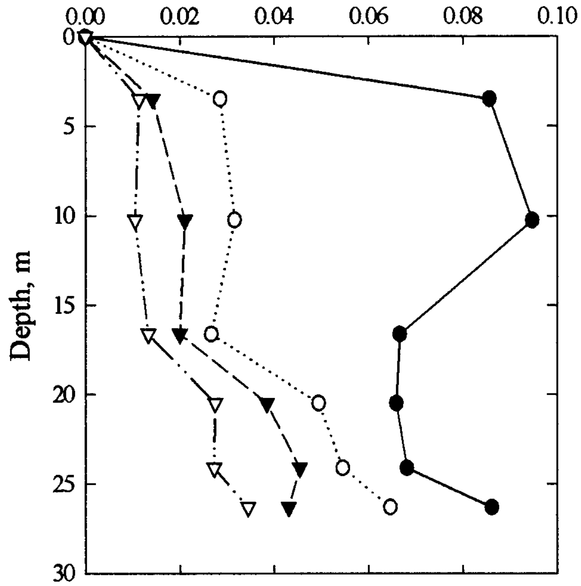

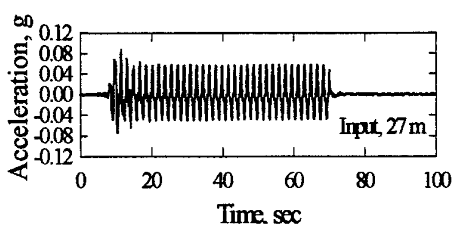

f = 0.6 Hz
a_{max} = 0.07 g

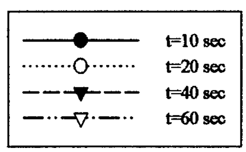

Model 3c-eq1

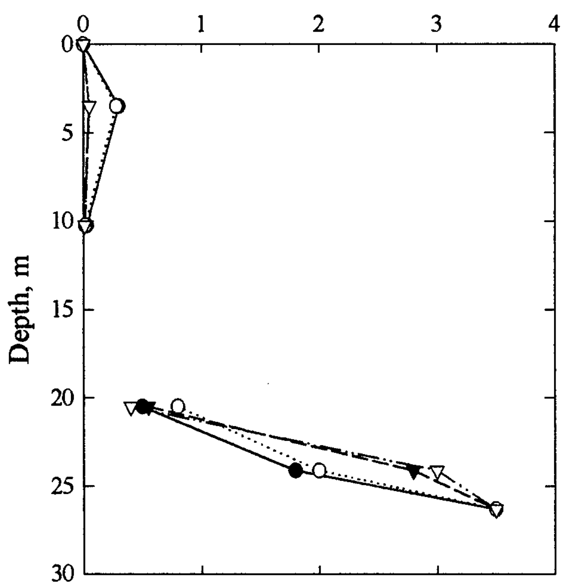

Model 3c-eq1

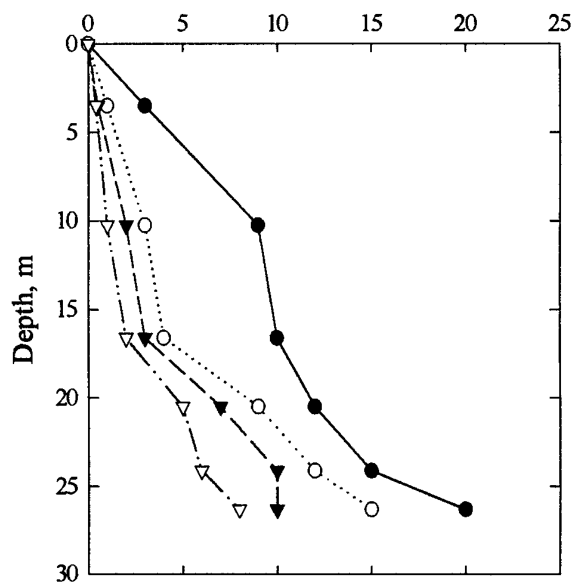

Model 3c Stress and strain isochrones

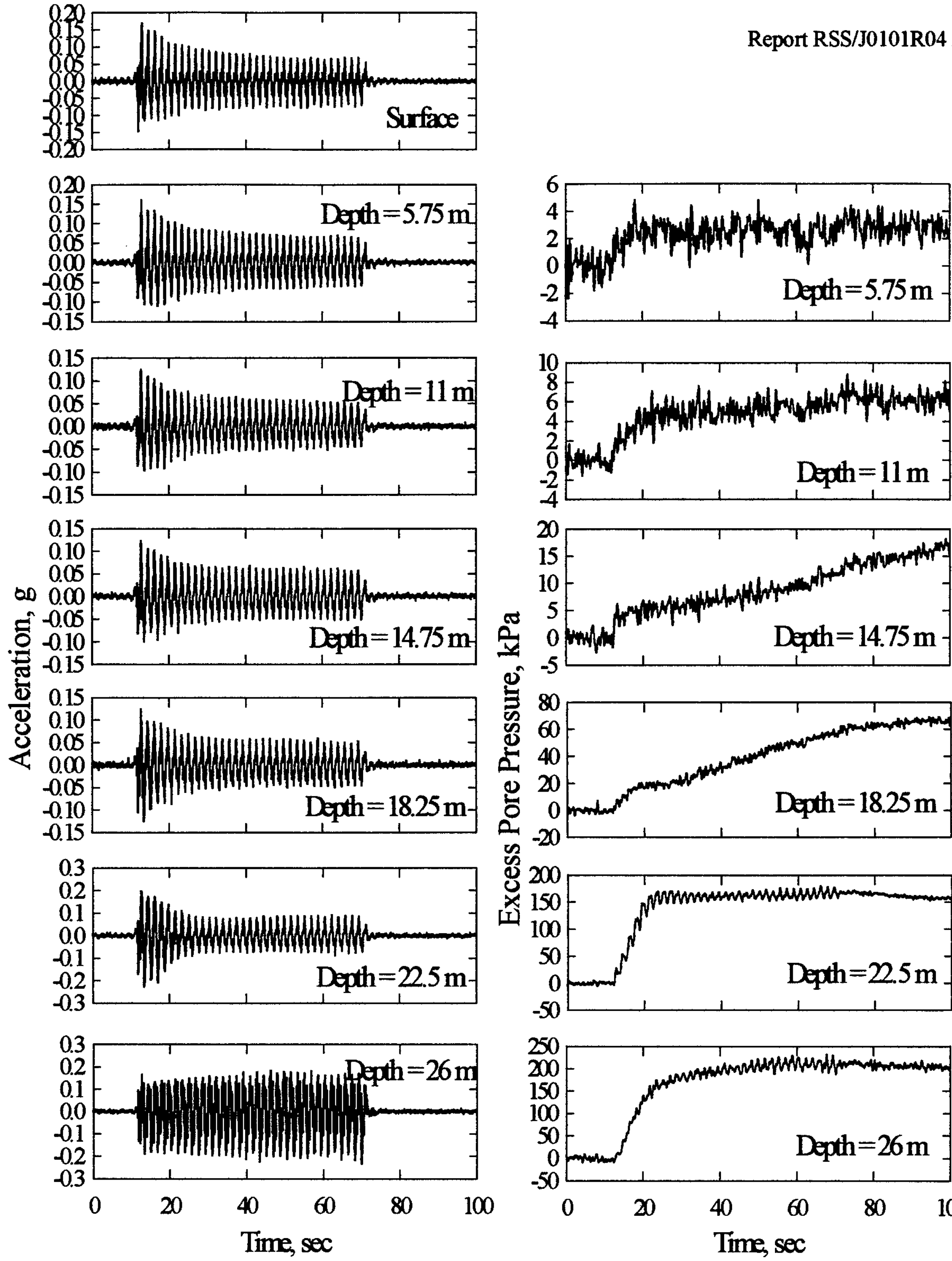

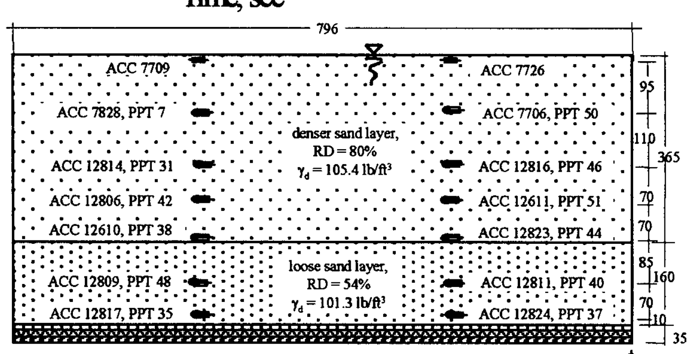

Cross-section through Model 3d

Model 3d

Model 3d-eql

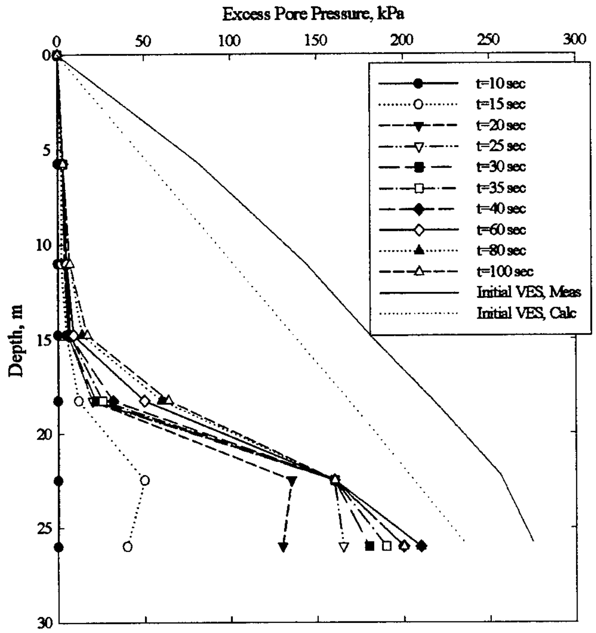

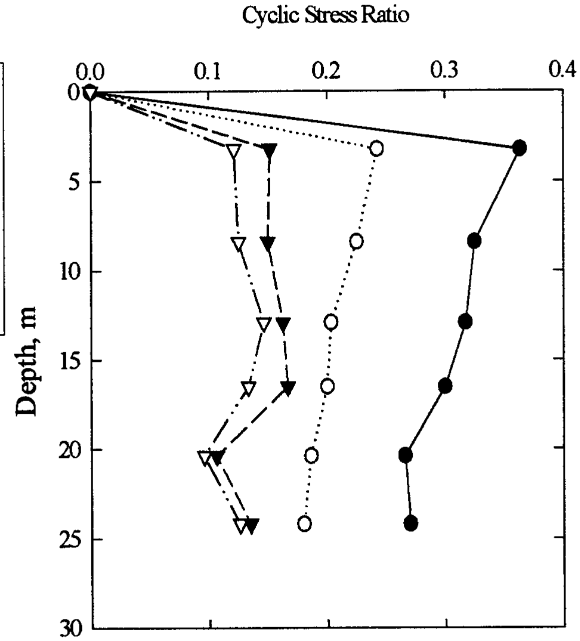

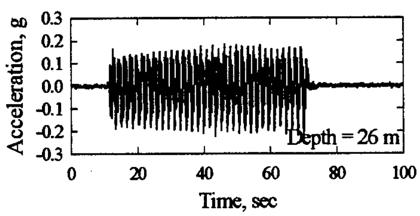

f = 0.6 Hz
a_{max} = 0.19 g

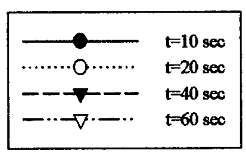

Model 3d-eql

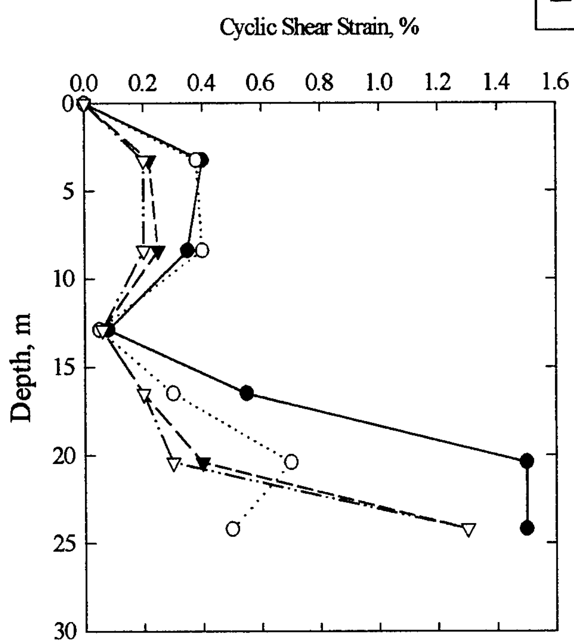

Model 3d-eql

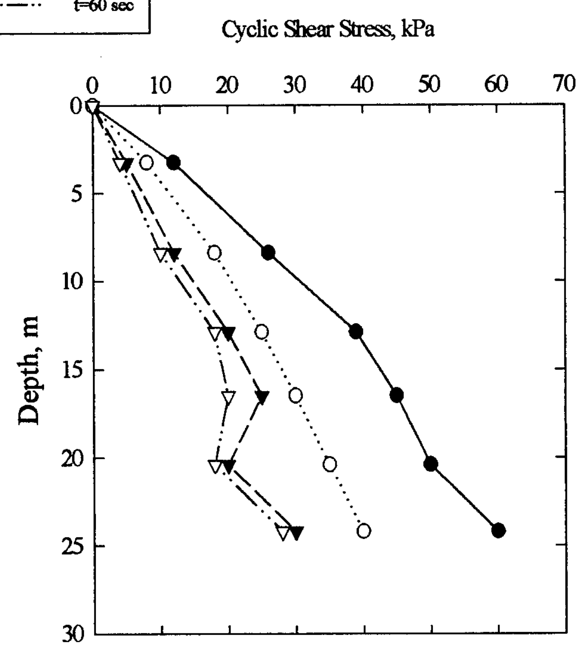

Model 3d Stress and strain isochrones

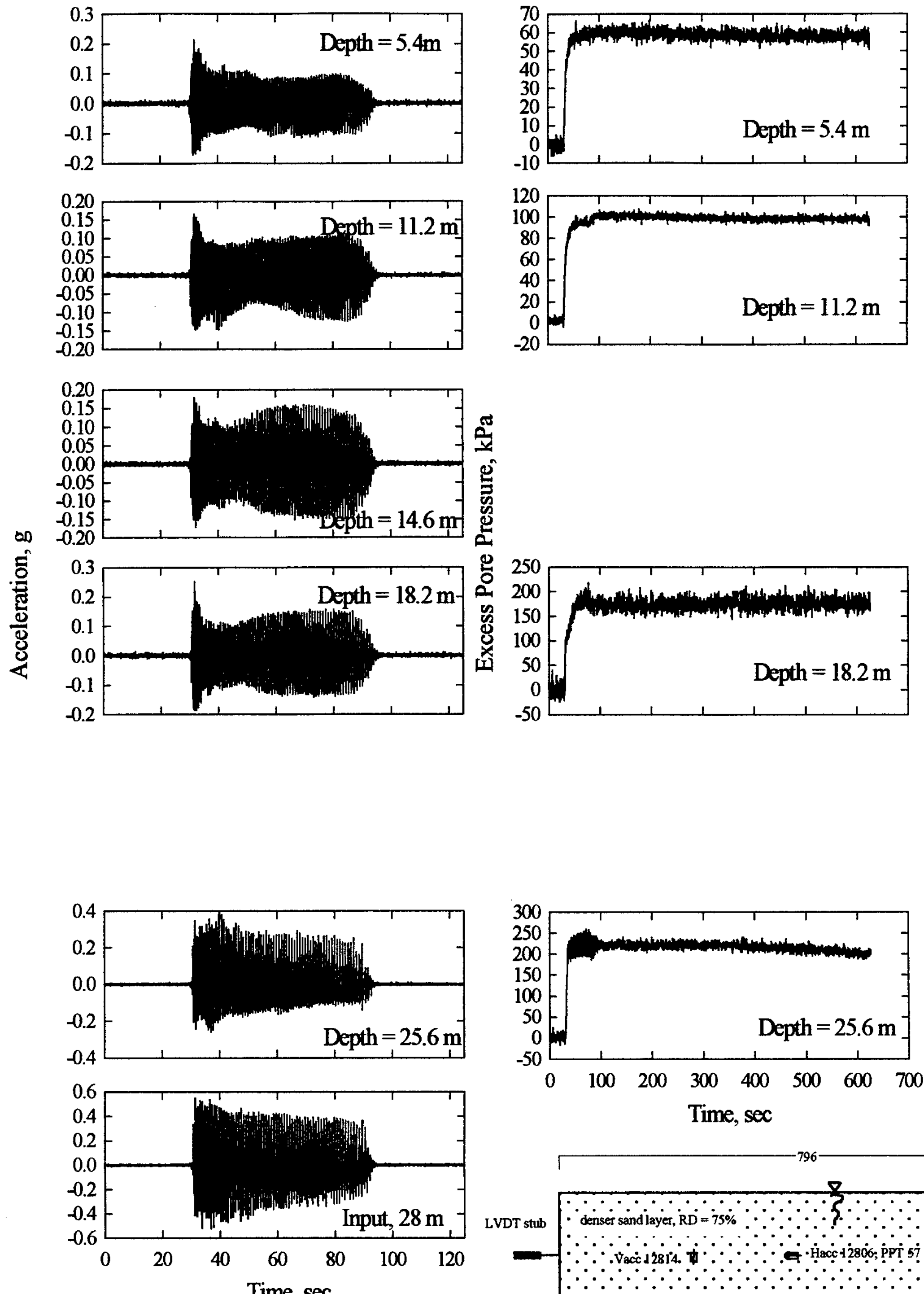

Acceleration, g
Depth = 5.4m
Depth = 11.2 m
Depth = 14.6 m
Depth = 18.2 m
Depth = 25.6 m
Input, 28 m
Time, sec
Excess Pore Pressure, kPa
Depth = 5.4 m
Depth = 11.2 m
Depth = 18.2 m
Depth = 25.6 m
Time, sec

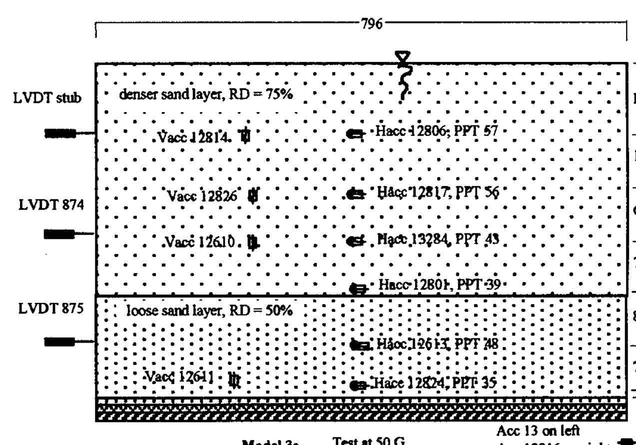

796
LVDT stub
LVDT 874
LVDT 875
denser sand layer, RD = 75%
loose sand layer, RD = 50%
Vacc 12814
Vacc 12826
Vacc 12610
Vacc 12611
Hacc 12806, PPT 57
Hacc 12817, PPT 56
Hacc 13284, PPT 43
Hacc 12801, PPT 39
Hacc 12613, PPT 48
Hacc 12824, PPT 35
108
115
69
71
80
70
12
35
365
160
Model 3e
Test at 50 G
Acc 13 on left
Acc 12816 on right

Model 3e

Model 3e (Archtest 2a, no weight)

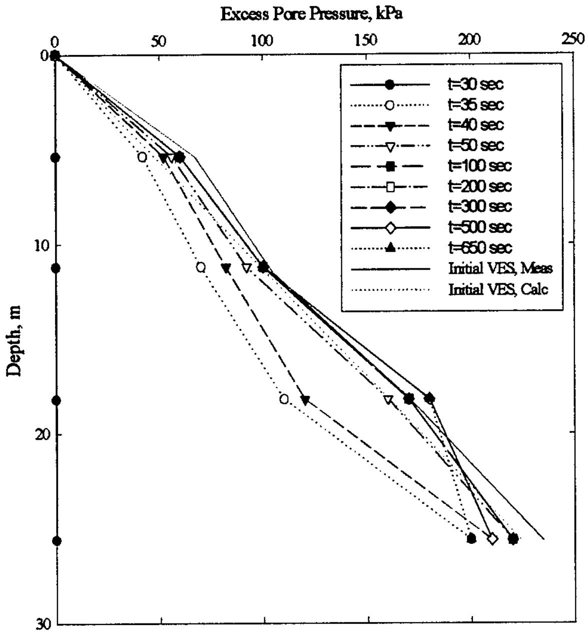

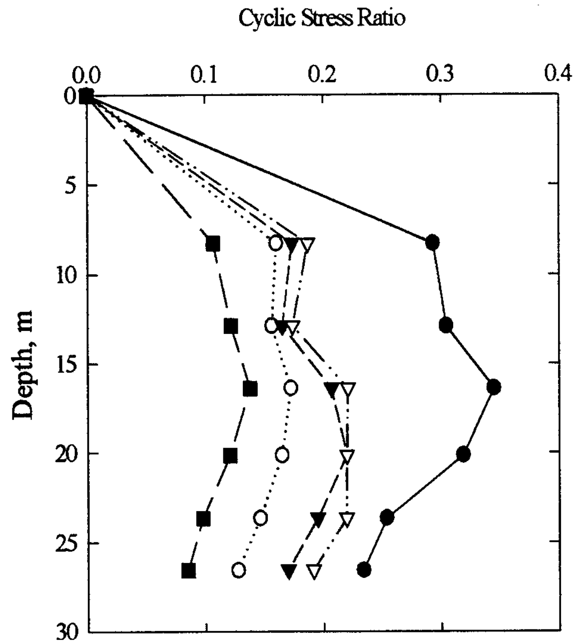

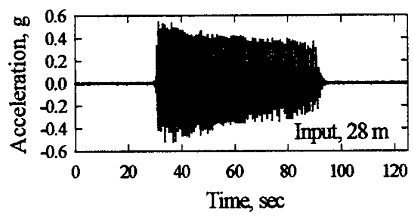

f = 1.2 Hz
a_{max} = 0.4 g

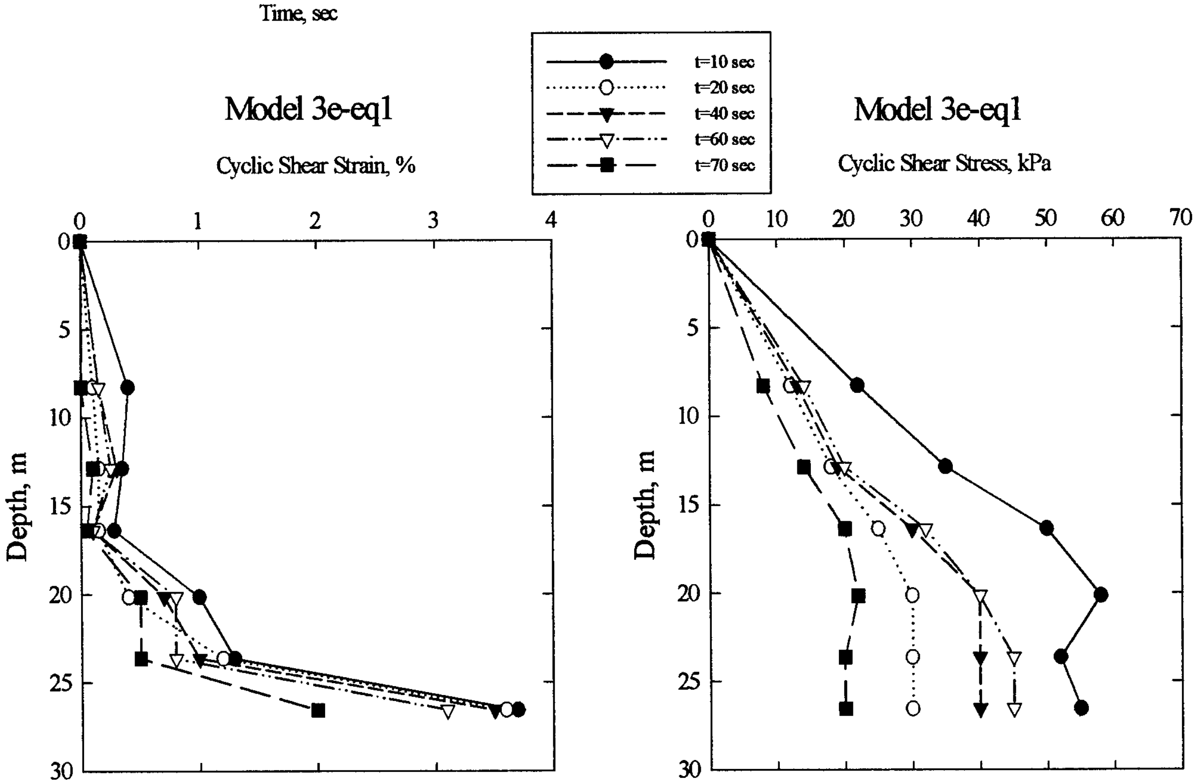

Model 3e Stress and strain isochrones

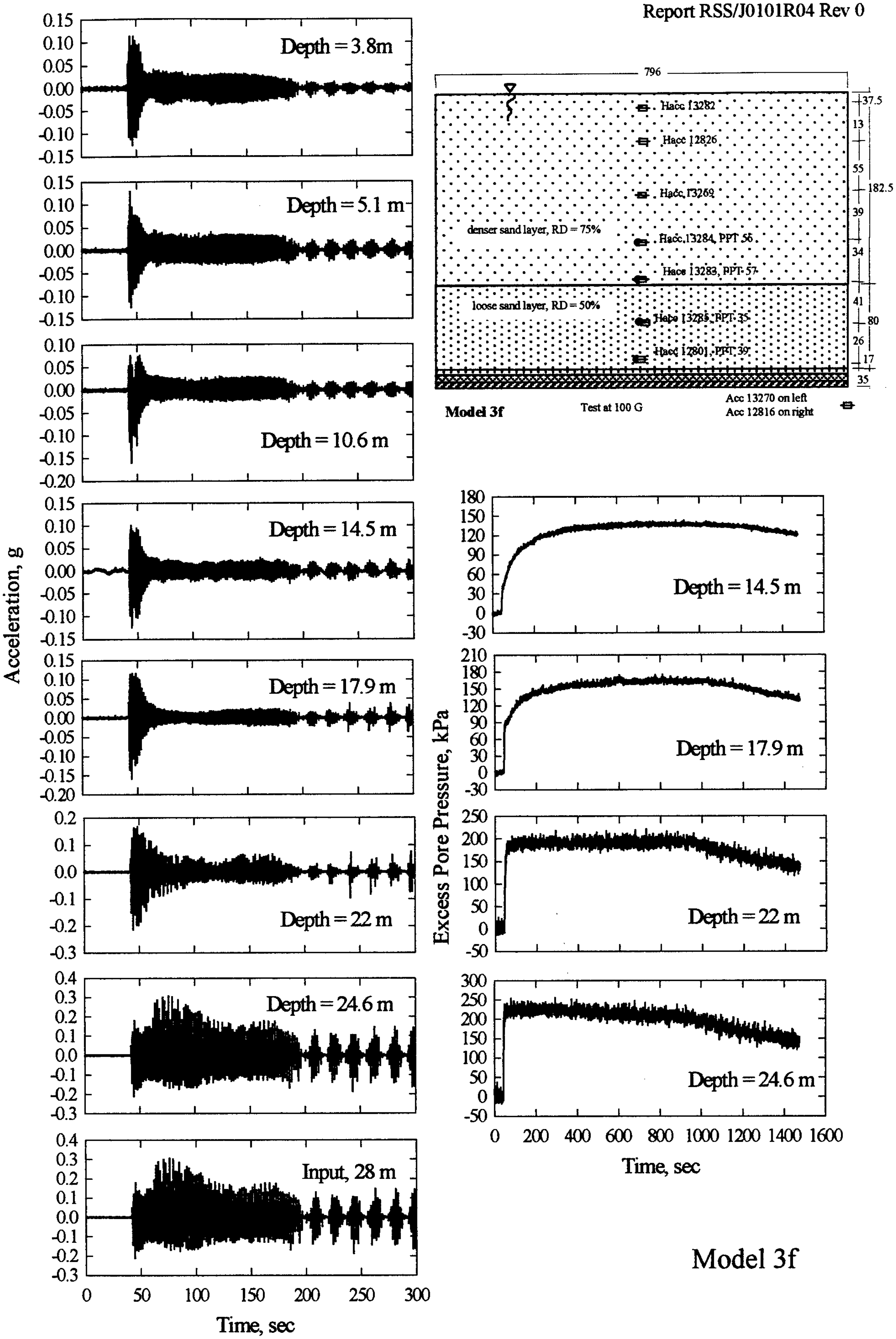

796
37.5
13
55
182.5
39
34
41
80
26
17
35
Hacc 13282
Hacc 12826
Hacc 13269
denser sand layer, RD = 75%
Hacc 13284, PPT 56
Hacc 13283, PPT 57
loose sand layer, RD = 50%
Hacc 13285, PPT 35
Hacc 12801, PPT 39
Model 3f
Test at 100 G
Acc 13270 on left
Acc 12816 on right
Depth = 3.8m
Depth = 5.1 m
Depth = 10.6 m
Depth = 14.5 m
Depth = 17.9 m
Depth = 22 m
Depth = 24.6 m
Input, 28 m
Acceleration, g
Time, sec
Excess Pore Pressure, kPa
Depth = 14.5 m
Depth = 17.9 m
Depth = 22 m
Depth = 24.6 m
Time, sec

Model 3f

Model 3f (Half Scale 100g)

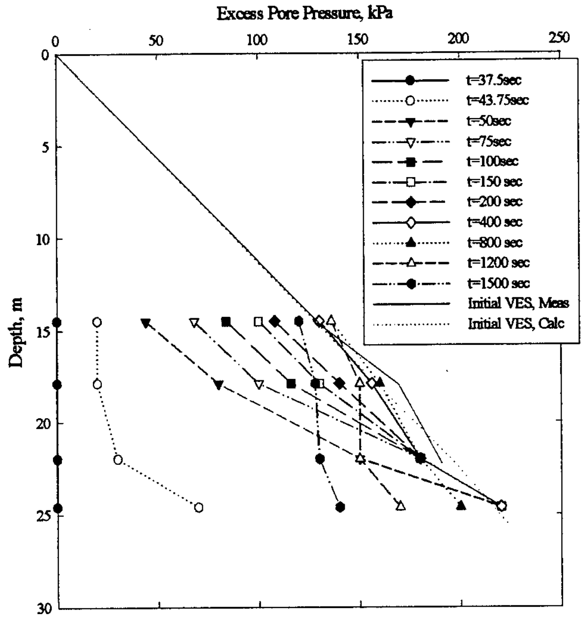

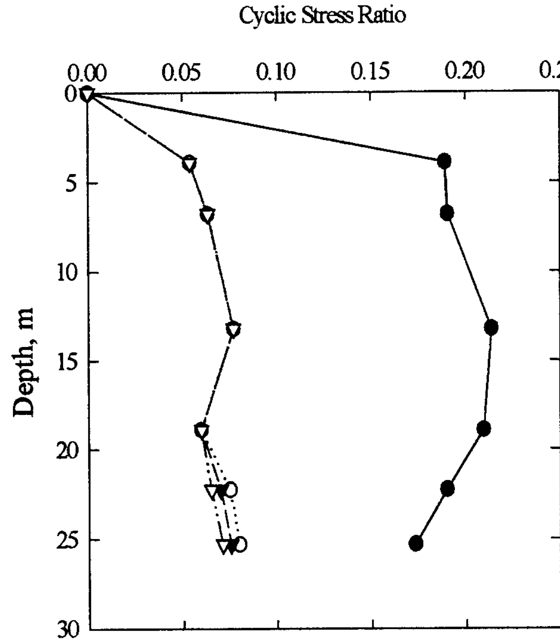

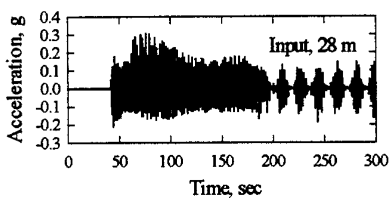

f = 0.6 Hz
a_{max} = 0.2 g

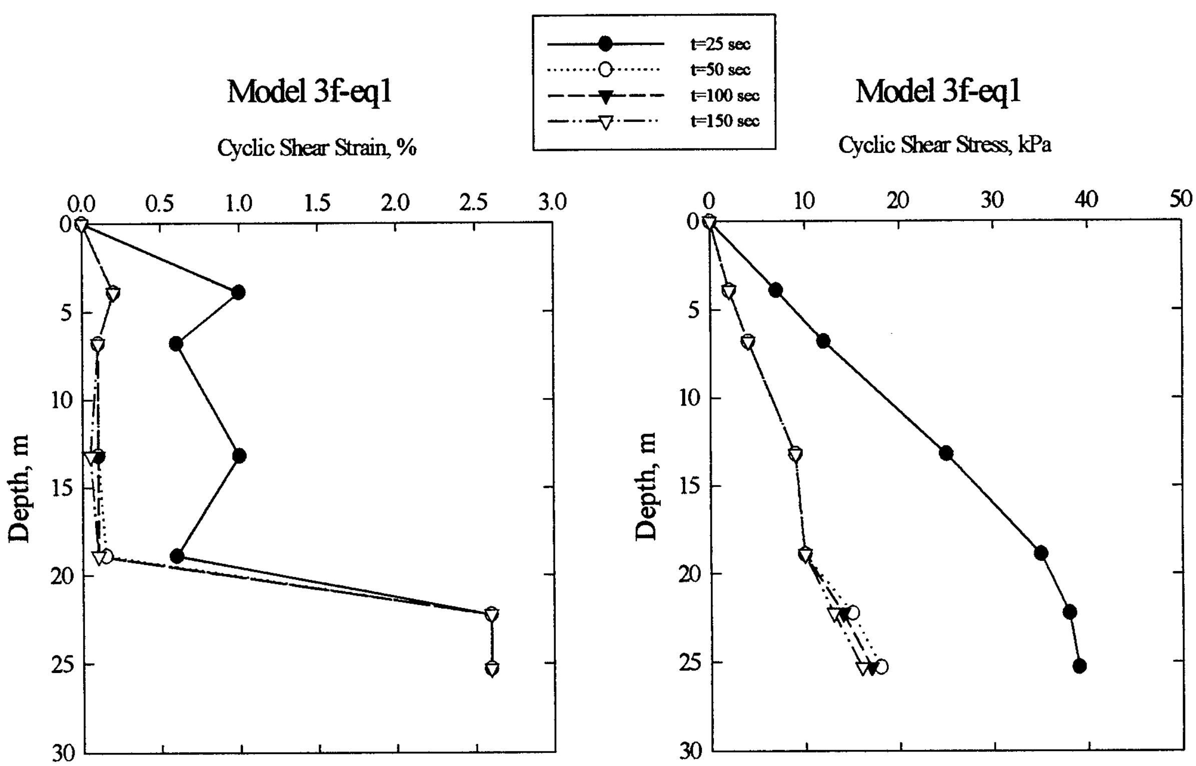

Model 3f Stress and strain isochrones

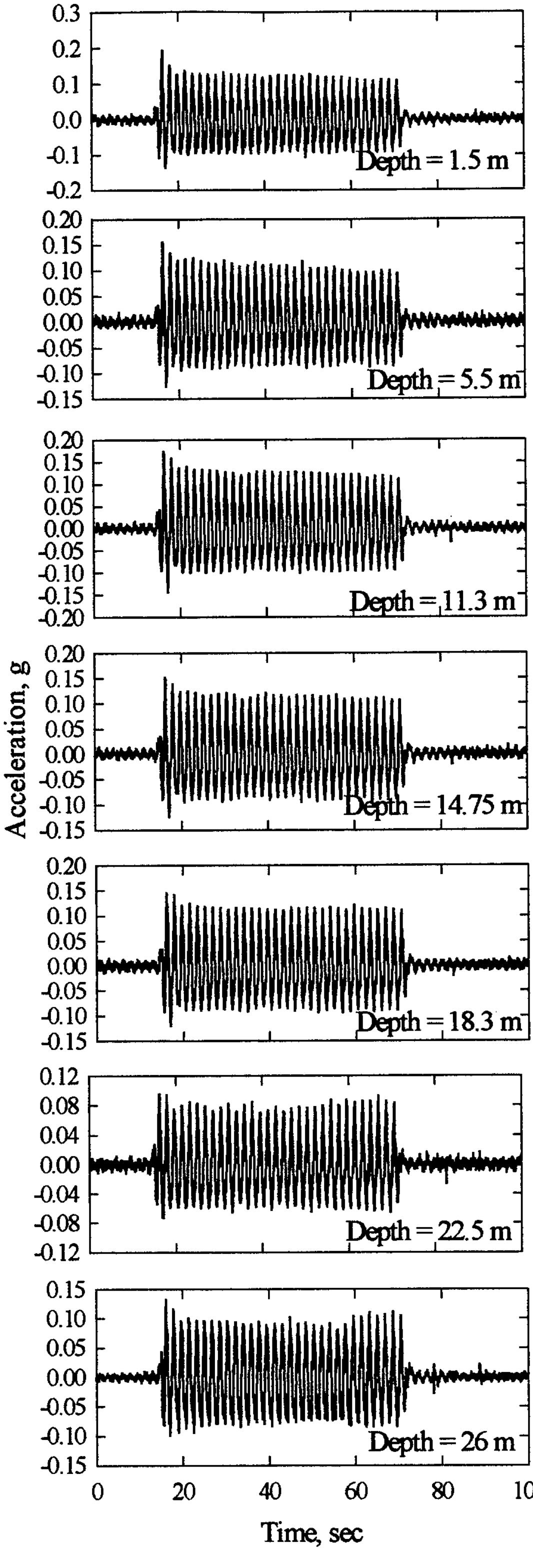
Acceleration, g
Depth = 1.5 m
Depth = 5.5 m
Depth = 11.3 m
Depth = 14.75 m
Depth = 18.3 m
Depth = 22.5 m
Depth = 26 m
Time, sec

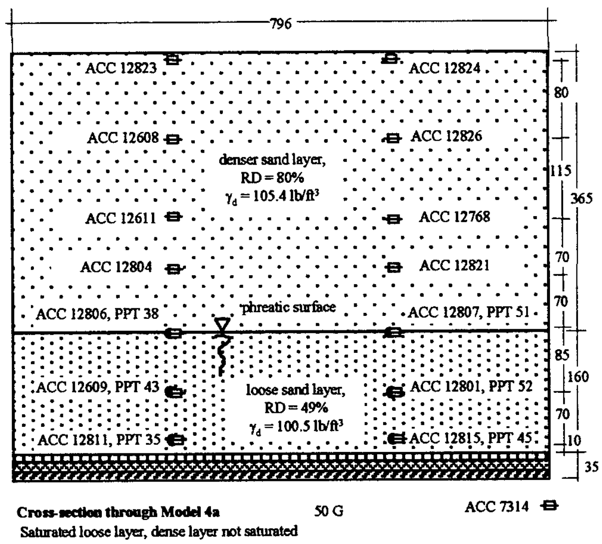
796
ACC 12823
ACC 12824
ACC 12608
ACC 12826
denser sand layer,
RD = 80%
γ_d = 105.4 lb/ft^3
ACC 12611
ACC 12768
ACC 12804
ACC 12821
ACC 12806, PPT 38
phreatic surface
ACC 12807, PPT 51
ACC 12609, PPT 43
loose sand layer,
RD = 49%
γ_d = 100.5 lb/ft^3
ACC 12801, PPT 52
ACC 12811, PPT 35
ACC 12815, PPT 45
80
115
365
70
70
85
160
70
10
35
Cross-section through Model 4a
50 G
ACC 7314
Saturated loose layer, dense layer not saturated

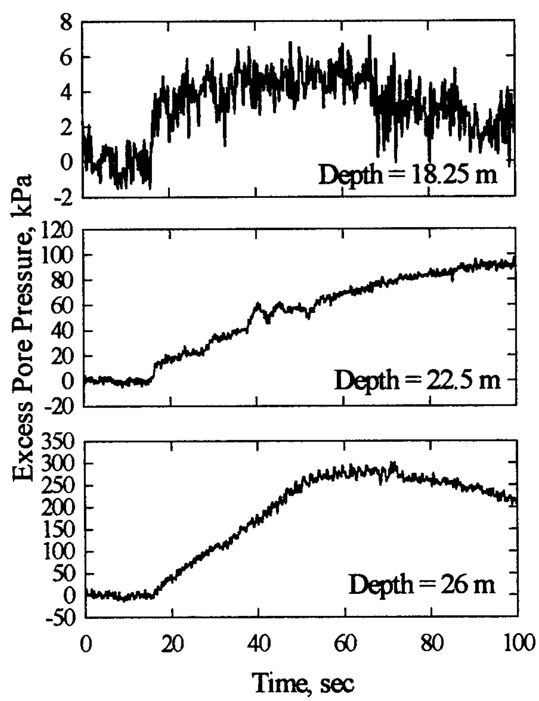
Excess Pore Pressure, kPa
Depth = 18.25 m
Depth = 22.5 m
Depth = 26 m
Time, sec

Model 4a

Model 4a-eq1

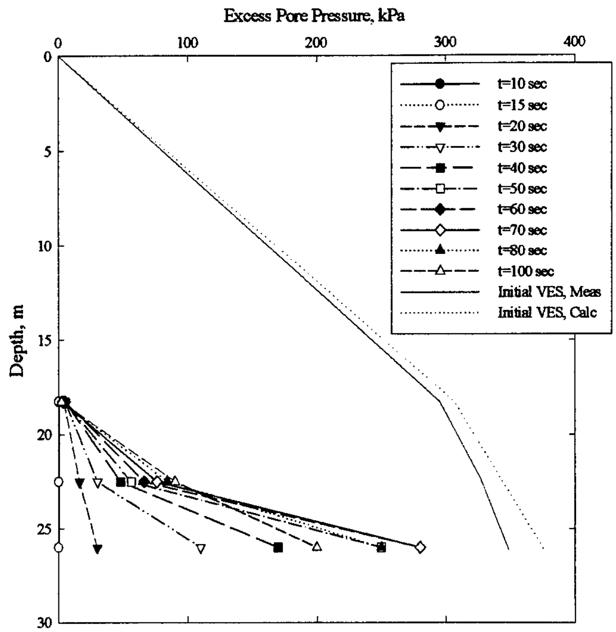

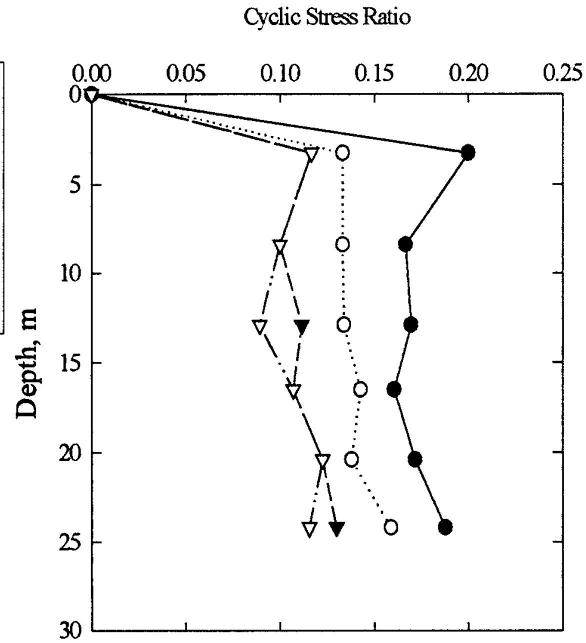

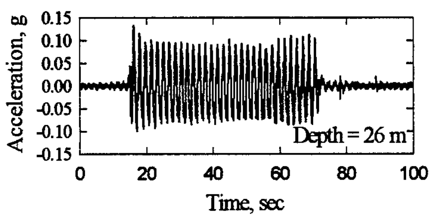

f = 0.6 Hz
a_{max} = 0.09 g

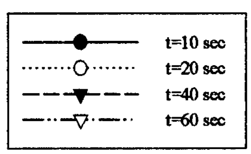

Model 4a-eq1

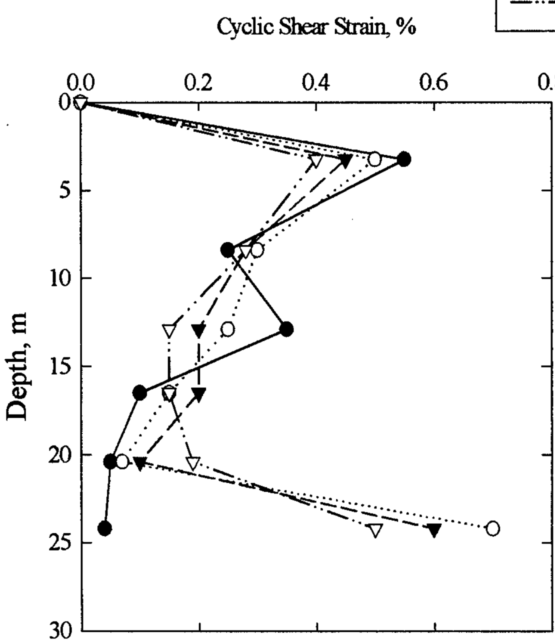

Model 4a-eq1

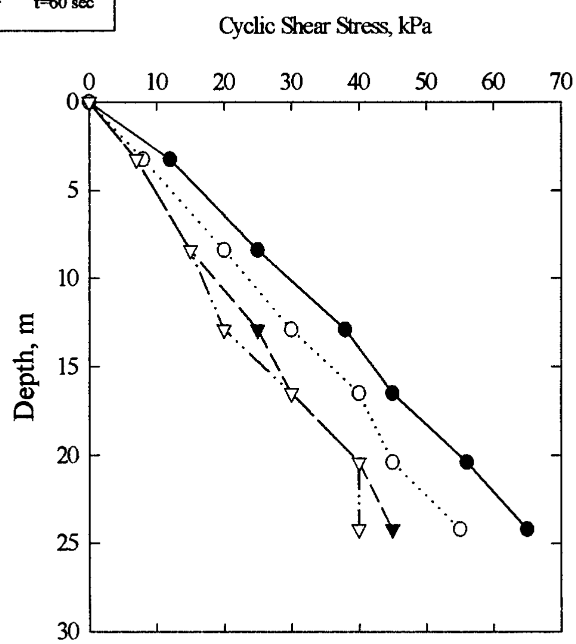

Model 4a Stress and strain isochrones

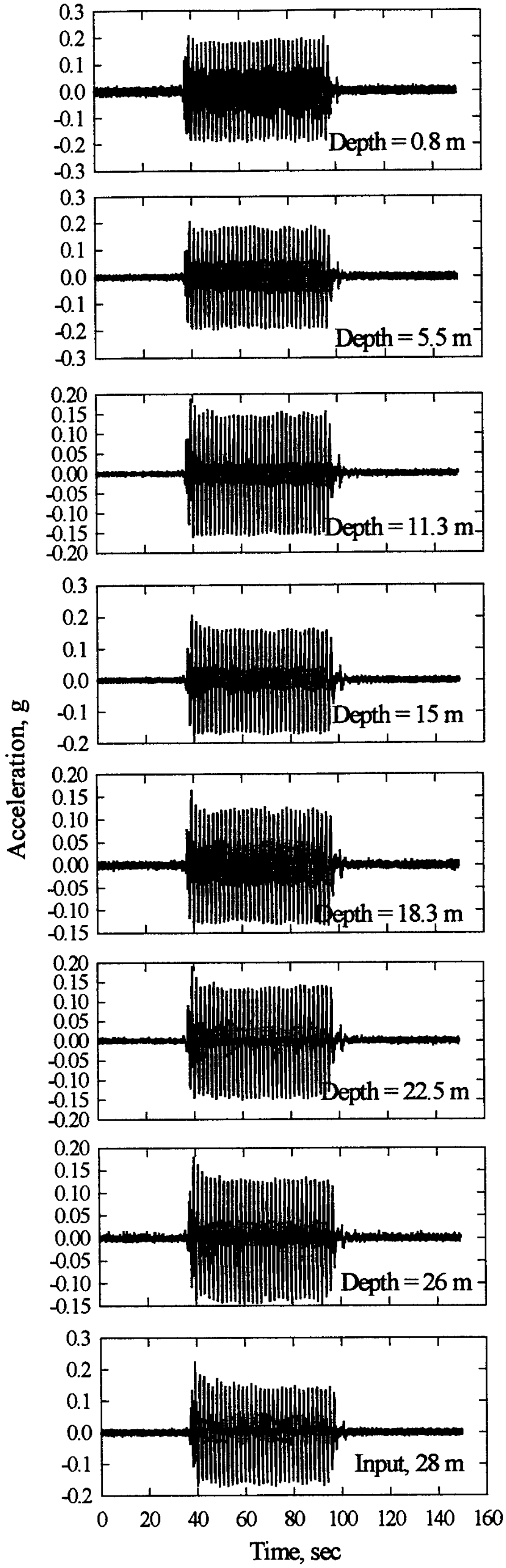
Acceleration, g
Depth = 0.8 m
Depth = 5.5 m
Depth = 11.3 m
Depth = 15 m
Depth = 18.3 m
Depth = 22.5 m
Depth = 26 m
Input, 28 m
Time, sec

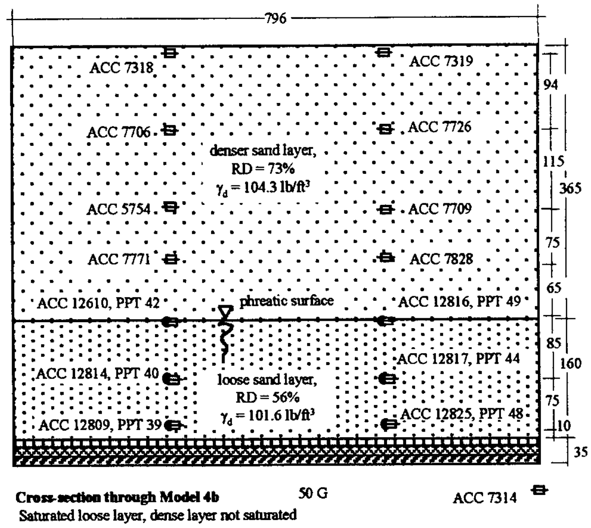
796
ACC 7318
ACC 7319
ACC 7706
ACC 7726
denser sand layer,
RD = 73%
γ_d = 104.3 lb/ft^3
ACC 5754
ACC 7709
ACC 7771
ACC 7828
ACC 12610, PPT 42
phreatic surface
ACC 12816, PPT 49
ACC 12817, PPT 44
ACC 12814, PPT 40
loose sand layer,
RD = 56%
γ_d = 101.6 lb/ft^3
ACC 12809, PPT 39
ACC 12825, PPT 48
94
115
365
75
65
85
160
75
10
35
Cross-section through Model 4b
50 G
ACC 7314
Saturated loose layer, dense layer not saturated

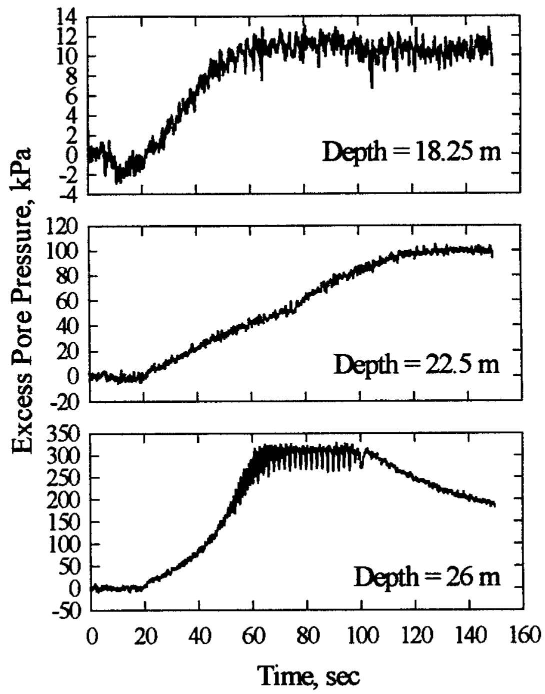
Excess Pore Pressure, kPa
Depth = 18.25 m
Depth = 22.5 m
Depth = 26 m
Time, sec

Model 4b

Model 4b-eq1

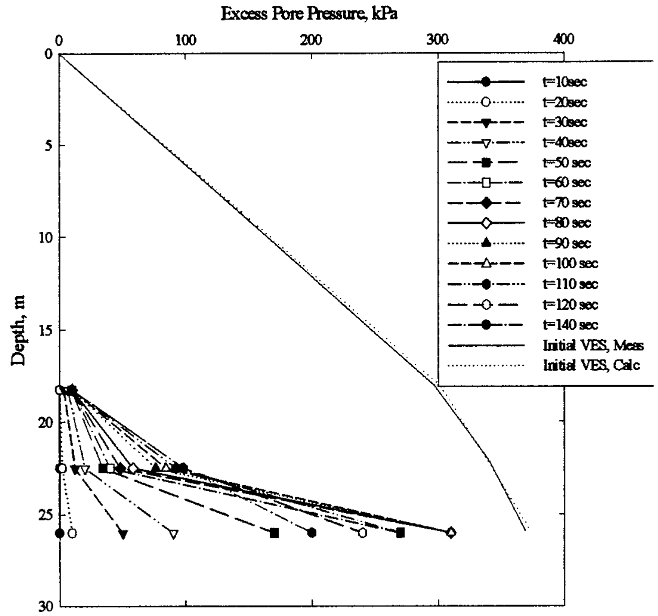

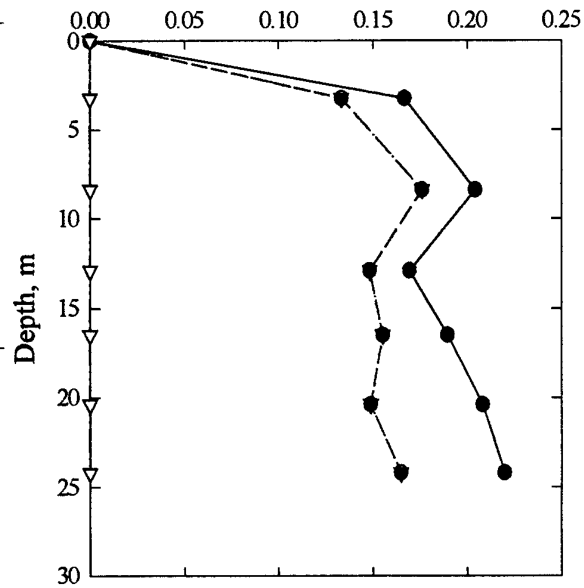

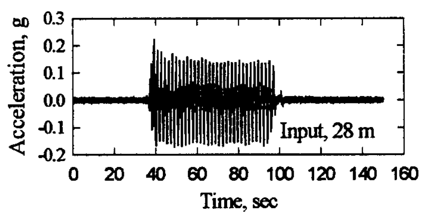

f = 0.6 Hz
a_{max} = 0.16 g

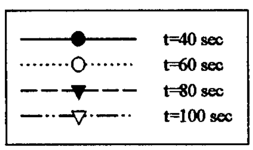

Model 4b-eq1

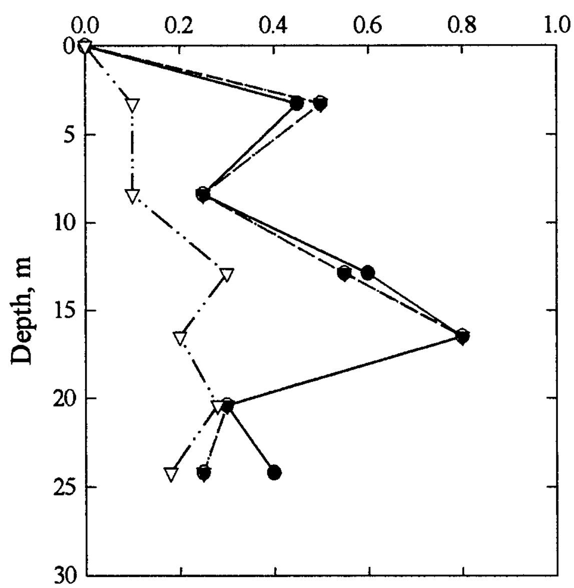

Model 4b-eq1

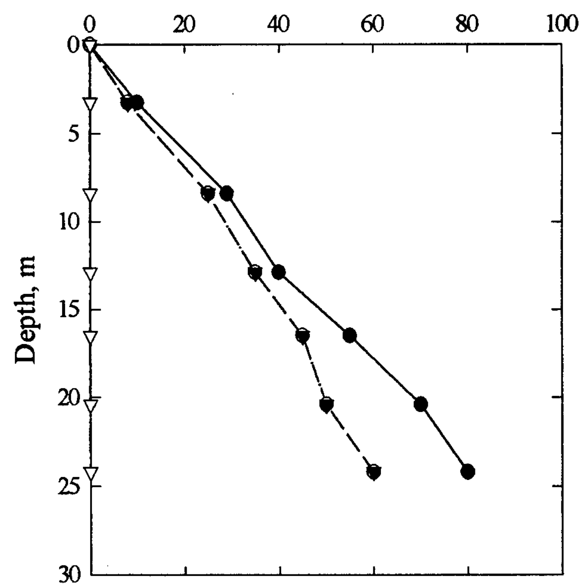

Model 4b Stress and strain isochrones

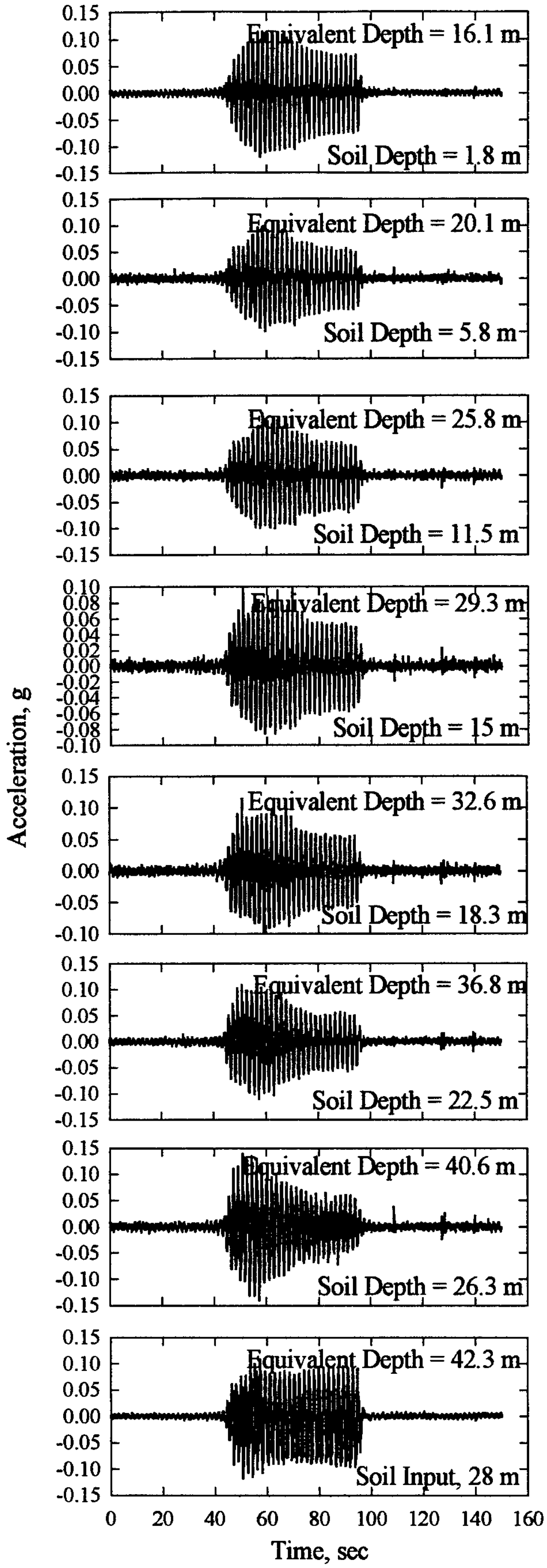
Equivalent Depth = 16.1 m
Soil Depth = 1.8 m
Equivalent Depth = 20.1 m
Soil Depth = 5.8 m
Equivalent Depth = 25.8 m
Soil Depth = 11.5 m
Equivalent Depth = 29.3 m
Soil Depth = 15 m
Equivalent Depth = 32.6 m
Soil Depth = 18.3 m
Equivalent Depth = 36.8 m
Soil Depth = 22.5 m
Equivalent Depth = 40.6 m
Soil Depth = 26.3 m
Equivalent Depth = 42.3 m
Soil Input, 28 m
Acceleration, g
Time, sec

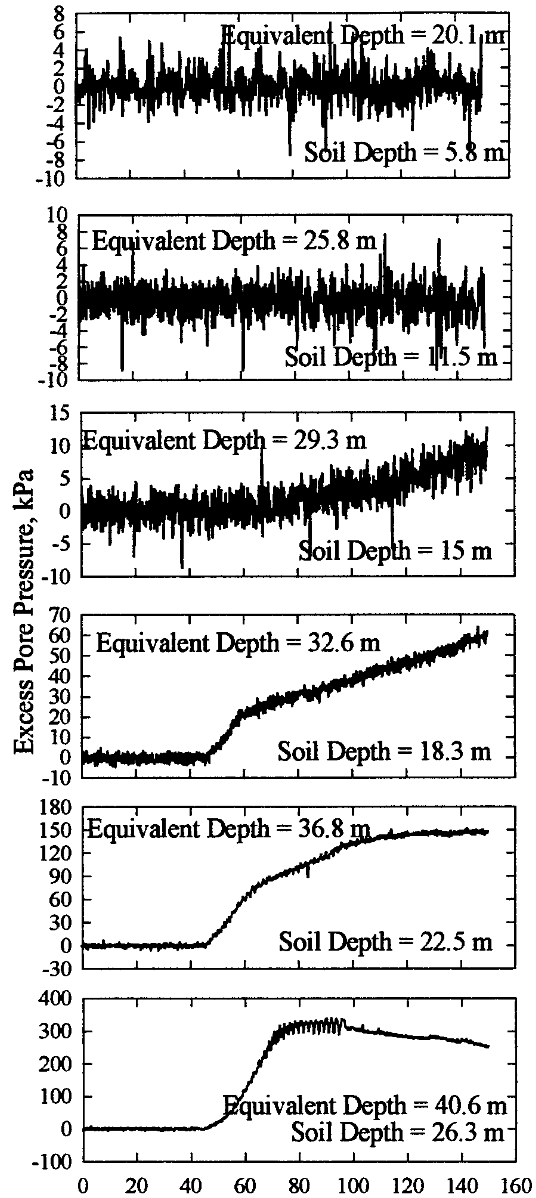
Equivalent Depth = 20.1 m
Soil Depth = 5.8 m
Equivalent Depth = 25.8 m
Soil Depth = 11.5 m
Equivalent Depth = 29.3 m
Soil Depth = 15 m
Equivalent Depth = 32.6 m
Soil Depth = 18.3 m
Equivalent Depth = 36.8 m
Soil Depth = 22.5 m
Equivalent Depth = 40.6 m
Soil Depth = 26.3 m
Excess Pore Pressure, kPa

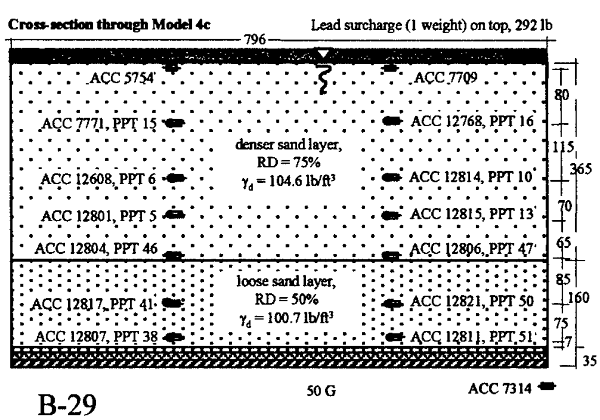
Cross-section through Model 4c
Lead surcharge (1 weight) on top, 292 lb
796
ACC 5754
ACC 7709
ACC 7771, PPT 15
ACC 12768, PPT 16
denser sand layer,
RD = 75%
γ_d = 104.6 lb/ft³
ACC 12608, PPT 6
ACC 12814, PPT 10
ACC 12801, PPT 5
ACC 12815, PPT 13
ACC 12804, PPT 46
ACC 12806, PPT 47
loose sand layer,
RD = 50%
γ_d = 100.7 lb/ft³
ACC 12817, PPT 41
ACC 12821, PPT 50
ACC 12807, PPT 38
ACC 12811, PPT 51
80
115
365
70
65
85
160
75
35
50 G
ACC 7314

Model 4c

Model 4c-eq1

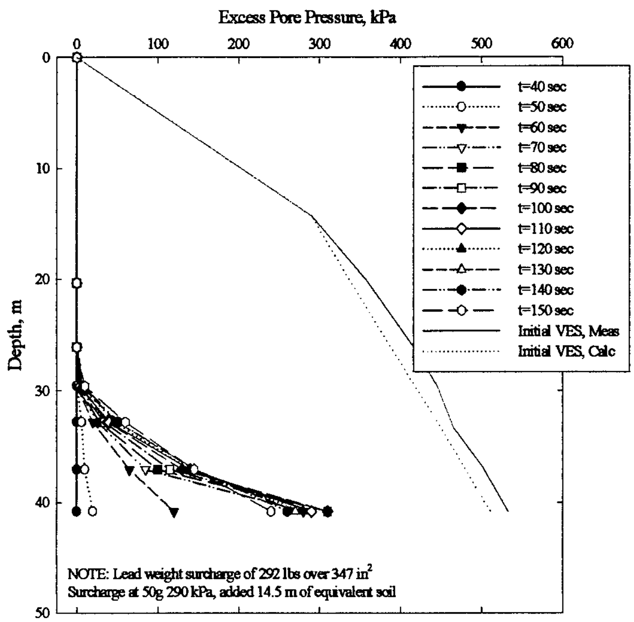

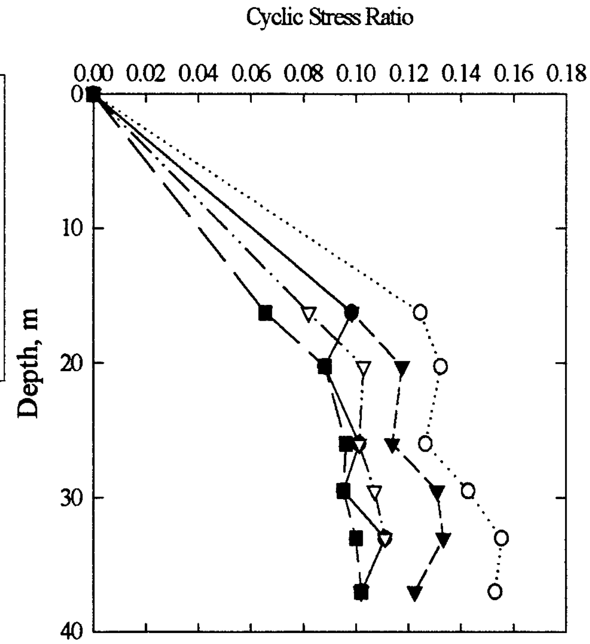

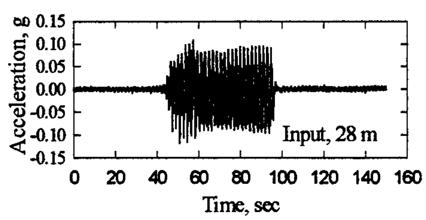

f = 0.6 Hz
a_{max} = 0.08 g

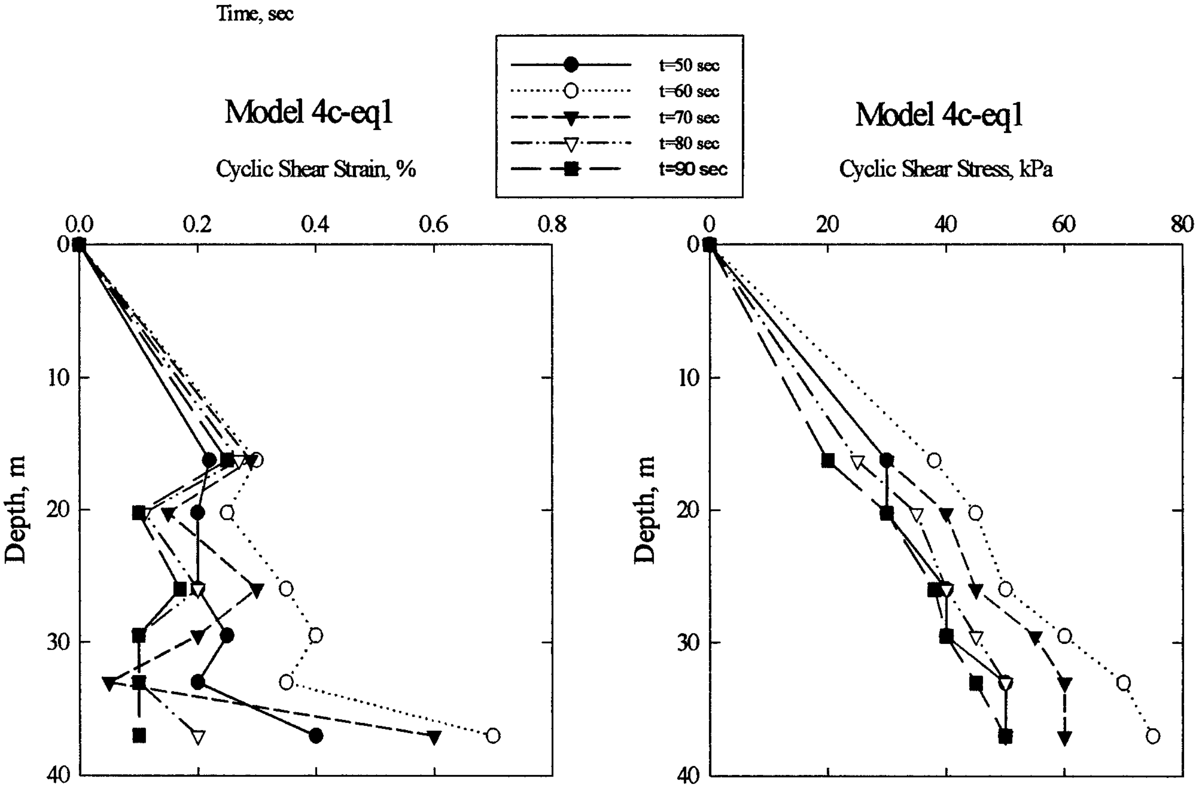

Model 4c Stress and strain isochrones

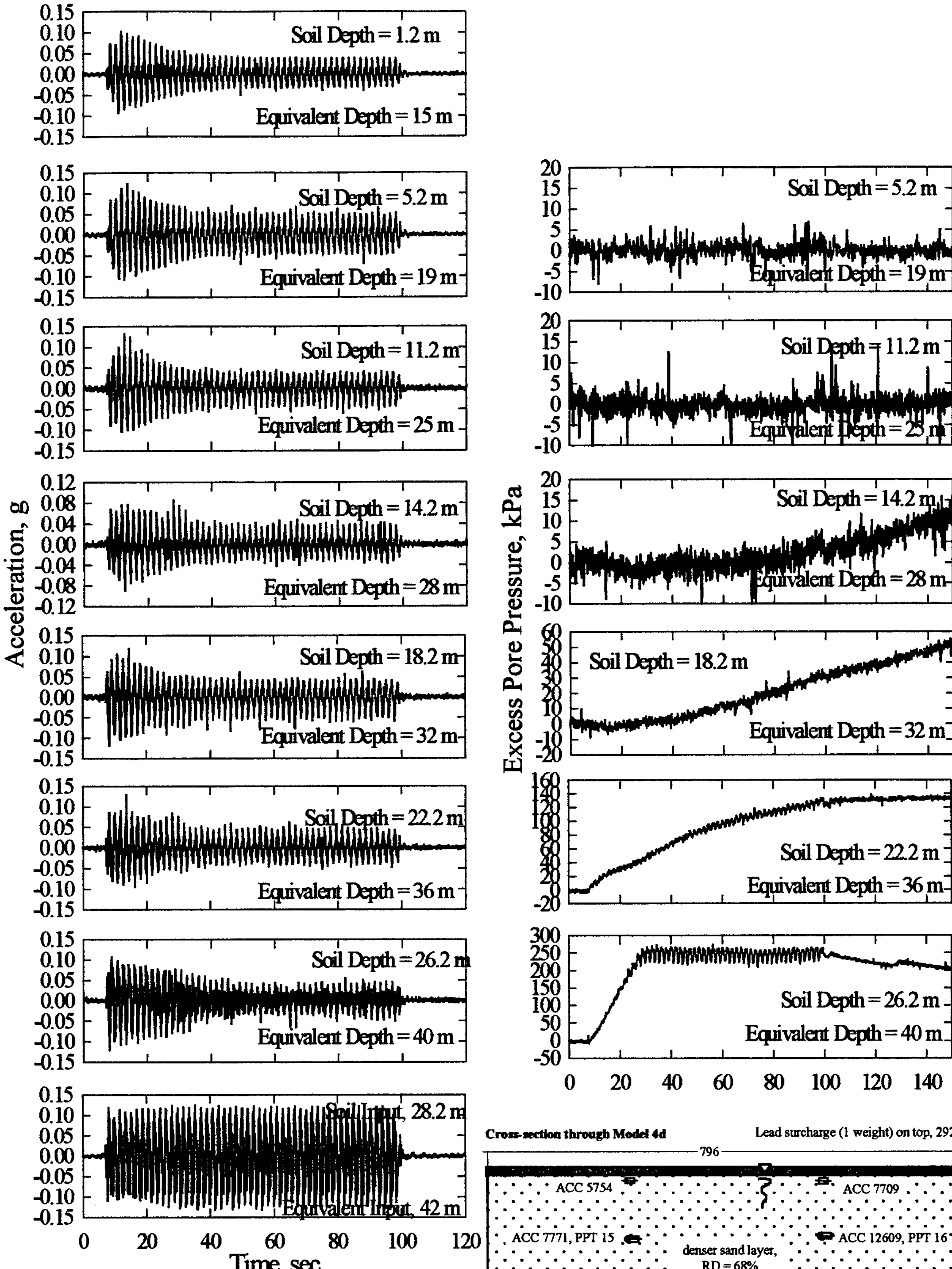

Soil Depth = 1.2 m
Equivalent Depth = 15 m
Soil Depth = 5.2 m
Equivalent Depth = 19 m
Soil Depth = 11.2 m
Equivalent Depth = 25 m
Soil Depth = 14.2 m
Equivalent Depth = 28 m
Soil Depth = 18.2 m
Equivalent Depth = 32 m
Soil Depth = 22.2 m
Equivalent Depth = 36 m
Soil Depth = 26.2 m
Equivalent Depth = 40 m
Soil Input, 28.2 m
Equivalent Input, 42 m
Acceleration, g
Time, sec
Excess Pore Pressure, kPa

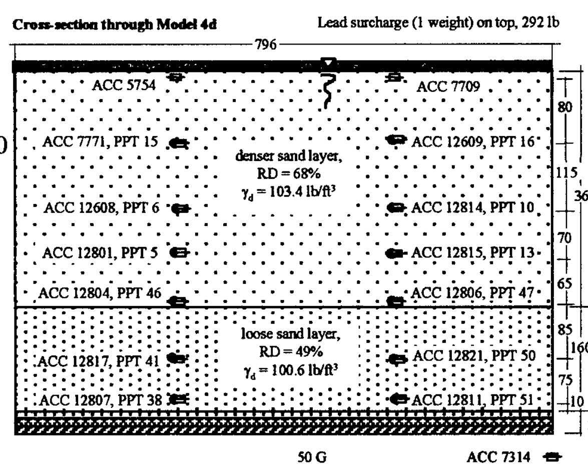

Cross-section through Model 4d
Lead surcharge (1 weight) on top, 292 lb
796
ACC 5754
ACC 7709
ACC 7771, PPT 15
ACC 12609, PPT 16
denser sand layer,
RD = 68%
γ_d = 103.4 lb/ft³
ACC 12608, PPT 6
ACC 12814, PPT 10
ACC 12801, PPT 5
ACC 12815, PPT 13
ACC 12804, PPT 46
ACC 12806, PPT 47
loose sand layer,
RD = 49%
γ_d = 100.6 lb/ft³
ACC 12817, PPT 41
ACC 12821, PPT 50
ACC 12807, PPT 38
ACC 12811, PPT 51
80
115
365
70
65
85
160
75
10
35
50 G
ACC 7314

Model 4d

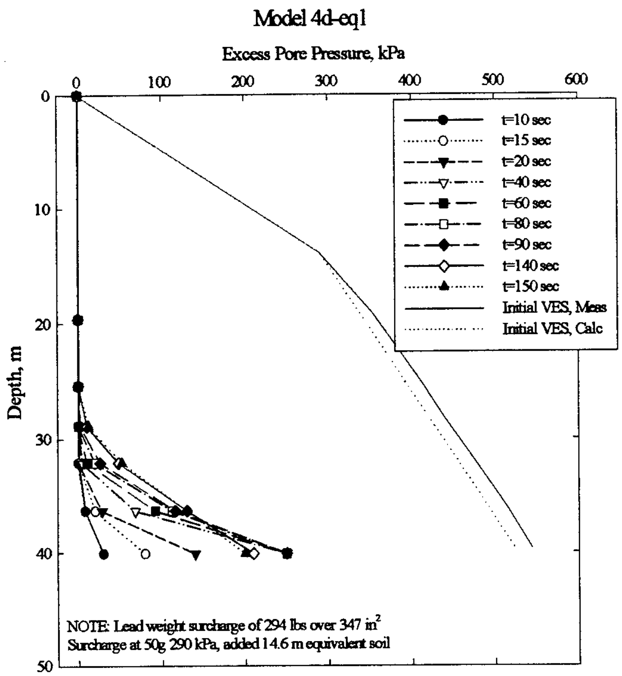

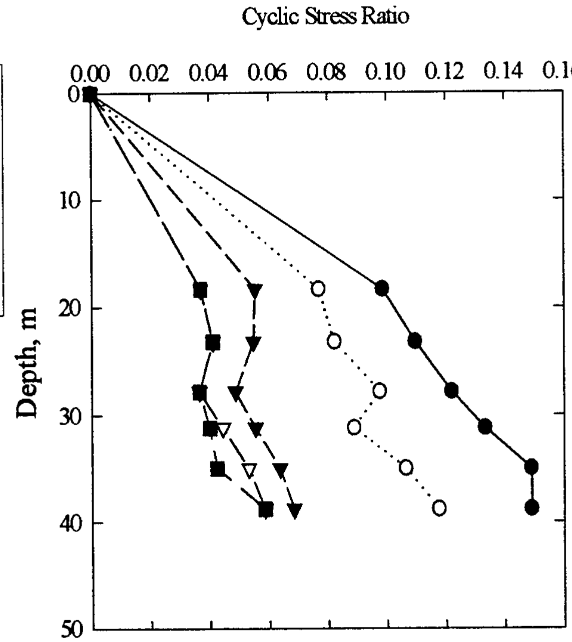

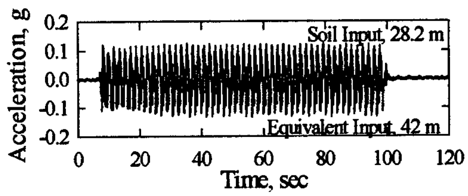

f = 0.6 Hz
a_{max} = 0.1 g

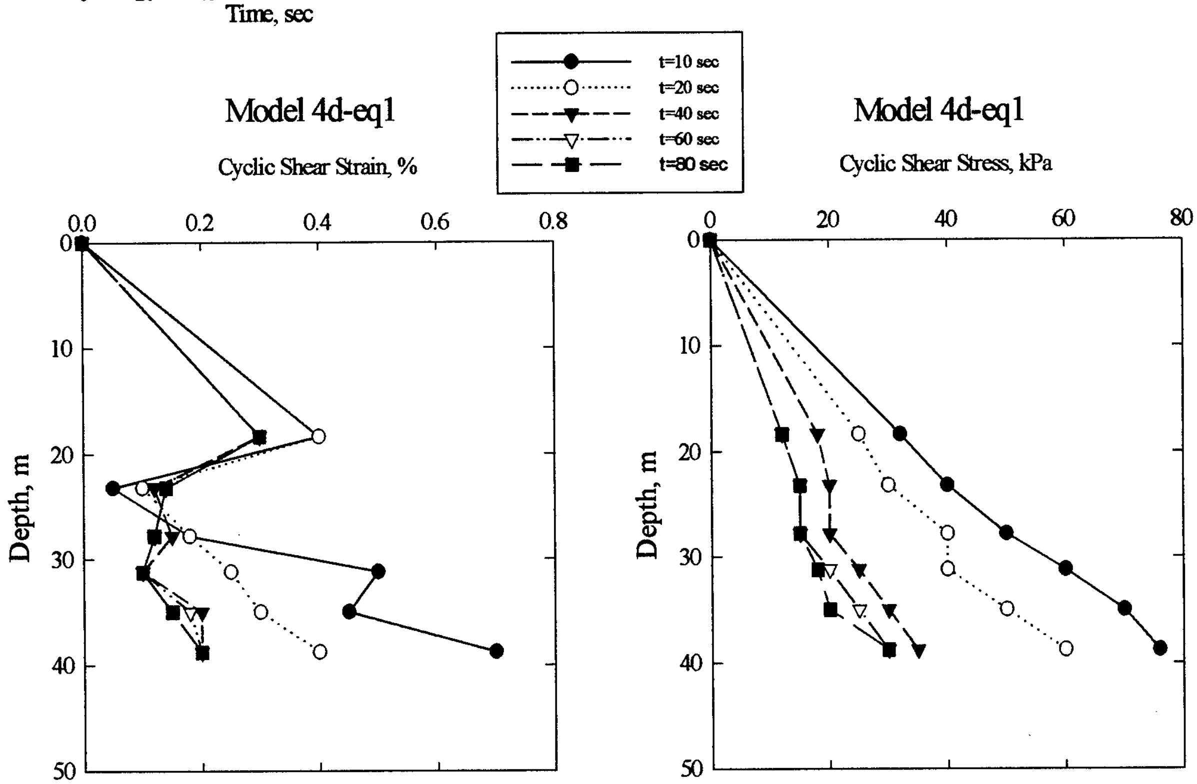

Model 4d Stress and strain isochrones

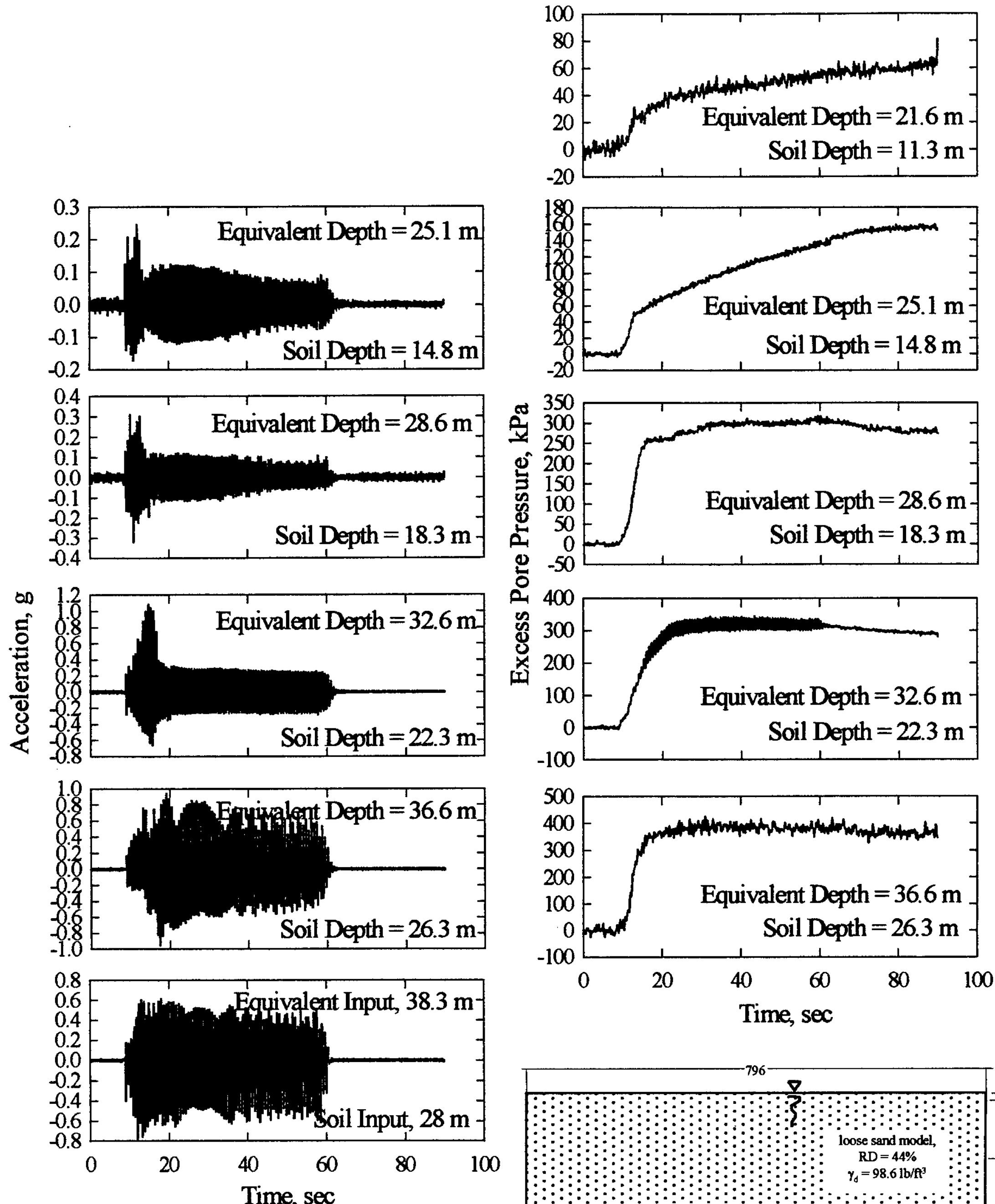
Acceleration, g
Equivalent Depth = 25.1 m
Soil Depth = 14.8 m
Equivalent Depth = 28.6 m
Soil Depth = 18.3 m
Equivalent Depth = 32.6 m
Soil Depth = 22.3 m
Equivalent Depth = 36.6 m
Soil Depth = 26.3 m
Equivalent Input, 38.3 m
Soil Input, 28 m
Time, sec
Excess Pore Pressure, kPa
Equivalent Depth = 21.6 m
Soil Depth = 11.3 m
Equivalent Depth = 25.1 m
Soil Depth = 14.8 m
Equivalent Depth = 28.6 m
Soil Depth = 18.3 m
Equivalent Depth = 32.6 m
Soil Depth = 22.3 m
Equivalent Depth = 36.6 m
Soil Depth = 26.3 m
Time, sec

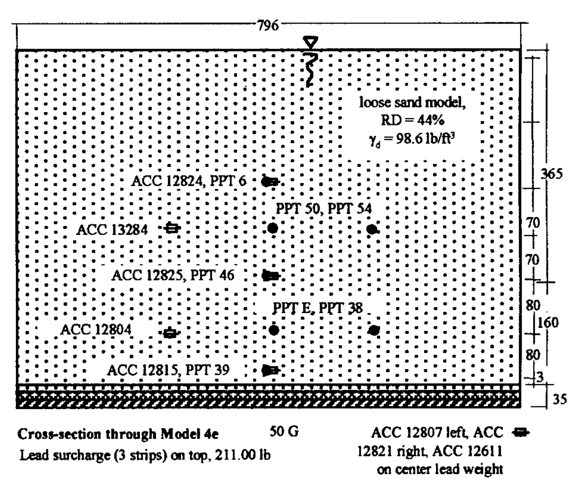
796
loose sand model,
RD = 44%
γ_d = 98.6 lb/ft³
ACC 12824, PPT 6
PPT 50, PPT 54
ACC 13284
ACC 12825, PPT 46
PPT E, PPT 38
ACC 12804
ACC 12815, PPT 39
365
70
70
80
160
80
3
35
Cross-section through Model 4e
50 G
Lead surcharge (3 strips) on top, 211.00 lb
ACC 12807 left, ACC 12821 right, ACC 12611 on center lead weight

Model 4e

Model 4e-eq1

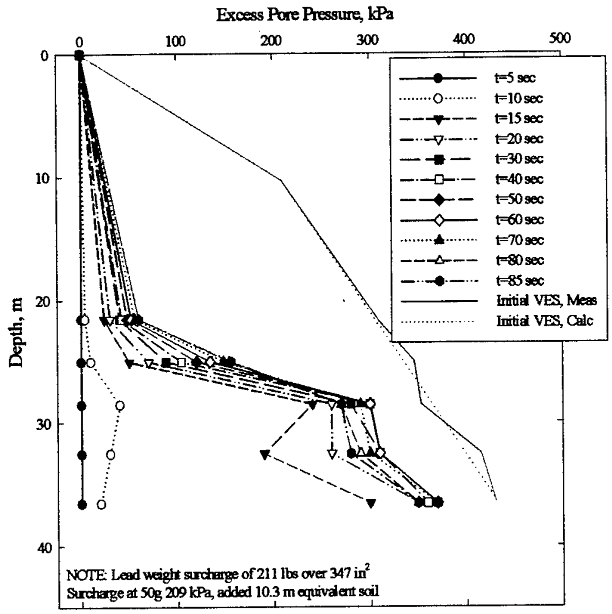

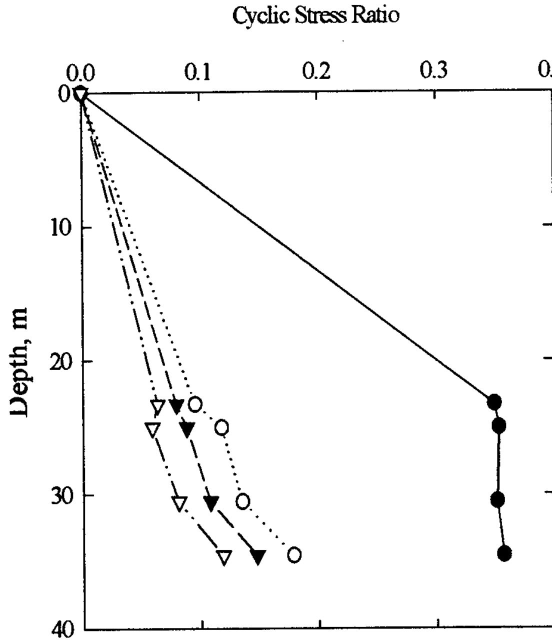

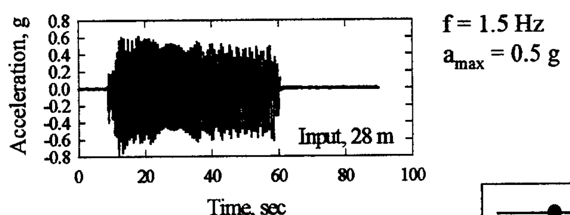

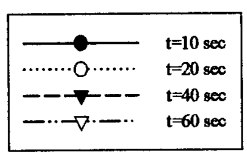

Model 4e-eq1

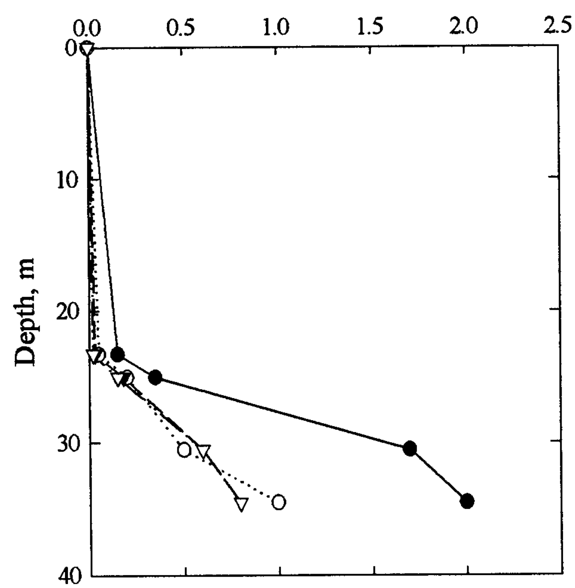

Model 4e-eq1

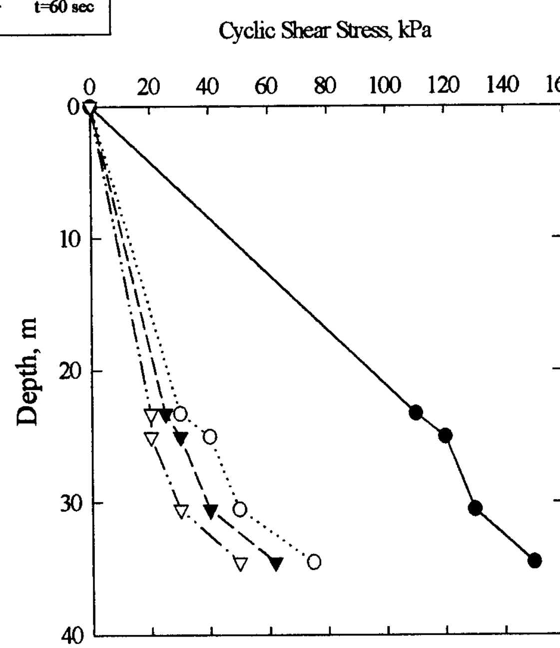

Model 4e Stress and strain isochrones

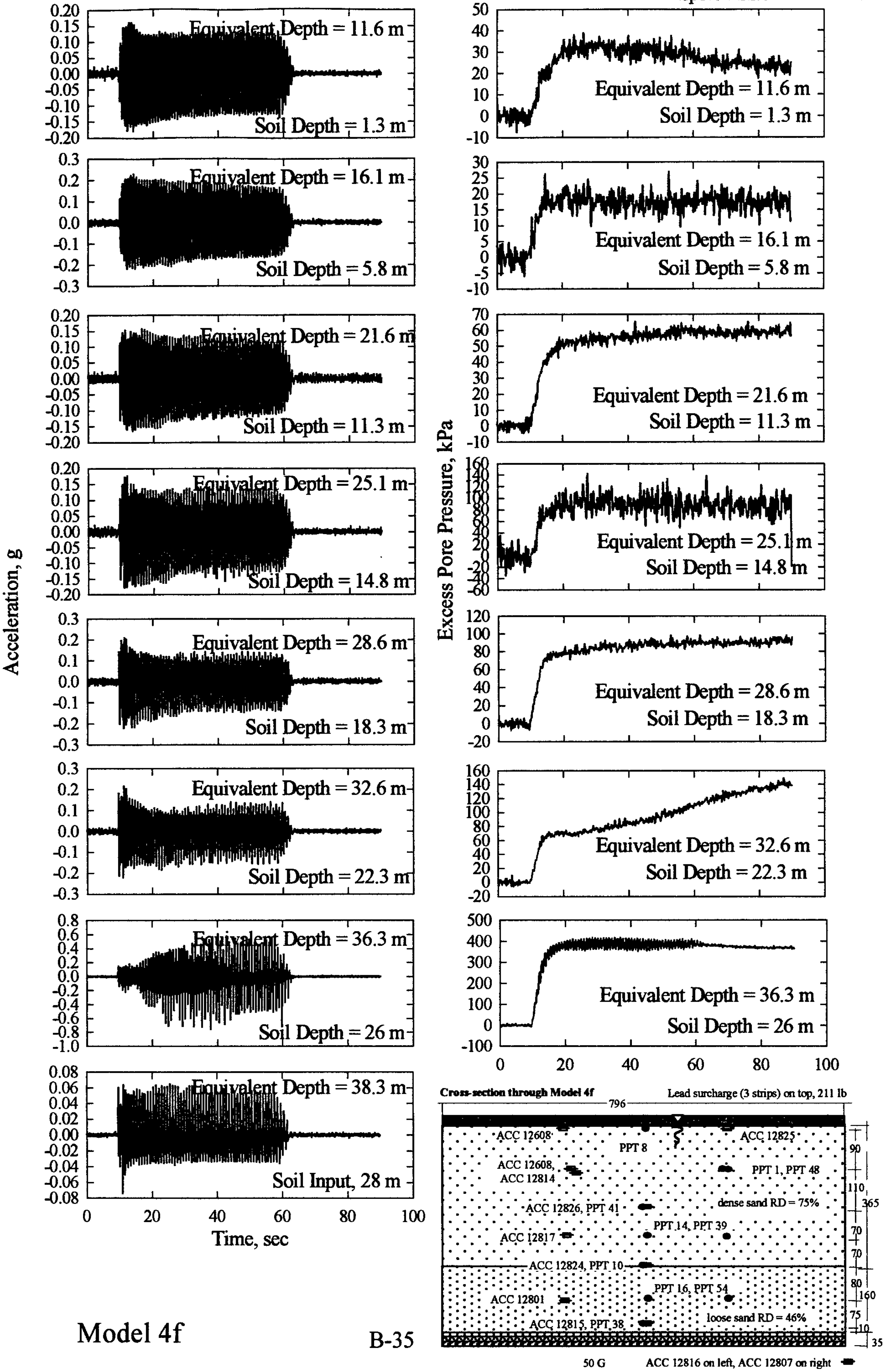
Acceleration, g
Equivalent Depth = 11.6 m
Soil Depth = 1.3 m
Equivalent Depth = 16.1 m
Soil Depth = 5.8 m
Equivalent Depth = 21.6 m
Soil Depth = 11.3 m
Equivalent Depth = 25.1 m
Soil Depth = 14.8 m
Equivalent Depth = 28.6 m
Soil Depth = 18.3 m
Equivalent Depth = 32.6 m
Soil Depth = 22.3 m
Equivalent Depth = 36.3 m
Soil Depth = 26 m
Equivalent Depth = 38.3 m
Soil Input, 28 m
Time, sec
Excess Pore Pressure, kPa
Cross-section through Model 4f
Lead surcharge (3 strips) on top, 211 lb
796
ACC 12608
ACC 12825
PPT 8
ACC 12608, ACC 12814
PPT 1, PPT 48
dense sand RD = 75%
ACC 12826, PPT 41
PPT 14, PPT 39
ACC 12817
ACC 12824, PPT 10
PPT 16, PPT 54
ACC 12801
loose sand RD = 46%
ACC 12815, PPT 38
50 G
ACC 12816 on left, ACC 12807 on right
90
110
365
70
70
80
160
75
10
35

Model 4f

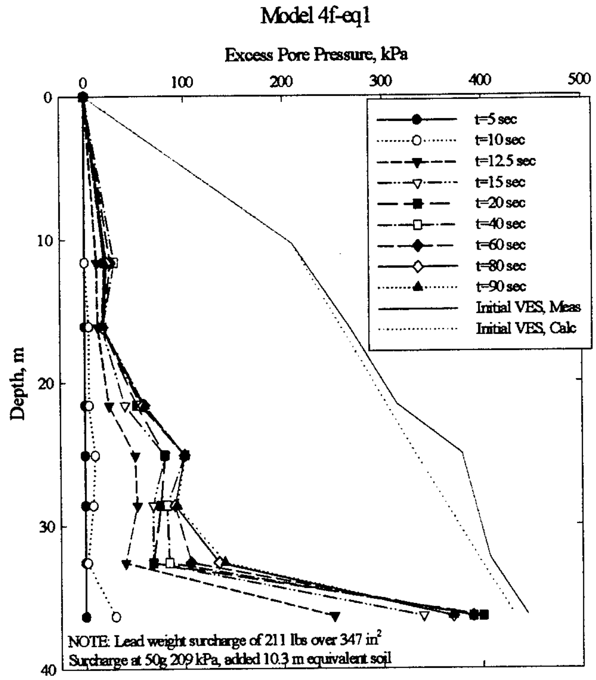

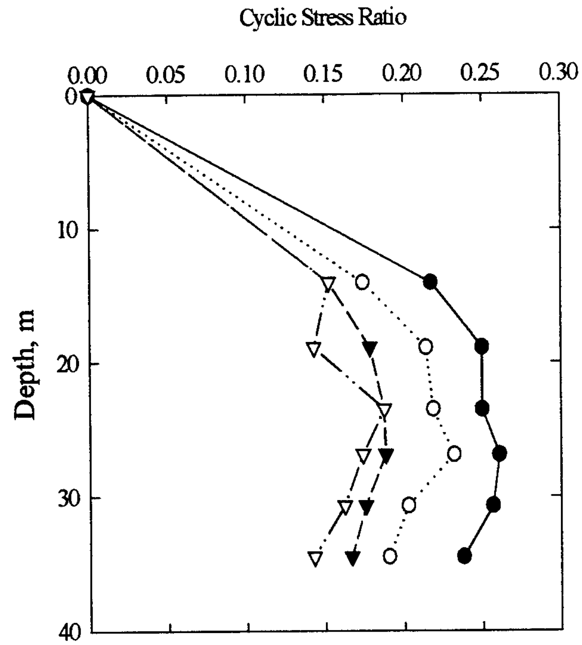

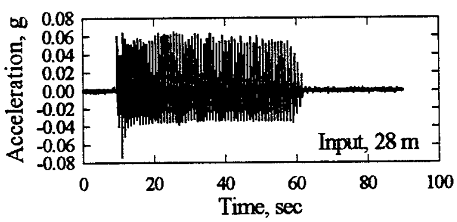

f = 1.2 Hz
a_{max} = 0.06 g

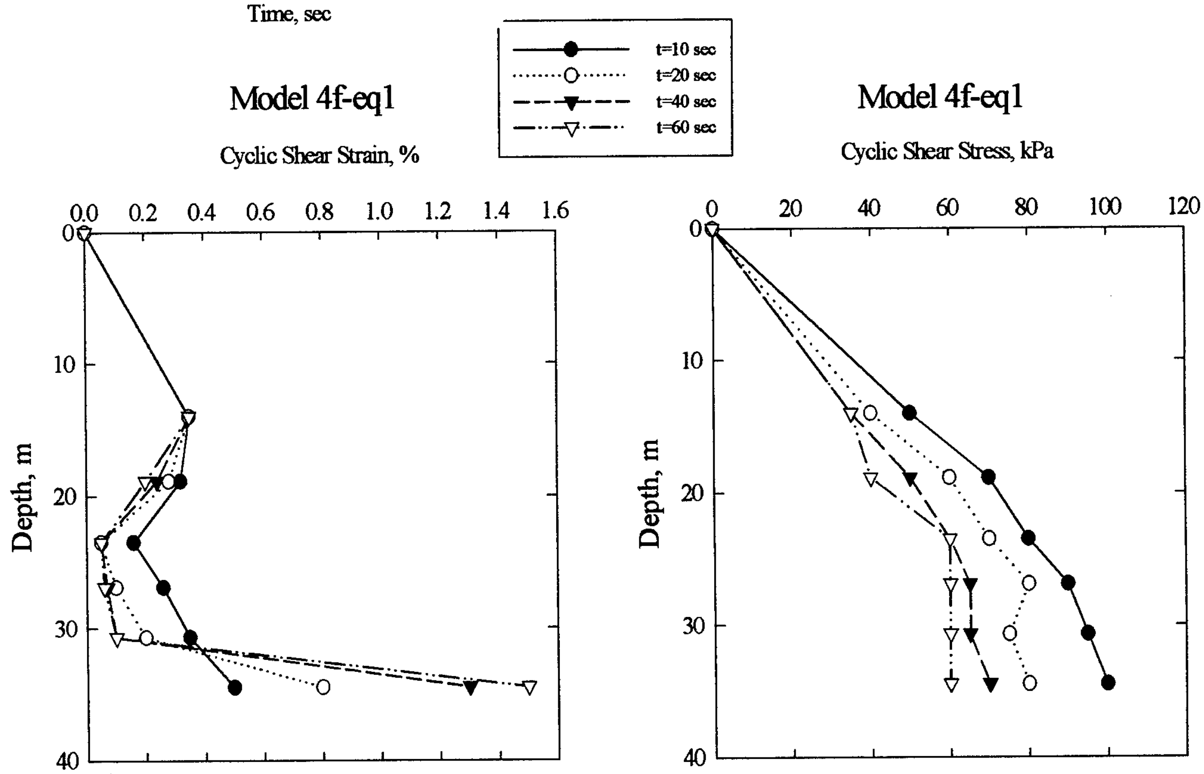

Model 4f Stress and strain isochrones

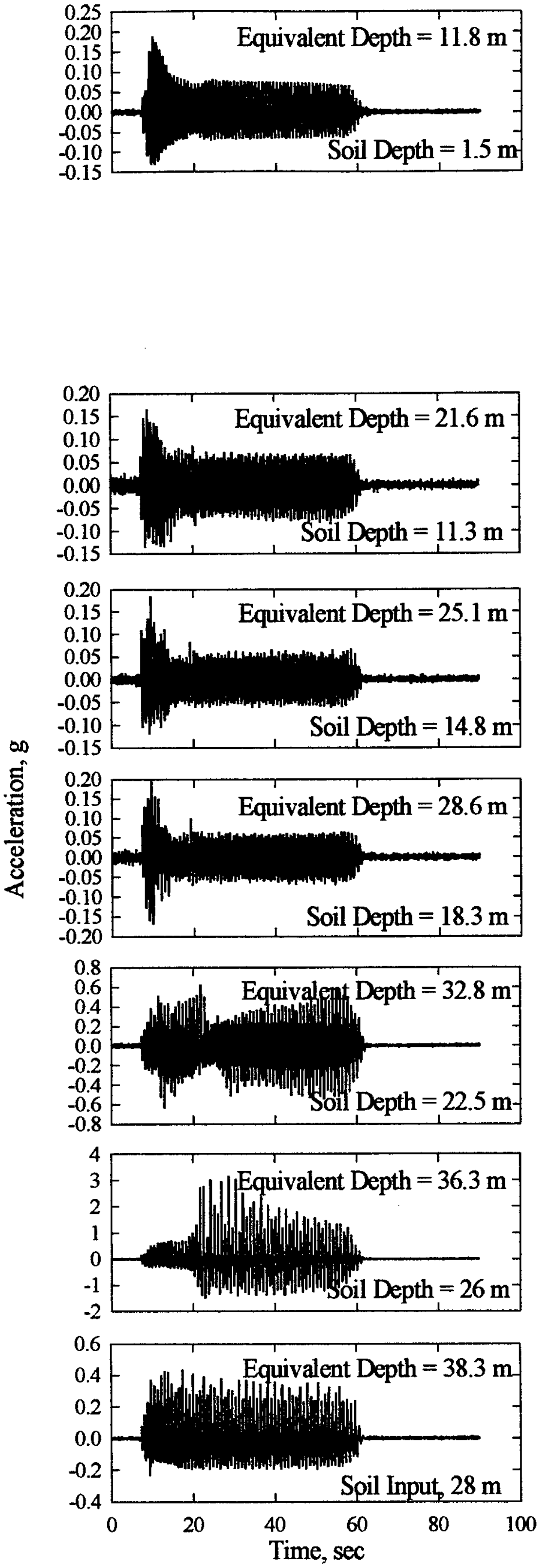
Equivalent Depth = 11.8 m
Soil Depth = 1.5 m
Equivalent Depth = 21.6 m
Soil Depth = 11.3 m
Equivalent Depth = 25.1 m
Soil Depth = 14.8 m
Equivalent Depth = 28.6 m
Soil Depth = 18.3 m
Equivalent Depth = 32.8 m
Soil Depth = 22.5 m
Equivalent Depth = 36.3 m
Soil Depth = 26 m
Equivalent Depth = 38.3 m
Soil Input, 28 m
Acceleration, g
Time, sec

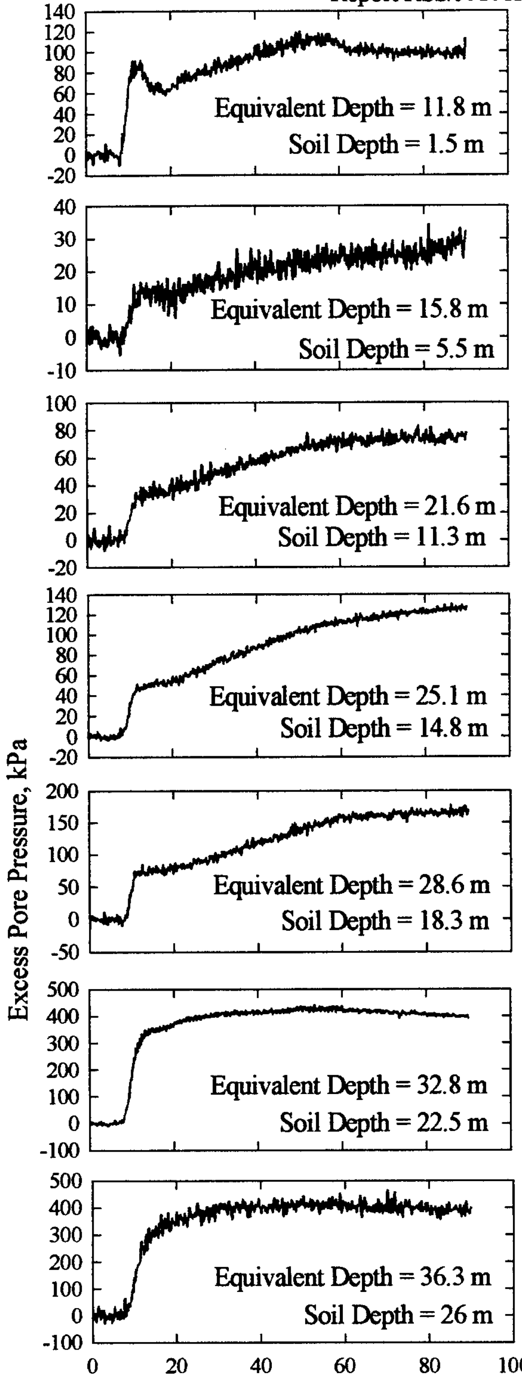
Equivalent Depth = 11.8 m
Soil Depth = 1.5 m
Equivalent Depth = 15.8 m
Soil Depth = 5.5 m
Equivalent Depth = 21.6 m
Soil Depth = 11.3 m
Equivalent Depth = 25.1 m
Soil Depth = 14.8 m
Equivalent Depth = 28.6 m
Soil Depth = 18.3 m
Equivalent Depth = 32.8 m
Soil Depth = 22.5 m
Equivalent Depth = 36.3 m
Soil Depth = 26 m
Excess Pore Pressure, kPa

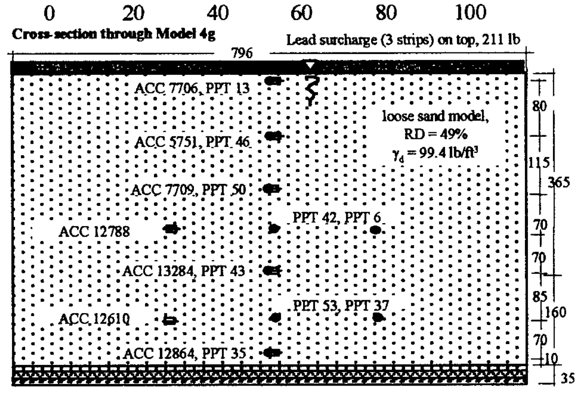
Cross-section through Model 4g
Lead surcharge (3 strips) on top, 211 lb
796
ACC 7706, PPT 13
ACC 5751, PPT 46
ACC 7709, PPT 50
ACC 12788
PPT 42, PPT 6
ACC 13284, PPT 43
ACC 12610
PPT 53, PPT 37
ACC 12864, PPT 35
loose sand model,
RD = 49%
γ_d = 99.4 lb/ft³
80
115
365
70
70
85
160
70
10
35
50G ACC 12821 on left & ACC 12611 on right, ACC 12807 on center lead weight

Model 4g

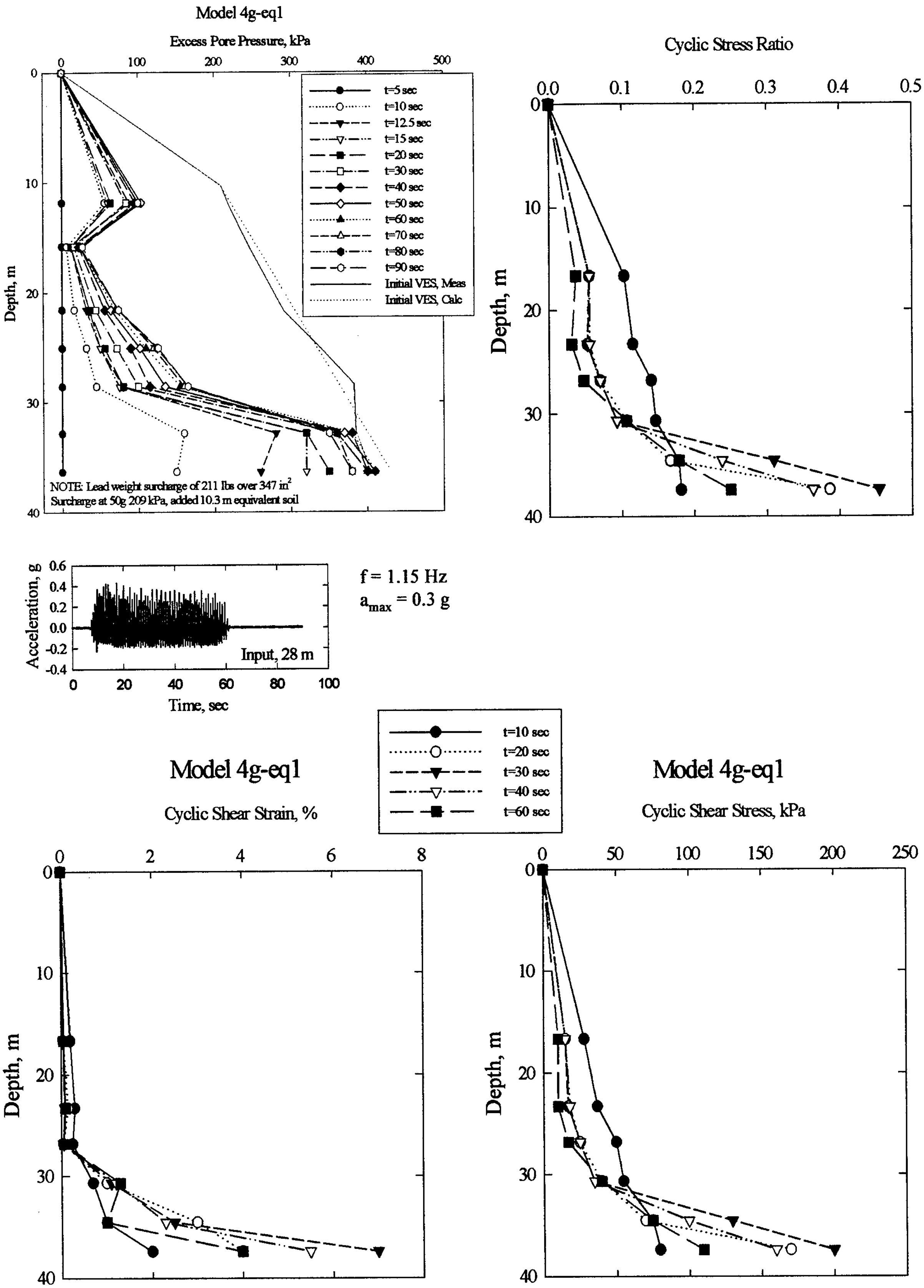

Model 4g Stress and strain isochrones

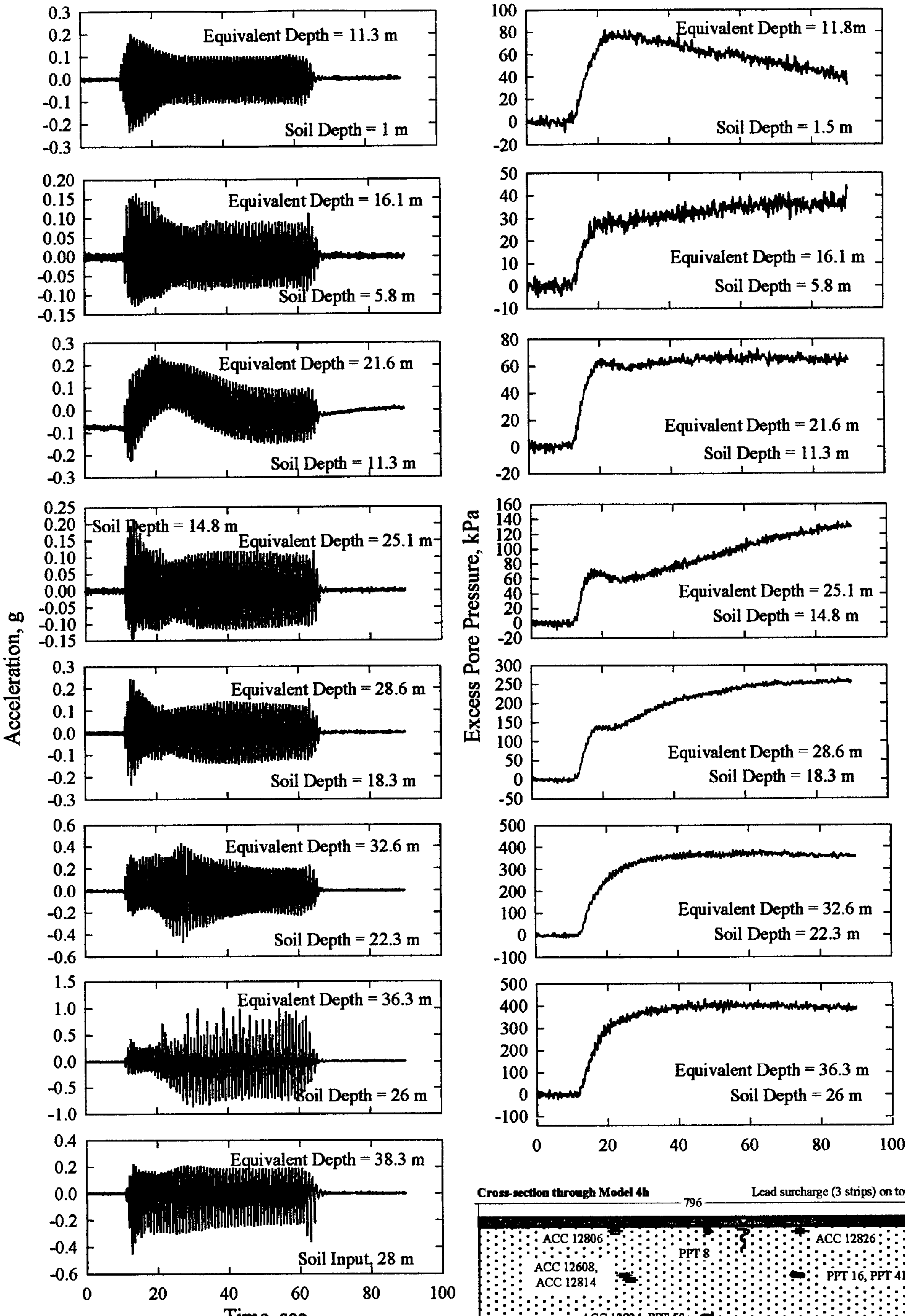
Acceleration, g
Excess Pore Pressure, kPa
Time, sec
Equivalent Depth = 11.3 m
Soil Depth = 1 m
Equivalent Depth = 11.8m
Soil Depth = 1.5 m
Equivalent Depth = 16.1 m
Soil Depth = 5.8 m
Equivalent Depth = 16.1 m
Soil Depth = 5.8 m
Equivalent Depth = 21.6 m
Soil Depth = 11.3 m
Equivalent Depth = 21.6 m
Soil Depth = 11.3 m
Soil Depth = 14.8 m
Equivalent Depth = 25.1 m
Equivalent Depth = 25.1 m
Soil Depth = 14.8 m
Equivalent Depth = 28.6 m
Soil Depth = 18.3 m
Equivalent Depth = 28.6 m
Soil Depth = 18.3 m
Equivalent Depth = 32.6 m
Soil Depth = 22.3 m
Equivalent Depth = 32.6 m
Soil Depth = 22.3 m
Equivalent Depth = 36.3 m
Soil Depth = 26 m
Equivalent Depth = 36.3 m
Soil Depth = 26 m
Equivalent Depth = 38.3 m
Soil Input, 28 m

Model 4h

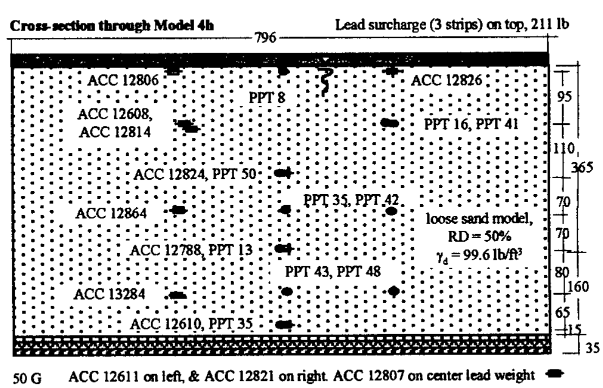
Cross-section through Model 4h
796
Lead surcharge (3 strips) on top, 211 lb
ACC 12806
PPT 8
ACC 12826
ACC 12608,
ACC 12814
PPT 16, PPT 41
ACC 12824, PPT 50
PPT 35, PPT 42
ACC 12864
loose sand model,
RD = 50%
γ_d = 99.6 lb/ft^3
ACC 12788, PPT 13
PPT 43, PPT 48
ACC 13284
ACC 12610, PPT 35
95
110
365
70
70
80
160
65
15
35
50 G
ACC 12611 on left, & ACC 12821 on right. ACC 12807 on center lead weight

Model 4h-eq1

Excess Pore Pressure, kPa

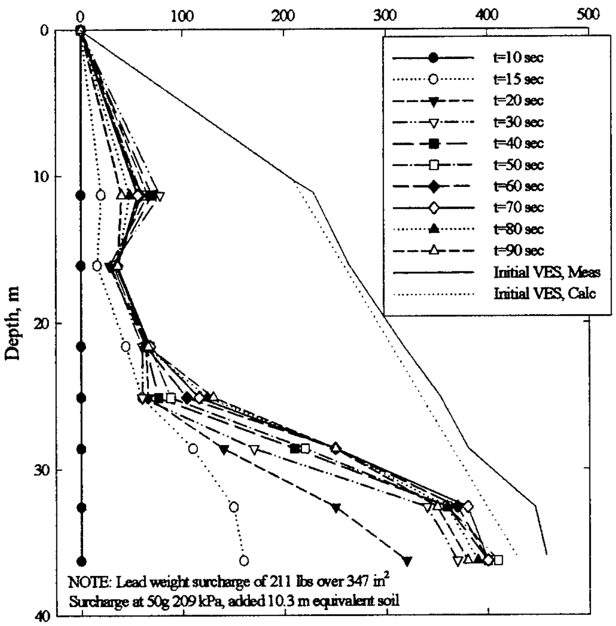

Cyclic Stress Ratio

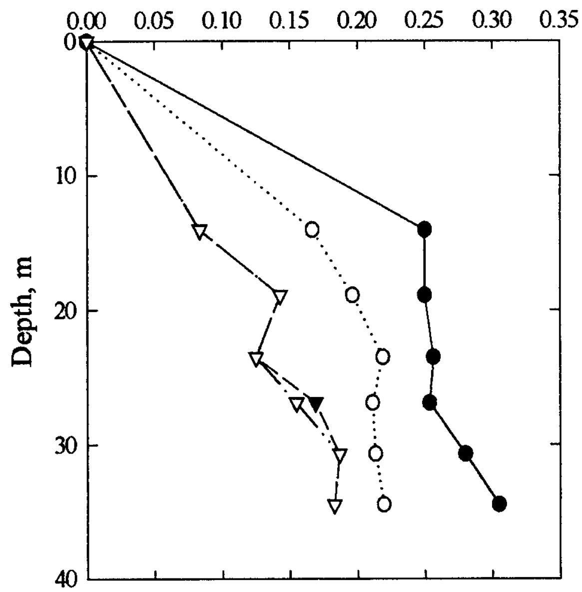

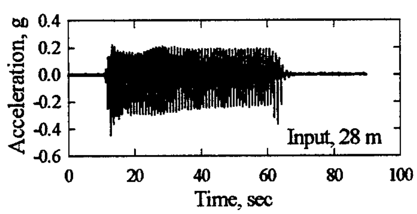

f = 1.1 Hz
a_{max} = 0.25 g

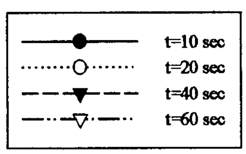

Model 4h-eq1

Cyclic Shear Strain, %

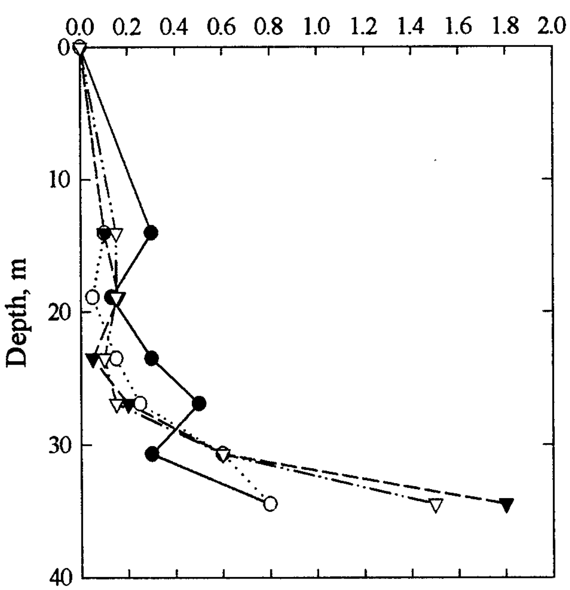

Model 4h-eq1

Cyclic Shear Stress, kPa

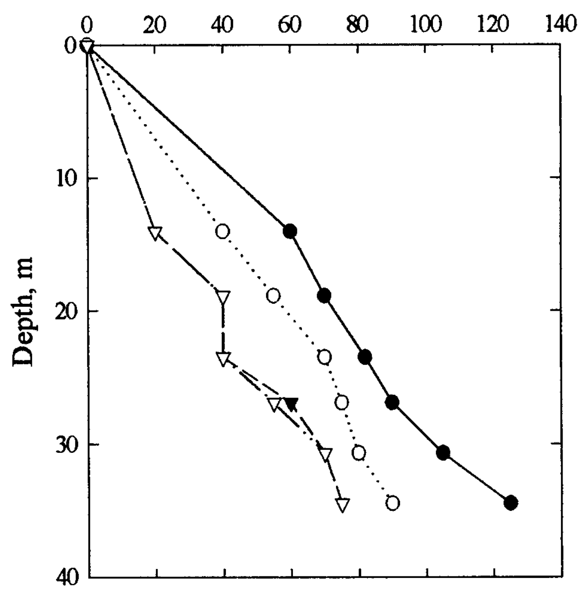

Model 4h Stress and strain isochrones

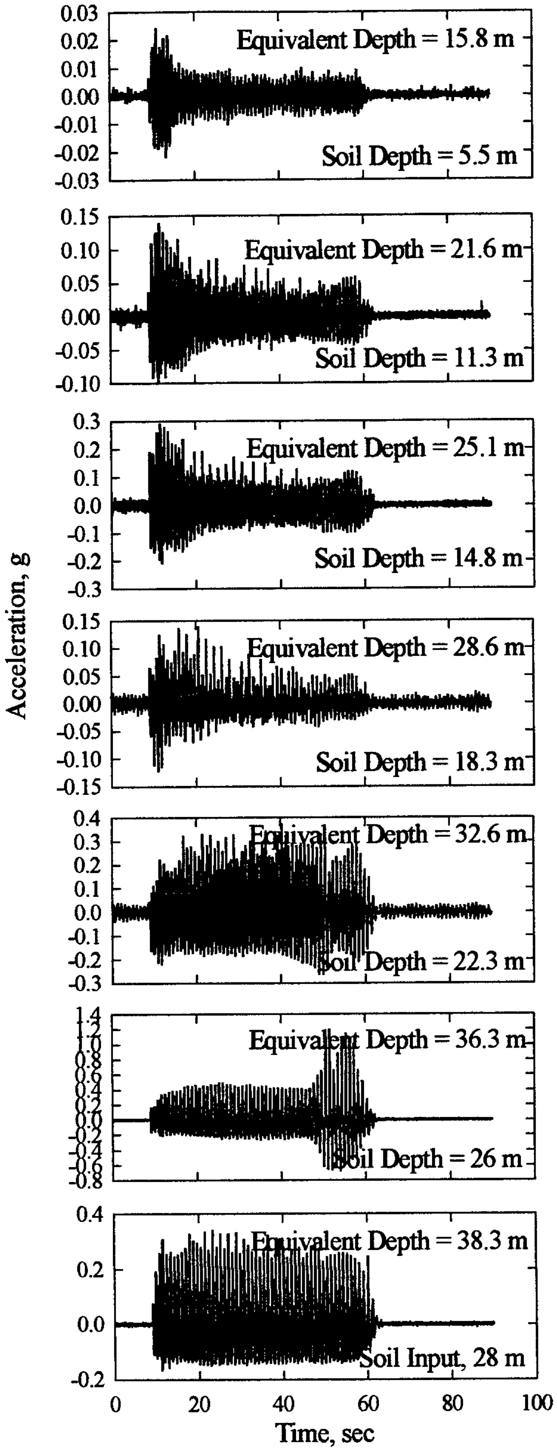

Acceleration, g
Equivalent Depth = 15.8 m
Soil Depth = 5.5 m
Equivalent Depth = 21.6 m
Soil Depth = 11.3 m
Equivalent Depth = 25.1 m
Soil Depth = 14.8 m
Equivalent Depth = 28.6 m
Soil Depth = 18.3 m
Equivalent Depth = 32.6 m
Soil Depth = 22.3 m
Equivalent Depth = 36.3 m
Soil Depth = 26 m
Equivalent Depth = 38.3 m
Soil Input, 28 m
Time, sec

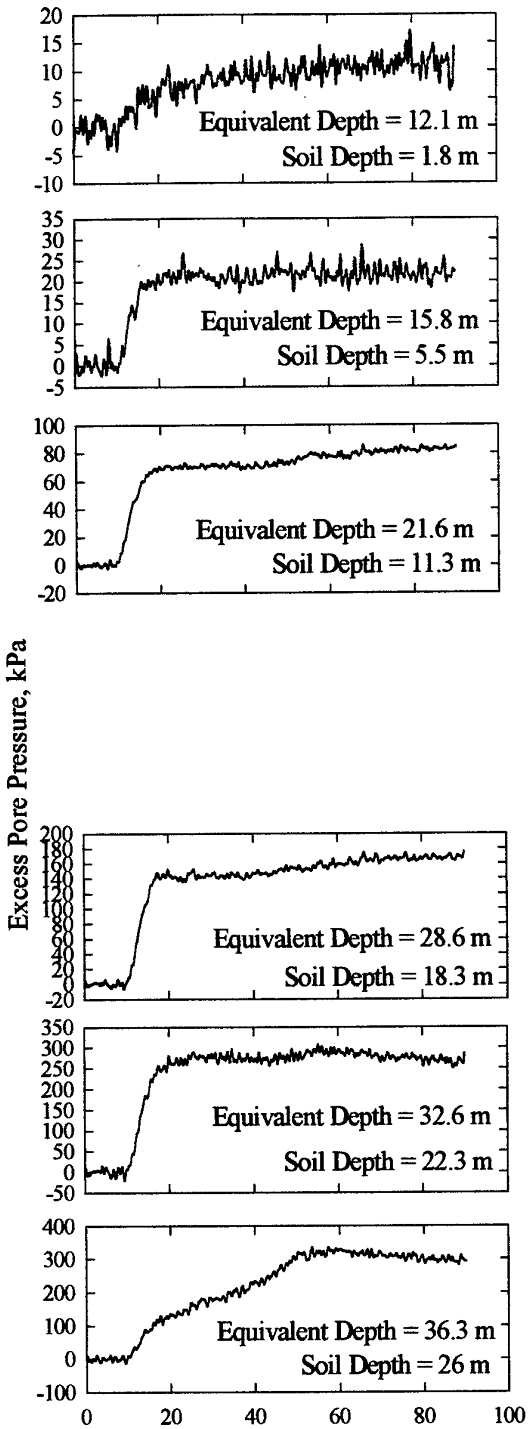

Excess Pore Pressure, kPa
Equivalent Depth = 12.1 m
Soil Depth = 1.8 m
Equivalent Depth = 15.8 m
Soil Depth = 5.5 m
Equivalent Depth = 21.6 m
Soil Depth = 11.3 m
Equivalent Depth = 28.6 m
Soil Depth = 18.3 m
Equivalent Depth = 32.6 m
Soil Depth = 22.3 m
Equivalent Depth = 36.3 m
Soil Depth = 26 m

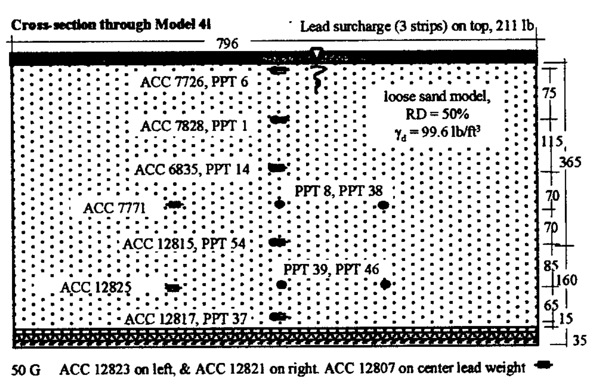

Cross-section through Model 4i
Lead surcharge (3 strips) on top, 211 lb
796
ACC 7726, PPT 6
ACC 7828, PPT 1
ACC 6835, PPT 14
PPT 8, PPT 38
ACC 7771
ACC 12815, PPT 54
PPT 39, PPT 46
ACC 12825
ACC 12817, PPT 37
loose sand model,
RD = 50%
γ_d = 99.6 lb/ft³
50 G ACC 12823 on left, & ACC 12821 on right. ACC 12807 on center lead weight

Model 4i

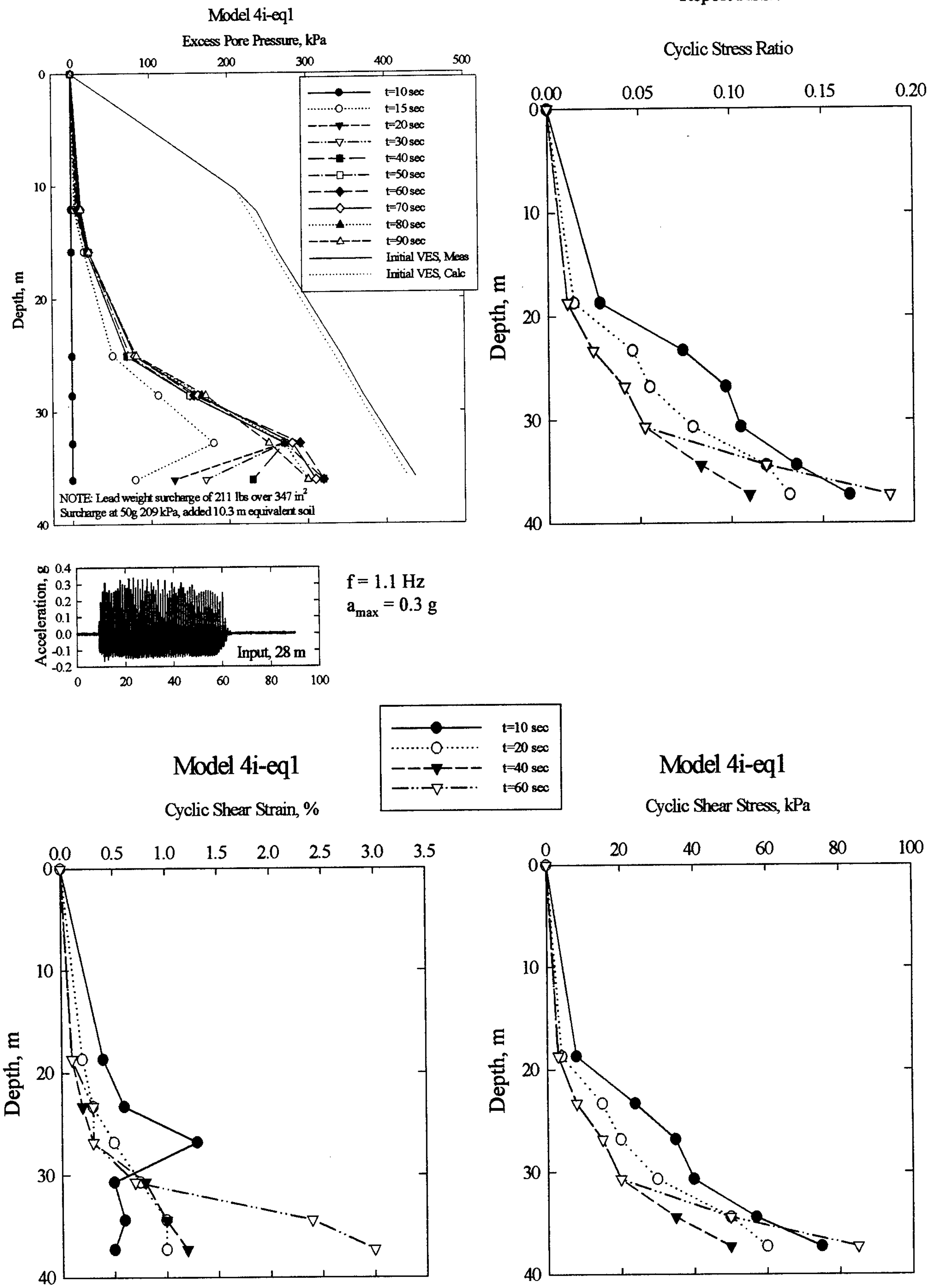

Model 4i Stress and strain isochrones

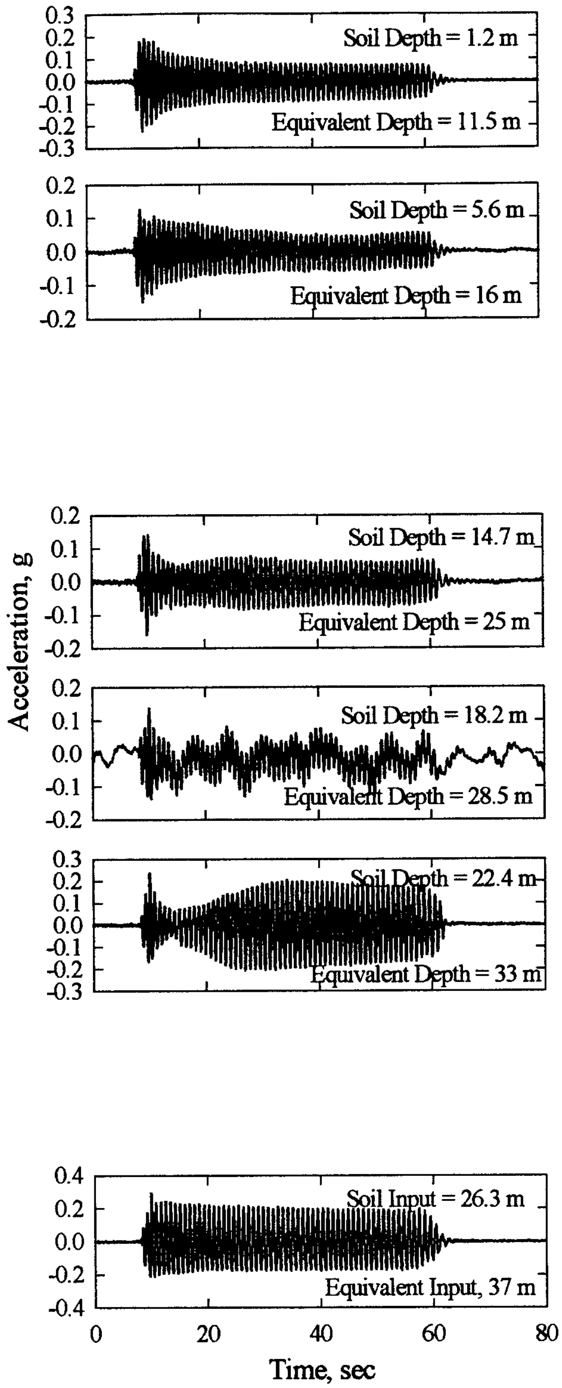
Soil Depth = 1.2 m
Equivalent Depth = 11.5 m
Soil Depth = 5.6 m
Equivalent Depth = 16 m
Soil Depth = 14.7 m
Equivalent Depth = 25 m
Soil Depth = 18.2 m
Equivalent Depth = 28.5 m
Soil Depth = 22.4 m
Equivalent Depth = 33 m
Soil Input = 26.3 m
Equivalent Input, 37 m
Acceleration, g
Time, sec

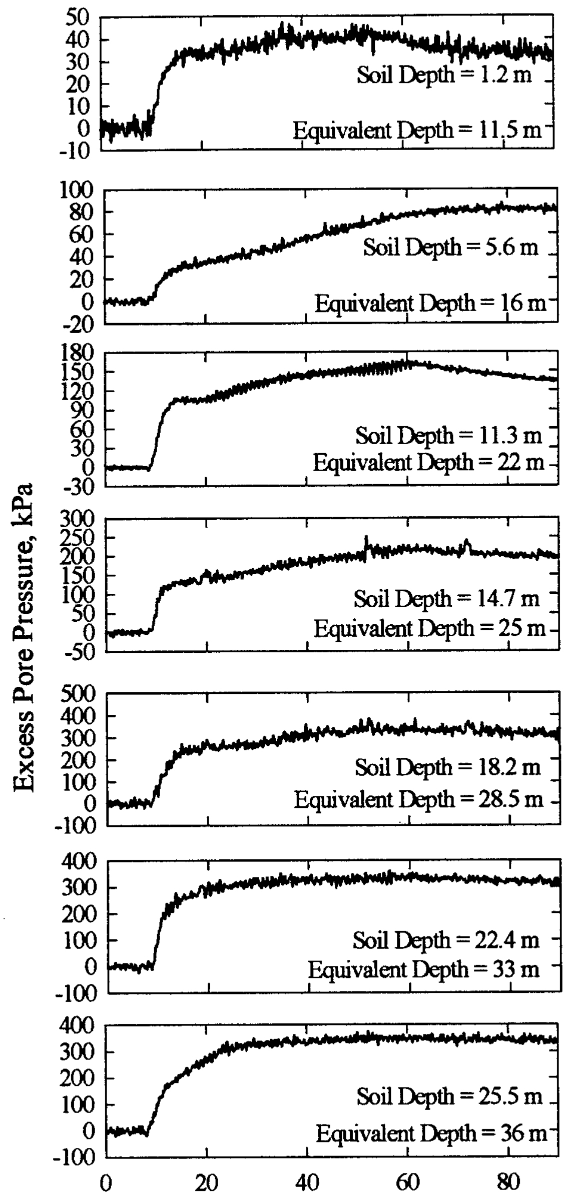
Soil Depth = 1.2 m
Equivalent Depth = 11.5 m
Soil Depth = 5.6 m
Equivalent Depth = 16 m
Soil Depth = 11.3 m
Equivalent Depth = 22 m
Soil Depth = 14.7 m
Equivalent Depth = 25 m
Soil Depth = 18.2 m
Equivalent Depth = 28.5 m
Soil Depth = 22.4 m
Equivalent Depth = 33 m
Soil Depth = 25.5 m
Equivalent Depth = 36 m
Excess Pore Pressure, kPa

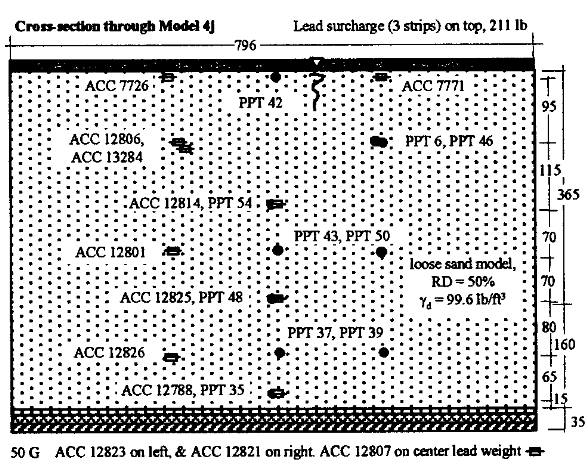
Cross-section through Model 4j
Lead surcharge (3 strips) on top, 211 lb
796
ACC 7726
PPT 42
ACC 7771
ACC 12806,
ACC 13284
PPT 6, PPT 46
ACC 12814, PPT 54
PPT 43, PPT 50
ACC 12801
loose sand model,
RD = 50%
γ_d = 99.6 lb/ft³
ACC 12825, PPT 48
PPT 37, PPT 39
ACC 12826
ACC 12788, PPT 35
95
115
365
70
70
80
160
65
15
35
50 G ACC 12823 on left, & ACC 12821 on right ACC 12807 on center lead weight

Model 4j

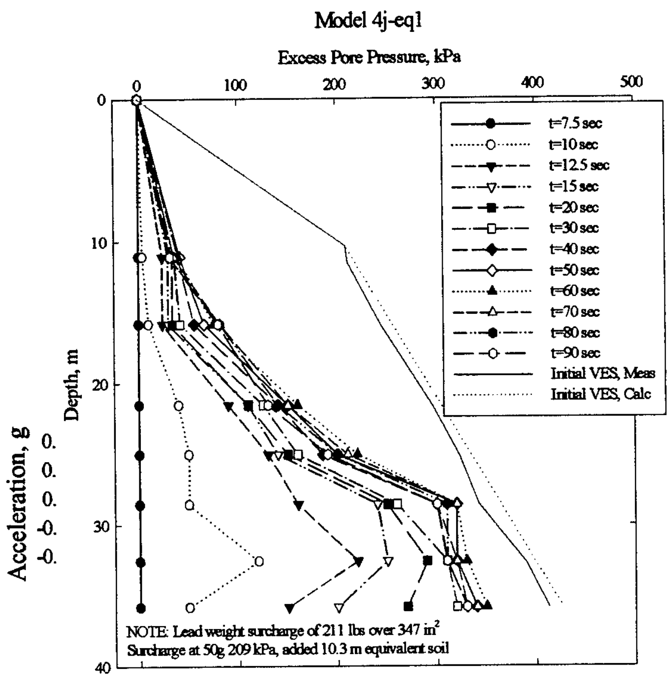

Model 4j Stress and strain isochrones

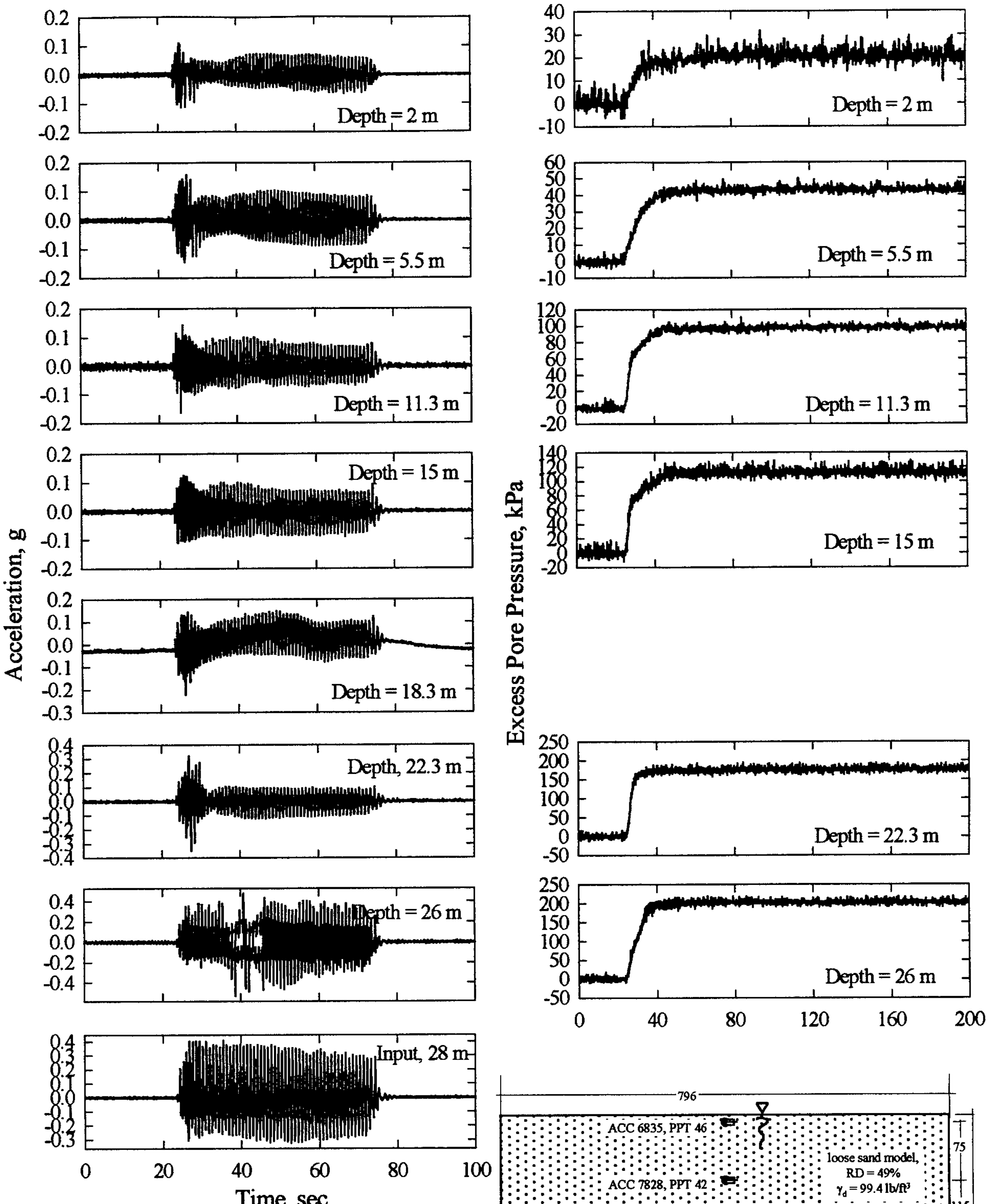

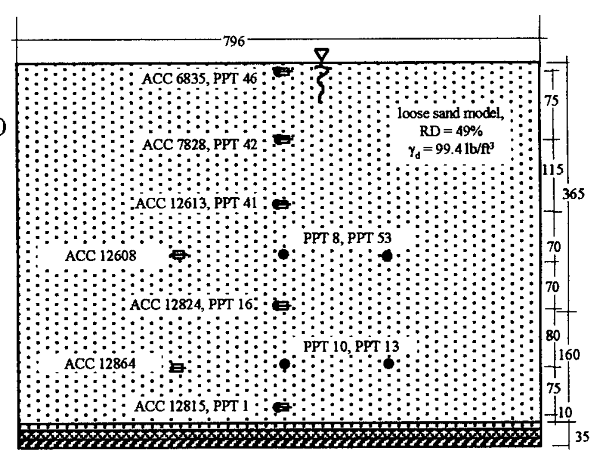

Model 4k

Cross-section through Model 4k 50 G ACC 12823 on left, & ACC 12821 on right

Model 4k-eq1

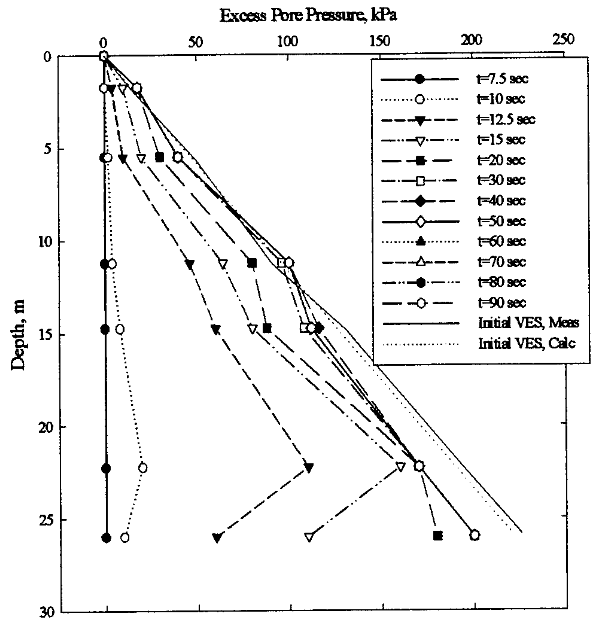

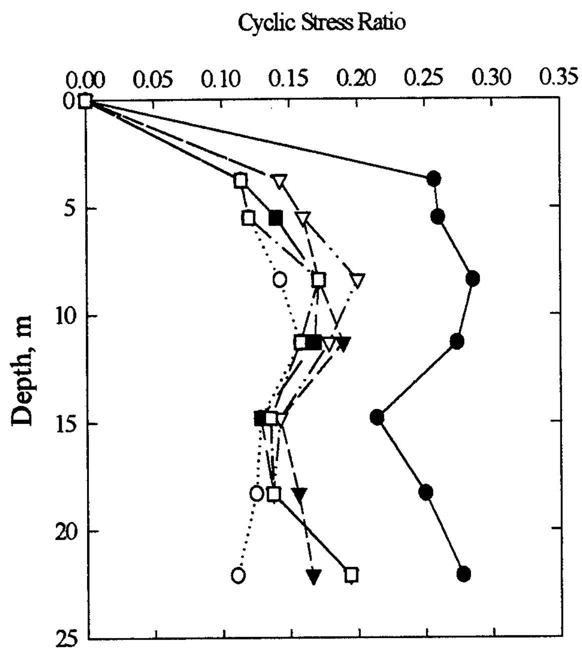

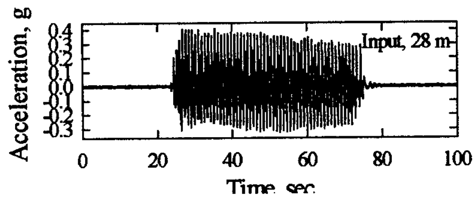

f = 1.1 Hz
a_{max} = 0.3 g

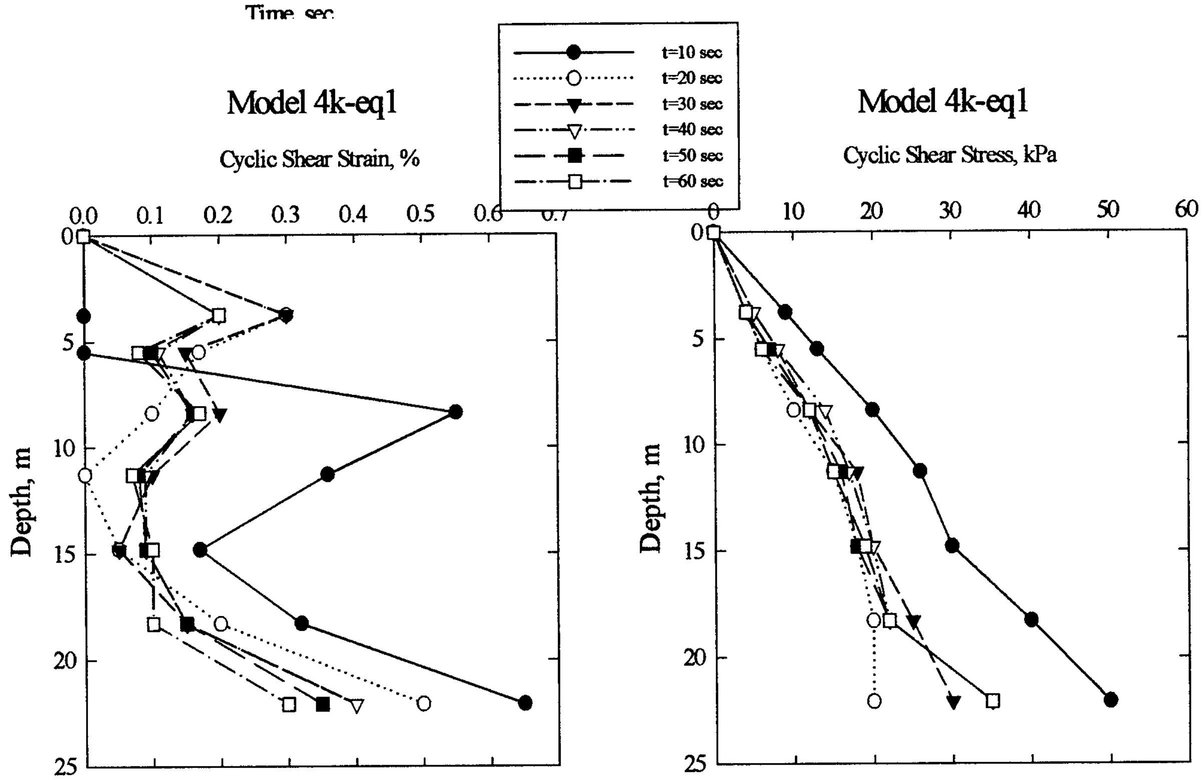

Model 4k Stress and strain isochrones

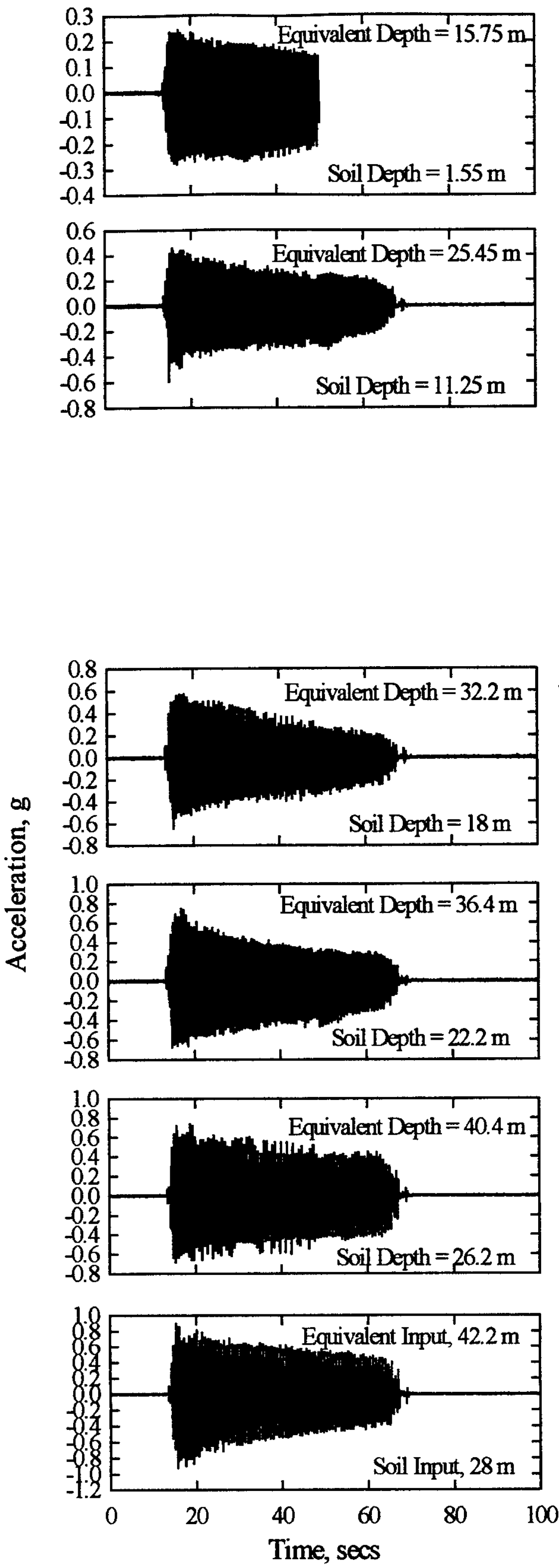

Equivalent Depth = 15.75 m
Soil Depth = 1.55 m
Equivalent Depth = 25.45 m
Soil Depth = 11.25 m
Equivalent Depth = 32.2 m
Soil Depth = 18 m
Equivalent Depth = 36.4 m
Soil Depth = 22.2 m
Equivalent Depth = 40.4 m
Soil Depth = 26.2 m
Equivalent Input, 42.2 m
Soil Input, 28 m
Acceleration, g
Time, secs

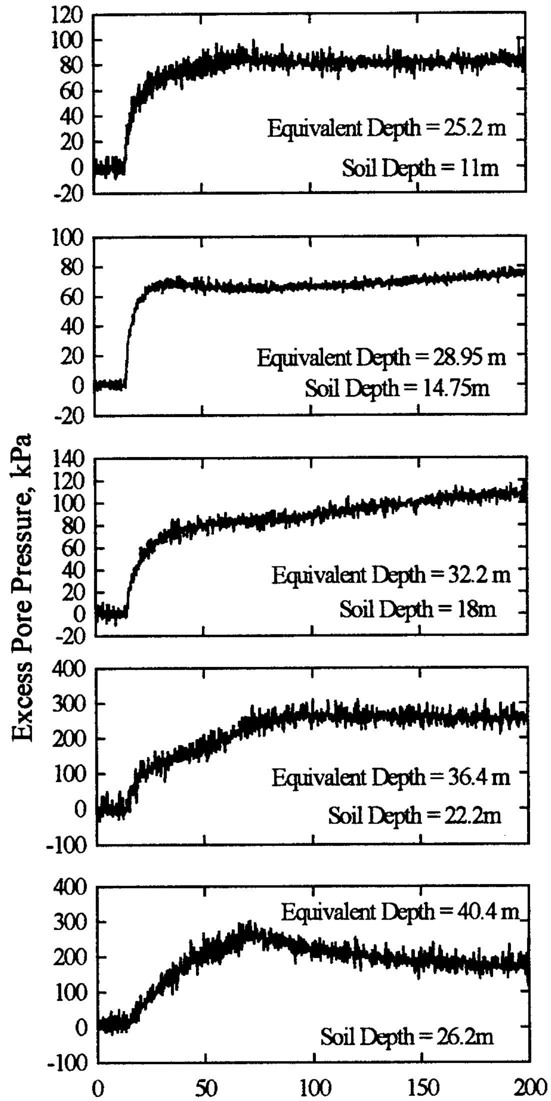

Equivalent Depth = 25.2 m
Soil Depth = 11m
Equivalent Depth = 28.95 m
Soil Depth = 14.75m
Equivalent Depth = 32.2 m
Soil Depth = 18m
Equivalent Depth = 36.4 m
Soil Depth = 22.2m
Equivalent Depth = 40.4 m
Soil Depth = 26.2m
Excess Pore Pressure, kPa

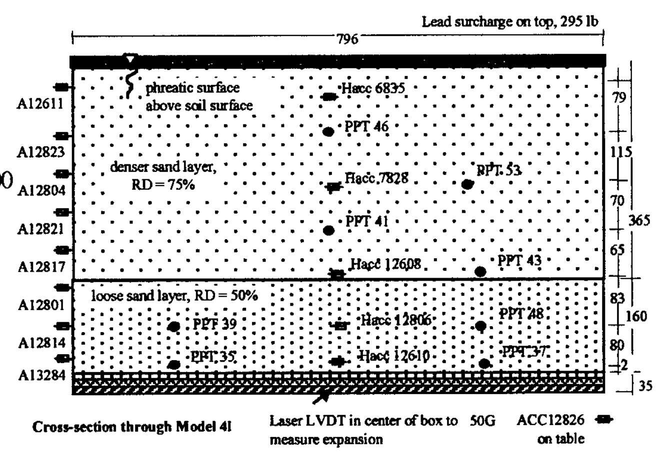

Lead surcharge on top, 295 lb
796
phreatic surface above soil surface
denser sand layer, RD = 75%
loose sand layer, RD = 50%
Hacc 6835
PPT 46
Hacc 7828
PPT 53
PPT 41
Hacc 12608
PPT 43
PPT 39
Hacc 12806
PPT 48
PPT 35
Hacc 12610
PPT 37
A12611
A12823
A12804
A12821
A12817
A12801
A12814
A13284
79
115
70
365
65
83
160
80
2
35
Cross-section through Model 41
Laser LVDT in center of box to measure expansion
50G
ACC12826 on table

Model 41

Model 4l (Box Sticking)

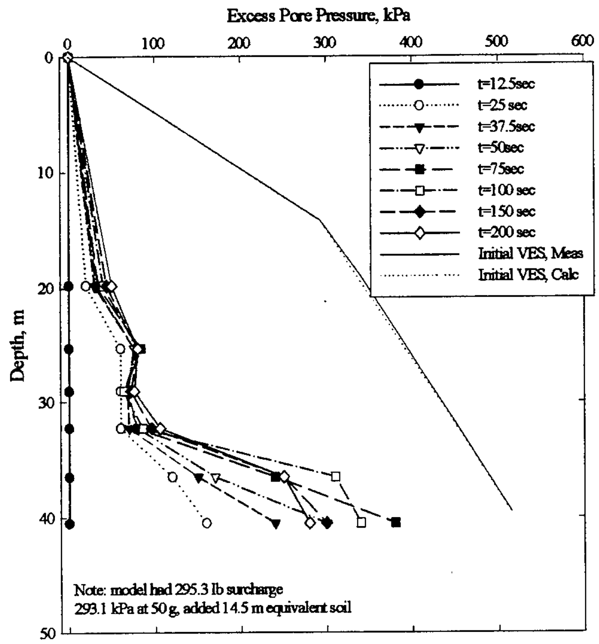

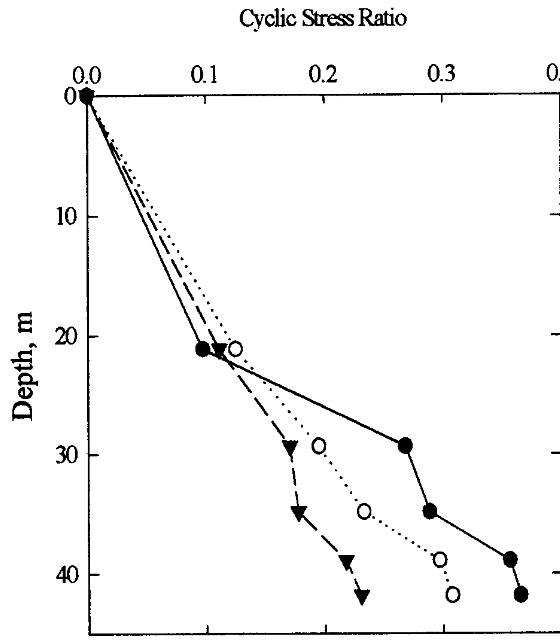

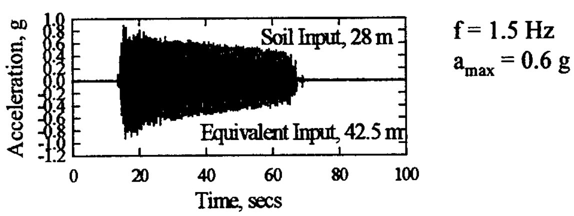

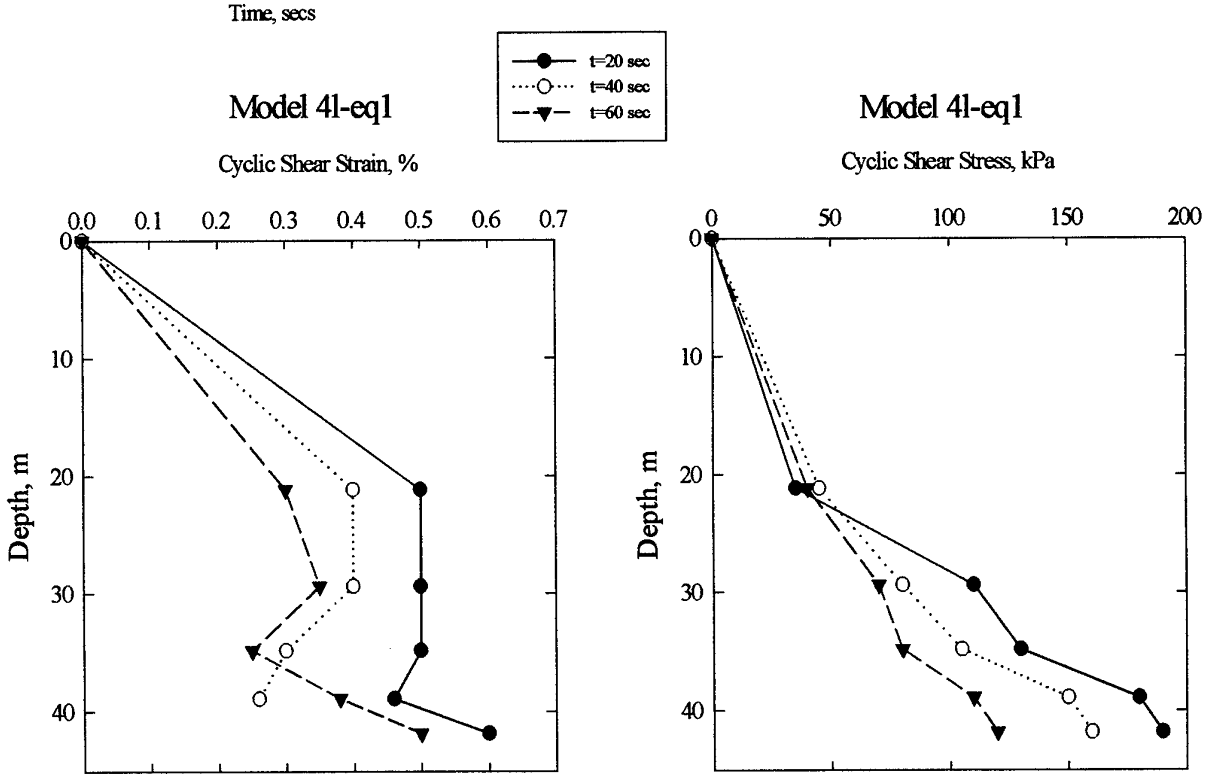

Model 4l Stress and strain isochrones

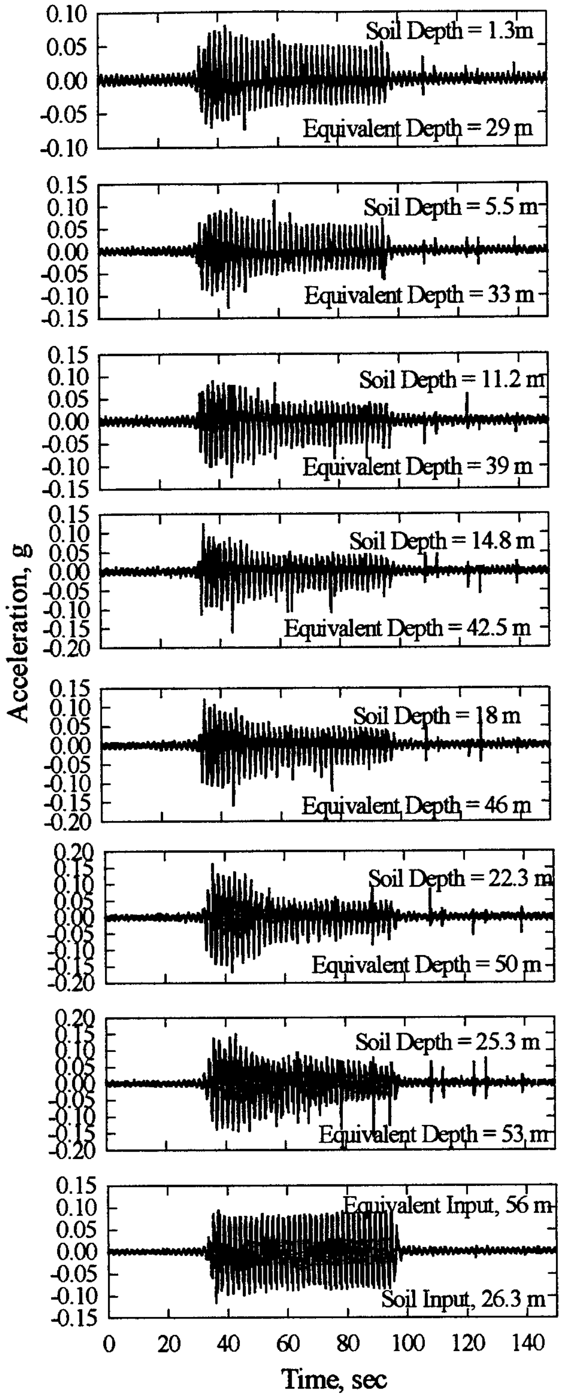
Acceleration, g
Soil Depth = 1.3m
Equivalent Depth = 29 m
Soil Depth = 5.5 m
Equivalent Depth = 33 m
Soil Depth = 11.2 m
Equivalent Depth = 39 m
Soil Depth = 14.8 m
Equivalent Depth = 42.5 m
Soil Depth = 18 m
Equivalent Depth = 46 m
Soil Depth = 22.3 m
Equivalent Depth = 50 m
Soil Depth = 25.3 m
Equivalent Depth = 53 m
Equivalent Input, 56 m
Soil Input, 26.3 m
Time, sec

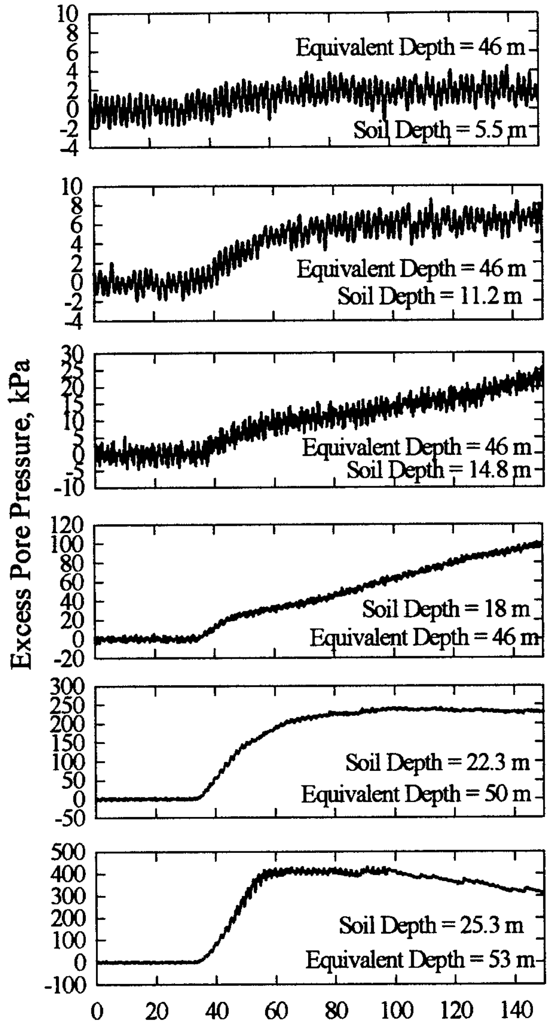
Excess Pore Pressure, kPa
Equivalent Depth = 46 m
Soil Depth = 5.5 m
Equivalent Depth = 46 m
Soil Depth = 11.2 m
Equivalent Depth = 46 m
Soil Depth = 14.8 m
Soil Depth = 18 m
Equivalent Depth = 46 m
Soil Depth = 22.3 m
Equivalent Depth = 50 m
Soil Depth = 25.3 m
Equivalent Depth = 53 m

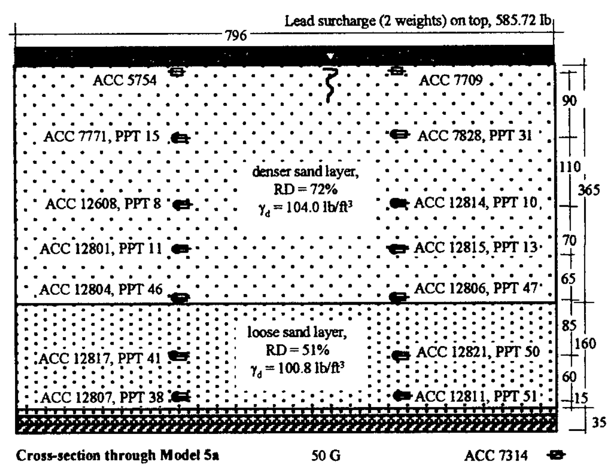
Lead surcharge (2 weights) on top, 585.72 lb
796
ACC 5754
ACC 7709
ACC 7771, PPT 15
ACC 7828, PPT 31
denser sand layer,
RD = 72%
γ_d = 104.0 lb/ft^3
ACC 12608, PPT 8
ACC 12814, PPT 10
ACC 12801, PPT 11
ACC 12815, PPT 13
ACC 12804, PPT 46
ACC 12806, PPT 47
loose sand layer,
RD = 51%
γ_d = 100.8 lb/ft^3
ACC 12817, PPT 41
ACC 12821, PPT 50
ACC 12807, PPT 38
ACC 12811, PPT 51
90
110
365
70
65
85
160
60
15
35
Cross-section through Model 5a
50 G
ACC 7314

Model 5a

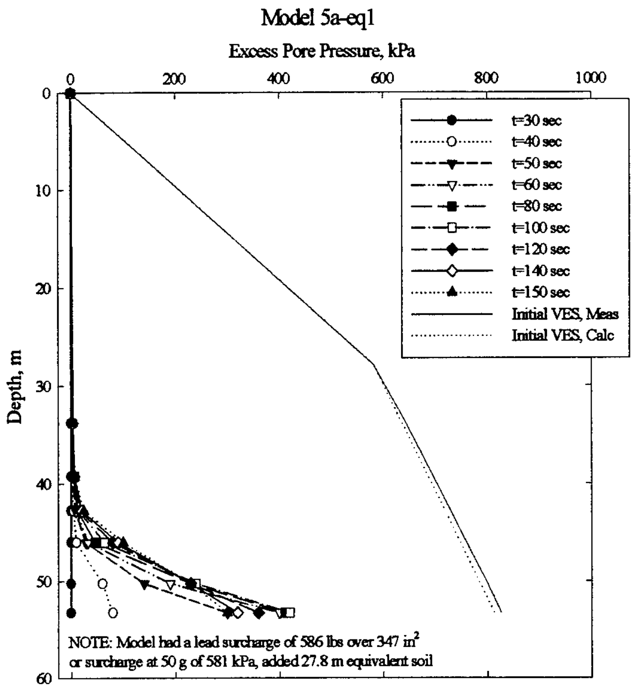

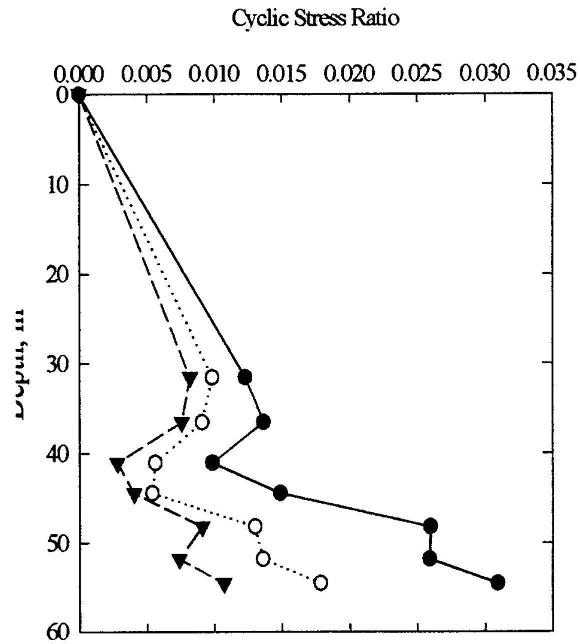

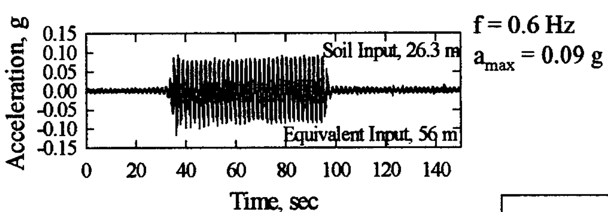

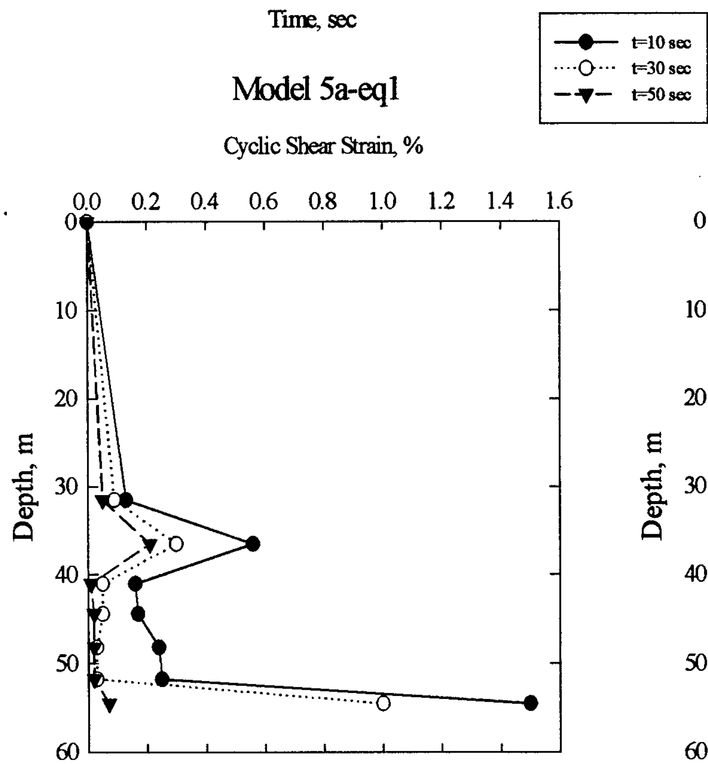

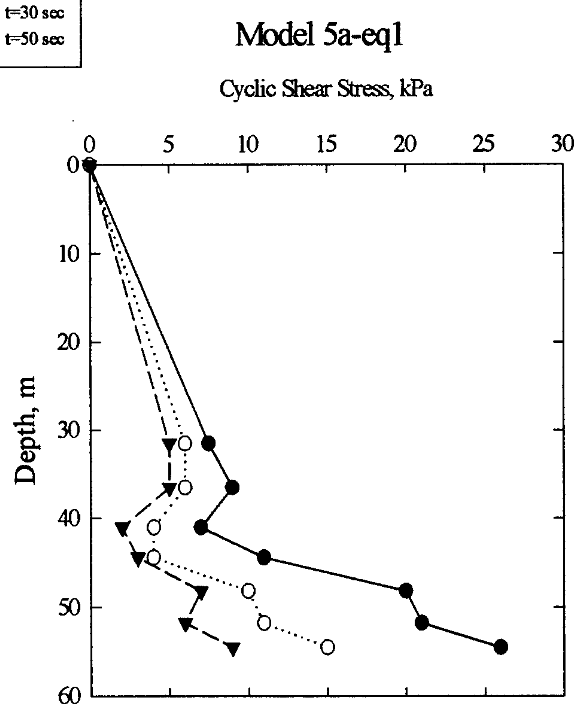

Model 5a Stress and strain isochrones

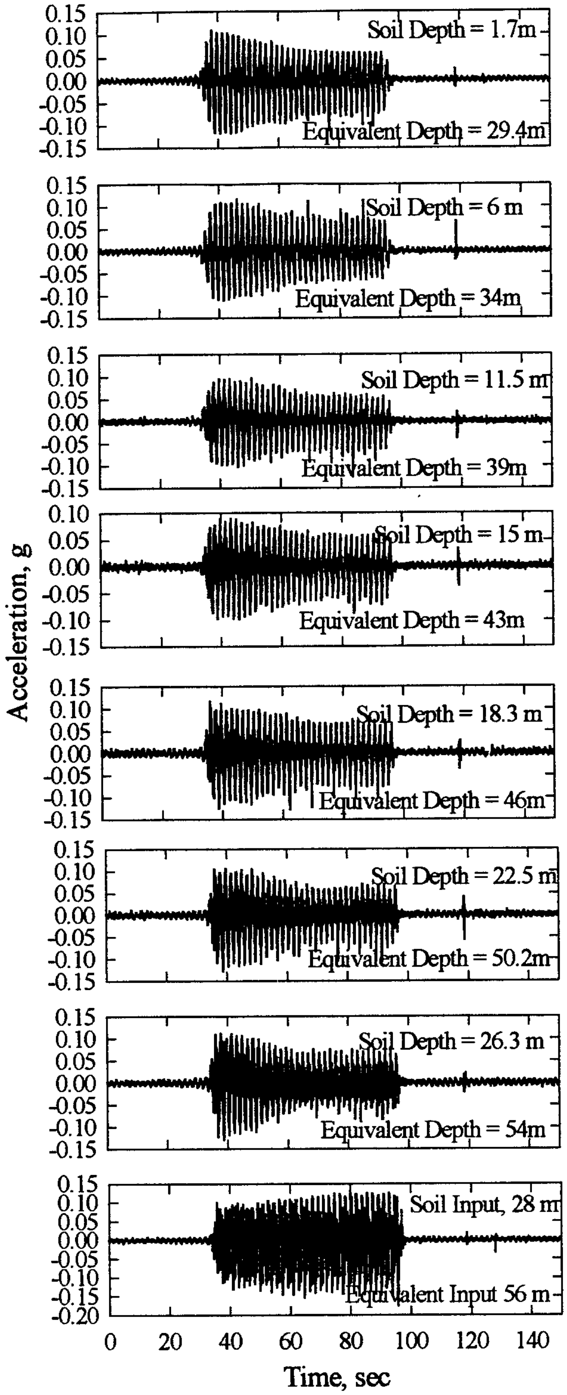

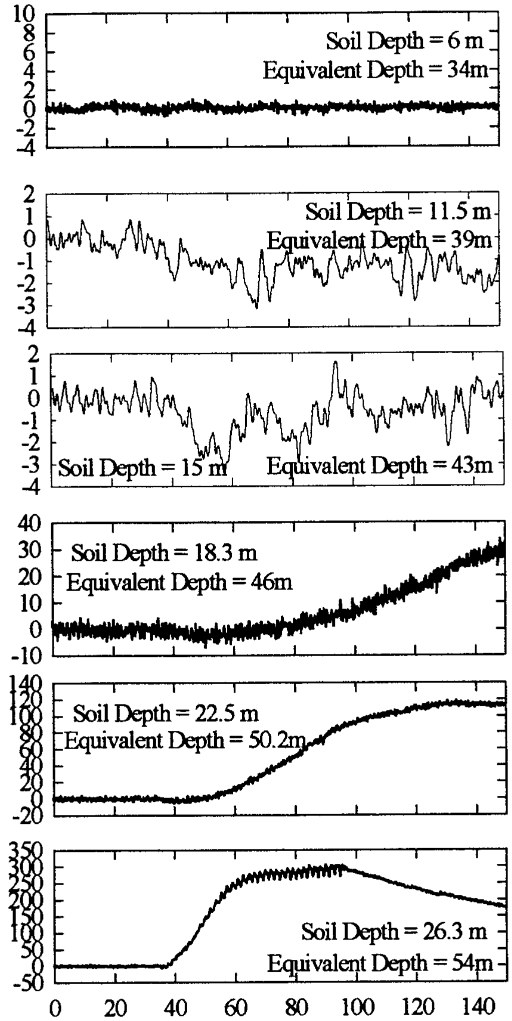

Model 5b

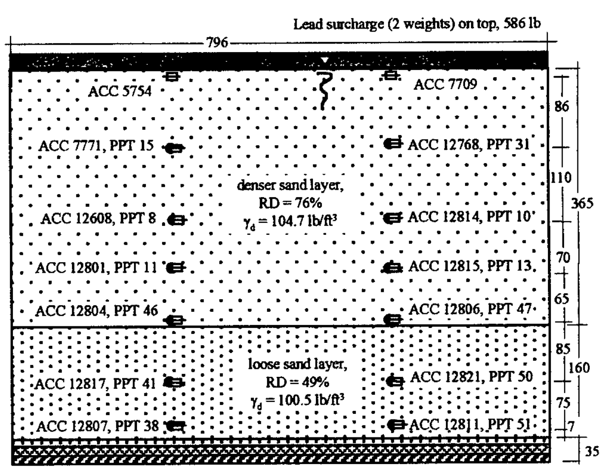

Cross-section through Model 5b

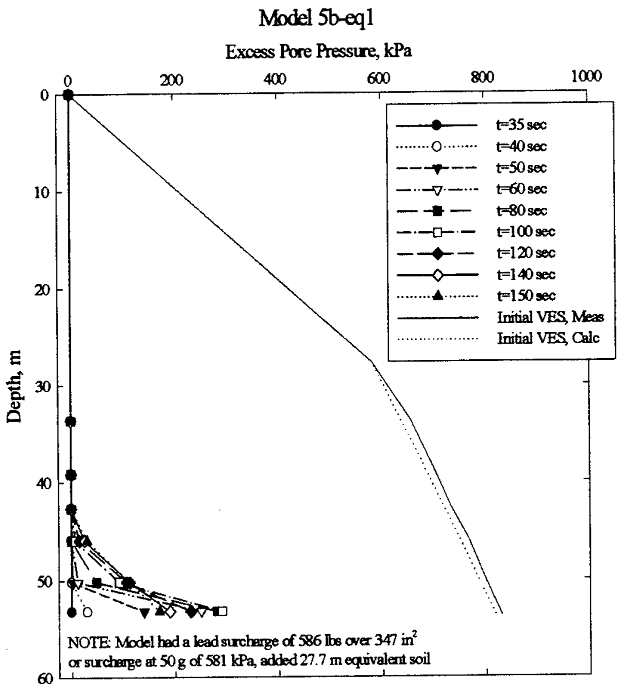

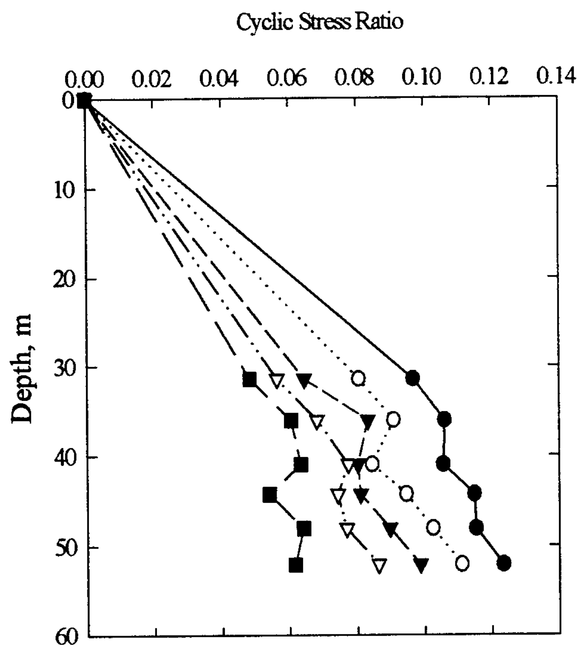

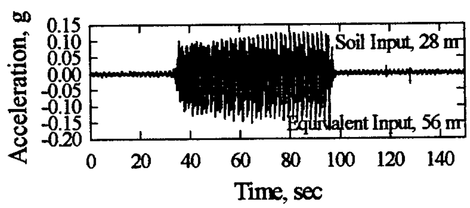

f = 0.6 Hz
a_{max} = 0.12 g

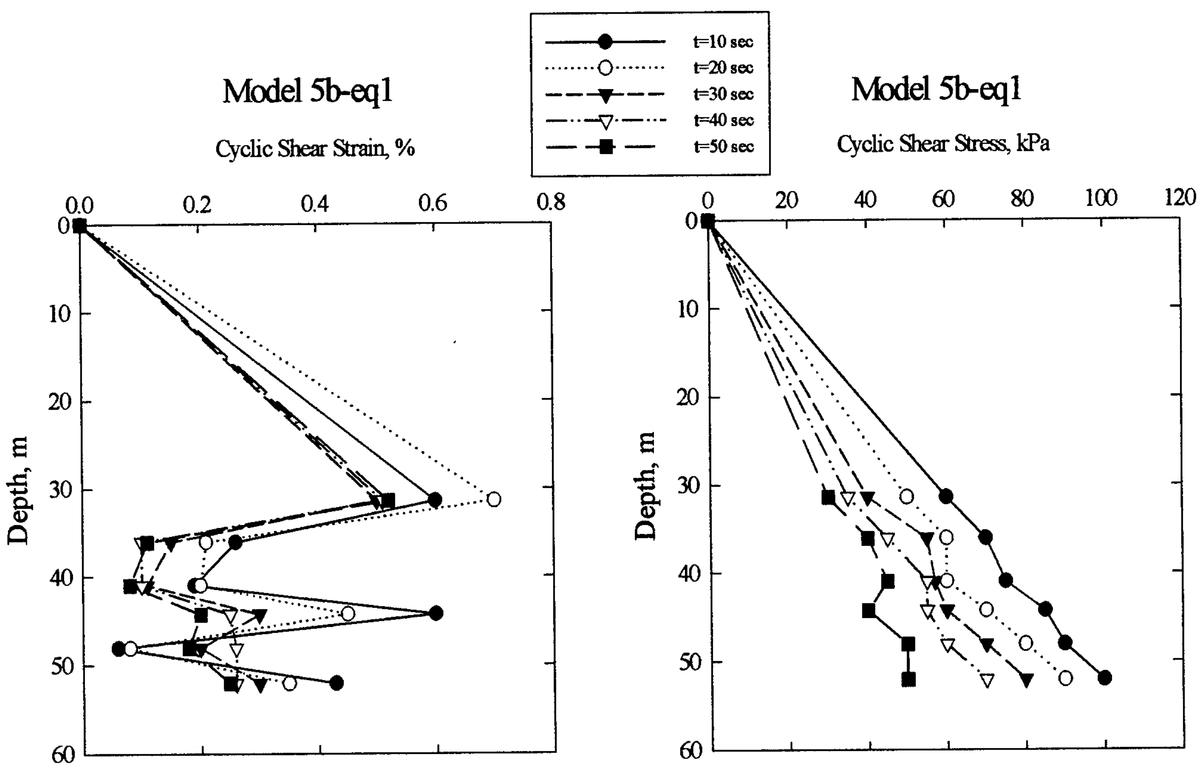

Model 5b Stress and strain isochrones

This test generated no useable data, Eq1 and 2 were particularly poor, Eq3 may have produced some information.

Model 5c

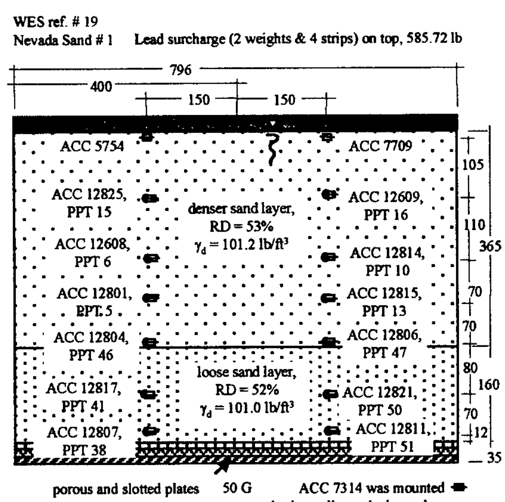

Cross-section through Model 5c

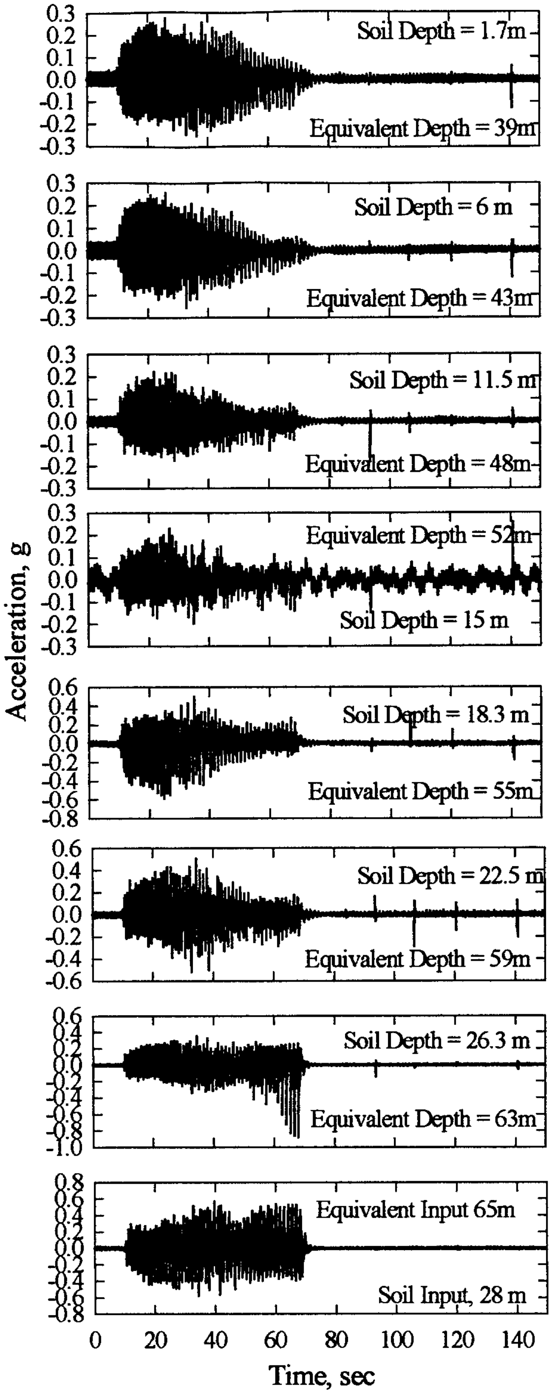

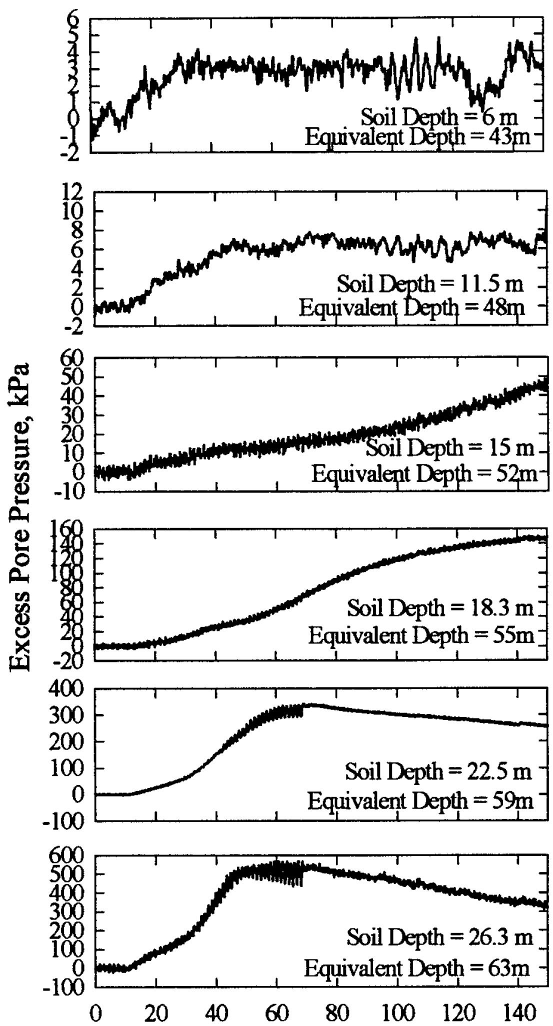

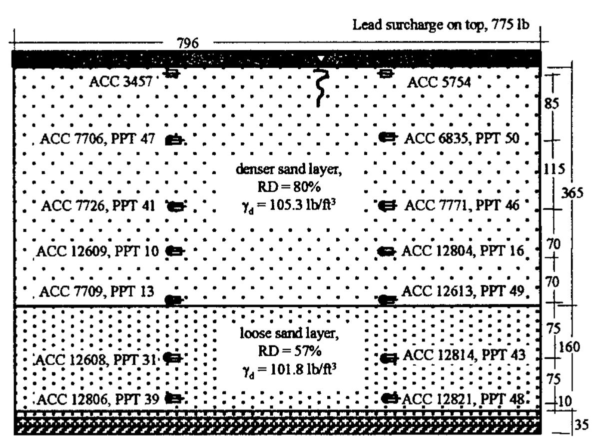

Cross-section through Model 5d

Model 5d

Model 5d-eq1

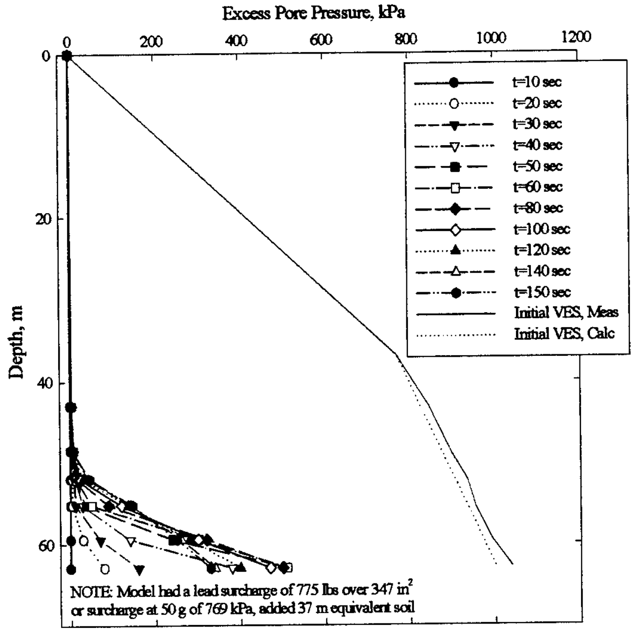

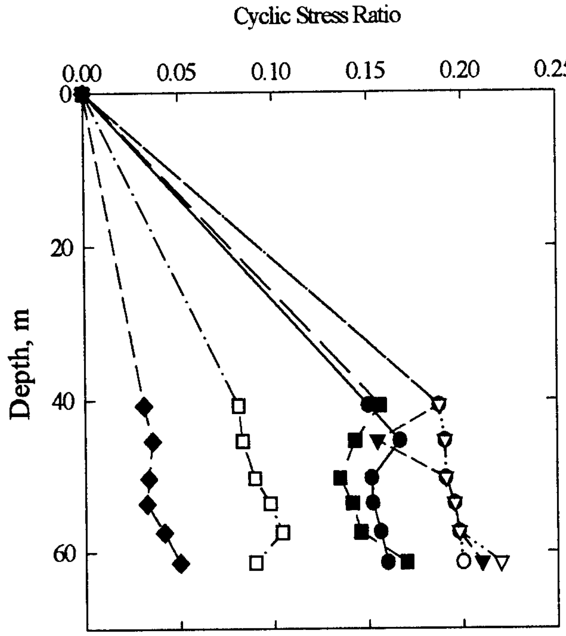

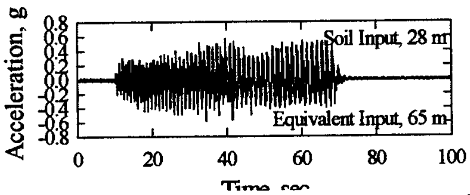

f = 1.6 Hz
a_{max} = 0.5 g

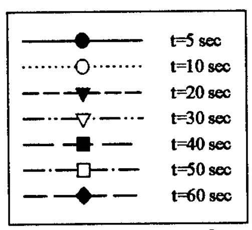

Model 5d-eq1

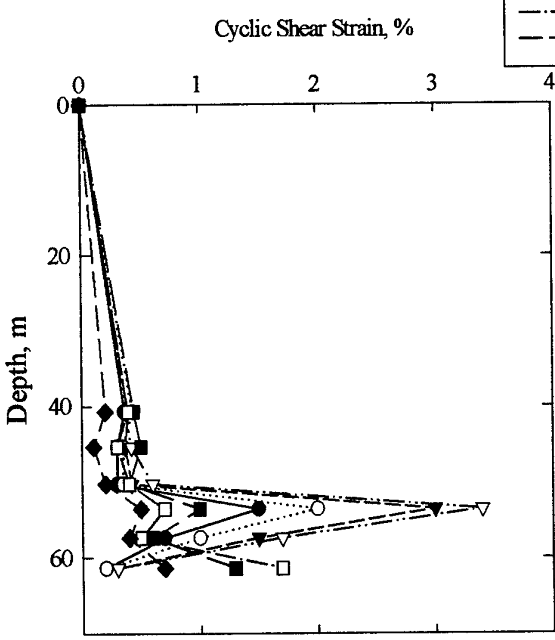

Model 5d-eq1

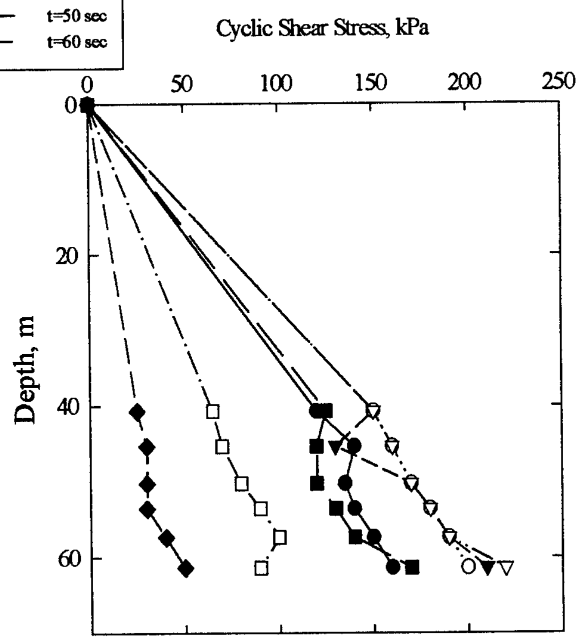

Model 5d Stress and strain isochrones

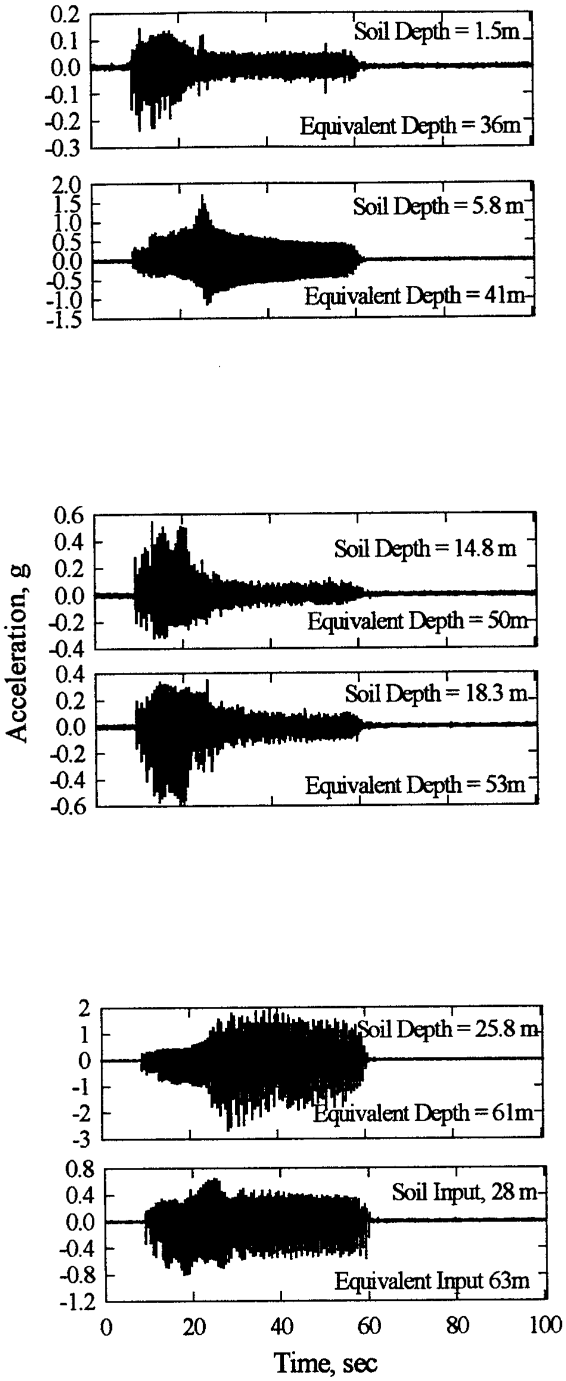

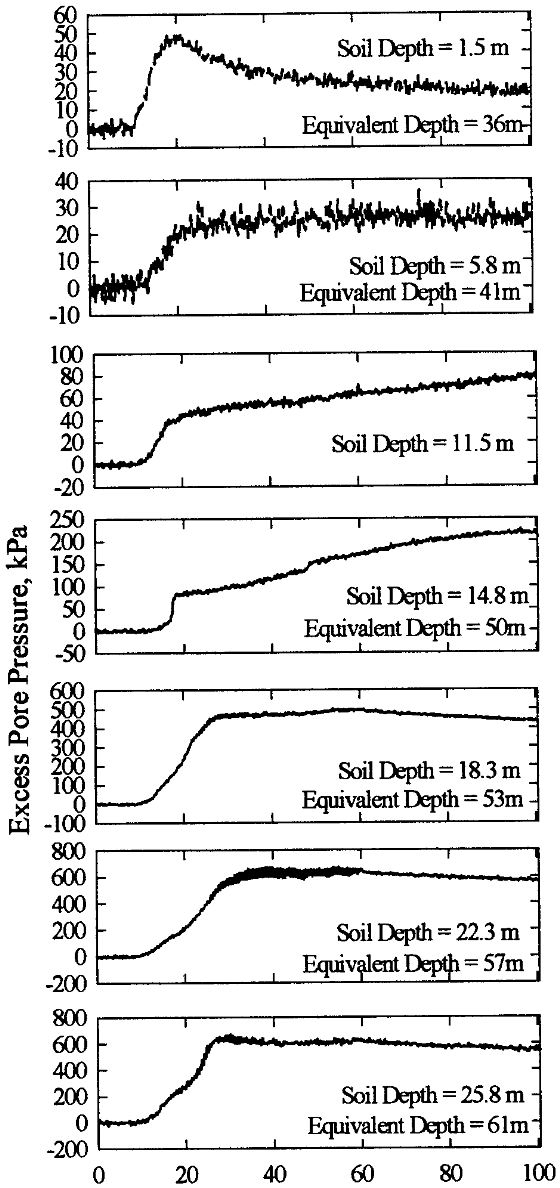

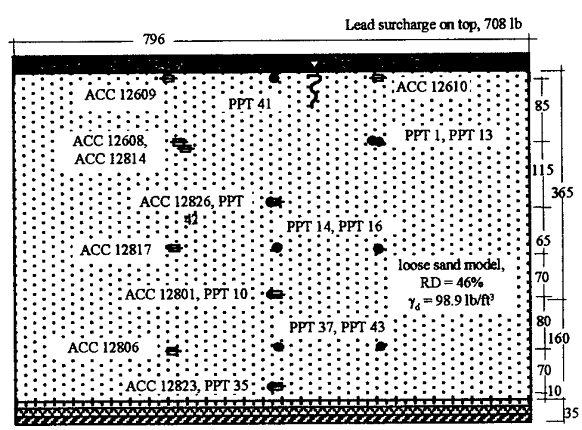

Cross-section through Model 5e 50 G ACC 12821 left, ACC 12807 right

Model 5e

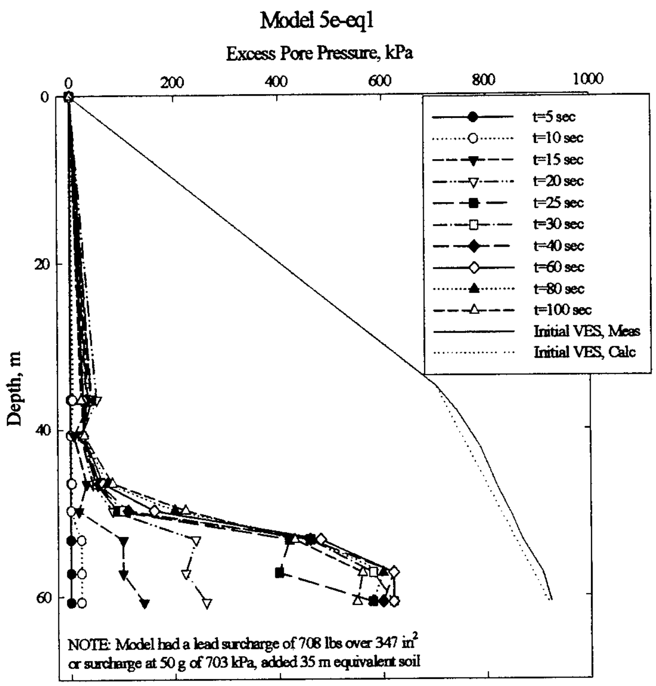

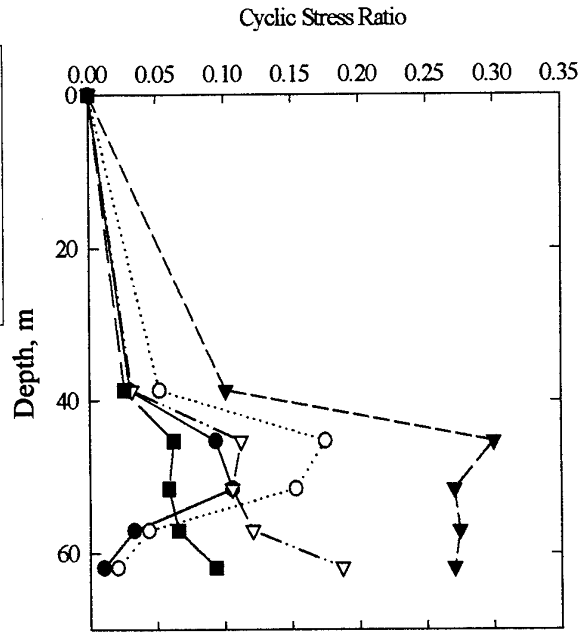

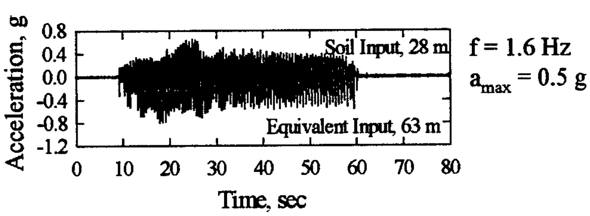

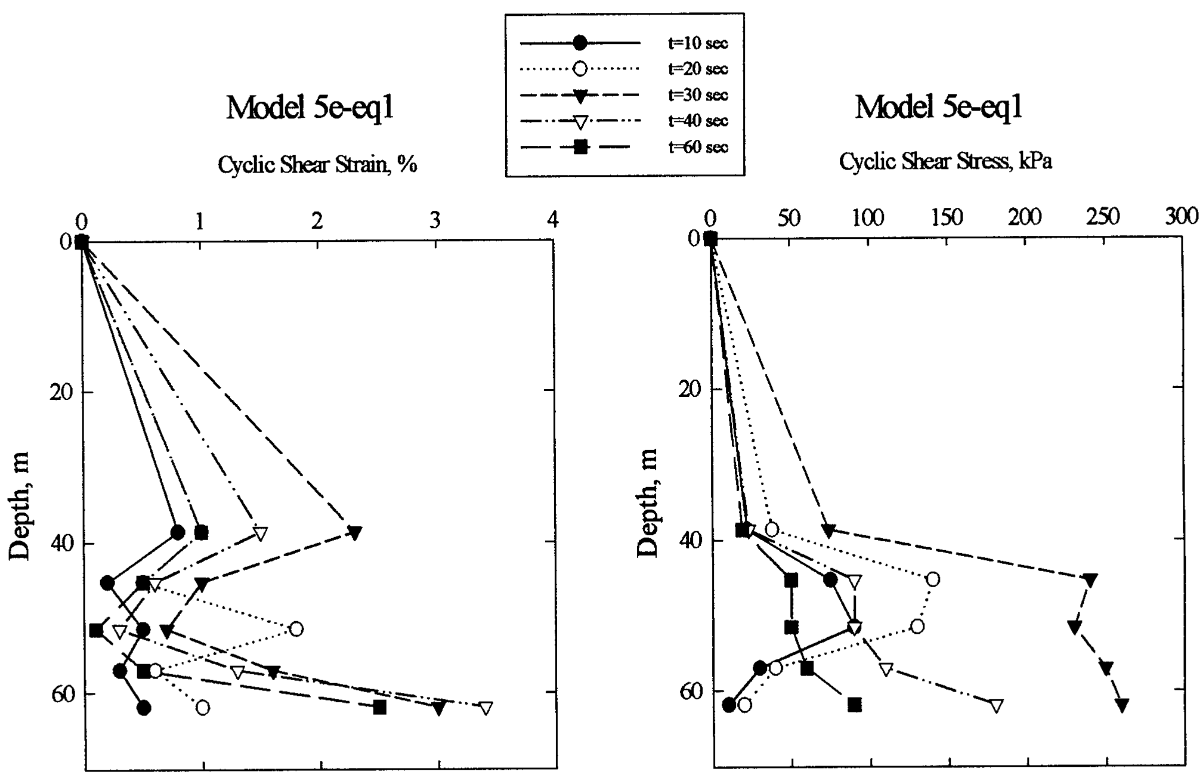

Model 5e Stress and strain isochrones

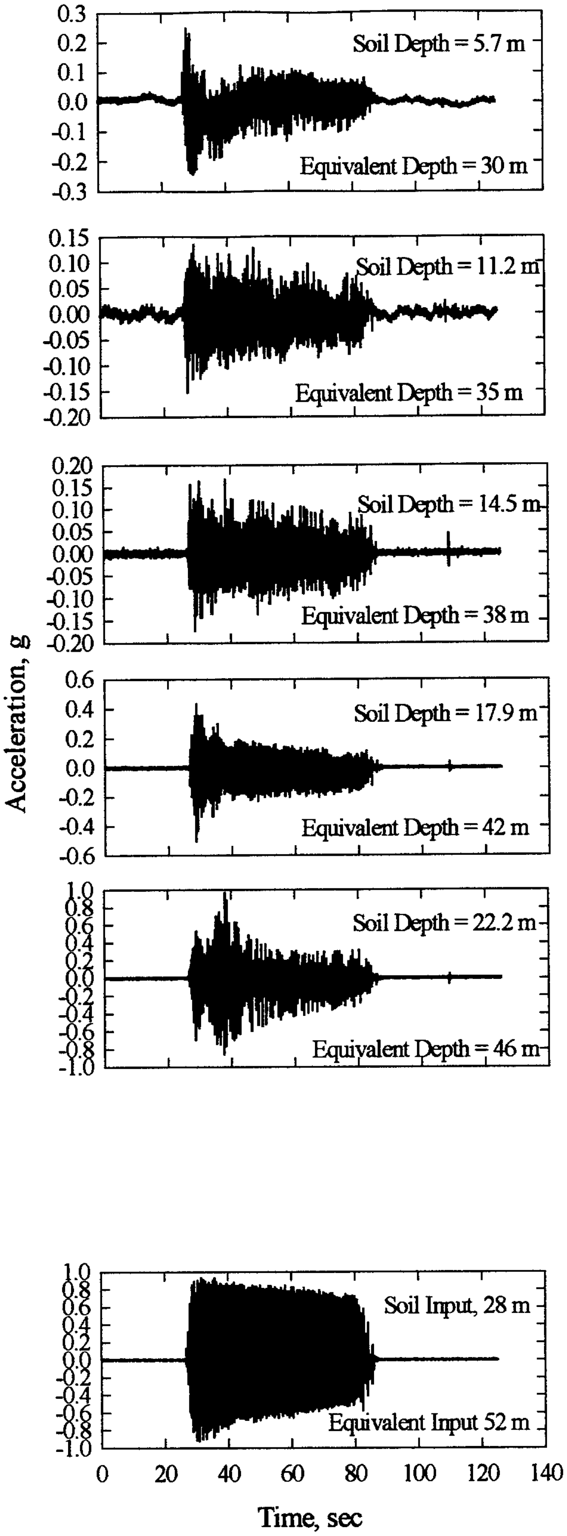
Soil Depth = 5.7 m
Equivalent Depth = 30 m
Soil Depth = 11.2 m
Equivalent Depth = 35 m
Soil Depth = 14.5 m
Equivalent Depth = 38 m
Soil Depth = 17.9 m
Equivalent Depth = 42 m
Soil Depth = 22.2 m
Equivalent Depth = 46 m
Soil Input, 28 m
Equivalent Input 52 m
Acceleration, g
Time, sec

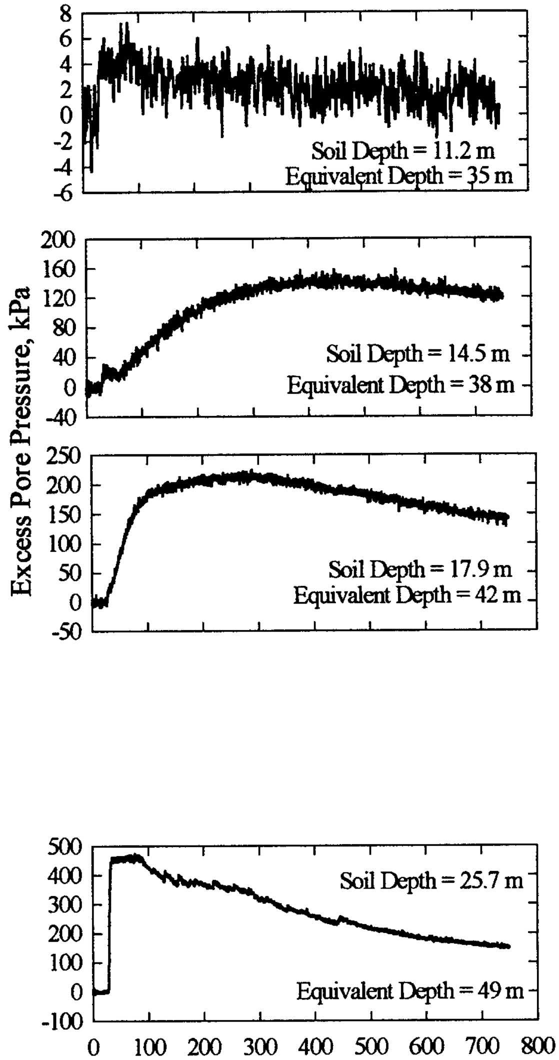
Soil Depth = 11.2 m
Equivalent Depth = 35 m
Soil Depth = 14.5 m
Equivalent Depth = 38 m
Soil Depth = 17.9 m
Equivalent Depth = 42 m
Soil Depth = 25.7 m
Equivalent Depth = 49 m
Excess Pore Pressure, kPa

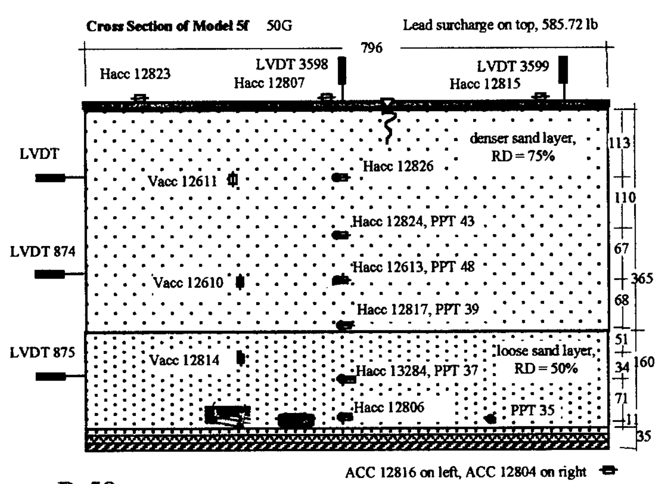
Cross Section of Model 5f 50G
Lead surcharge on top, 585.72 lb
796
Hacc 12823
LVDT 3598
Hacc 12807
LVDT 3599
Hacc 12815
denser sand layer, RD = 75%
LVDT
Hacc 12826
Vacc 12611
Hacc 12824, PPT 43
LVDT 874
Hacc 12613, PPT 48
Vacc 12610
Hacc 12817, PPT 39
LVDT 875
Vacc 12814
loose sand layer, RD = 50%
Hacc 13284, PPT 37
Hacc 12806
PPT 35
113
110
67
365
68
51
34
160
71
11
35
ACC 12816 on left, ACC 12804 on right

Model 5f

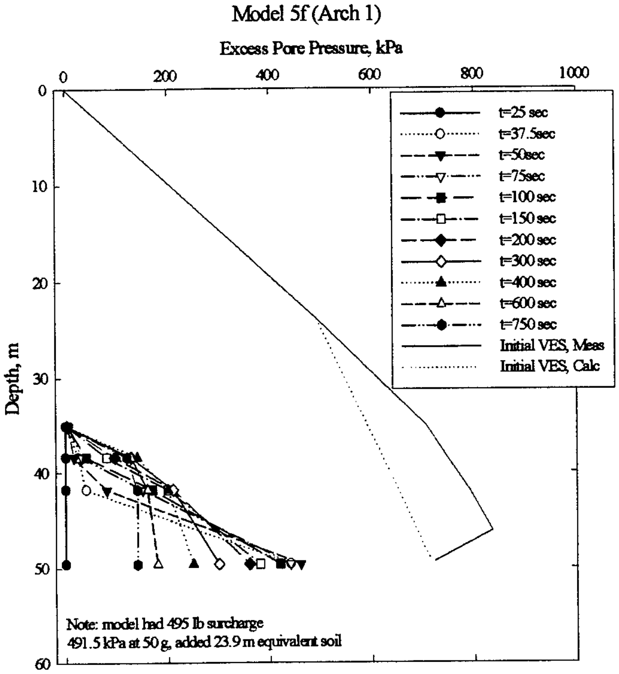

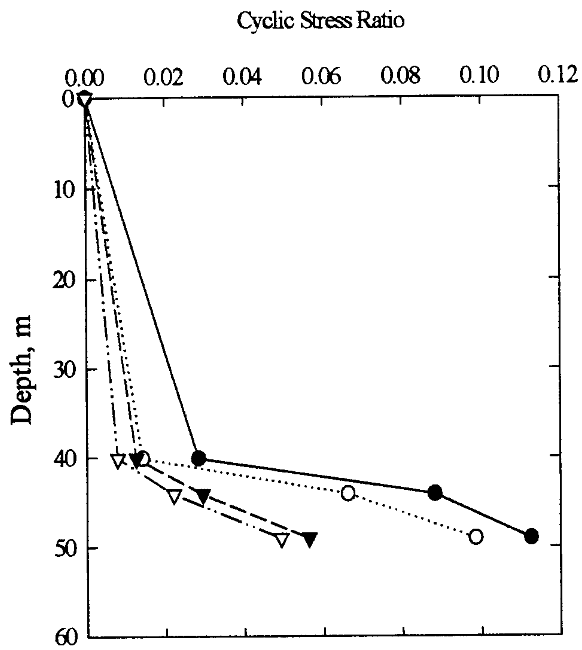

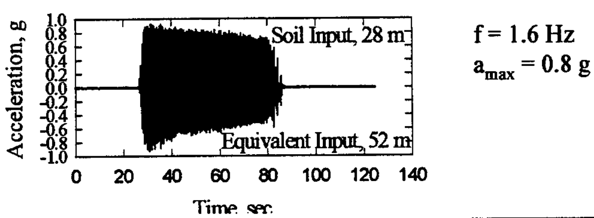

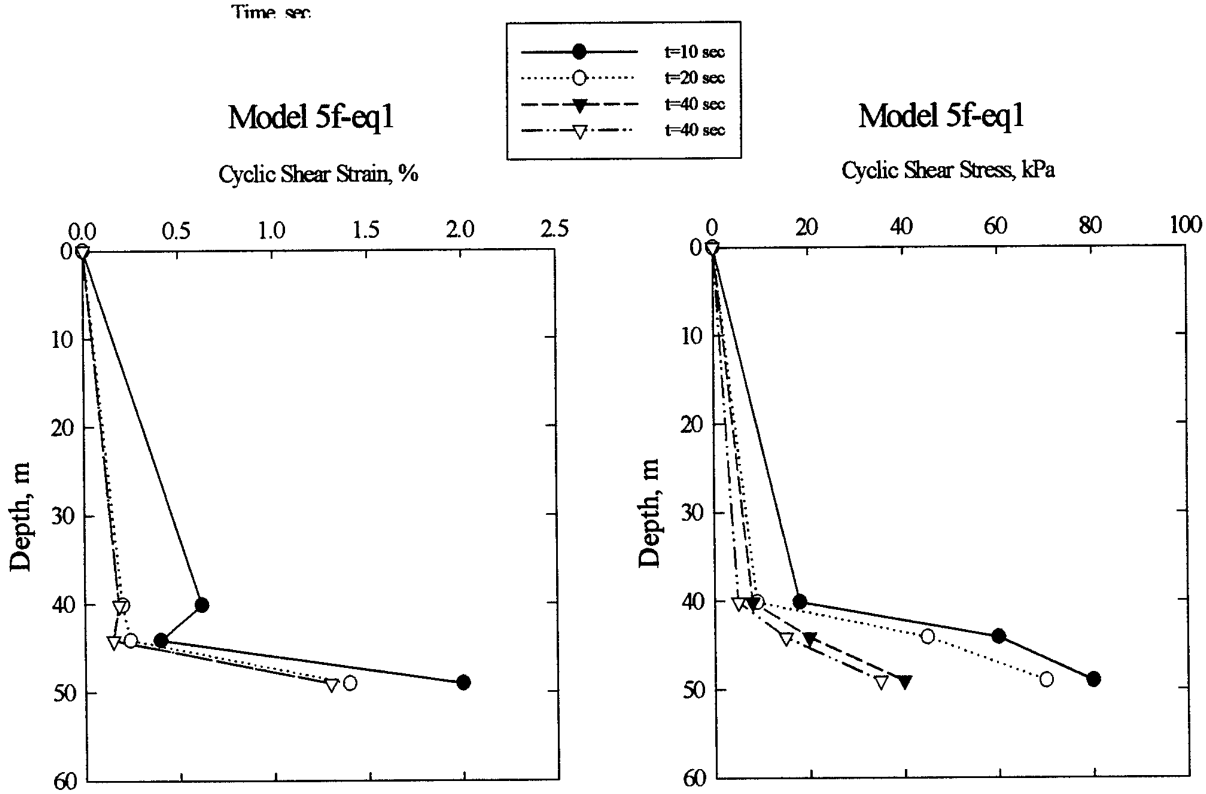

Model 5f Stress and strain isochrones

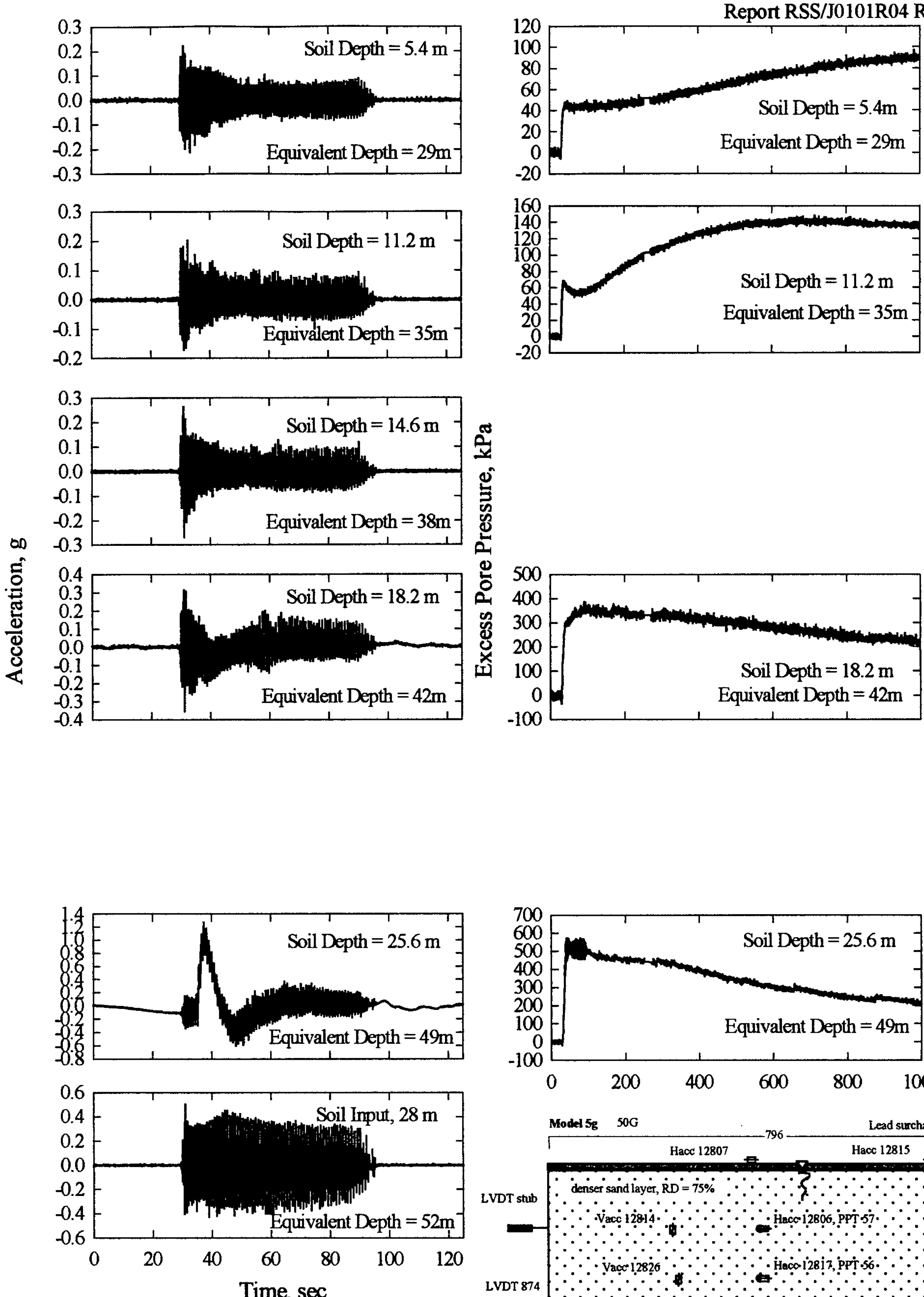

Acceleration, g
Soil Depth = 5.4 m
Equivalent Depth = 29m
Soil Depth = 11.2 m
Equivalent Depth = 35m
Soil Depth = 14.6 m
Equivalent Depth = 38m
Soil Depth = 18.2 m
Equivalent Depth = 42m
Soil Depth = 25.6 m
Equivalent Depth = 49m
Soil Input, 28 m
Equivalent Depth = 52m
Time, sec
Excess Pore Pressure, kPa
Soil Depth = 5.4m
Equivalent Depth = 29m
Soil Depth = 11.2 m
Equivalent Depth = 35m
Soil Depth = 18.2 m
Equivalent Depth = 42m
Soil Depth = 25.6 m
Equivalent Depth = 49m

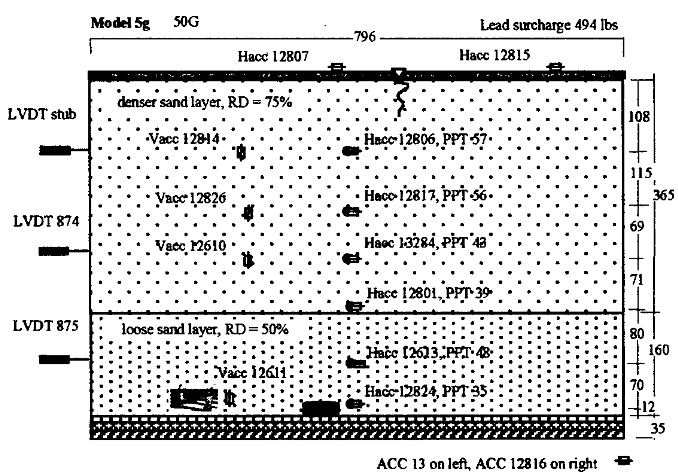

Model 5g 50G
796
Lead surcharge 494 lbs
Hacc 12807
Hacc 12815
LVDT stub
denser sand layer, RD = 75%
Vacc 12814
Hacc 12806, PPT 57
Vacc 12826
Hacc 12817, PPT 56
LVDT 874
Vacc 12610
Hacc 13284, PPT 43
Hacc 12801, PPT 39
LVDT 875
loose sand layer, RD = 50%
Hacc 12613, PPT 48
Vacc 12611
Hacc 12824, PPT 35
108
115
365
69
71
80
160
70
12
35
ACC 13 on left, ACC 12816 on right

Model 5g

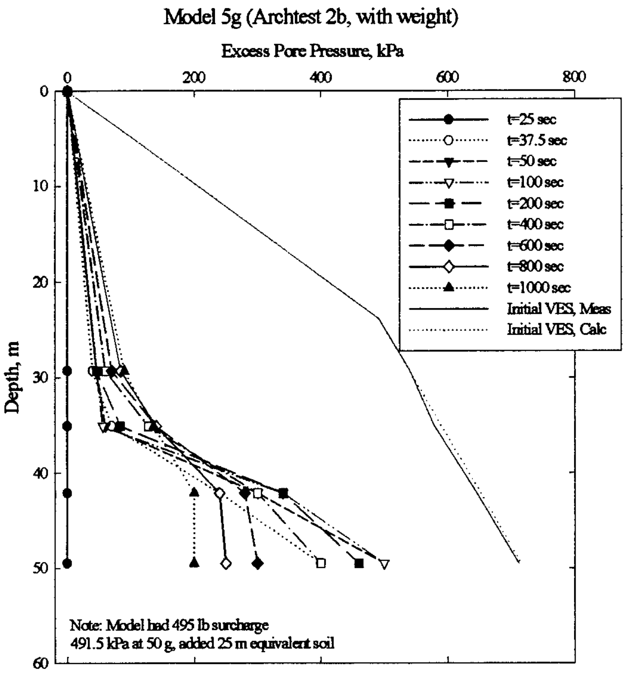

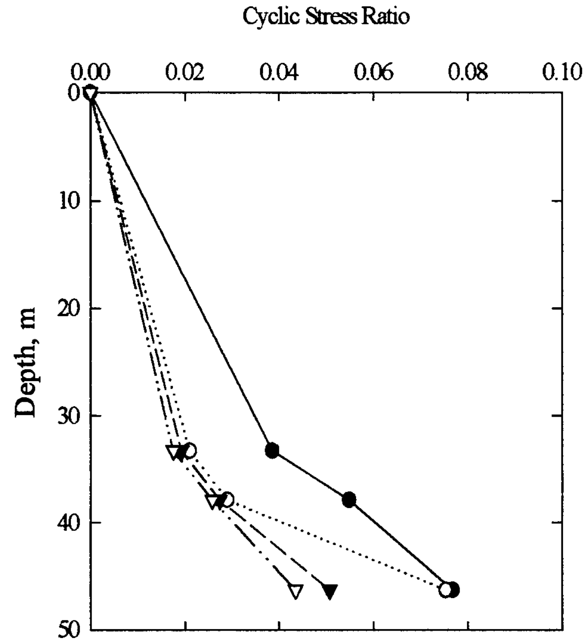

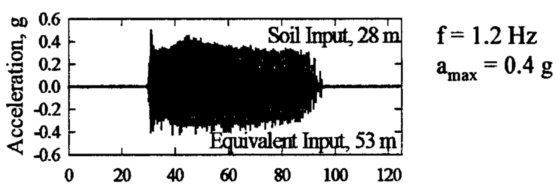

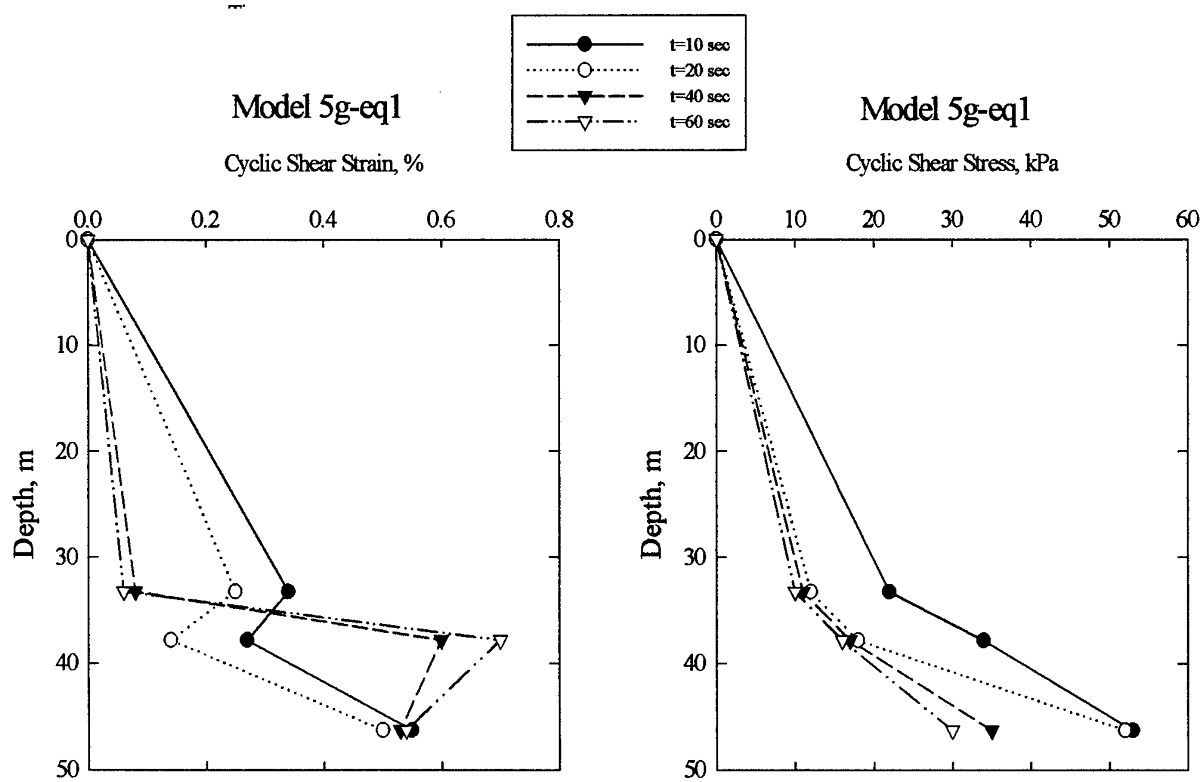

Model 5g Stress and strain isochrones

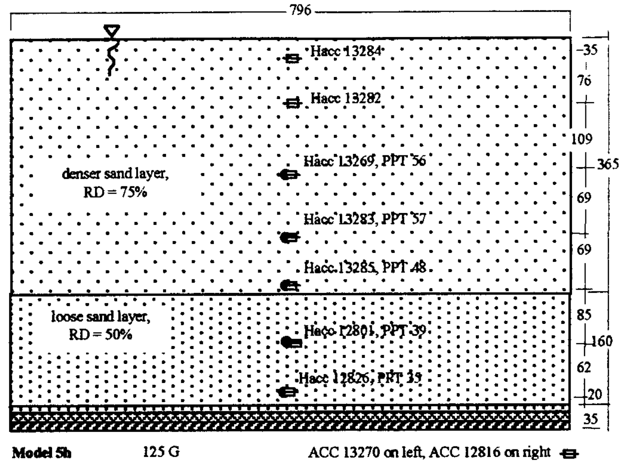
796
Hacc 13284
Hacc 13282
Hacc 13269, PPT 56
Hacc 13283, PPT 57
Hacc 13285, PPT 48
denser sand layer,
RD = 75%
loose sand layer,
RD = 50%
Hacc 12801, PPT 39
Hacc 12826, PPT 33
35
76
109
365
69
69
85
160
62
20
35
Model 5h
125 G
ACC 13270 on left, ACC 12816 on right

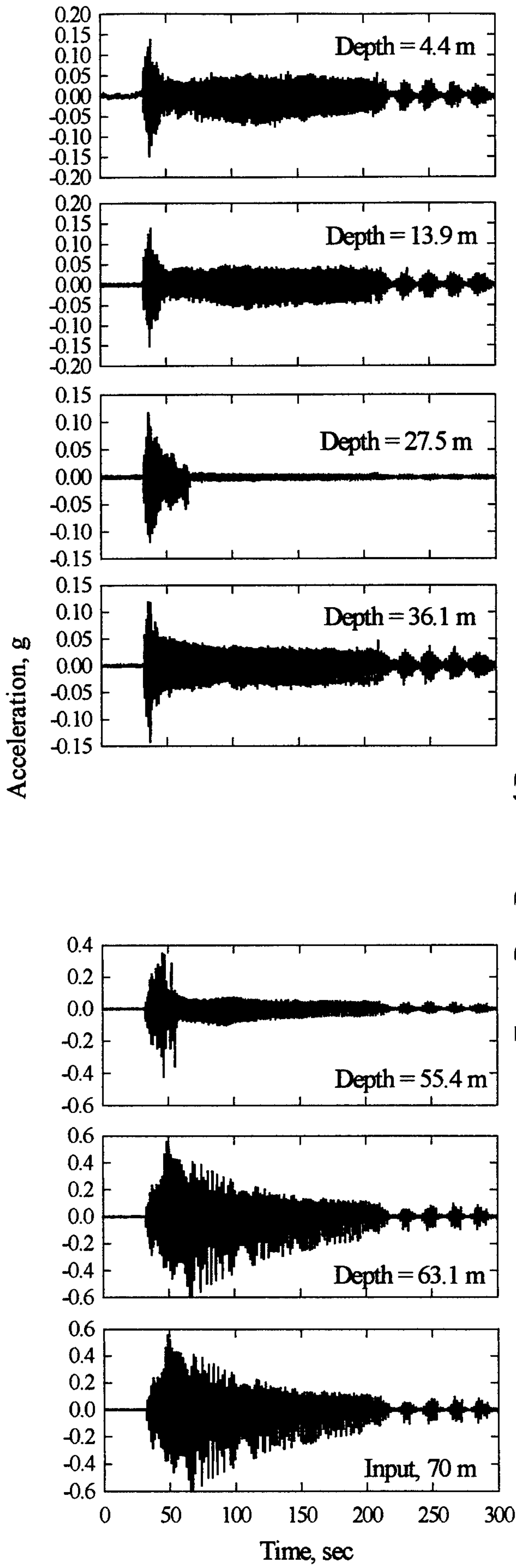
Acceleration, g
Depth = 4.4 m
Depth = 13.9 m
Depth = 27.5 m
Depth = 36.1 m
Depth = 55.4 m
Depth = 63.1 m
Input, 70 m
Time, sec

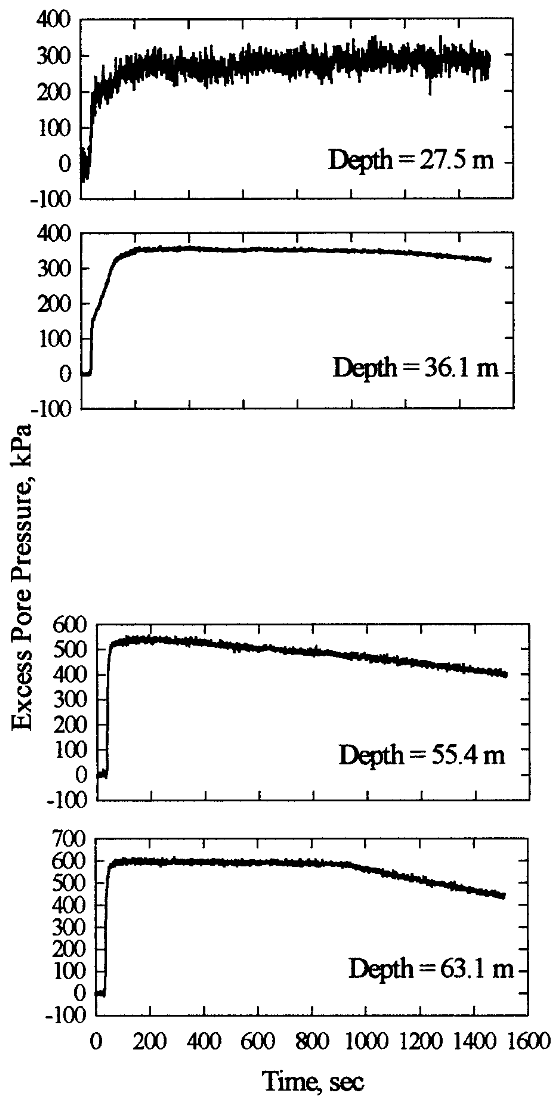
Excess Pore Pressure, kPa
Depth = 27.5 m
Depth = 36.1 m
Depth = 55.4 m
Depth = 63.1 m
Time, sec

Model 5h

Model 5h (No Weight 125g)

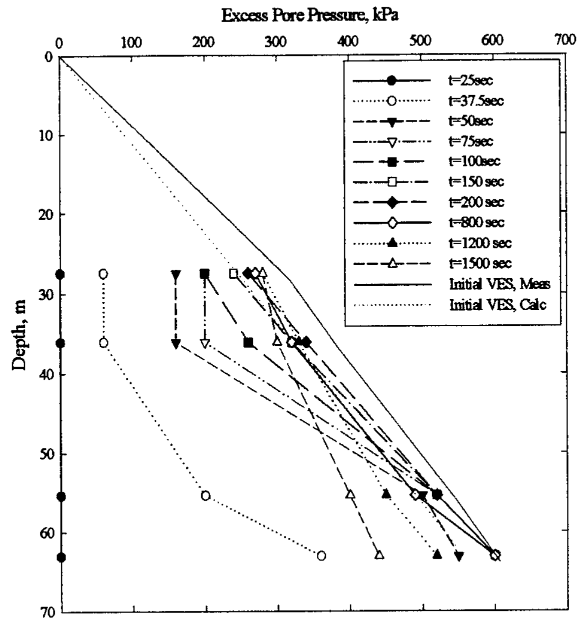

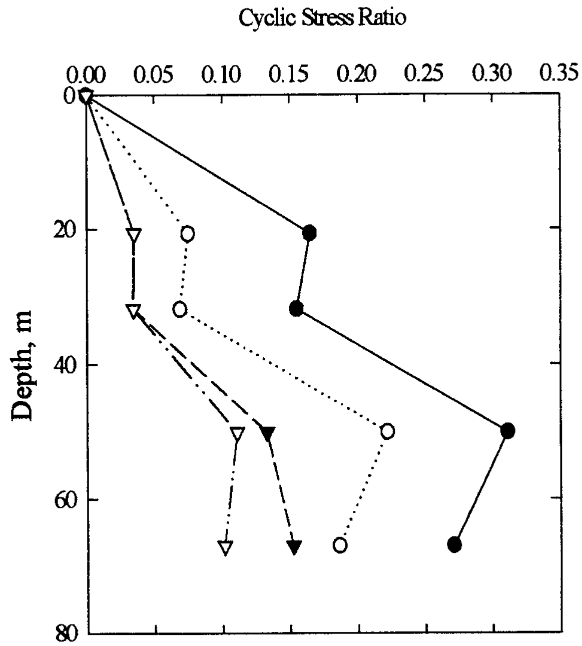

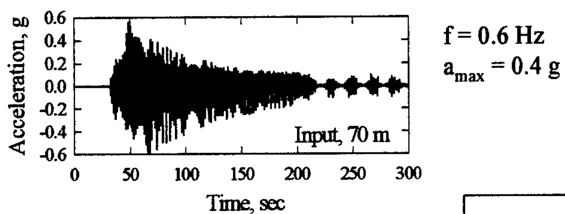

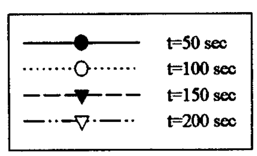

Model 5h-eq1

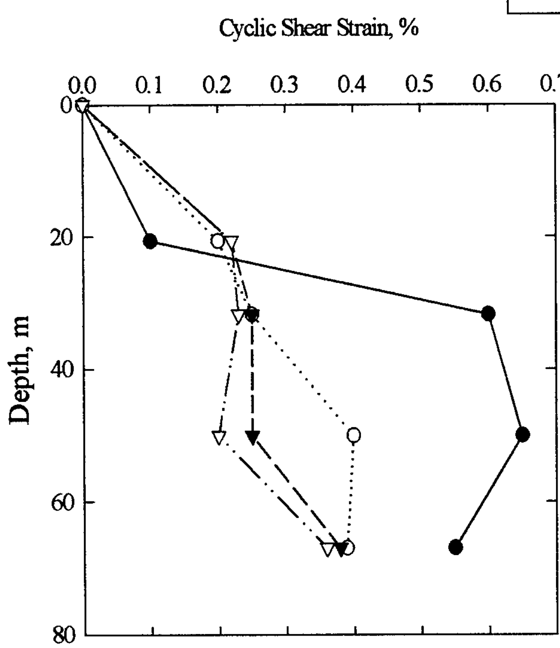

Model 5h-eq1

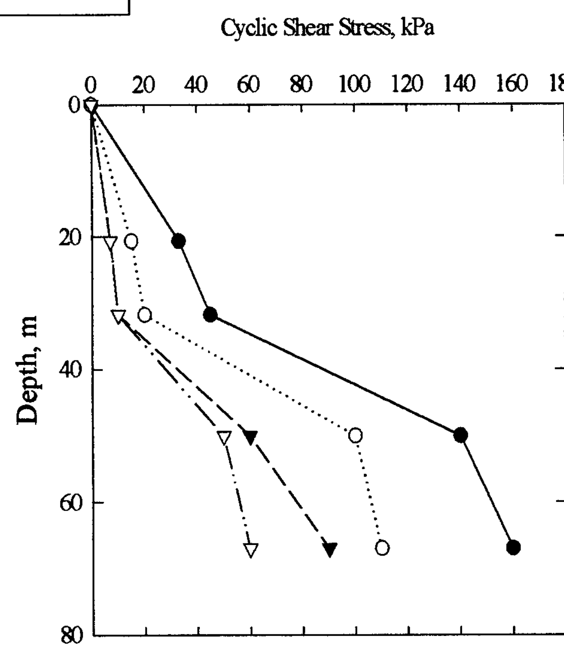

Model 5h Stress and strain isochrones

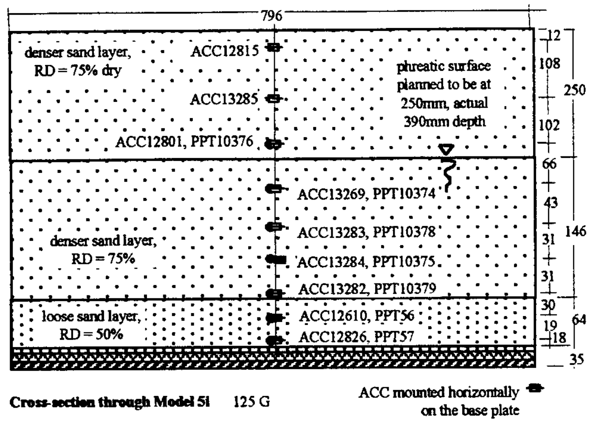

Cross-section through Model 5i 125 G

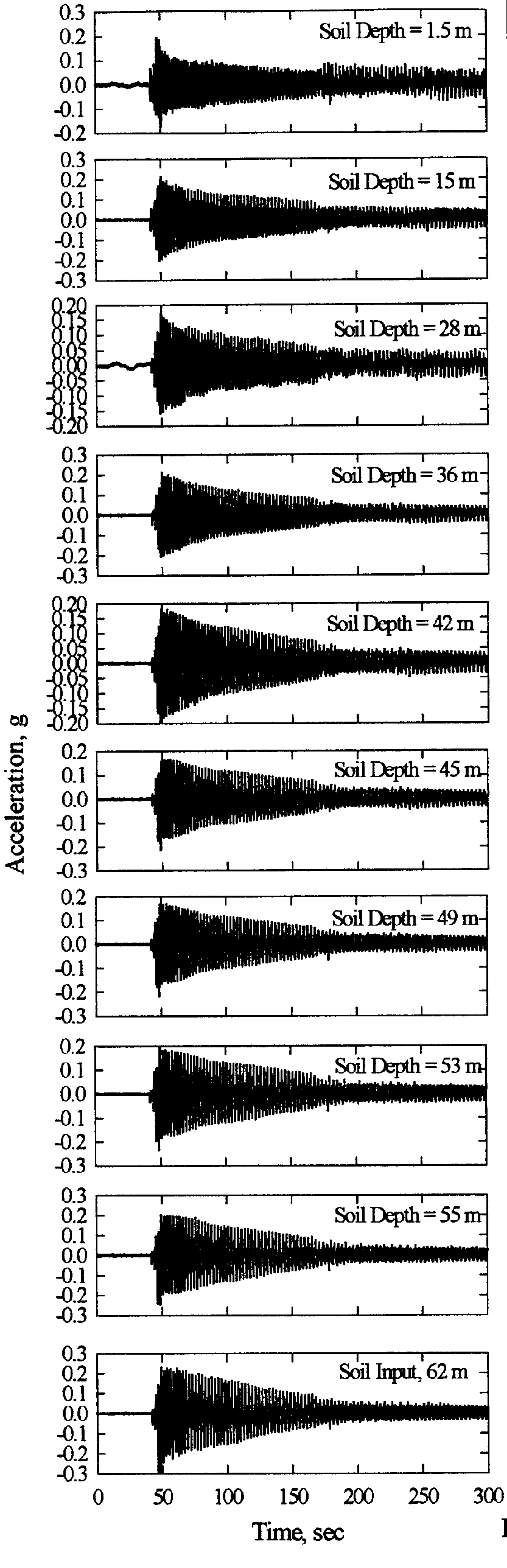

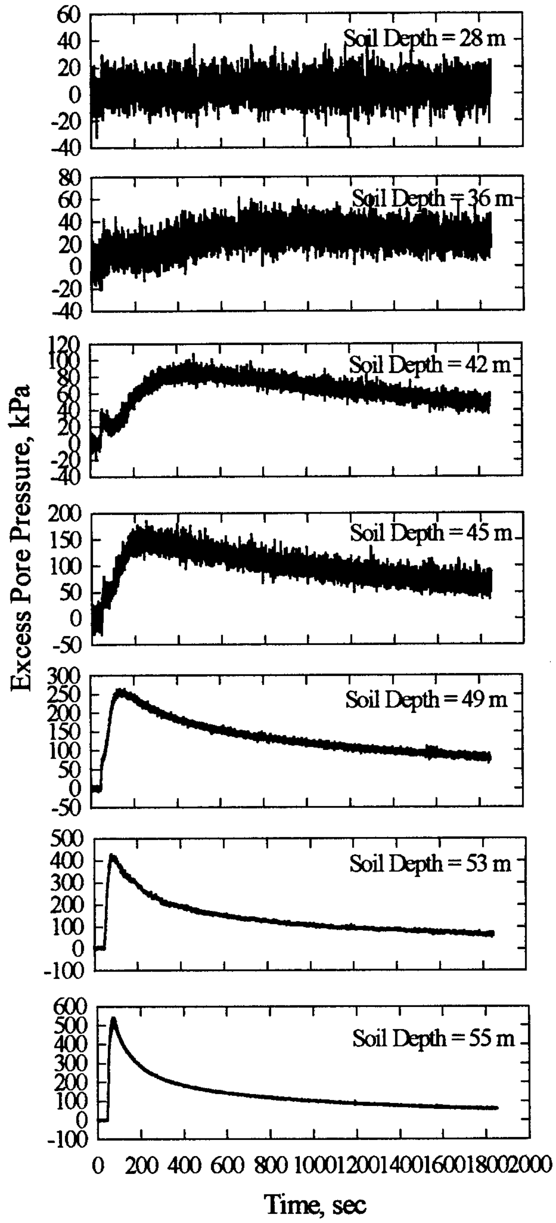

Model 5i

Model 5i (Dry Surcharge 125g)

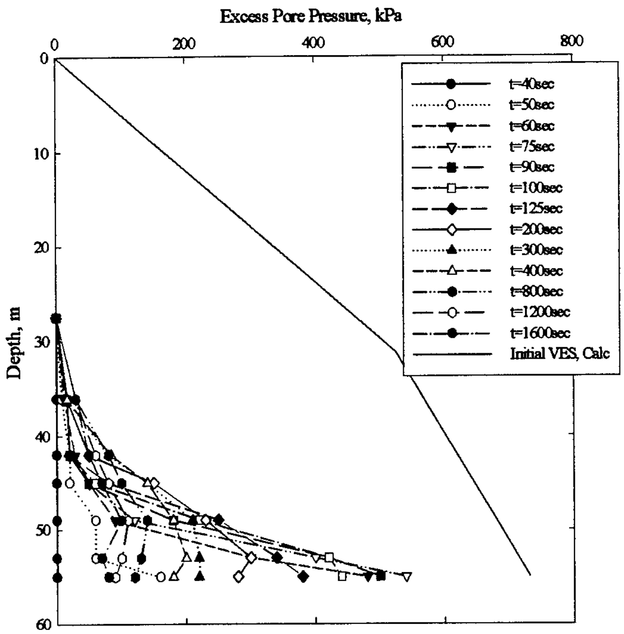

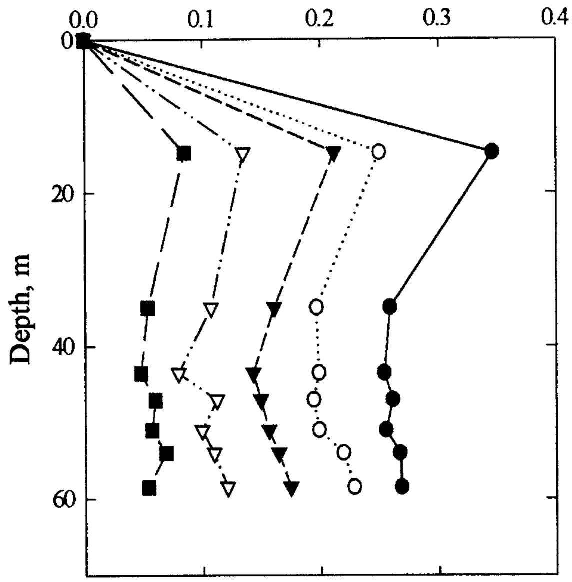

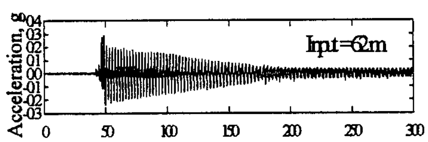

f = 0.43 Hz
a_{max} = 0.22 g

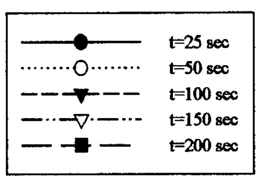

Model 5i-eq1

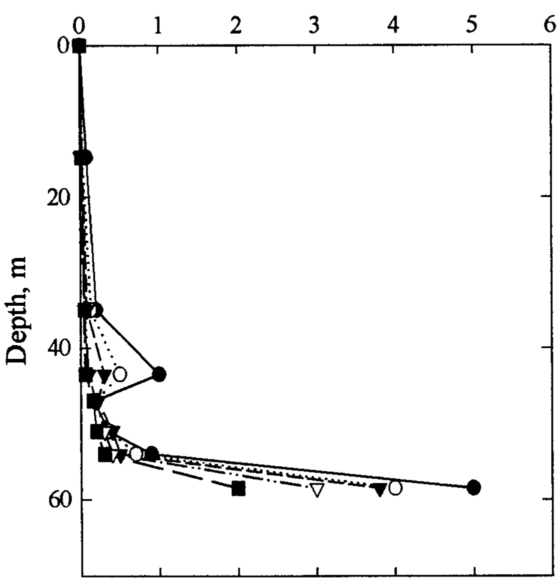

Model 5i-eq1

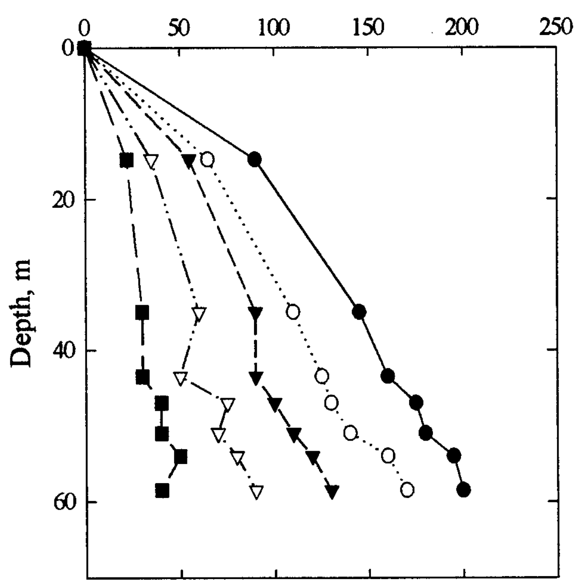

Model 5i Stress and strain isochrones